Hunting for carotenoid-derived retrograde signals that regulate plastid development

Xin Hou

April 2018

A thesis submitted for the degree of
Doctor of Philosophy of
The Australian National University

Declaration

Except where otherwise indicated, this thesis is my own original work.

Xin Hou
Xin.Hou@anu.edu.au
25 April 2018

This thesis is dedicated to my beloved parents
Mr Tao Hou and Madam Yu Qin Liu,
who raised and educated me.

Acknowledgements

My deepest gratitude goes to my supervisor, Professor Barry Pogson from the Australian National University. You not only provided me the opportunity to take on this exciting journey towards an independent scientist but also mentored me along the way. I sincerely appreciate the academic freedom, intellectual stimulation and professional mentorship provided by you throughout my PhD study. You have firmly supported me to hold my position as a righteous man and highlighted integrity as the most precious characteristic of a junior researcher and teacher.

My sincere gratitude to the members of my supervisory panel, Professor Anthony Millar and Dr Christopher Cazzonelli: thank you for being such inspirational figures and approachable advisors during my PhD study. Your advice and guidance have been invaluable at critical steps in my project.

I am deeply grateful to Professor Barbara van Leeuwen who recently retired from ANU Research School of Biology, and Professor Nicholas Glasgow who recently retired from ANU Medical School. They encouraged me to join ANU, one of the world top universities, and to start my second PhD study on a campus full of brilliant academics.

Special thanks go to these helpful and supportive people in the Pogson Lab: Dr Derek Collinge, Dr Nasia Nazir, Dr Gonzalo Estavillo, Dr Andrew Bowerman, Dr Peter Crisp, Dr Kai Chan, Dr Su Yin Phua, John Rivers, Estee Tee and Diep Ganguly. In addition to the helpful discussion over many talks and meetings, the happy hours we spent together at morning teas, birthday celebrations, lab retreats and Plant Energy Biology Conference adventures are shiny pearls in my memory. Many thanks also go to the members of neighbouring laboratories at ANU Research School of Biology, ANU John Curtin School of Medical Research and Australian Commonwealth Scientific and Industrial Research Organisation for kindly providing the key research materials for completing this research.

Contribution of collaborators enriched my research presented in this thesis. In particular, I would like to acknowledge the assistance from Dr Ralf Weslch, Dennis Schlossarek and Carmen Schubert (Faculty of Biology II, University of Freiburg) on PSY activity assays and protein-protein interaction assays using split ubiquitin system. I thank Ms Jiwon Lee (Centre

for Advanced Microscopy, ANU) for technical supports in Transmission electron microscopy. I thank the kind assistance from Dr Yan Wang and Professor James Whelan (School of Life Sciences, La Trobe University) on confocal microscopy.

Massive thanks to the ANU and the Australian Research Council for funding my tuition fees and stipend for my PhD study. This project was made possible through funding from the Australian Research Council Centre of Excellence in Plant Energy Biology.

Last but not least, my gratitude goes to my beloved wife, Dr June Liu: thank you for your patience, understanding and unconditional support throughout this long and tough journey. I will not be able to go through this amazing journey without you.

Thanks to all these who have trusted and helped me!

Abstract

In plants, carotenoids are essential for photosynthesis and photoprotection. However, carotenoids are not the end-products of the pathway: apocarotenoids are produced by carotenoid cleavage dioxygenases (CCDs) or non-enzymatic processes. Apocarotenoids are more soluble or volatile than carotenoids, but they are not simply breakdown products as there can be modifications post cleavage and functions include hormones, volatiles or signals. Evidence is emerging for a class of apocarotenoids herein referred to as Apocarotenoid Signals (ACSs) that have regulatory roles throughout plant development beyond those ascribed to ABA and strigolactone. In the present study, we provide evidence that ACS2, a *cis*-carotenoid-derived retrograde signal, regulates plastid development during both skotomorphogenesis and photomorphogenesis.

cis-carotenoids produced early in the carotenoid pathway may serve as substrates for the production of novel ACSs that regulate nuclear gene expression, metabolic homeostasis and leaf development. When and where they accumulate and what physiological functions they may serve in higher plants remain unclear. *cis*-carotenoids are not easily detected in most plant tissues, except in the absence of carotenoid isomerase (CRTISO) activity when photoisomerisation rate-limits the isomerisation of tetra-*cis* to all-*trans*-lycopene. The accumulation of *cis*-carotenoids in Arabidopsis *crtiso* mutant (*carotenoid and chloroplast regulation 2*, *ccr2*) tissues was observed in plant tissues grown under extended darkness (i.e. shorter photoperiod) and coincided with a perturbation in chloroplast development that caused leaf yellowing. A forward genetic screen identified an epistatic interaction between the ζ-carotene isomerase (*ziso*) and *ccr2* which could restore plastid development, and revealed that di-*cis*-ζ-carotene, tri-*cis*-neurosporene and tetra-*cis*-lycopene are likely substrates for the generation of an ACS, named ACS2. Transcriptomics analysis of *ccr2 ziso* mutant tissues revealed that photosynthesis associated nuclear gene expression (*PhANG*) was activated through the down-regulation of genes involved in repressing photomorphogenesis. We identified an alternative splice mutant of *det1,* a repressor of photomorphogenesis, which could restore PLB formation and cotyledon greening following de-etiolation in *ccr2*. Chemical inhibition of carotenoid cleavage dioxygenase activity provided evidence that ACS2 posttranscriptionally maintains protochlorophyllide oxidoreductase (POR) protein levels

acting downstream of DET1 to control PLB formation and plastid development.

Phytoene synthase (PSY) is a major rate-controlling enzyme that catalyses the initial step of carotenoid biosynthesis and is hence under multi-level regulation. Alteration of *PSY* gene expression, protein levels or enzyme activity can exert profound effects on carotenoid composition and plant development. Here we show that four mutants of PSY: *psy*-4, *psy*-90, *psy*-130 and *psy*-145 reduced *cis*-carotenoids to levels below a threshold and suppressed ACS2 which negatively regulates plastid development in *ccr2*. The restoration of plastid development in the four *ccr2 psy* double mutants was caused by decreased PSY activity and reduced protein levels due to altered PSY-AtOR (ORANGE) interaction, but not by changed localization of PSY. This study reveals a novel role of PSY, modulating carotenoid-derived retrograde signals and regulating plastid development.

Contents

Chapter 1: Carotenoid biosynthesis and cleavage in Arabidopsis

1.1 Introduction

Carotenoids are a group of lipid-soluble isoprenoids with a C_{40} polyene backbone that contain various numbers of conjugated double bonds functioning as a chromophore (Hirschberg, 2001; Eckardt, 2002; Takaichi and Mochimaru, 2007; Maresca et al., 2008). In nature, carotenoids are synthesised by all photosynthetic organisms (i.e cyanobacteria, algae and higher plants), as well as some non-photosynthetic organisms such as fungi and bacteria (Ruiz-Sola and Rodriguez-Concepcion, 2012; Nisar et al., 2015). Animals do not normally synthesize carotenoids, but can ingest them in their dietary intake (McGraw et al., 2006; Baron et al., 2008). However, as one of the only a few exceptions, aphids can make their own carotenoids (Moran and Jarvik, 2010).

There are two types of carotenoids: non-oxygenated and oxygenated carotenoids. The end of non-oxygenated carotenoids can be cyclized at one or both sides (Baroli and Niyogi, 2000). Carotenoids are best known as pigments and scents which are mostly non-oxygenated. They accumulate in specialized plastids called chromoplasts which store carotenoids in plastoglobules, fibrillar, tubular, membranous or even crystalline carotenoid storage structures (Vishnevetsky et al., 1999a; Walter and Strack, 2011; Shumskaya and Wurtzel, 2013). An important role of these carotenoids is to provide distinct colours, scents and flavours in flowers, fruits and seeds to attract animals and insects for pollination and seed dispersal. In addition, the colourful carotenoid compounds furnishing these organs can contribute to economic value (Hirschberg, 2001).

Besides non-oxygenated carotenoids (carotenes), the other major class of carotenoids are oxygenated at the terminal rings so they contain one or more oxygen atoms. The oxygenated carotenoids such as lutein, violaxanthin, neoxanthin and zeaxanthin, are referred to as xanthophylls (DellaPenna and Pogson, 2006; Shumskaya and Wurtzel, 2013).

Interestingly, the composition of carotenoids in all flowering plants is very similar. Lutein (45% of total carotenoids), violaxanthin (10 - 15%), neoxanthin (10 - 15%) and β-carotene (25 - 30%)

are the most abundant carotenoids in plants (Britton, 1993; Pogson et al., 1998). In contrast to chromoplasts which accumulate non-oxygenated carotenoids, chloroplasts accumulate xanthophylls and β-carotene. Therefore, xanthophylls and β-carotene are referred to as "chloroplast carotenoids" in the following sections.

Most chloroplast carotenoids, together with chlorophylls, are associated with pigment-binding proteins located in thylakoid membranes, with β-carotene being abundant in reaction centres of photosystems I and II and xanthophylls mostly found in light-harvesting complexes (Green and Durnford, 1996). This suggests that chloroplast carotenoids may play major roles other than providing plant organs with colours, scents and flavours.

Chloroplast carotenoids stabilize membranes and xanthophylls act as accessory pigments in the light-harvesting antennae by absorbing light at 450 - 570 nm and transferring the energy to chlorophylls which do not absorb light effectively in this range (Demmig-Adams et al., 1996). In addition to light harvesting, chloroplast carotenoids protect photosynthetic apparatus from photooxidative damage, in which β-carotene and xanthophylls are both actively involved. Quenching of ^{3}Chl and $^{1}O_2$ (Kuhlbrandt, 1994; Baroli and Niyogi, 2000) and dissipating the excess excitation energy in a non-radiative manner (Niyogi, 1999, 2000), namely nonphotochemical quenching (NPQ), are examples of photoprotection provided by carotenoids.

In addition to their roles in photosynthetic tissues, carotenoids are also required in etiolated seedlings to form a prolamellar body (PLB) that promotes photomorphogenesis upon illumination (Park et al., 2002; Rodriguez-Villalon et al., 2009b). Moreover, carotenoids are precursors of phytohormones such as plant growth regulator ABA (abscisic acid) and strigolactones, a root transmissible hormone inhibiting plant shoot branching (Nambara and Marion-Poll, 2005; Xie et al., 2010).

Carotenoids are also important to human health. For example, they are precursors of retinal (vitamin A) (Fraser and Bramley, 2004) and can act as antioxidants (Fiedor and Burda, 2014). Carotenoids are linked to reducing age-related macular degeneration and the risk of certain cancers (Snodderly, 1995; Nishino et al., 2000).

Arabidopsis (*Arabidopsis thaliana*) cannot be used to directly explore biological processes located in chromoplasts because it lacks this type of plastid. Therefore, plant systems that synthesize and sequester carotenoids, for example, flowers of marigold (*Tagetes erecta*) and

daffodil (*Narcissus pseudonarcissus*) and fruits of tomato (*Solanum lycopersicum*) and pepper (*Capsicum annuum*) were used to achieve the first advances in carotenoid biosynthesis (Hirschberg, 2001; Fraser and Bramley, 2004; Zhu et al., 2010). On the other hand, carotenoids that accumulate in chloroplasts can be studied using Arabidopsis. Characterization of Arabidopsis mutants *lut*, *npq* and *aba*, which are impaired in xanthophyll biosynthesis, has greatly advanced the study on the role of xanthophylls in photoprotection (Pogson et al., 1996; Pogson et al., 1998; Niyogi, 1999; Pogson and Rissler, 2000; Tian et al., 2004; Kim and DellaPenna, 2006).

To date, there are a few useful genomic tools which facilitate research on the process and regulation of carotenoid biosynthesis. AtIPD, the *Arabidopsis thaliana* Isoprenoid Pathway Database (www.atipd.ethz.ch), is a database that can be searched for isoprenoid pathway models, enzyme activities and subcellular localization of enzymes. Integrating information on isoprenoid pathway genes from other databases including AraCyc (www.arabidopsis.org/biocyc), BioPathAt (Lange and Ghassemian, 2005), KEGG (www.genome.jp/kegg) as well as information from the literatures (Vranova et al., 2011), AtIPD makes a remarkable resource in exploring the regulation of carotenoid biosynthesis.

A range of proteomics databases such as AtCHLORO (www.grenoble.prabi.fr/at_chloro) are also available for study on carotenoid biosynthesis in Arabidopsis. In AtCHLORO database, proteomics data includes protein molecular weights, peptide sequences, MS/MS spectra and chromatographic retention times. So far, this database has been compiled using information of hundreds of proteins identified from purified leaf chloroplasts and their compartments (Cheng et al., 2002). Isoprenoid-pathway-related proteomic databases can now be found in a web portal named MASCP Gator (gator.mascproteomics.org).

1.2 The biosynthesis of carotenoids

Regarding the biosynthesis of carotenoids, two pathways are reviewed in the following sections: the plastidial methylerythritol phosphate (MEP) pathway which produce the C_5 building blocks, isopentenyl pyrophosphate (IPP) and dimethylallyl pyrophosphate (DMAPP), for C_{40} polyene backbone (Figure 1.1); and the carotenoid biosynthesis pathway to produce various carotenoids (Figure 1.2). A generalized carotenoid biosynthesis pathway in plants can

be found via web portals PlantCyc (http://pmn.plantcyc.org/PLANT/NEWIMAGE?type=PATHWAY&object=CAROTENOID-PWY).

The synthesis of the C_5 building blocks, IPP and DMAPP, occurs *de novo* in plastids (Chappell, 1995). IPP and DMAPP are both derived predominantly from glyceraldehyde 3-phosphate and pyruvate as initial substrates by the MEP pathway, although they can also be generated by mevalonic acid (MVA) pathway in the cytosol (Lichtenthaler, 1999; Eisenreich et al., 2001; Rodriguez-Concepcion and Boronat, 2002). The condensation of three IPP molecules and one DMAPP molecule produces geranylgeranyl diphosphate (GGPP, also named as geranylgeranyl pyrophosphate, C_{20}). This reaction is catalysed by GGPP synthase (GGPPS or GGDS) (Farre et al., 2010).

The first committed step in plant carotenoid biosynthesis pathway is the condensation of two GGPP molecules by phytoene synthase (PSY) to produce C_{40} phytoene (Misawa et al., 1994). Phytoene is converted into bright red all-*trans*-lycopene in four desaturation reactions catalysed by phytoene desaturase (PDS), ζ-carotene desaturase (ZDS), and two *cis-trans* isomerases, ζ-carotene isomerase (ZISO) and carotenoid isomerase (CRTISO) (Isaacson et al., 2002; Park et al., 2002; Breitenbach and Sandmann, 2005; Li et al., 2007). Interestingly, in bacteria, all desaturation and isomerization reactions are carried out by only one enzyme, carotene desaturase (CrtI) (Sandmann, 2009).

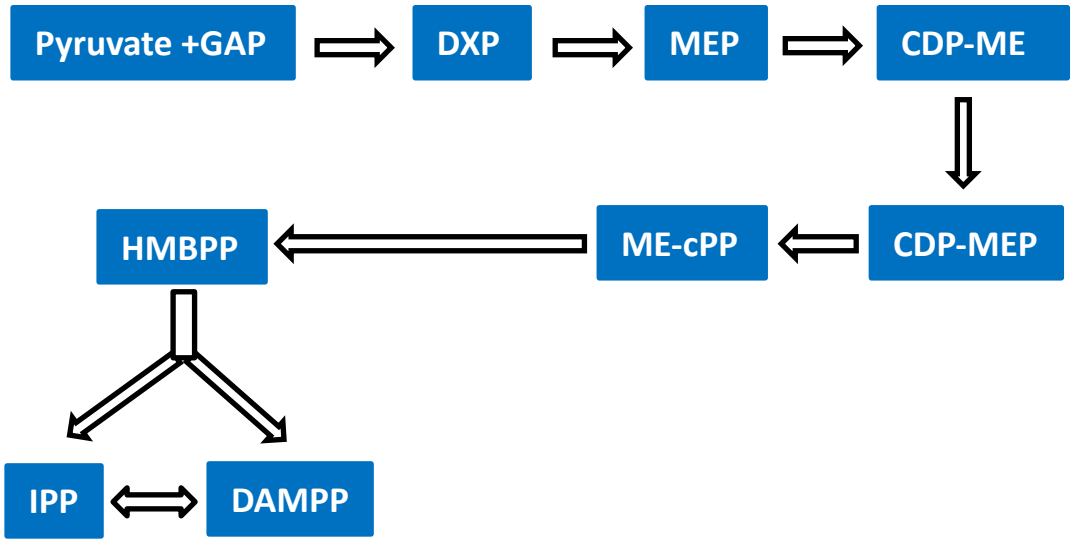

Figure 1.1 A schematic process of the MEP pathway.

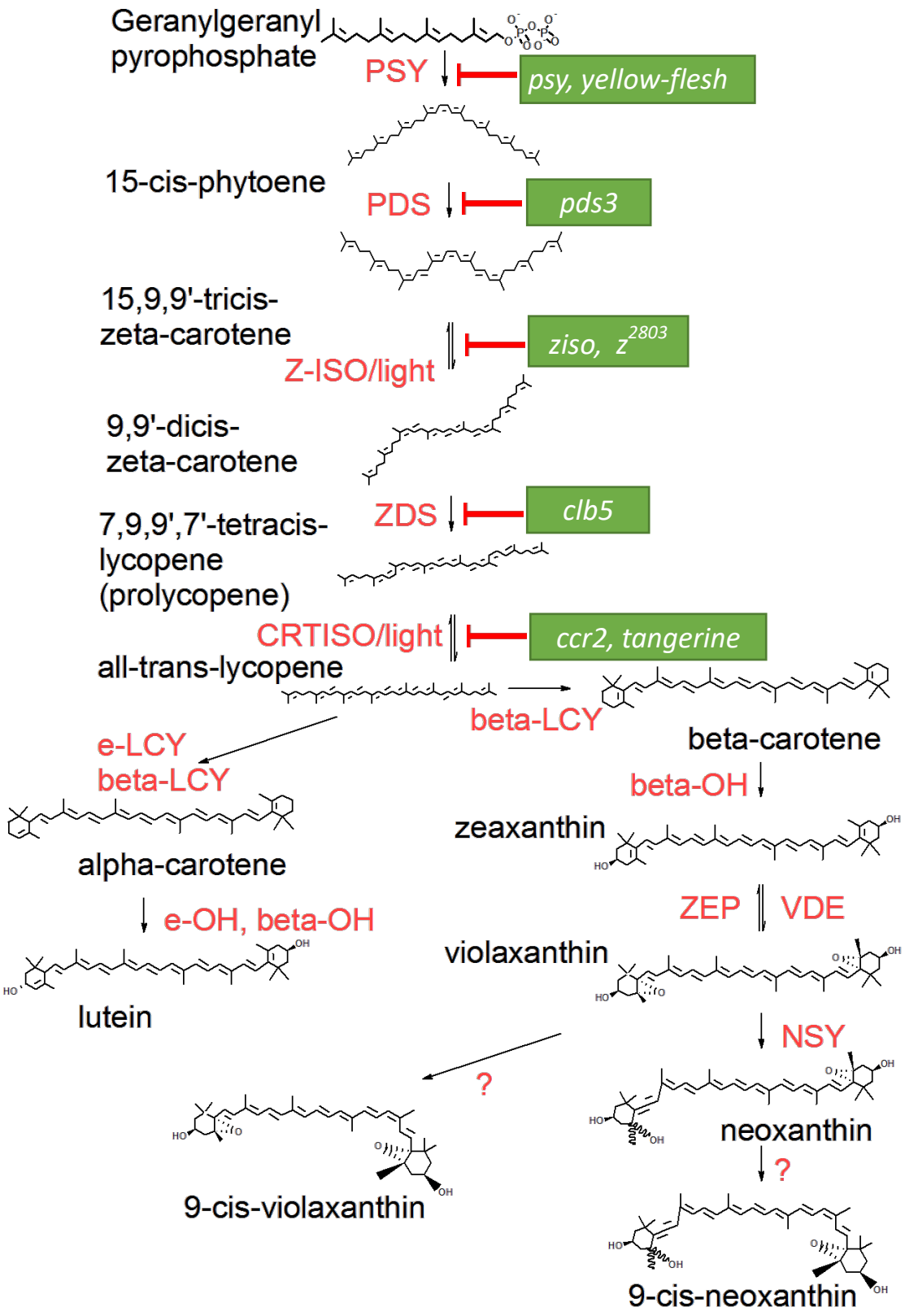

Figure 1.2 The biosynthesis of carotenoids. Question marks indicate unknown enzymes; mutants in the *cis*-carotenoid pathway are shown in green boxes. Geranylgeranyl pyrophosphate is also named as geranylgeranyl diphosphate.

Lycopene represents the branch point of carotenoid pathway. It is cyclized at one end by lycopene β-cyclase (LCYB), and at the other end by lycopene ε-cyclase (LCYE) or LCYB, to produce β,ε-carotene (α-carotene) or β,β-carotene (simply β-carotene), respectively (Cunningham et al., 1996). The introduction of hydroxyl moieties into the cyclic ends is carried out by the two di-iron non-heme β-carotene hydroxylase (BCH) and cytochrome P450 type hydroxylases (CYP97A and CYP97B) to produce zeaxanthin from β-carotene, or by P450 type ε-ring carotene hydroxylase (CYP93C) to produce lutein from α-carotene (Sun et al., 1996; Bouvier et al., 1998a; Tian et al., 2003). Lutein is the endpoint of the α-carotene branch.

Zeaxanthin is converted to violaxanthin via antheraxanthin by zeaxanthin epoxidase (ZEP), and violaxanthin deepoxidase (VDE) reverses this reaction by turning violaxanthin back to zeaxanthin, giving rise to the xanthophyll cycle to protect plants against high light stress (Demmig-Adams et al., 1996; Marin et al., 1996). Antheraxanthin and violaxanthin are then converted to neoxanthin by neoxanthin synthase (NXS) (Al-Babili et al., 2000; Bouvier et al., 2000).

Carotenoids can be cleaved to produce apocarotenoids. In Arabidopsis, a family of nine carotenoid cleavage dioxygenases (CCDs) have been found to catalyse the oxidative cleavage of carotenoids (Walter and Strack, 2011). Apocarotenoids and CCDs are reviewed in section 1.5.

The following sections review the details of MEP pathway and carotenoid biosynthesis pathway.

1.2.1 MEP pathway and synthesis of GGPP

The MEP pathway comprises seven biosynthetic steps and the enzymes catalysing each step have been identified (Rodriguez-Concepcion, 2010; Walter and Strack, 2011). All of the enzymes are encoded by single-copy nuclear genes in Arabidopsis (Rodriguez-Concepcion and Boronat, 2002; Phillips et al., 2008). These enzymes are found to localize in stroma of plastids via varies molecular and proteomic approaches (Querol et al., 2002; Hsieh et al., 2008; Joyard et al., 2009; Ferro et al., 2010).

DXP synthase (DXS, At4g15560), the first enzyme in MEP pathway, catalyses the condensation of glyceraldehyde-3-phosphate and pyruvate to produce 1-deoxy-D-xylulose 5-phosphate (DXP). By research on mutants such as *cla1-1* albino, it has been suggested that the first step

of the pathway is essential. Due to a loss-of-function of DXS, the Arabidopsis *cla1-1* mutant produces almost no leaf carotenoids and chlorophylls, therefore the mutant can only be maintained on media containing sucrose or the dephosphorylated form of DXP (Mandel et al., 1996; Estevez et al., 2000; Estevez et al., 2001). Unlike Arabidopsis, most plants have at least two classes of DXS isoforms which are encoded by small gene families. DXS isozymes of all classes have been found functional in carotenoid biosynthesis (Walter et al., 2002; Krushkal et al., 2003; Cordoba et al., 2011).

In the second and third step, DXP reductoisomerase (DXR, At5g62790) catalyses the intramolecular rearrangement and reduction of DXP to produce MEP, followed by the conversion of MEP to 4-(cytidine 5'-diphospho)-2-C-methyl-D-erythritol (CDP-ME) by MEP cytidylyltransferase (MCT, At2g02500). These two steps, especially the second step, are essential for Arabidopsis seedling viability, as suggested by a complete arrest of tomato seedling development induced by DXR inhibitor fosmidomycin which also inhibits carotenoid biosynthesis in fruits (Budziszewski et al., 2001; Rodriguez-Concepcion et al., 2001; Xing et al., 2010).

In the following steps, CDP-ME is phosphorylated by CDPME kinase (CMK, At2g26930), and the product CDP-ME 2-phosphate (CDP-ME2P) is converted into 2-C-methyl-D-erythritol 2,4-cyclodiphosphate (ME-cPP) by ME-cPP synthase (MDS, At1g63970). ME-cPP is then converted into two isomers IPP and DMAPP (5:1 mixture) via 4-hydroxy-3-methylbut-2-enyl diphosphate (HMBPP), catalysed by HMBPP synthase (HDS, At5g60600) and HMBPP reductase (HDR, At4g34350), respectively. HDR, which catalyses the last step in MEP pathway, has also been found to be a key enzyme. HDR is regulated by post-transcriptional feedback within the pathway according to research on Arabidopsis mutation *clb6* which is defective in the function of this enzyme (Guevara-Garcia et al., 2005).

There is also an enzymatic interconversion between IPP and DMAPP, catalysed by IPP isomerase (IDI). It is possible that this interconversion is used to control different molar ratios between the two isomers to produce different classes of isoprenoids. Unlike the MEP pathway enzymes, IDI is encoded by two genes IDI1 (At5g16440) and IDI2 (At3g02780) in Arabidopsis.

So far, two strategies have been used to identify essential steps in MEP pathway: overexpression of single gene followed by analysis of carotenoid content alteration, and analysis of transcript level alterations and their potential correlation with carotenoid

accumulation. In Arabidopsis, overexpression of *CLA1-DXS* gene increased total carotenoids in light-grown seedlings by 1.3-fold (Estevez et al., 2001), and overexpression of *DXR* also up-regulated carotenoids biosynthesis (Carretero-Paulet et al., 2006). While constitutive overexpression of *HDR* gene in Arabidopsis showed no significant increase in carotenoid levels in etioplasts, carotenoid biosynthesis in green seedlings were clearly up-regulated (Botella-Pavia et al., 2004).

The transcription of *DXS* gene is strikingly up-regulated during fruit ripening in tomato, which also showed a strong correlation with the increase of lycopene content in fruit (Lois et al., 2000). *DXS3*, *DXR* and *HDR* transcripts increased with the accumulation of xanthophylls in maize (*Zea mays*) kernel endosperm (Vallabhaneni and Wurtzel, 2009). The transcription of *HDR* in Arabidopsis also exhibits strong up-regulation in correlation with carotenoid accumulation during seedling deetiolation (Botella-Pavia et al., 2004).

Taken together, the flux from MEP pathway to carotenoids may be controlled by DXS, DXR and HDR which are suggested to be rate-limiting enzymes in the pathway.

The assembly of four C_5 units into C_{20} molecule GGPP is carried out by GGPPS which catalyses the sequential and linear condensation of three molecules of IPP to an allylic primer DMAP. This step provides building blocks not only for carotenoid biosynthesis but also for gibberellin phytohormones and the phytyl side chain of chlorophylls, tocopherols and a large variety of diterpenes.

Thus far, 12 putative *GGPPS* genes have been identified from sequenced Arabidopsis genome (Lange and Ghassemian, 2003) (www.atipd.ethz.ch), of which five have been characterized but only two were found to be located in plastids (Okada et al., 2000). In tomato, two plastidial isoforms of GGPPS enzyme were also characterized (Ament et al., 2006); in maize, the expression of only one out of three *GGPPS* genes described was shown to positively correlate with kernel endosperm carotenoid content (Vallabhaneni and Wurtzel, 2009).

The presence of several GGPPS isoforms in most plants studied suggests that different isoforms may be involved in the synthesis of specific classes of isoprenoids. Consistently, GGPPS and PSY have been identified from multi-enzyme complexes in chromoplasts and this association can facilitate direct conversion of IPP and DMAP into phytoene (Islam et al., 1977; Maudinas et al., 1977; Camara, 1993). In maize, the transcription of genes encoding *DXS*, *DXR*

and *HDR* also showed significant correlation with that of the only *GGPPS* gene involved in carotenoid biosynthesis (Vallabhaneni and Wurtzel, 2009).

It has been hypothesized that in carotenoid biosynthesis, precursor formation, their conversion to C_{40} backbone and further modifications form a co-ordinately regulated reaction chain, where carotenogenesis-associated GGPPS isoforms and enzymes in MEP pathway jointly channel well-regulated supply of metabolites and building blocks for carotenoid biosynthesis (Walter and Strack, 2011). However, it remains largely to be tested if metabolite channelling is a valid mechanism for the production of carotenoids in plant.

1.2.2 Synthesis of the first carotenoid in the pathway: phytoene

The first committed step in carotenoid biosynthesis is the formation of 15-*cis*-phytoene (also referred to as phytoene thereafter), a colourless compound, from two GGPP molecules. This step is catalysed by PSY that is probably the best-studied enzyme in plant carotenoid biosynthesis (Beyer et al., 1989; Hirschberg, 2001; Fraser and Bramley, 2004). The formation of phytoene by PSY involves two steps: the head-to-head condensation of two GGPP molecules to form the intermediate pre-phytoene diphosphate, followed by the elimination of the diphosphate group and a molecular structure rearrangement to form phytoene.

Being an entry-point enzyme of carotenogenesis, PSY is strongly regulated therefore regarded as the major rate-limiting enzyme in carotenoid biosynthetic flux (Hirschberg, 2001; Giuliano et al., 2008; Cazzonelli and Pogson, 2010). Altered *PSY* expression often affects carotenoid content in plants (Ducreux et al., 2005; Fraser et al., 2007; Maass et al., 2009; Welsch et al., 2010; Cao et al., 2012). Interestingly, overexpression of PSY may not boost up the carotenoid flux as expected; instead it could lead to dwarf phenotypes along with altered carotenoid content in various tissues (Fray et al., 1995; Busch et al., 2002). The mechanism could be due to depleted GGPP pools for biosynthesis of phytohormones such as gibberellin and/or down-regulation of PSY by co-suppression effects.

As discussed in section 1.2.1, it has been found that PSY activity is associated with enzymes GGPPS and IDI in a huge enzyme complex (up to 200 kD), which may facilitate channelling isoprenoid precursors formed in the stroma (Camara, 1993; Fraser et al., 2000). The enzyme complex likely localizes in membranes because phytoene is a hydrophobic carotenoid. Indeed PSY enzymes have been detected on membranes in all kinds of plastids (Dogbo et al., 1988;

Bonk et al., 1997; Fraser et al., 2000; Welsch et al., 2000; Li et al., 2008b) but GGPPS and IDI have been found soluble (Joyard et al., 2009). A study of PSY localization in white mustard (Arabidopsis relative) found that PSY was isolated from both membrane and stroma fractions, but PSY activity was detected only in membrane pellets (Welsch et al., 2000). Together with other results, this suggests that membrane association was required for the activity of PSY.

While there is only one *PSY* gene (At5g17230) in Arabidopsis, most plants have gene families encoding PSY (Ruiz-Sola and Rodriguez-Concepcion, 2012). There are at least three *PSY* homologues in tomato, carrot (*Daucus carota*), rice (*Oryza sativa*), maize and cassava (*Manihot esculenta*), and two genes encoding PSY isoforms in tobacco (Fraser et al., 1999; Busch et al., 2002; Giorio et al., 2008; Li et al., 2008b; Welsch et al., 2008; Arango et al., 2010). The expression of Arabidopsis *PSY* gene has been found in all photosynthetic and non-photosynthetic tissues (Welsch et al., 2003), and is correlated with other genes in the carotenoid pathway and MEP pathway as well as *GGPPS* (Meier et al., 2011).

In other plants, some PSY isoforms are expressed in chloroplasts in photosynthetic tissue, while others predominantly in other plastids such as chromoplasts in non-photosynthetic tissues. For example, tomato *PSY2* transcripts were detected in all tissues and leaves showed the highest transcription level, whereas *PSY1* transcripts were found to be extremely abundant in fruits at ripening stage (Kachanovsky et al., 2012). Maize *PSY1* is expressed in seed endosperm while *PSY3* transcripts have been predominantly detected in root (Li et al., 2008a; Li et al., 2008b).

Among the three well-characterized PSY isoforms in both maize and rice, PSY3 is expressed strongly in root and its transcription is regulated in response to drought, salt and abiotic stresses in roots (Li et al., 2008a; Li et al., 2008b). The regulation of *PSY3* gene expression plays an essential role in ABA biosynthesis by determining root carotenoid biogenesis channelled into ABA formation, consistent to which ABA-response elements have been identified from *PSY3* promoter in rice (Welsch et al., 2008).

Similar with tomato, it has been also elucidated that the formation of carotenoids involved in photosynthesis in maize leaves requires another *PSY* homologue, *PSY2* (Li et al., 2008a; Li et al., 2008b). Meanwhile, phylogenetic analysis on rice *PSY* (*OsPSY*) homologues indicated that *PSY2* was likely the common ancestor of *PSY1* and *PSY3* genes, suggesting the presence of a single-copy *PSY* gene originally in higher plants (Welsch et al., 2008).

1.2.3 From phytoene to lycopene

The chromophore of carotenoids contains a series of conjugated double bonds. Phytoene is an uncoloured carotene with only a central conjugated core of three double bonds. Naturally or artificially introducing additional double bonds by desaturation steps to phytoene confers carotenoids to different colours ranging from yellow, orange to red (Schmidt-Dannert et al., 2000; Cazzonelli and Pogson, 2010).

In the following steps of the carotenoid biosynthesis pathway in plants, four desaturation and two isomerization reactions introduce conjugated double bonds into phytoene to form the red-coloured all-*trans*-lycopene, sequentially via phytofluene, ζ-carotenes, neurosporene and pro-lycopene. These reactions are carried out by two desaturases and two isomerases.

1.2.3.1 Desaturases

As mentioned above, through four desaturation steps, phytoene is transformed into tetra-*cis*-lycopene (ψ,ψ-carotene) which possesses eleven conjugated double bonds, sequentially via di-*cis*-phytofluene (7,8,11,12,7',8'-hexahydro-ψ,ψ-carotene), tri-*cis*-ζ-carotene (7,8,7',8'-tetrahydro-ψ,ψ-carotene) and tri-*cis*-neurosporene (7,8-dihydro-ψ,ψ-carotene), and the number of conjugated double bonds is increased to five, seven and nine, respectively (Hirschberg, 2001; Fraser and Bramley, 2004). As the number of conjugated double bonds increases, the absorption of the C_{40} polyene chain is shifted towards longer wavelengths, which confers pale-yellow colour to ζ-carotene, orange colour to neurosporene, and red colour to lycopene (Cunningham and Gantt, 1998; Zhu et al., 2010).

In plant and cyanobacteria, the desaturation steps are catalysed by phytoene desaturase synthase (PDS) and ζ-carotene desaturase (ZDS) (Fraser and Bramley, 2004; Sandmann, 2009). PDS introduces *trans* double bonds at the 11, 11′ positions to form 9,15,9'-tri-*cis*-ζ-carotene, while ZDS introduces *cis* double bonds to form 7,9,9',7'-tetra-cis-lycopene (Giuliano et al., 2002).

In contrast, nonphotosynthetic bacteria and fungi require only a single CrtI enzyme (phytoene desturase) to catalyse all desaturation steps and form all-t*rans*-lycopene as the final product (Bartley et al., 1999). This was supported by an experiment overexpressing bacterial (*Erwinia herbicola*) CrtI along with daffodil (*Narcissus pseudonarcissus*) PSY and/or daffodil lycopene β-cyclase, and consequently obtaining the accumulation of phytoene, lycopene, β-carotene,

lutein and zeaxanthin in rice endosperm (golden rice) (Beyer et al., 2002; Al-Babili et al., 2006). The complicated desaturation and isomerization steps in plants generate several *cis*-carotene intermediates that may play regulatory roles within carotenoid biosynthesis.

Arabidopsis PDS (encoded by At4g14210) and ZDS (encoded by At3g04870) (www.arabidopsis.org) and both have been identified from chloroplast envelope membrane sub-fraction by proteomic approaches (Joyard et al., 2009). Similar to GGPPS and PSY, the membrane-bound PDS from chloroplasts and chromoplasts was also detected in a large protein complex (350 kD), which is consistent with the proposed multi-enzyme complex containing membrane-associated PDS, ZDS and other enzymes in the carotenoid pathway to convert phytoene to cyclic carotenes (Cunningham and Gantt, 1998).

PDS has also been found in soluble fractions (e.g. stroma) from Arabidopsis chloroplasts and other plastids but the soluble forms were inactive and associated with chaperone proteins (Al-Babili et al., 1996; Bonk et al., 1997; Lopez et al., 2008b). It has been hypothesized that the association of PDS with chaperones is important for its activation through insertion into plastid membranes (Al-Babili et al., 1996; Bonk et al., 1997). ZDS was also found in chloroplast stroma and PDS in the thylakoid fraction (Mann et al., 2000). It remains to be elucidated what carotenogenic enzymes are in the membrane-associated PDS complex and if it also contains chaperone proteins as shown for the stroma complex. Future studies need to address the molecular mechanism of multi-enzyme association and coordination/regulation to perform the highly-regulated carotenoid biosynthesis process.

Besides membrane association, the carotenoid desaturases also need to bind redox cofactors for their activity (Nievelstein et al., 1995). In accordance with this, all desaturases and isomerases in carotenoid biosynthesis possess a conserved flavin-binding motif near their N-terminuses (Sandmann, 2009; Schaub et al., 2012). Evidences for the requirement of oxidized plastoquinone as an electron carrier for the desaturation reactions were from the characterization of *pds1* and *pds2* mutants in Arabidopsis, where the impaired plastoquinone biosynthesis was accompanied with accumulation of phytoene (Norris et al., 1995).

A plastidial terminal oxidase (PTOX) was identified as a second component of the redox chain required for carotenoid desaturation, based on the characterization of another phytoene-accumulating Arabidopsis mutant, *immutans* (*im*) (Wu et al., 1999; Carol and Kuntz, 2001). The *im* mutant shows variegated phenotype comprising green and albino sectored leaves due

to accumulation of phytoene and reduced photosynthetic carotenoids (Aluru et al., 2001). Plastoquinone is reduced in carotene desaturation reactions, and PTOX, as a plastoquinol-O_2 oxidoreductase, regenerates the oxidized plastoquinone required for the desaturases. Genetic lesions in *PTOX* hence lead to accumulation of phytoene in both leaves (chloroplasts) and fruit (chromoplasts), resulting in albino phenotypes such as white 'ghost' tomato (Josse et al., 2000).

While the above results suggested PTOX as an essential cofactor involved in carotenoid desaturation in both photosynthetic and non-photosynthetic tissues, other studies showed that PTOX is not absolutely required for carotenoid desaturases in photosynthetic tissues, implying the existence of an alternative, PTOX-independent plastoquinol-O_2 oxidoreduction pathway (Carol and Kuntz, 2001; Shahbazi et al., 2007). Supporting this hypothesis, NADH dehydrogenase also catalyses the reduction of plastoquinone using electron donors in stroma (Burrows et al., 1998; Endo et al., 2008). However, the regulatory mechanisms to balance PTOX and NADH dehydrogenase and its biological implications have remained unclear.

1.2.3.2 Isomerases

Phytoene exists predominantly as the 15-*cis* isomer in carotenoid biosynthesis pathway in all higher plants, while the predominant isomer of lycopene has the more stable all-*trans* configuration, suggesting the requirement of *cis*-*tans* transition (isomerisation) (Beyer and Kleinig, 1991), possibly catalysed by isomerase(s) in the pathway. Catalysed by PDS, the 15-*cis*-phytoene is converted to tri-*cis*-ζ-carotene, but this intermediate needs to be isomerized at the 15-*cis* double bond to form di-*cis*-ζ-carotene before two further desaturation steps can occur under the catalysis of ZDS (Bartley et al., 1999; Matthews et al., 2003; Breitenbach and Sandmann, 2005).

Although the above isomerization can occur in the presence of light in the chloroplasts of green tissues, another enzyme is required in other plastids to carry out the isomerization in the absence of light (Breitenbach and Sandmann, 2005; Li et al., 2007). The enzyme ZISO has been found to catalyse this *cis*-*trans* transition enzymatically in plant. Based on the characterization of maize *y9* and Arabidopsis *zic* mutants accumulating tri-*cis*-ζ-carotene in the dark, *ZISO* has been cloned from both plants (Li et al., 2007; Chen et al., 2010). In fact *ZISO* exists in all plants and algae, where its activity is required in both light-exposed and light-deprived tissues, though the activity can be partially compensated by photoisomerization (Li

et al., 2007; Chen et al., 2010). Possessing membrane-spanning domains, ZISO is also predicted to be a membrane-associated enzyme, but it is yet to be determined whether this plastid-targeted enzyme is integrated into envelope or thylakoid membranes (Zybailov et al., 2008; Ishikawa et al., 2009).

Only one single gene encodes ZISO (At1g10830) in Arabidopsis, but two transcripts are produced by this gene. *ZISO1.1* encodes a functional enzyme and is expressed in all tissues, while *ZISO1.2* encodes a truncated protein that lacks the predicted transmembrane domains and possesses no enzymatic activity. Most other plants, including maize and rice, also have a single gene encoding ZISO, but interestingly no alternate transcripts have been found (Chen et al., 2010).

Through another two desaturation steps, ZDS introduces two more *cis*-double bonds at the 7-8 and 7'-8' positions of di-*cis*-ζ-carotene, forming tetra-*cis*-lycopene (pro-lycopene) (Breitenbach and Sandmann, 2005; Sandmann, 2009). In the presence of light, photoisomerization is sufficient to convert pro-lycopene to all-*trans*-lycopene (Cazzonelli and Pogson, 2010). However in the dark or nonphotosynthetic tissues, a second round of enzymatic isomerization must be carried out by another isomerase (Park et al., 2002; Cazzonelli and Pogson, 2010).

A carotenoid isomerase (CRTISO) was identified by characterizing tomato *tangerine* and Arabidopsis *ccr2* (*carotenoid and chloroplast regulatory 2*) mutants (Isaacson et al., 2002; Park et al., 2002). Tomato *tangerine* mutant has orange fruit, yellowish young leaves and pale flowers (Isaacson et al., 2002). In the Arabidopsis *ccr2* mutant, etiolated seedlings accumulate poly-*cis* carotenes including pro-lycopene in etioplasts and the change of carotenoid content is correlated with the lack of PLBs. In wild type Arabidopsis, cyclic xanthophylls lutein and violaxanthin are associated with PLBs which form the lattice of etioplast tubular membranes to disperse into chloroplast thylakoids upon illumination (Park et al., 2002).

CRTISO isomerizes *cis*-bonds (at 7,9 and 7',9' positions) in pro-lycopene and forms all-*trans*-lycopene (Isaacson et al., 2004). To be active, CRTISO requires membrane-association and a flavin adenine dinucleotide (FAD) cofactor in a reduced form. Interestingly, although CRTISO shows some sequence similarity to plant PDS and ZDS, unlike both of them, it lacks desaturase activity and catalyses reactions that do not involve net electron transfer (Isaacson et al., 2004; Yu et al., 2011). CRTISO shares 20 – 30% amino acid identity to bacterial carotenoid

desaturases CrtI, particularly at the N-terminal FAD-binding domain which is conserved in all desaturases and cyclases (Sandmann, 2009; Schaub et al., 2012). Apart from *CCR2*/*CRTISO1* (At1g06820) encoding a functional CRTISO enzyme in Arabidopsis, *CRTISO2* (At1g57770) has also been proposed to encode a protein named CRTISO2 (Lange and Ghassemian, 2003), although no enzymatic activity has been detected from CRTISO2 (Park et al., 2002).

It has been proposed that the *cis*-carotenes produced in carotenoid biosynthesis may serve as novel signalling molecules and regulate chloroplast biogenesis and plant development under certain circumstances (Kachanovsky et al., 2012). As the defective CRTISO genes in Arabidopsis *ccr2* and tomato *tangerine* cause accumulation of *cis*-carotenes (Park et al., 2002; Kachanovsky et al., 2012), CRTISO may play an important regulatory role in the carotenoid pathway and plant development. However, at present no convincing results are available to support the above hypothesis.

1.2.3.3 The complication of carotene desaturation

Bacterial *crtI* genes encode desaturases that can convert phytoene to neurosporene with three desaturation steps (first gene cloned in *Rhodobacter capsulatus*), or to lycopene with four steps (first gene cloned in *Erwinia herbicola*) (Armstrong et al., 1989; Bartley and Scolnik, 1989), while *crtI*-like desaturase gene *al-1* from the fungus *Neurospora crassa* encodes a desaturase that can convert phytoene to 3,4-dehydrolycopene through five steps (Hausmann and Sandmann, 2000). Similarly, the diapophytoene desaturase CrtN is also diverse on the number of desaturation steps (Raisig and Sandmann, 1999; Tao et al., 2005). Though *crtI* and *crtN* genes can be classed into three clusters by phylogenetic analysis, each of them encodes a single desaturase that is sufficient for the entire desaturation and *cis*-*trans* transition process in carotenoid biosynthesis.

Quite differently, in cyanobacteria and plant there are two desaturases (PDS/CrtP and ZDS/CrtQb) and two isomerases (ZISO and CRTISO) to catalyse the conversion of 15-*cis*-phytoene to all-*trans*-lycopene (Chamovitz et al., 1990; Chamovitz et al., 1991; Pecker et al., 1992; Albrecht et al., 1995; Breitenbach et al., 1998; Bartley et al., 1999). The plant poly-*cis* pathway from phytoene to lycopene generates a number of *cis*-carotene intermediates (Clough and Pattenden, 1979; Goodwin, 1983) which may serve regulatory roles in carotenoid biosynthesis, plant development or stress responses.

In a study on tomato mutant *yellow-flesh* (*r*) and *tangerine* (*t*), the transcription of *PSY* in fruit was shown to be eliminated by single mutant r^{2997}, while the transcription of *PSY* was partially restored in the double mutant r^{2997}/t^{3002}. Because t^{3002} has a mutation in the gene *CRTISO*, it has been suggested that the accumulated pro-lycopene and tri-*cis*-neurosporene in carotenoid biosynthesis pathway act as signalling molecules to regulate the transcription of *PSY* and might also produce regulatory signals for other pathways in plant development (Kachanovsky et al., 2012). This provides a possible explanation for why plants use a complicated poly-*cis* pathway that involves four enzymes in carotenogenesis.

Though CrtI and the enzymes in poly-*cis* pathway both convert 15-*cis*-phytoene to all-*trans*-lycopene, biochemically they are not identical (Sandmann, 2009; Walter and Strack, 2011). While CrtI alone forms all-*trans*-lycopene without detectable intermediates, all of the *cis*-configured intermediates in the plant poly-*cis* pathway exist in detectable concentrations (Isaacson et al., 2004). Furthermore, tri-*cis*-neurosporene and pro-lycopene can both be cleaved by CCDs to produce *cis*-configured apocarotenoids that may serve as signalling molecules, particularly when their concentrations are altered under stress or during disturbance of carotenoid biosynthesis (also see section 1.5). The activity of CRTISO is then important not only for carotenoid biosynthesis but also for controlling the level of *cis*-carotenes, that themselves or after cleavage may serve as signalling molecules.

Besides the regulatory mechanism described above, other regulatory loops may also exist in tomato fruit, as suggested by a study using Virus Induced Gene Silencing (VIGS) to examine the functions of carotenogenic enzymes (Fantini et al., 2013). The transcription of *ZISO* was induced when *PDS* was silenced, and similarly *CRTISO* transcript was increased when *ZDS* was silenced. Two functional units comprising PDS/ZISO and ZDS/CRTISO, respectively, were hence proposed to be under the regulation of two regulatory loops which may sense the levels of downstream *cis*-confirmed carotenoids (such as prolycopene) or the derivatives (Fantini et al., 2013).

In another study addressing the reason why “golden rice” is yellow (golden) instead of red, the expression of bacterial *crtI* gene was suggested to greatly up-regulate the endogenous carotenoid biosynthesis in the target tissue in rice by a feedback loop. The absence of *cis*-carotenes including pro-lycopene due to the bypass of the poly-*cis* pathway, and/or the constitutive production of all-*trans*-lycopene, both mediated by bacterial *ctrI* gene in the

transgenic rice, were proposed to initiate the feedback regulation (Schaub et al., 2005). Despite that the expression of intrinsic carotenoid biosynthesis genes in rice was shown unchanged, the lack of *cis*-carotenes can still be speculated to lie in protein expression and/or enzymatic activity.

1.2.4 Cyclization of lycopene

An essential modification of the linear C_{40} backbone of all-*trans*-lycopene is the cyclization of both ends as a branch point of the carotenoid biosynthesis pathway to generate diversified carotenoid. Formation of cyclic terminal groups is initiated by proton attack at the terminal C-1,2 double bond of the hydrocarbon chain. Two types of cyclic terminal groups can be generated by enzymatic cyclization: ε- and β-rings, and they only differ in the position of the double bond in the ring, which depends on the nature of the cyclase enzyme (Fraser and Bramley, 2004). A β-ring only has one conformation because the double bond within the ring is in conjugation with the backbone, while a ε-ring can rotate within a range because its double bond is not in conjugation (Ruiz-Sola and Rodriguez-Concepcion, 2012).

At this branch point the carotenogenesis pathway bifurcates to β,β-carotenoids with two β rings (*e.g.* β-carotene and derived β,β-xanthophylls such as zeaxanthin, violaxanthin and neoxanthin) and β,ε-carotenoids with one β-ring and one ε-ring (*e.g.* α-carotene and derived β,ε-xanthophylls such as lutein) (Hirschberg, 2001). The formation of ε,ε-ring carotenoids is uncommon in plants, and has only been found in a few species. For example, lettuce (*lactuca sativa*) can produce a ε,ε-xanthophyll named lactucaxanthin, via ε-carotene (Phillip and Young, 1995; Cunningham and Gantt, 2001). In plant, two different lycopene cyclases carry out the formation of β- and ε-rings: LCYB creates β-rings, and LCYE forms ε-rings (Cunningham et al., 1993; Pecker et al., 1996; Ronen et al., 1999; Cunningham and Gantt, 2001).

While LCYE normally generates only one ring at one end of the linear lycopene, LCYB creates one β-ring at each end of the C_{40} backbone to produce the bicyclic β-carotene via a monocyclic γ-carotene (β,ψ -carotene) (Walter and Strack, 2011). The two cyclases together can hence catalyse the conversion of lycopene to α-carotene containing one β- and one ε-ring, via the monocyclic δ-carotene (ε,ψ-carotene), which initiates the other branch of the carotenoid pathway (Ronen et al., 1999). Interestingly, only a single amino acid determines the molecular nature of LCYE to stop after the first cyclization, as verified by a mutated Arabidopsis LCYE

with only Lysine448 changed to Histidine but leading to the formation of two ε-rings (Cunningham and Gantt, 2001).

Under the catalysis of only LCYE (without LCYB) in maize, the monocyclic δ-carotene and uncommon bicyclic ε,ε-carotene can both be synthesized by the cyclization of either one or both ends of the hydrocarbon backbone, respectively (Bai et al., 2009). In another study, the characterization of Arabidopsis *lut2* mutant possessing a defective *LCYE* gene showed no accumulation of any ε-ring carotenoid, while β-cyclization is intact (Pogson et al., 1996). Taken together, LCYE has been proposed to be rate-limiting in the formation of lutein in carotenoid biosynthesis.

It has been proposed that the cyclases are also membrane-associated proteins and involved in enzyme complexes that coordinate related steps in the carotenoid pathway (Cunningham and Gantt, 1998). LCYB has been identified from envelop membranes by proteomic approaches, although the existence of enzyme complexes involving LCYB and/or LCYE has remained to be verified (Joyard et al., 2009). It has been further hypothesized that the absence of ε,ε-carotenoids in most plants is due to enzyme complexes containing both LCYE and LCYB or only the later (Cunningham and Gantt, 1998; Bai et al., 2009). Consequently, the relative amounts or activities of the two cyclases in plant may determine the proportion of β,β- and β,ε-carotenoids (Pogson et al., 1996; Ronen et al., 2000; Harjes et al., 2008).

All carotenoid cyclases, including crtY from nonphotosynthetic bacteria, CrtL from cyanobacteria and plant LCYB and LCYE, have been shown to require an FAD cofactor in a reduced form with no net redox in catalysis (Yu et al., 2010). This character requires a conserved FAD-binding domain in all carotenoid cyclases, although similarity of these cyclases is rather low. It is hypothesized that plant cyclases were originated from CrtL, and that LCYE in plant might be evolved from LCYB by gene duplication (Klassen, 2010). Consistently, all carotenoid-synthesizing organisms form β-rings from the linear C_{40} backbone, while only photosynthetic organisms produce ε-rings (Kim and DellaPenna, 2006), suggesting that LCYE was a descendant of LCYB.

While LCYE is typically encoded by single-copy genes in most plants, LCYB is encoded by small gene families in some plants, or by single-copy genes in others (*e.g.* maize and rice (Cunningham et al., 1996; Lange and Ghassemian, 2003; Chaudhary et al., 2010) (www.phytozome.net). In Arabidopsis, two single-copy genes with significant homology

encode LCYB (At3g10230) and LCYE (At5g57030) (www.arabidopsis.org). In tomato, there are two *LCYB* genes with significant homology, *LCYB1*/*CRTL-B1* and *LCYB2*/*CRTL-B2*. They share 53% similarity in amino acid sequence. The expression of *LCYB1* was found mainly in leaves and flowers, and its transcription was down-regulated during fruit ripening (Pecker et al., 1996; Ronen et al., 2000). LCYB2 is chromoplast-localized, and its expression was mainly found in fruit (Ronen et al., 2000). LCYB2 also shows similarity to the pepper capsaxanthin-capsorubin synthase (CCS) (Ronen et al., 2000).

Introducing daffodil *LCYB* gene introduced into tomato plastid genome led to almost eliminated lycopene and significantly elevated β-carotene in tomato fruits. Meanwhile the total carotenoids were increased by more than 50% (Apel and Bock, 2009). In another interesting test with potato, the introduction of an antisense fragment of *LCYE* gene under the control of a tuber-specific promoter to down-regulate the expression of potato *LCYE* gene led to significantly increased β,β-carotenoids including β-carotene. However, in contrast to expectation, the level of lutein was not reduced and total carotenoids increased up to 2.5-fold (Diretto et al., 2006). These results together raised a hypothesis that the activities and gene expression of not only cyclases but also other key enzymes in carotenoid biosynthesis pathway are regulated by a complex mechanism involving metabolic feedback to dynamically control the flux of the whole pathway.

1.2.5 The formation of xanthophylls

The cyclic α- and β-carotenes are further hydroxylated at positions C-3 and C-3’ of each ionone ring to produce the oxygenated carotenoids, xanthophylls (lutein and zeaxanthin from α- and β-carotenes, respectively) (Zhu et al., 2010). Lutein is the end of the α-carotene branch of the carotenoid pathway. On the β-carotene branch, zeaxanthin undergoes two-step epoxidation at positions C-5,6 and C-5’,6’ of the 3-hydroxy β-rings to yield antheraxanthin (epoxidated at one ring) and then violaxanthin. Violaxanthin can be de-epoxidated into zeaxanthin via antheraxanthin in the xanthophyll cycle to dissipate excess light energy, or converted to neoxanthin, making an end of the β,β-branch of the pathway (Hirschberg, 2001; Zhu et al., 2010; Walter and Strack, 2011).

1.2.5.1 Hydroxylases

The introduction of hydroxyl moieties to α- and β-carotene at the 3,3'-position of ionone rings is carried out by two different types of carotenoid hydroxylase specific for β- or ε-rings with possible crossover (Kim et al., 2009; Kim et al., 2010). The ferredoxin-dependent non-heme di-iron enzymes (BCH type) catalyse the hydroxylation of β-rings and convert β-carotene to β,β-xanthophylls, while the heme-containing cytochrome P450 hydroxylases (CYP97 type) perform the hydroxylation of both β- and ε-rings and convert α-carotene to the β,ε-xanthophyll lutein (Pogson et al., 1996; Sun et al., 1996; Tian and DellaPenna, 2001; Tian et al., 2004; Kim and DellaPenna, 2006).

In most plants, both BCH type and CYP97 type hydroxylases are encoded by gene families. Normally a *CYP97* gene family consists of three lineages (A, B and C) whereas *BCH* genes are in small gene families. BCH type hydroxylases share similarity with the bacteria crtZ and cyanobacteria CrtR-B enzymes that also perform the hydroxylation of β-rings (Tian and DellaPenna, 2004; Galpaz et al., 2006). At least four genes encoding two BCH type hydroxylases and two CYP97 type hydroxylases were found in Arabidopsis: *BCH1*/*AtB1* (At4g25700), *BCH2*/*AtB2* (At5g52570), *CYP97A3*/*LUT5* (At1g31800) and *CYP97C1*/*LUT1* (At3g53130) (Sun et al., 1996; Tian and DellaPenna, 2001; Tian et al., 2004; Kim and DellaPenna, 2006). Interestingly, as indicated by phylogenetic study, *BCH* genes were originated by duplication from a common ancestor after the separation of monocot and dicot, while the origination of *CYP97* lineages happened much earlier, before the green algae and higher plant split point (Kim et al., 2009; Bak et al., 2011). It has hence been proposed that the two branches in the carotenoid pathway synthesizing β,β- and β,ε-xanthophylls evolved independently and the enzymes involved in each branch may be regulated independently as well (Kim and DellaPenna, 2006).

The functions and specificities of the four Arabidopsis hydroxylases have been studied with multiple mutants (Kim et al., 2009; Kim et al., 2010). A quadruple mutant showed albino phenotype and a complete loss of xanthophylls, and the accumulated α- and β-carotenes were only about 10% of the wild-type levels (Kim et al., 2009), suggesting that the four hydroxylases are essential and sufficient for carotenoid biosynthesis in Arabidopsis. Triple mutants with intact CYP97C1 still maintained near normal lutein levels, suggesting that CYP97C1 can effectively catalyse the hydroxylation of both β- and ε-rings of α-carotene (Kim et al., 2009).

Based on analysis of multiple mutants, CYP97A3 is most effective at hydroxylating the β-rings of α-carotene but it also has low activity toward the ε-rings; both CYP97A3 and CYPC1 have limited hydroxylation activity towards the β-rings of β-carotene (Kim et al., 2009). BCH enzymes were found most active in the conversion of β-carotene to β,β-xanthophylls by hydroxylating the β-rings, although they can also hydroxylate the ε- and β-rings of α-carotene with a low activity (Sandmann et al., 2006; Kim et al., 2009). In fruits, seed and flowers which accumulate β,β-xanthophylls, *BCH* genes show differential expression with one isogene predominantly expressed in a certain tissue (Ruiz-Sola and Rodriguez-Concepcion, 2012). One explanation lies in that the differential expression of *BCH* genes facilitates the regulation of xanthophylls biosynthesis in a tissue-specific manner.

A fifth Arabidopsis hydroxylase CYP97B3 (At4g15110) has also been identified and indicated to be phylogenetically related to CYP97A3 and CYP97C1. CYP97B3 showed hydroxylase activity when overexpressed in both *E. coli* and transgenic plants. However, given that CYP97B3 was excluded from the quadruple mutant experiment, the *in vivo* activity of this enzyme may require association with the other hydroxylases, or it may not be functional in carotenoid biosynthesis (Kim et al., 2009; Kim et al., 2010). Future research can be carried out to characterize Arabidopsis CYP97B3-defective mutants to examine the *in vivo* activity of CYP97B3 and address its role in the carotenoid pathway.

Similar to other P450 proteins, all three Arabidopsis CYP97 type hydroxylases possess conservative transmembrane motifs (Chapple, 1998), which suggest them to be membrane-associated enzymes. In agreement with this view, all of them have been detected only in chloroplast envelope membrane fractions (Joyard et al., 2009). These results also support the hypothesis that enzymes involved in carotenoid biosynthesis form protein complexes to coordinate the metabolic flux through the pathway, because many other enzymes in the pathway have also been localized in membranes, as discussed in previous sections in this review. The BCH hydroxylases in Arabidopsis also have four transmembrane helices, suggesting their localization in envelope or thylakoid membranes (Cunningham and Gantt, 1998), but experimental data are yet to be presented to support the deduction.

1.2.5.2 Xanthophyll cycle

While the hydroxylation of α-carotene forms lutein, one of the end-products in carotenogenesis, the hydroxylation of β-carotene produces zeaxanthin that initiates the

xanthophyll cycle (or violaxanthin cycle) protecting photosynthesis apparatus against excessive light energy (Jahns et al., 2009). The xanthophyll cycle is localized in plant thylakoid membranes and it involves several xanthophylls and cofactors (Hager and Holocher, 1994; Gilmore, 1997; Hirschberg, 2001).

The production of violaxanthin, in dark or under light conditions which do not exceed the photosynthesis capacity, is catalysed by zeaxanthin epoxidase (ZEP) in two steps with antheraxanthin as an intermediate. While under these conditions violaxanthin is the major pigment in the xanthophyll cycle, in excessive light it is de-epoxidized by violaxanthin de-epoxidase (VDE) into zeaxanthin that is more effective in the thermal dissipation of excess excitation energy (Demmig-Adams et al., 1996; Cunningham and Gantt, 1998).

The interconversion of zeaxanthin and violaxanthin plays an essential role in adapting plants to different light conditions by flexibly switching between light-harvesting state and dissipative state (Bassi et al., 1993; Hirschberg, 2001). Interestingly, the two enzymes in the xanthophyll cycle are on opposite side of the thylakoid membrane, with VDE on the lumen side and ZEP on the chloroplast stromal side (Demmig-Adams et al., 1996; Hieber et al., 2000; Yamamoto, 2006).

As a monooxgenase, ZEP has been found to require ferredoxin, FAD and NADPH, implicating reduced ferredoxin as the reductant for the epoxidase reaction (Bouvier et al., 1996). In agreement with these results, a FAD-binding domain has also been found in ZEP (Marin et al., 1996). The cDNA of *Zep1*, the first gene encoding ZEP, was cloned from *Nicotiana plumbaginifolia* (ABA-defective mutant *aba2*) and pepper (Bouvier et al., 1996). Characterization of Arabidopsis mutants *npq1* and *npq2* identified *VDE*/*NPQ1* (At1g08550 encoding Arabidopsis VDE) and *ZEP*/*NPQ2*/*ABA1* (At5g67030 encoding Arabidopsis ZEP), respectively (Niyogi et al., 1998; Niyogi, 1999). The *npq1* mutant showed significantly reduced non-photochemical quenching (NPQ) as well as consequently increased photoinhibition. The *npq2* mutant was actually identified in a screening for ABA-deficient mutants and found to constitute a new allele in Arabidopsis mutant *aba1*, where a defective *ZEP* gene was characterized (Niyogi et al., 1998). The characterization of these Arabidopsis mutants and identification of *ZEP* and *VDE* genes have defined the key role that the xanthophyll cycle plays in plant photoprotection.

1.2.5.3 Production of Neoxanthin

Violaxanthin is converted to neoxanthin by neoxanthin synthase (NXS), which represents the final step in the classical carotenoid biosynthesis pathway. Both 9-*cis*-neoxanthin and 9-*cis*-violaxanthin can be cleaved by Nine-*cis*-epoxy-dioxygenase (NCED), products of which can be further modified to form the plant growth regulator ABA (Seo and Koshiba, 2002; Chinnusamy et al., 2008). NCEDs are further discussed in section 1.5. Surprisingly, the first studies trying to identify genes encoding enzymes with NXS activity led to the cloning of genes that were homologous to *LCYB* and *CCS*, which encodes CCS enzyme involved in the production of keto-xanthophylls capsanthin and capsorubin conferring the red colour in pepper fruit chromoplasts (Bouvier et al., 1994).

Another interesting result was that the tomato NXS enzyme turned out to be nearly identical to LCYB2, suggesting the possibility of a bi-functional NXS in tomato. It is possible that NXS can catalyse both the conversion of lycopene to β-carotene and the production of neoxanthin from violaxanthin (Ronen et al., 2000). However, given that neoxanthin is still produced in LCYB2-defective tomato mutants, there should be an independent NXS enzyme (Ronen et al., 2000).

A novel gene encoding ABA4, a chloroplast membrane protein in Arabidopsis, was shown to be involved in neoxanthin synthesis. The *aba4* mutant displayed reduced levels of ABA and was more sensitive to oxidative stress than wild-type leaves, demonstrating the requirement of neoxanthin in ABA biosynthesis (Dall'Osto et al., 2007; North et al., 2007). Although, similar with many other enzymes in Arabidopsis carotenoid biosynthesis, ABA4 was found to be localized in chloroplast envelope membranes. The *ABA4* gene (At1g67080) exhibits different expression patterns when compared to other genes in the carotenoid pathway (Ruiz-Sola and Rodriguez-Concepcion, 2012).

1.2.6 Cross-talk between MEP and carotenoid pathways

As discussed in section 1.2.1 in this review, the channelling of C_5 precursors (prenyl diphosphate) to the carotenoid biosynthesis pathway has been proposed to be under fine regulation to ensure that the building blocks will be supplied when necessary. In accordance to this view, cross-talk between the MEP pathway and the carotenoid pathway has been suggested by recent studies.

Tomato PSY1 had been deemed as the only rate-limiting enzyme in fruit carotenogenesis, until

results suggested that DXS from the MEP pathway possibly catalysed the first regulatory step in carotenoid biosynthesis during tomato fruit ripening, and that an active cross-talk might exist between DXS and PSY to efficiently tune up carotenoid accumulation in the fruits (Lois et al., 2000). In agreement with the above observations, overexpression of Arabidopsis DXS and HDR, the key flux-controlling enzymes in the MEP pathway, up-regulated carotenoid biosynthesis in light-grown photosynthetic tissues. However, increased carotenoid levels were not seen in etiolated tissues (Botella-Pavia et al., 2004; Rodriguez-Villalon et al., 2009a), probably because the expression and activity of PSY in dark-grown seedlings are suppressed as reported in another study (Toledo-Ortiz et al., 2010).

Overexpression of *PSY* in photosynthetic tissues led to unexpected dwarf phenotypes and reduced carotenoid levels, possibly due to lack of other isoprenoids including the gibberellins resulting from a depleted GGPP pool (Fray et al., 1995) (Also described in section 1.2.2). Taken together, coordination between the MEP pathway and the carotenoid pathway can deliver balanced precursor supply to carotenoid biosynthesis and problems may arise if the cross-talk is 'broken'.

In plants such as Arabidopsis (Botella-Pavia et al., 2004; Wille et al., 2004), tomato (Lois et al., 2000) and pepper (Bouvier et al., 1998b), evidence has shown a close regulatory connection between key genes in MEP pathway and carotenoid pathway, particularly those at rate-limiting/flux-controlling steps. As an example, the expression of Arabidopsis MEP pathway genes *DXS* and *HDR* was suggested to coordinate the induction of *PSY* triggered by illumination during the deetiolation process (von Lintig et al., 1997; Botella-Pavia et al., 2004).

Consistently, in another study on phytochrome-mediated light signals regulating the expression of *PSY* in Arabidopsis, PIF1, the transcription factor that directly binds to the promoter of *PSY* gene to repress its transcription in etiolated seedlings, was shown to be degraded after interaction with photoactivated phytochromes (PHY), leading to a rapid increase of *PSY* transcription level and a burst in the production of carotenoids to meet the requirements in chloroplast development upon exposure to light (Castillon et al., 2007; Toledo-Ortiz et al., 2010). PIFs also bind to *DXS* promoter and repress its transcription (Leivar et al., 2009; Toledo-Ortiz et al., 2010). In the above studies, the derepression of *DXS* was also observed along with that of *PSY*, although *DXS* promoter lacks the G-box motif which has been found in *PSY* promoter as a binding site of PIF1 (Leivar et al., 2009; Toledo-Ortiz et al., 2010).

In addition to transcription level, increased PSY activity during deetiolation was found to stimulate the accumulation of DXS enzyme at post-transcriptional level via metabolite feedback (Guevara-Garcia et al., 2005). However, the metabolites that are involved in the feedback remain to be identified. On the other hand, elevated level of DXP (the product of DXS enzyme) appears to be correlated with up-regulated *PSY* gene expression and PSY enzyme activity (to a lower extent) in tomato fruit (Lois et al., 2000; Rodriguez-Concepcion et al., 2001).

As a summary, the cross-talk between MEP and carotenoid pathways rely on the coordination at transcriptional level and post-transcriptional feedback mechanisms. The cross-talk occurs to not only ensure an appropriate supply of prenyl diphosphate precursors for carotenoid biosynthesis at different developmental stages, but also maintain an efficient entry of the precursors to carotenoid pathway.

1.3 Localization of the carotenoid biosynthetic metabolon

In plant, carotenoid biosynthesis occurs on plastid membranes and the pathway enzymes are encoded by nuclear genes (Cuttriss et al., 2011). The enzymes involved in the carotenoid pathway have been proposed to form a metabolon that holds multiple coordinating enzymes together by noncovalent interactions and channels the intermediary products through enzyme complex(es) along the pathway (Bassard et al., 2012; Quinlan et al., 2012; Shumskaya and Wurtzel, 2013). In agreement with this view, carotenoid pathway intermediates have been found largely absent (Wurtzel, 2004; Quinlan et al., 2012), and enzyme complexes with high molecular weights containing carotenoid biosynthesis enzymes have been identified from plastids (Al-Babili et al., 1996; Bonk et al., 1997; Cunningham and Gantt, 1998; Lopez et al., 2008a). The formation of metabolon results in interactions between enzymes and may affect their activities and localization. However, little is known about the localization and regulation of this dynamic metabolon, the carotenoid biosynthetic machinery.

1.3.1 Where is the key enzyme PSY localized?

PSY catalyses the entry point of GGPP to carotenoid pathway, and hence acts as the head of a proposed enzyme metabolon. Though the only Arabidopsis PSY enzyme and rice PSY isoforms are found to localize to plastoglobuli (Shumskaya et al., 2012; Shumskaya and Wurtzel, 2013) attached to thylakoids (in chloroplast) (Austin et al., 2006), not all PSYs localize identically. Additionally, details of plastoglobular association in nonphotosynthetic plastids have

remained unclear. Maize PSY1 isozyme differs from others in that its physical localization can be altered and depends on its allelic variant (Shumskaya et al., 2012).

Sequence alignment showed that maize PSY1 had an Asn168 compared with a Serine of other PSYs at the same position, and a Thr257 that is occupied by a Proline in other PSYs (Shumskaya et al., 2012). The molecular basis of the unique dual localization of maize PSY1 to stroma or attached to membranes is thus reflected by sequence difference. A T257P mutation in maize PSY1 strikingly altered it localization by forming unusual spikes that stretched chloroplasts and caused a morphological change from round elliptical to diamond with sharp corners where spikes touched envelope membrane. A second N168S mutation restored the stroma localization of the progenitor PSY1. The altered localization of the T257P mutant and morphological change of chloroplasts were suggested to result from increased activity of PSY1, because the mutated enzyme was located in fibrillar plastoglobuli which is formed when the concentrations of carotenoids are high (Shumskaya et al., 2012). The introduction of a second D285E mutation to the T257P mutant of PSY1 inactivated the enzyme and restored its stromal localization (Shumskaya et al., 2012). An interesting hypothesis based on this study is that, by forming different types of plastoglobuli, fibrillar or globular, PSY1 isoforms may direct carotenogenesis to different plastid compartments.

1.3.2 Enzyme metabolon: localization and regulation

Answering some questions on PSY localization has opened more questions on where and how the entire carotenoid pathway is reconstituted.

In Arabidopsis chloroplasts, only a few enzymes in carotenoid biosynthesis are found in thylakoids, while most others, if not all (because localization of some enzymes are undetermined), are identified in envelope membranes (Joyard et al., 2009). If the metabolon is localized on envelope membranes, how are carotenoids delivered to thylakoids to play important roles in photosynthesis and photoprotection? Could the pathway be carried out on two sites: envelope and thylakoids, with two independent metabolons producing carotenoids possessing different biological functions? If there is a metabolon on thylakoids, why are many carotenogenesis enzymes missing from, or undetectable in this structure? The distinctive localization of most PSYs on plastoglobuli attached to thylakoids suggests that PSY may be physically separated from the remainder of the pathway. If so, how is PSY recruited to form a

complete pathway?

The dynamically localized maize PSY1, either being soluble in stroma or attaching to carotenoid crystals that can touch membranes (Shumskaya et al., 2012), may suggest a dynamic assembly of the metabolon, recruiting carotenoid enzymes as needed to meet dynamic requirements in a living cell. In a dynamic fashion, localization of all carotenoid enzymes on one site would not be necessary. Or maybe the putative metabolon consists of a few enzyme complexes to coordinate carotenoid biosynthesis. Associated questions would be on the trafficking of carotenoids. If there are more than one enzyme complexes in the metabolon, transporters for metabolic intermediates are yet to be described. Although envelope localized carotenoid pathway can supply substrates for ABA synthesis, part of which happens outside of plastid (Cutler et al., 2010), carotenoids need to be transferred to thylakoids by a certain mechanism, probably via vesicular transport.

While many carotenoid enzymes are localized to the envelope in chloroplasts, these enzymes are observed in plastoglobuli in chromoplasts, the plastid mainly sequesters carotenoids. Chromoplast carotenoids may hence be synthesized in plastoglobuli rather than being formed elsewhere and sequestered in plastoglobuli. How is the carotenoid pathway reconstituted in plastoglobuli? If there is a different metabolon in chromoplast recruiting carotenoid enzymes via different mechanisms, what happens to these enzymes during chloroplast to chromoplast transition? Because plastids are dynamic organelles that alter their structures and metabolism under developmental regulations (Egea et al., 2011), the re-assembly and re-localization of the carotenoid metabolon would be inevitable, if this putative carotenoid biosynthesis machinery actually exists.

1.4 Regulation of carotenoid biosynthesis

Despite the many in-depth studies on plant carotenoid biosynthesis, it has been a challenge to gain a clear insight into the mechanisms by which this pathway is regulated. The regulation of carotenoid biosynthesis is carried out in response to various development requirements and environmental stimuli. Here I review the progress on the regulation of carotenoid pathway at both transcriptional and post-transcriptional levels.

1.4.1 Carotenogenic gene transcription

Controlling the transcription of genes is the first level of regulation of carotenoid biosynthesis. The transcriptional regulation of caroteogenetic genes, MEP pathway gene and *GGPPS* (see sections 1.2.1 and 1.2.2) are correlated to dynamically maintaining a proper metabolite flux in response to developmental and environmental stimuli. In this section, I will focus on the roles of light signalling, developmental signals and epigenetic regulation in modulating carotenoid biosynthesis in Arabidopsis and other systems such as ripening tomato fruit. Transcriptional regulation of carotenoid genes by other yet-to-be-identified developmental or environmental factors, for example the reduction of LCYE mRNA abundance in tetra-*cis*-lycopene accumulating Arabidopsis plants (Cuttriss et al., 2007), is not reviewed here.

1.4.1.1 Light signalling

In this section, I review the regulation of carotenoid biosynthesis by multiple light signalling factors, while in chapters 3, 4 and 5, I study the regulation of plastid development by carotenoid-derived retrograde signals via light signalling factors.

Studies on the regulation of carotenoid biosynthesis in photosynthetic and nonphotosynthetic tissues have revealed that light plays predominant roles in the induction of carotenogenic gene expression during deetiolation and the development of fruits and flowers (Romer and Fraser, 2005; Howitt and Pogson, 2006). The light signal is transduced to chemical signal by photoreceptors, chromoproteins that participate in the regulation of carotenoid pathway genes, particularly at transcription level (Pizarro and Stange, 2009). This section will mainly discuss the regulatory functions of light on carotenoid biosynthesis in photosynthetic tissues.

When plant seeds germinate in dark, phoptomorphogenesis is repressed and the seedlings are etiolated. The cotyledons of etiolated seedlings contain etioplasts instead of chloroplasts, and carotenoids are localized in PLB, a lattice of tubular membranes that defines etioplasts (Park et al., 2002; Cuttriss et al., 2007). Upon exposure to light, plant seedlings deetiolate with etioplasts differentiating into chloroplasts and a burst of carotenoid biosynthesis in chloroplasts to facilitate photosynthetic development (Romer and Fraser, 2005).

As reviewed in section 1.2.6, expression of Arabidopsis carotenoid pathway genes and MEP pathways genes, especially rate-determining genes such as *PSY* and *DXS*, is up-regulated with high correlation during the deetiolation process after illumination (von Lintig et al., 1997;

Botella-Pavia et al., 2004; Ghassemian et al., 2006; Castillon et al., 2007; Toledo-Ortiz et al., 2010; Meier et al., 2011). Besides these two key genes, the transcription of *LCYB* was shown to increase by 5-fold when Arabidopsis and tomato seedlings were transferred from low light to high light (Hirschberg, 2001). In maize, the up-regulation of *PSY2* gene expression during deetiolation was suggested to depend on phytochromes (phys), a family of photoreceptors. (Li et al., 2008a). While the transcription of maize *LCYB* and *VDE* can also be induced by red light illumination, the transcription of ZEP appeared to remain at a similar level, suggesting that the expression of carotenoid genes is dependent on the functions of phys and cryptochromes (CRYs) (Woitsch and Romer, 2003). In tobacco, the induction of carotenoid gene expression was also found to involve different photoreceptors (Woitsch and Romer, 2003).

Photoreceptors include the phytochrome family (phy A – phy E), the CRY family and the phototropins. The phy family absorbs red and far-red light, whereas the CRYs and the phototropins absorb blue and UV light (Briggs and Olney, 2001; Franklin et al., 2005; Briggs et al., 2007). Phys have been the best studied photoreceptors. The signalling induced by phys requires transcription factors such as HY5 (Elongated Hypocotyl 5), LAF1 (Long After Far-Red Light 1) and PIF (Phytochrome-Interacting Factor) (Chattopadhyay et al., 1998; Ballesteros et al., 2001; Tepperman et al., 2001; Al-Sady et al., 2006; Leivar and Quail, 2011).

HY5 is a bZIP-containing transcription activator (Basic Leucine Zipper Domain, bZIP) that binds to red, far-red, blue and white light responsive elements (LREs) (Yadav et al., 2002; Pizarro and Stange, 2009). In Arabidopsis, the photoreceptor phy A promotes the binding of HY5 to the LREs in *PSY* gene promoter, and consequently elevates its transcription (von Lintig et al., 1997). Consistently, the suppression of tomato *HY5* gene expression by RNAi (or antisense RNA) also led to significant reduction of carotenoid and chlorophyll levels in leaf and fruit (Liu et al., 2004). The LREs bound by HY5 possess ATCTA box and G-boxes; other light-responsive promoters can also have a Z-box (ATCTATTCGTATACGTGTCAC) that can be activated by phys and/or CRY1 (Yadav et al., 2002; Welsch et al., 2003; Botella-Pavia et al., 2004).

Unlike HY5, the PIF family proteins are transcription repressors containing basic helix-loop-helix (bHLH) motifs (Castillon et al., 2007; Bae and Choi, 2008; Leivar and Quail, 2011). Besides the function of PIF1 in the regulation of *PSY* gene expression, some members among PIF1, PIF3, PIF4 and PIF5 also coordinate carotenoid and chlorophyll biosynthesis with chloroplast

development during deetiolation. This was indicated by an up-regulation of transcription of the genes involved in the differentiation of chloroplasts and chlorophyll biosynthesis as well as carotenogenesis (Leivar et al., 2009; Stephenson et al., 2009; Toledo-Ortiz et al., 2010).

Accumulation of the PIF family proteins in etiolated seedlings has also been observed (Leivar et al., 2008; Shen et al., 2008; Shin et al., 2009). Actually, PIF proteins including PIF1 were found to repress *PSY* gene transcription and carotenoid biosynthesis even in deetiolated Arabidopsis plants (Toledo-Ortiz et al., 2010), suggesting a 'life-long' regulation of carotenoid genes at the transcriptional level. Because a *PSY* gene with a truncated promoter lack G-boxes is still up-regulated during deetiolation (Welsch et al., 2003), there may be other transcription factors besides PIFs which carry out the light-responsive regulation of *PSY* and other genes. Another explanation would be that PIFs also bind to motifs other than G-boxes in the promoter area of carotenoid genes including *PSY* and *DXS*. This is discussed in section 1.2.6.

COP1, a RING motif–containing E3 ligase that promotes the ubiquitin-mediated proteolysis, has been suggested to be another negative regulator of light-mediated gene expression (Saijo et al., 2003; Seo et al., 2003; Sullivan and Deng, 2003). In dark, Arabidopsis COP1 interacts with transcription factors such as HY5 and LAF1, triggering their degradation via the 26S proteasome, and thus represses the expression of carotenoid genes (Holm et al., 2002; Seo et al., 2003; Yanagawa et al., 2004). Upon the exposure of plants to light, CRY and phy proteins were found to bind and consequently inactivate COP1 by direct interaction causing conformational changes, followed by the release of transcription factors including HY5 and LAF1 (Wang et al., 2001; Cashmore, 2003). In tomato, RNAi induced gene slicing of *COP1* showed elevated accumulation of carotenoids (Liu et al., 2004). The dark-grown Arabidopsis seedlings with impaired *COP1* gene or treated with paclobutrazol (PAC, an inhibitor of gibberellin biosynthesis) showed a partially deetiolated phenotype and higher total carotenoid levels compared to wild-type plants, which was accompanied by up-regulated *PSY* gene expression and enhanced PSY enzyme activity, suggesting the involvement of COP1 in the regulation of carotenogenesis (Rodriguez-Villalon et al., 2009a, b).

In Arabidopsis, another two repressors of photomorphogenesis, the deetiolated-1 (DET1) and UV-damaged DNA binding protein 1 (DDB1), can form a complex and interact with COP1. The formation of the complex can promote the ubiquitination of transcription factors and down-regulate carotenoid biosynthesis (Schroeder et al., 2002; Lau and Deng, 2012). Recent

research has also indicated that DET1 and DDB1 forms complex with the ubiquitin-conjugating enzyme variant COP10, and the so called CDD (COP10-DET1-DDB1) complex physically interacts with COP1, promoting degradation of positive transcription factors such as HY5 to repress photomorphogenesis (Yanagawa et al., 2004; Lau et al., 2011). In tomato *high pigment* (*hp*) mutants that accumulate enhanced levels of carotenoids in fruits, the *hp1* mutation is located in *DDB1* (Azari et al., 2010) and *hp2* mutation in *DET1* (Davuluri et al., 2005), both of which have been found to regulate light-mediated plastid development (Benvenuto et al., 2002).

1.4.1.2 Developmental signals

Carotenoid biosynthesis is dynamically regulated throughout the plant life cycle by developmental signals and in response to external environmental stimuli (Cazzonelli and Pogson, 2010). Photomorphogenesis, regulated by light signal that is discussed in section 1.4.1.1, is also a developmental process. In this section, other developmental signals controlling carotenoid profile in fruit, flower and seed are discussed.

In most plants, carotenoid composition and its regulation during fruit and flower development are distinct from that arising in vegetative tissue (Hirschberg, 2001; Sandmann et al., 2006). The changes in carotenoid composition during ripening are predominantly controlled via the regulation of transcription of carotenoid genes (Giovannoni, 2001). An increased transcription of MEP pathway key gene *DXS*, followed by that of *PSY*, *PDS* and other genes encoding desaturases and isomerases in the carotenoid pathway, were observed during the ripening process, resulting in a burst of carotenoid biosynthesis (Pecker et al., 1992; Corona et al., 1996; Bramley, 1997; Lois et al., 2000) .

Interestingly, the expression of cyclase genes *LCYB* and *LCYE* was shown to diminish simultaneously (Ronen et al., 1999). The differential gene expression in carotenoid biosynthesis hence lead to an increased flux through the initial stages of the pathway and a restriction to end products, which results in a massive accumulation of lycopene while xanthophylls are eliminated (Giuliano et al., 1993; Fraser et al., 1994; Pecker et al., 1996; Alba et al., 2005). In accordance to this view, the tomato mutant *delta* accumulates δ-carotene in the fruit due to an increased transcription of *LCYE* (Ronen et al., 1999), while the observed accumulation of β-carotene in another mutant *beta* is caused by an up-regulation of the expression of *LCYB2* (Ronen et al., 2000). Tomato *LCYB2* promoter has *cis*-elements such as

RAP2.2 and ERE (ethylene responsive element) to which transcription factors can bind and trigger regulation of carotenoid accumulation in fruits and flowers (Dalal et al., 2010), though these transcription factors and the up-stream signalling pathway are yet to be defined. A similar differential expression pattern of carotenoid genes during fruit development has been observed in satsuma mandarin (*Citrus unshiu* Marc) (Ikoma et al., 2001) and pepper (Kuntz et al., 1992; Romer et al., 1993; Bouvier et al., 1996; Bouvier et al., 1998b).

In flower development, transcriptional control of carotenoid pathway genes has also been suggested as the key mechanism in regulating carotenoid biosynthesis (Schledz et al., 1996; Ronen et al., 1999; Mann et al., 2000; Moehs et al., 2001). Lutein and lutein fatty acid esters are the major carotenoids found in marigold petals, the content of which varies between varieties resulting in light yellow to dark orange colours of flowers (Moehs et al., 2001). The abundance of *PSY* and *DXS* transcripts was found to correlate positively with lutein levels in marigold petals. It was reported that the expression of *LCYE* gene was significantly induced during marigold flower development while that of *LCYB* gene was unchanged, suggesting that the transcriptional levels of *LCYE* gene, probably as well as enzyme activity, control the flux through the β,ε-branch of the carotenoid pathway to convert lycopene into lutein (Moehs et al., 2001).

In Arabidopsis, low levels of lutein and β,β-xanthophylls were observed in etioplasts in dry seeds, and consistently an efficient conversion of β-carotene into β,β-xanthophylls (possibly followed by the formation of ABA) was also detected. This can be explained by results from the analysis of microarray-based gene expression databases, which indicated high levels of *BCH2* and *BCH1* transcripts in mature Arabidopsis seeds. Unlike tomato, the transcriptional regulation of carotenoid pathway genes in Arabidopsis has largely remained to be described. Although an increased carotenoid biosynthesis was observed in etioplasts after Arabidopsis seed germination in dark (Park et al., 2002; Ghassemian et al., 2006; Rodriguez-Villalon et al., 2009a), no molecular mechanism has been reported regarding the regulation of carotenoid expression in this process.

1.4.1.3 Epigenetic regulation

The epigenetic regulation of a carotenoid pathway gene, *CRTISO*, has been reported in Arabidopsis. The characterization of the *ccr1* (*carotenoid and chloroplast regulatory 1*) mutant revealed a gene encoding histone methyltransferase (SET DOMAIN GROUP 8, SDG8) that

methylates histone H3 on Lys4/36 (H3K4/36). Similar to *ccr2*, *ccr1* also has reduced lutein in leaves and accumulated *cis*-carotenoids in etiolated seedlings, which is correlated with the reduction in *CRTISO* transcript abundance. The suppressed expression of *CRTISO* has been suggested to result from an altered methylation status of the chromosome surrounding this gene, which is due to the absence of SDG8 activity in *ccr1* (Cazzonelli et al., 2009b). The changed carotenoid profile in *ccr1* and *ccr2* has been proposed to cause increased shoot branching, possibly by the reduced carotenoid substrates for strigolactone biosynthesis, which links carotenoid pathway to the regulation of plant development (Cazzonelli and Pogson, 2010).

1.4.2 Post-transcriptional regulation

The regulation of carotenoid biosynthesis also happens at post-transcriptional levels. In many cases including some transgenic plants, the profile of carotenoid gene expression does not correlate with carotenoid accumulation; post-transcriptional regulation can explain many of these results. In this section, I review the regulation of carotenoid composition via modulating enzyme activities and through storage and degradation of carotenoids.

1.4.2.1 Enzyme activities and levels

Post-transcriptional regulation has been observed in carotenoid and MEP pathways in many plants. A few examples have been discussed under other topics in this review, and are summarized as following.

During deetiolation, increased PSY activity initiates metabolite feedback and leads to the accumulation of DXS enzyme at post-transcriptional level (section 1.2.6). Substrate specificities of hydroxylases in the carotenoid pathway along with differential expression of isogenes likely lead to tissue-specific accumulation of xanthophylls (section 1.2.5.1). Most enzymes in carotenoid biosynthesis are membrane-associated and the localization of carotenoid enzymes is at least one of essential factors that determine their activities (section 1.2 and 1.3). The presence of a metabolon or large enzyme complexes may also affect enzyme activities by protein-protein interaction, and modulate enzyme activities in a source-regulation fashion by metabolite channelling (section 1.3).

There are many other examples in the regulation of carotenoid biosynthetic enzyme activities. Reportedly PSY and OR family proteins including AtOR and AtOR-like, interact directly with

each other in plastids. OR proteins were shown to be major post-transcriptional regulators of PSY; overexpression of AtOR increases the protein level of enzymatically active PSY whereas *ator atro-like* double mutant exhibits significant reduction of PSY. Interestingly, a mutual regulation exists between PSY and OR proteins as altered PSY expression also changes AtOR protein levels (Zhou et al., 2015). In addition, plastid enzyme GGPP synthase 11 (GGPPS11) physically interacts with enzymes that use GGPP to produce carotenoids and chlorophylls, including PSY (Ruiz-Sola et al., 2016). This is consistent with the existence of a metabolon that contains GGPPS and PSY in chromoplasts producing carotenoid at high levels (Camara, 1993; Fraser et al., 2000). All desaturases and isomerases in carotenoid biosynthesis, LCYB, LCYE and ZEP possess a conserved flavin-binding motif (Marin et al., 1996; Isaacson et al., 2004; Sandmann, 2009; Yu et al., 2010; Yu et al., 2011; Schaub et al., 2012), suggesting an essential role of redox balance in the activities of these enzymes. In particular, the two desaturases, PDS and ZDS, require oxidized plastoquinone as an electron carrier for enzymatic reactions (Norris et al., 1995), which suggests that their activity is connected to photosynthetic electron transport chain which is localized on thylakoid membranes. From another angle, this also reflects the importance of membrane-association to the activities of carotenoid pathway enzymes. The MEP pathway enzymes DXR and HDR were both found to be thioredoxin targets (Balmer et al., 2003; Wong et al., 2003; Lemaire et al., 2004), suggesting the activities of the two enzymes to be also redox-regulated, because thioredoxins are small redox proteins reduced in chloroplasts by ferredoxin-thoiredoxin reductase, consequently up-regulating target proteins through reducing specific disulfide groups (Buchanan et al., 2002).

Another interesting example of the regulation of enzyme activity in carotenoid biosynthesis is the modulation of xanthophyll cycle enzymes, ZEP and VDE. ZEP is localized on the chloroplast stromal side of thylakoid membrane while VDE on the lumen side (Demmig-Adams et al., 1996; Hieber et al., 2000; Yamamoto, 2006). ZEP functions the best at neutral pH which is observed in dark or under low light, whereas VDE is in the lumen at such pH, being soluble but inactive. Under high light, the proton flow driven into the lumen by photosynthetic proton pump reduces the pH. As a result, VDE binds to thylakoid membrane from lumen side, being activated and converting violaxanthin into zeaxanthin which protects photosynthetic apparatus by dissipating excess light energy (Hieber et al., 2000; Yamamoto, 2006; Li et al., 2009b).

During daffodil flower development, carotenoid production is significantly increased, but interestingly the transcription of *PSY* gene is decreased from flower stage 1 to stage 4 (Al-Babili et al., 1996; Schledz et al., 1996). However, the protein level of PSY and PDS is elevated during stage 1 and 2 (Al-Babili et al., 1996; Schledz et al., 1996). These results indicate a post-transcriptional regulation mechanism in daffodil flower development.

Moreover, not all PSY and PDS enzyme molecules are associated with membrane and thus active (Al-Babili et al., 1996; Schledz et al., 1996). The presence of soluble and inactivated forms of PSY and PDS suggests a more complicated post-transcriptional regulation in carotenoid biosynthesis during daffodil flower development. The formation of metabolon in chromoplast, probably on the membrane, is essential for carotenogenesis during flower development. Given that all the carotenoid enzymes are encoded by nuclear genes, understanding how the proteins are imported into the chromoplast and assembled into large enzyme complexes will certainly contribute to elucidating the regulation of carotenoid pathway at post-transcriptional level. A strong up-regulation of chaperone proteins Hsp70 and Cpn60 in chromoplasts was observed during this process (Bonk et al., 1996), which may facilitate the correct folding of the imported proteins and their assembly into active enzyme complexes.

Despite many studies proposing a feedback/forward-feed mechanism of transcriptional and/or post-transcriptional regulation of carotenogenic genes by phytoene, lycopene, *cis*-carotenes including tri-*cis*-neurosporene, tetra-*cis*-lycopene and other metabolites (Schaub et al., 2005; Cuttriss et al., 2007; Qin et al., 2007; Bai et al., 2009; Cazzonelli et al., 2010; Kachanovsky et al., 2012), solid evidence is yet to be presented for a complete elucidation of the mechanisms.

1.4.2.2 Storage and degradation

The regulatory mechanisms discussed so far belong to ‘source regulation’, whereas mechanisms such as sequestration and storage, belonging to ‘sink regulation’, are also plausible. The biogenesis of a plastid defines its type, and thus profoundly affects the accumulation of carotenoid in the plastid by determining its storage capacity.

In chloroplasts, carotenoids are localized in photosynthetic apparatuses in membrane, while in chromoplasts the storage of carotenoids (normally with esterification) is achieved by their association with specified lipoprotein structures containing proteins known as fibrillins

(Vishnevetsky et al., 1999a; Vishnevetsky et al., 1999b). The formation of carotenoid-lipoprotein complexes relies on the hydrophobic nature of carotenoids, which confers them a much higher stability when associated with lipoproteins than in chloroplast membranes (Merzlyak and Solovchenko, 2002). The fibrillin-carotenoid conjugates form plastoglobuli that consists of a layer polar lipid and protein covering non-polar components (15 - 25% carotenoids) in the center, or fibrillar, tubular, membranous even crystalline structures that contains pure carotenoid crystals in chromoplasts (Deruere et al., 1994; Vishnevetsky et al., 1999a).

Studies have identified specific fibrillins, namely chromoplast protein C (CHRC) and chromoplast protein D (CHRD). The 35-kD CHRC, found in cucumber (*Cucumis sativus*) flowers, is abundant in flowers but absent in chloroplasts and its expression is greatly induced by gibberellin GA_3 (Smirra et al., 1993; Vainstein et al., 1994; Vishnevetsky et al., 1997). The 14-kD CHRD demonstrates similar expression and localization profiles and hormone response (LibalWeksler et al., 1997). A suppression of *CHRC* expression by RNAi in tomato reduced carotenoid accumulation by 30%, suggesting the dependence of carotenoid sequestration on fibrillins (Leitner-Dagan et al., 2006a; Leitner-Dagan et al., 2006b); vice versa, inhibition of carotenoid biosynthesis affects the expression of *CHRC* and *CHRD* at both transcriptional and post-transcriptional levels (Vishnevetsky et al., 1999b).

Taken together, the storage of carotenoids relies on the type of plastids and specific plastidial structures for sequestration. In *PSY*-overexpressing Arabidopsis lines, despite enhanced expression of *PSY* in all tissues, the carotenoid levels in chloroplasts of photosynthetic tissues remained almost the same as in wild type plants, whereas that in nonphosynthetic tissue (seed-derived calli) was increased by up to 100-fold (Maass et al., 2009). These results support the view that the type of plastids determines the capacity of carotenoid storage.

Other determinants of carotenoid storage are the size and replication (number) of plastids. In support of this view, a cauliflower (*Brassica oleracea* var. *botrytis*) mutant o*r* was found to abnormally accumulate carotenoid, particularly β-carotene, resulting in an orange color in the edible tissue that is normally white (Li et al., 2001; Lu et al., 2006). Mutant *or* showed no increase in carotenoid biosynthesis but rather it developed chromoplast-like plastids that contain membranous compartments instead of leucoplasts (Paolillo et al., 2004). Most interestingly, plastid division was remarkably arrested in the *or* mutant and few or only single

plastid was seen in affected cells (Lu et al., 2006).

The *OR* gene encodes a DnaJ-like protein which possibly acts as a co-chaperone that targets substrates to DnaK/Hsp70 for proper folding and assembly (Paolillo et al., 2004; Lu et al., 2006). DnaJ-type proteins possess conserved Cys-rich domains, and a member of them was also found to participate in plastid division (Giuliano and Diretto, 2007). Consistently, Hsp21, another chaperone protein from tomato, was also found to promote chloroplast to chromoplast transition, in turn resulting in the accumulation of carotenoid (Neta-Sharir et al., 2005). The protein-protein interaction between PSY and OR is studied in chapter 5.

In the tomato *high pigment* mutants *hp1* and *hp2* that have been briefly discussed in section 1.4.1.1, striking accumulation of carotenoids was observed, likely due to elevated plastid biogenesis (Liu et al., 2004; Davuluri et al., 2005; Kolotilin et al., 2007; Azari et al., 2010). The *DDB1* gene that is mutated in *hp1* (Azari et al., 2010), and the *DET1* gene mutated in *hp2* (Davuluri et al., 2005), are both involved in light-mediated regulation of carotenogenesis and plastid biogenesis (Benvenuto et al., 2002). However, no increase in carotenoid gene expression was observed in tomato lines with suppressed *DET1* expression, instead the size and/or number of plastids were elevated (Kolotilin et al., 2007). Similarly, the tomato *hp3* mutant has a defective *ZEP* gene that is involved in xanthophyll cycle and also linked to ABA biosynthesis, conferring an enhancement of carotenoid accumulation by increasing both plastid numbers and the size of plastid compartment; strongly reduced ABA production was also observed in this mutant (Galpaz et al., 2008).

Although the mechanisms of carotenoid homeostasis are poorly understood, it has been proposed that the steady-state levels of carotenoids are determined by the rate of biosynthesis, storage capacity and their degradation. The rate of carotenoid degradation was assumed to be slow, as the yellow-orange carotenoids in senescing autumn leaves normally last long. However, data using $^{14}CO_2$ pulse-chase labeling showed that the degradation rate of carotenoids in Arabidopsis was much higher than expected (Beisel et al., 2010). Non-enzymatic oxidation and enzymatic cleavage might both contribute to the turnover of carotenoids, but the enzymatic cleavage of carotenoids may only break down a very minor portion of the carotenoid pool, as suggested by a much higher (several orders of magnitudes) rate of photooxidative loss of β-carotene and xanthophylls than the rate of ABA biosynthesis via the cleavage of violaxanthin and neoxanthin by NCED (Simkin et al., 2003; Beisel et al.,

2010).

Members of the CCD family have different substrate preference, and have been proposed to contribute to carotenoid degradation by enzymatic cleavage in nonphotosynthetic tissues of plants including maize and potato (Campbell et al., 2010; Vallabhaneni et al., 2010). However, in general the expression profile of CCD family enzymes has a better correlation with apocarotenoid biosynthesis than with the degradation of carotenoids (Walter and Strack, 2011). The roles of CCDs and NCEDs in the production of apocarotenoids are discussed in detail in section 1.5.

To summarize, conflicting results thus far still discourage the proposed contribution of CCDs to the homeostasis of carotenoids. Apart from CCDs that cleave carotenoids with specificity, lipoxygenases and peroxidases can nonspecifically break down carotenoid by oxidative degradation (Leenhardt et al., 2006b). Furthermore, nonenzymatic degradation of carotenoids, including photochemical damage and degradation under other oxidative stresses, would also contribute to carotenoid homeostasis, though how this is balanced with carotenoid biosynthesis and storage remains completely unclear.

1.5 Synthesis and function of apocarotenoid signals in plants

Section 1.5 has been published as a review paper (Hou et al., 2016) and is inserted "as is" in this chapter.

Carotenoids are not the end-products of the pathway: apocarotenoids are produced by CCDs or non-enzymatic processes. Apocarotenoids are more soluble or volatile than carotenoids, but they are not simply breakdown products as there can be modifications post cleavage and functions include hormones, volatiles or signals. Evidence is emerging for a class of apocarotenoids herein referred to as Apocarotenoid Signals (ACSs) that have regulatory roles throughout plant development beyond those ascribed to ABA and strigolactone. In this context, we review studies of carotenoid feedback regulation, chloroplast biogenesis, stress signalling, and leaf and root development, which provides evidence that apocarotenoids may fine-tune plant development and responses to environmental stimuli.

1.5.1 Carotenoid cleavage products play regulatory roles in plants

Enzymatic and non-enzymatic oxidative cleavage of carotenoids produces biologically-

important carotenoid derivatives, apocarotenoids. CCD enzymes catalyse carotenoid cleavage at specific double bonds (Walter and Strack, 2011). Non-enzymatic apocarotenoid formation can occur via singlet oxygen ($^1O_2$) attack, primarily on β-carotene (Havaux, 2014). Regardless of metabolic origin, apocarotenoids help fine-tune carotenogenesis, plant development and environmental responses, in part *via* changes in nuclear gene expression, and retrograde (plastid-to-nucleus) signaling (Pogson et al., 2008). Apocarotenoids have also been shown to inhibit mammalian cancer cell proliferation by altering gene expression (Sharoni et al., 2012). Thus, the discovery and characterization of novel carotenoid derivatives *in planta* provide new opportunities for plant development research. Here we review recent studies of carotenoid catabolism and discuss how apocarotenoids may regulate plant development.

1.5.2 Apocarotenoid biosynthesis: enzymatic and non-enzymatic processes

The CCDs are an evolutionarily-conserved family of non-heme, iron-dependent enzymes that catalyse carotenoid oxidative cleavage (Harrison and Bugg, 2014). CCDs typically act by incorporating oxygen atoms between adjacent carbon atoms along the conjugated carotenoid backbone. Some CCD cleavage reactions require isomerization to form substrate isomers favourable for cleavage (McQuinn et al., 2015). In *Arabidopsis* there are nine CCDs categorised according to their enzymatic specificities, and they determine CCD nomenclature in other species. Five CCD members are in the nine-*cis*-epoxy carotenoid dioxygenase subfamily (NCED2, NCED3, NCED5, NCED6, NCED9); and participate in ABA synthesis (Tan et al., 2003). NCEDs have been extensively reviewed (Nambara and Marion-Poll, 2005) and will not be discussed further here. CCD1, CCD4 and CCD7 have broad substrate specificity, whilst CCD8 may be specific for strigolactone synthesis (Figure 1.3) (Alder et al., 2012). One additional CCD subfamily, dubbed 'CCD2' (and not to be confused with NCED2), has also been identified in *Crocus sativus*; it produces saffron flavour and fragrance apocarotenoids (Frusciante et al., 2014).

The roles and specificities of CCDs have long been debated. Our understanding of CCDs comes mostly from *in vitro* enzymatic assays, and "*in bacterio*" heterologous expression analysis using *Escherichia coli* engineered to accumulate particular carotenoids (Cunningham and Gantt, 1998). Studies of CCD1 enzymes from many species indicate they possess the broadest

substrate specificity. CCD1s cleave various linear, monocyclic and bicyclic carotenoids, regardless of their stereochemistry, and in various positions along the carbon backbone (Figure 1.3) (Vogel et al., 2008; Ilg et al., 2014). Significantly, this concurs with *in vitro* findings (Simkin et al., 2004a). CCD1s are localised to the cytoplasm (Auldridge et al., 2006) although they may also associate with the outer chloroplast membrane (Simkin et al., 2004a), and seem to have roles in fruit and flower volatile production (Simkin et al., 2004b; Mathieu et al., 2005; Baldermann et al., 2010). In some species however, CCD1 gene duplication has occurred, leading to functional specialisation. In *Crocus sativus CsCCD1a* expression is induced upon dehydration stress (Rubio et al., 2008). The differing substrate specificities of *Solanum lycopersicum* CCD1a and CCD1b also suggest functional specialisation (Ilg et al., 2014). However, it is unclear whether CCD1s were recruited from volatile production to other functions or *vice versa*.

The role of *Medicago truncatula* CCD1 in producing the apocarotenoid mycorradicin is another prominent example of a non-volatile-production role for CCD1. Mycorradicin is the yellow pigment that accumulates to high levels in roots of many plant species upon colonisation with arbuscular mycorrhiza (AM) (Fester et al., 2002a); and is produced from cleavage of root carotenoids (Klingner et al., 1995; Fester et al., 2002b). Mycorradicin is often esterified in plants, although the free di-acid form has also been detected (Schliemann et al., 2006). Its production appears associated with that of various C_{13} apocarotenoids, primarily the cyclohexenone blumenol (and its glycoside derivatives), which also accumulate upon AM colonisation (Maier et al., 1995); cleavage of C_{40} carotenoids to produce C_{14} mycorradicin naturally yields two C_{13} apocarotenoids. RNAi silencing of *CCD1* expression in *Medicago* roots led to accumulation of the C_{27} apocarotenoids 3-hydroxy-α-10'-apocarotenal, and other C_{27} apocarotenoids (Floss et al., 2008). CCD7 is believed to cleave the initial carotenoid substrate in a two-step pathway leading to mycorradicin and the cyclohexenone derivatives (Floss et al., 2008). Blumenol derivatives are responsible for systemic suppression of additional AM-colonisation following initial colonisation (Vierheilig et al., 2000); detailed descriptions of AM-induced apocarotenoids and their roles are found elsewhere (Akiyama, 2007).

CCD4 enzymes generally cleave carotenoids (especially β-carotene) at the 9,10-double bond when tested *in vitro* and *in bacterio* (Huang et al., 2009). However, the substrate specificity of CCD4 is still unclear. Recent work suggests zeaxanthin and β,β-epoxyxanthophylls are also

substrates for CCD4-mediated 9,10-cleavage in *Arabidopsis* leaves and that the apocarotenoids formed are sequestered as glycosides (Latari et al., 2015). Other CCD4 enzymes appear specific for 7,8-cleavage. Satsuma mandarin (*Citrus unshiu*) CCD4 enzymes cleave β-cryptoxanthin and zeaxanthin asymmetrically at 7,8/7',8' positions to yield β-citraurin and apo-8'-β-carotenal (Ma et al., 2013). Many CCD4 enzymes seem to have a role in carotenoid catabolism, particularly in carotenoid-sink tissues such as flowers (Rubio et al., 2008), fruits (Brandi et al., 2011), seeds (Gonzalez-Jorge et al., 2013) and tubers (Campbell et al., 2010). Similarly to CCD1, CCD4 genes exist as duplicates in many species, and often differ in substrate selectivity, tissue localisation and regulation of expression (Ohmiya et al., 2006; Ahrazem et al., 2010; Lashbrooke et al., 2013; Rubio-Moraga et al., 2014). In some species, however, CCD4 duplicates share such high identity in their amino acid and promoter sequences that they may simply be allelic variants, such as *Cs*CCD4a and *Cs*CCD4b from *C. sativus* (Ahrazem et al., 2010; Rubio-Moraga et al., 2014).

CCD4 cleavage may also produce apocarotenoids with biological activity. RNAi knockdown of CCD4 in potato (*Solanum tuberosum*), in addition to increasing carotenoid levels caused elongated tubers and increased stolon-like growth (Campbell et al., 2010). Similar phenotypes are seen under heat stress (Jefferies and Mackerron, 1987). Campbell *et al*. speculates that the CCD4 apocarotenoid product might therefore be an important regulator of heat stress responses, most-likely derived from 9,10-asymmetric cleavage of all-*trans*-β-carotene, based on *in vitro* data (Bruno et al., 2015). Accordingly, the CCD4 homologue *CsCCD4a* is also induced by heat (Rubio et al., 2008). CCD4 may also metabolise ζ-carotenes to create an apocarotenoid signaling molecule(s), herein called ACS1 (Avendano-Vazquez et al., 2014)(see next section).

CCD7's primary role is to catalyse the first step in strigolactone biosynthesis, namely 9',10'-cleavage of 9-*cis*-β-carotene to give 9-*cis*-β-apo-10'-carotenal (Figures 1.3 and 1.4) (Booker et al., 2004; Alder et al., 2012). Additionally, CCD7 may also catalyse the initial 9,10-cleavage required for mycorradicin synthesis (Figures 1.3 and 1.4) (Floss et al., 2008; Vogel et al., 2010). *In vivo* assays suggest CCD7 also cleaves lycopene and ζ-carotene at the 9,10 bonds, albeit slowly (Booker et al., 2004; Schwartz et al., 2004).

CCD8 follows CCD7 in strigolactone biosynthesis by catalysing an unusual oxidative cleavage and intramolecular cyclisation of 9-*cis*-apo-10'-carotenal to yield the strigolactone precursor, carlactone (Figures 1.3 and 1.4) (Alder et al., 2012). Interestingly, CCD8 also cleaves *trans*-apo-

10'-carotenal to yield apo-13-carotenone, which was originally postulated to be the strigolactone precursor. Although the biological relevance of this reaction is unclear as it is ten-fold slower than carlactone formation (Alder et al., 2012), it should be noted that phylogenetic studies in maize, rice and sorghum suggest a subset of CCD8 enzymes may synthesise non-strigolactone apocarotenoids (Vallabhaneni et al., 2010).

Biologically active apocarotenoids often undergo additional enzymatic transformations prior to and/or following oxidation. Carotenoid isomerisation is often crucial; ABA and strigolactone biosynthesis both require 9-*cis* substrates (Schwartz et al., 2003; Alder et al., 2012). We know little about the mechanism of these isomerisations. In rice D27 catalyses the *trans*-9-*cis* conversion needed for subsequent CCD7 cleavage and strigolactone synthesis. Orthologs of D27 exist in other plants and are the only known isomerase involved in apocarotenoid metabolism (Lin et al., 2009; Alder et al., 2012).

Apocarotenoids can also form non-enzymatically by oxidative cleavage, and two of these have roles in stress signalling. They are described in more details below (see Non-enzymatically-generated apocarotenoid signals).

Plant apocarotenoid formation is responsive to environmental and developmental cues which not only affect CCD enzymes but also regulate carotenogenic gene expression. This is discussed further in Box 1.1.

1.5.3 Novel or uncharacterised apocarotenoid signals play regulatory roles *in planta*

Recent studies suggest a number of uncharacterised ACSs modulate plant developmental and/or stress responses. This is in addition to phytohormones such as ABA and strigolactones, new aspects of which are still being discovered (Fan et al., 2009; Seto and Yamaguchi, 2014). In fact, the structure of apocarotenoids suggests that they can play signaling roles. Most apocarotenoids contain an α,β-unsaturated carbonyl moiety, which can easily react with the nucleophilic moieties of biological molecules (Farmer and Mueller, 2013). Reactive electrophilic species (RES) can react with thiols on transcription factors, altering gene expression (Levonen et al., 2004); this is how apocarotenoids mediate apoptosis (Liu et al., 2008) and retinoid signaling (Eroglu et al., 2012) in mammals. The relationships between apocarotenoid structure and signalling activity however, remain unclear (Linnewiel et al., 2009)

in most instances. Indeed, most plant ACSs remain unidentified.

One uncharacterized ACS, which we dub 'ACS1', alters leaf development and chloroplast

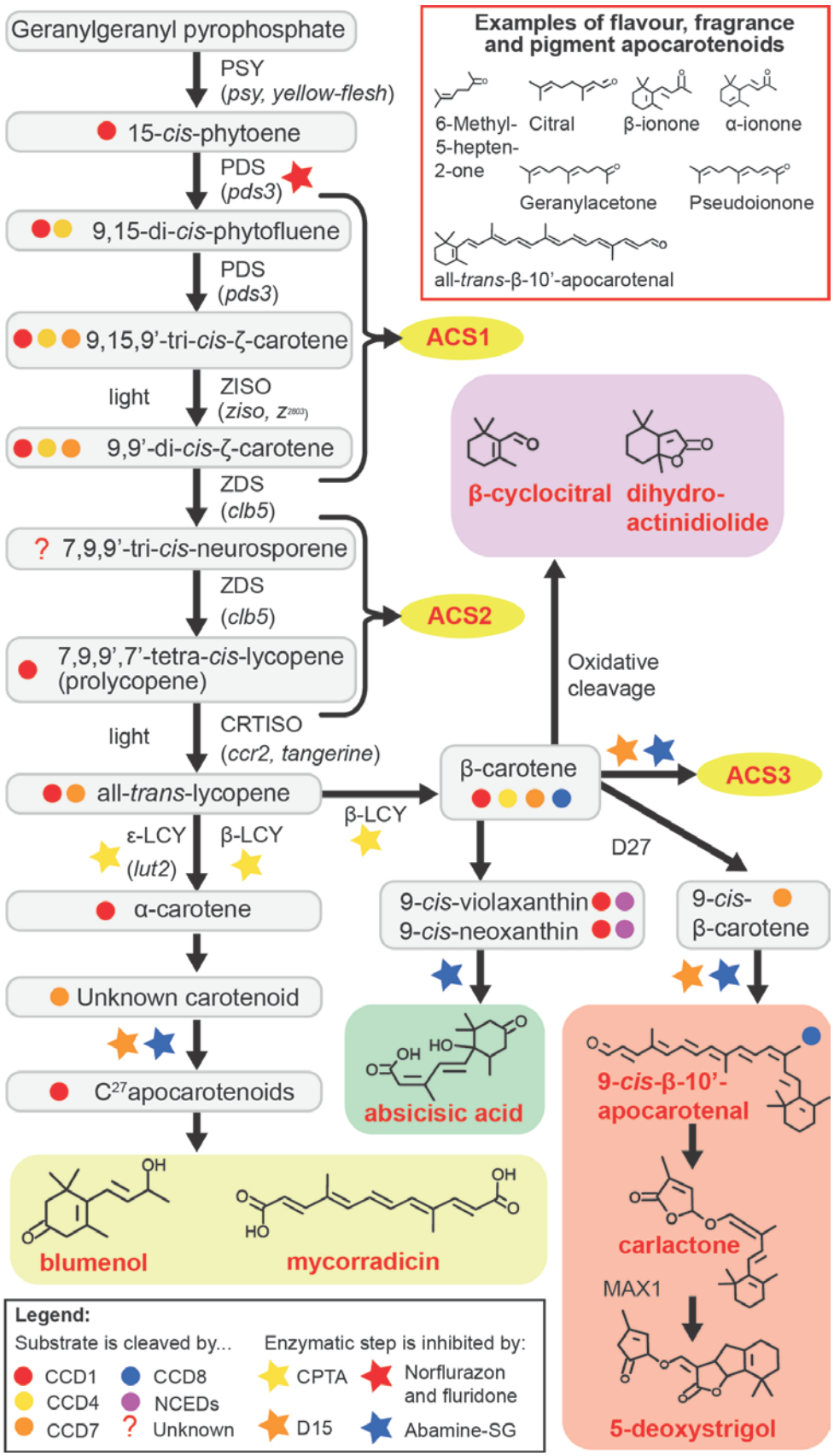

Figure 1.3 Apocarotenoid biosynthesis. Many carotenoids are cleaved to form apocarotenoids through enzymatic reactions. Nine-*cis*-epoxy-dioxygenase (NCED) cleaves 9-*cis*-violaxanthin and 9-*cis*-neoxanthin to yield the precursor of ABA. The Carotenoid Cleavage Dioxygenase (CCD) enzymes cleave carotenoids to yield various apocarotenoids. CCD7 and CCD8, for example, contribute to strigolactone synthesis following β-carotene isomerisation by D27. The CCD8 product carlactone is further elaborated by the P450 enzyme MAX1, and possibly other unknown enzymes before yielding strigolactones (5-deoxystrigol is depicted as an example). CCD7 and CCD1 contribute to the formation of mycorradicin and blumenol derivatives, which accumulate in AM-colonised roots. CCD7 cleaves an unknown carotenoid substrate (possibly lutein or an ε,ε-xanthophyll) to yield a C_{27} apocarotenoid which is further cleaved by CCD1. The end products mycorradicin and blumenol are often further glycosylated. One ACS, β-cyclocitral, is formed via non-enzymatic cleavage of β-carotene. *cis*-carotene-derived apocarotenoids may also be important plant development signals. We propose at least two groups of unidentified Apocarotenoid Signals, ACS1 and ACS2, function in a range of processes, including feedback regulation, based on evidence from mutants in the *cis*-carotene pathway (i.e. *Arabidopsis* mutants *psy, pds3, ziso, clb5* and *ccr2,* and *S. lycopersicum* mutants *yellow-flesh, z^{2803}* and *tangerine*). Another unidentified signal, ACS3, seems to be derived from β-carotene cleavage and functions in root development. Some apocarotenoids are flavour, fragrance and pigment apocarotenoids (mainly in carotenoid sink tissues); these are depicted in the top-right panel. CCD cleavage activities have been denoted by coloured circles next to the carotenoid substrates (see colour code). Given the importance of chemical inhibitors in the study of apocarotenoid biosynthesis, the enzymatic targets of norflurazon, fluridone, CPTA, D15 and abamine-SG have been annotated with coloured stars (see colour code).

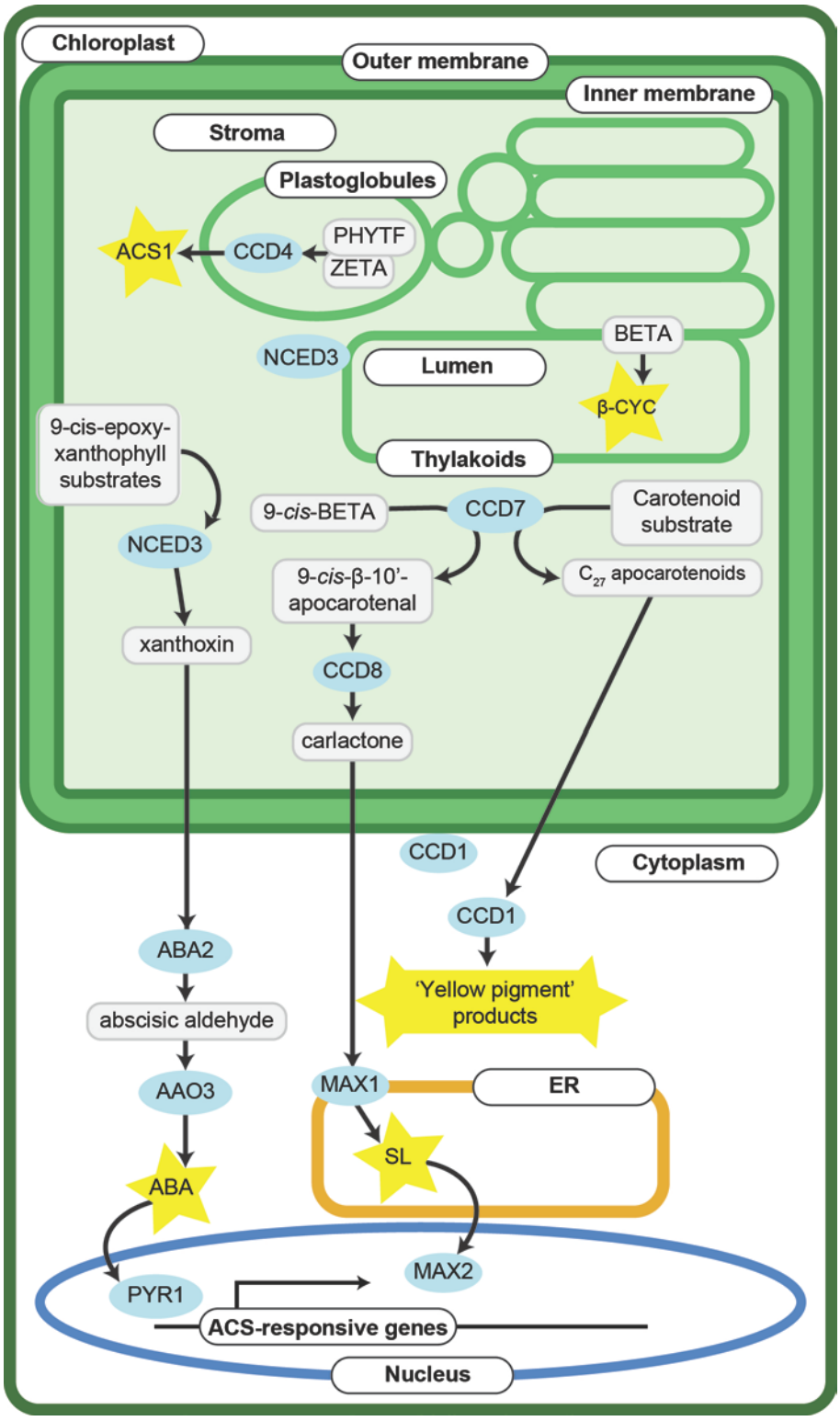

Figure 1.4 Apocarotenoid signal generation and perception take place across several subcellular compartments. In this scheme, the biosynthesis of some known (ABA, SL, 'Yellow Pigment' products, β-cyclocitral) and novel (ACS1) ACSs are placed in the context of a plant cell, and the various chloroplastic compartments. The carotenoid precursors are typically found in chloroplast membranes, such as PSII-associated β-carotene. The 9-*cis*-

epoxyxanthophyll ABA precursors are believed to be inner membrane-embedded, given the necessary carotenogenic enzymes are also localised here. ζ-carotene and phytofluene, putative ACS1 precursors, are believed to accumulate in the plastoglobules. It is not known where the precursors for strigolactones (9-*cis*-β-carotene) and the yellow-pigment products (unknown) are localised. These substrates are cleaved by CCD and NCED enzymes, save for β-carotene, which is cleaved by singlet-oxygen to yield β-cyclocitral. CCD4 is localised to the plastoglobules, consistent with its putative role in ACS1 generation. CCD7 and CCD8 are localised to the stroma, as are the NCEDs involved in ABA biosynthesis (although transient association with the stroma-facing thylakoid membrane has also been observed). Subsequent modification of ACS precursors may occur in the cytoplasm or other organelles, as depicted for ABA, SL and yellow pigment products. Unknown mechanisms must export these precursors from the chloroplast. Notably, elaboration of carlactone to strigolactones may occur in the endoplasmic reticulum, based on localisation predictions for MAX1, a strigolactone biosynthetic enzyme downstream of CCD8. CCD1, localised to the cytosol (but also known to associate with the cytoplasm-facing outer chloroplast membrane), further cleaves C_{27}-apocarotenoid substrates to yield the yellow pigment products. ACSs may then interact with receptors, such as for ABA, which binds to PYR/PYL/RCARs (denoted here as PYR) and SL to MAX2, to effect biological response(s). It is not known how, or where, the yellow pigment products, ACS1-3 and β-cyclocitral exert their effects. Abbreviations: AAO3, *Arabidopsis* aldehyde oxidase 3; ABA, abscisic acid; ABA2, short-chain dehydrogenase/reductase ABA2; BETA, β-carotene; β-CYC, β-cyclocitral; ER, endoplasmic reticulum; MAX1, more axillary growth 1; MAX2, more axillary growth 2; PHYTF, phytofluene; PYR1, pyrabactin resistance 1; ZETA, ζ-carotene.

Box 1.1 Environmental and developmental stimuli regulate apocarotenoid formation

Many examples exist of changes in apocarotenoid accumulation in response to environmental and/or developmental cues. This, together with genetic and biochemical studies demonstrate that some apocarotenoids have regulatory roles *in planta*. The nature of the environmental and developmental stimuli that alter apocarotenoid formation may in some cases also reflect the ecological roles of apocarotenoids (e.g. as pollinator attractants). Examples of stimuli that affect apocarotenoid formation are summarised in Table 1.1.

Environmental and developmental stimuli also alter the expression of many carotenoid biosynthetic genes, altering carotenoid composition, which may in turn promote production of specific apocarotenoids (Tuan et al., 2013a; Tuan et al., 2013b; Lao et al., 2014). However, the relationship between carotenoid and apocarotenoid levels is not always straightforward as expression and localisation of substrates and enzymes will affect apocarotenoid production.

Table 1.1 Environmental stimuli that regulate apocarotenoid formation and CCD enzymes involved

Environmental stimulus	Species	CCD enzyme involved	Apocarotenoids produced	Refs.
Light	*Petunia hybrida*	CCD1	β-ionone	(Simkin et al., 2004b)
Light	*Phaseolus vulgaris*	Unknown	3-hydroxy-β-ionone	(Kato-Noguchi, 1996)
Seed dehiscence and dark-induced leaf senescence	*Arabidopsis thaliana*	CCD4	Possibly β-carotene-derived apocarotenoids	(Gonzalez-Jorge et al., 2013)
Wounding, heat, cold, osmotic stress	*Crocus sativus*	CCD4c	Possibly β-ionone and β-cyclocitral	(Rubio-Moraga et al., 2014)

Abbreviations: CCD, carotenoid cleavage dioxygenase.

biogenesis (Avendano-Vazquez et al., 2014). The *Arabidopsis chloroplast biogenesis 5* (*clb5*) mutant, lacking ζ-carotene desaturase (ZDS) function, accumulates *cis*-carotenes upstream of ZDS (Figure 1.3). *Clb5* plants also exhibits needle-like, translucent leaves and strong suppression of nuclear- and plastid-encoded genes required for chloroplast biogenesis, photosynthetic activity and carotenoid biosynthesis. Genetic and biochemical analyses demonstrated the *clb5* leaf and transcriptional phenotypes were due to cleavage of

phytofluene and/or ζ–carotene isomers to produce ACS1 (Figure 1.3). That is, blocking accumulation or cleavage by CCD4 of these carotenes rescues leaf development and gene expression patterns (Avendano-Vazquez et al., 2014). Curiously, past *in vitro* studies suggest *cis*-ζ-carotene isomers are not CCD4 substrates (Huang et al., 2009), but this does not preclude phytofluene or *cis*-ζ-carotene cleavage *in planta* and demonstrates the need for multiple lines of evidence when determining *in vivo* carotenoid substrates for CCDs.

What is ACS1 and where might it be produced? Proteomics and GFP-tagging data indicate CCD4 is localised to plastoglobules (Figure 1.4) (Ytterberg et al., 2006; Lundquist et al., 2012). In chromoplasts, these plastidic structures accumulate high levels of carotenoids (Rubio et al., 2008; Frusciante et al., 2014) and chloroplastic plastoglobules may also contain carotenoids. Thus, it is likely the first step in ACS1 biosynthesis might be in these suborganellar structures, but the structure, the number of steps in its biosynthesis and its mechanism of action are all unknown.

cis-carotenoids in tomato (*Solanum lycopersicum*) fruit may yield ACS2. *SlPSY1* transcription, eliminated in the *yellow-flesh* mutant r^{2997}, is partially recovered in the double mutant r^{2997}/t^{3002} (Figure 1.3). *PSY1* transcription recovery seems linked to accumulation of tetra-*cis*-lycopene and various neurosporene isomers present in the t^{3002} tomato, which lacks a functional CRTISO. Either of these two *cis*-carotenoids might be precursors of ACS2. Consistent with our theory, expression of *PSY1* is not rescued in the loss-of-function *PSY*/*ZISO* double mutant r^{2997}/z^{2803}that lacks the aforementioned *cis*-carotenoids (Figure 1.3) (Kachanovsky et al., 2012).

ACS3, derived from the β,β-branch of the carotenoid pathway, regulates periodic root branching and lateral root (LR) capacity in *Arabidopsis* in conjunction with the oscillatory LR-clock gene expression network (Van Norman et al., 2014). Treatment of *Arabidopsis* seedlings with the carotenoid cleavage inhibitor D15 reduced LR capacity, similarly to that seen upon carotenoid biosynthesis inhibition (i.e. via Norflurazon and CPTA treatment) and in carotenogenic mutants (*clb6* and *psy*, Figure 1.3). Genetic analysis suggests that the reduced LR-capacity was not related to ABA or strigolactone signaling, demonstrating the existence of a yet to be identified ACS3. Analysis of the *lut* mutants revealed ACS3 was not derived from the ε,β-carotenoid pathway branch, indicating ACS3 is derived from a β,β-carotenoid (Van Norman et al., 2014).

Are there other ACSs? Metabolic feedback within the carotenoid and MEP pathways at transcriptional and/or post-transcriptional levels is essential for regulating carotenoid biosynthesis *in planta* (Qin et al., 2007; Bai et al., 2009; Rodriguez-Villalon et al., 2009a; Ruiz-Sola and Rodriguez-Concepcion, 2012) and feedback metabolites may originate from the plant poly-*cis* carotenoid pathway, in which phytoene is converted to lycopene. In bacteria, CrtI converts 15-*cis*-phytoene to all-*trans*-lycopene, whereas plants, algae and cynobacteria require two desaturases and two isomerases that are highly conserved (Sandmann, 2009). The *cis*-configured intermediates produced by these enzymes may be susceptible to cleavage and modification to form plant-specific regulatory signals, thereby fine-tuning the carotenoid pathway in response to stimuli (Kachanovsky et al., 2012).

1.5.4 Non-enzymatically-generated apocarotenoid signals act as photooxidative stress signals

Non-enzymatically-generated apocarotenoids can also be signals (Estavillo et al., 2012). Singlet oxygen ($^1O_2$) quenching by β-carotene in photosystem II forms various β-apocarotenoids via an unknown mechanism, presumably involving oxidative cleavage (Gonzalez-Perez et al., 2011; Havaux, 2014). β-cyclocitral and β-ionone were shown to accumulate in *Arabidopsis* within minutes of strong high-light treatment (Ramel et al., 2012). Similarly, the *Arabidopsis* mutant *ch1,* which lacks chlorophyll *b* and overproduces $^1O_2$, accumulates β-cyclocitral under moderately-elevated light (Ramel et al., 2013b). *Arabidopsis* exposed to physiologically-relevant concentrations of β-cyclocitral increased the expression of stress response, environmental-interaction and $^1O_2$ marker genes, and reduced that of development, growth and cellular biogenesis genes. These changes increased tolerance to photooxidative stress (Ramel et al., 2012). Moreover, while β-ionone treatment led to only moderate induction of one $^1O_2$ gene marker, dihydroactinidiolide (DHA), derived from β-ionone, elicited gene expression patterns correlating with enhanced photooxidative stress-tolerance (Ramel et al., 2012; Shumbe et al., 2014).

Intriguingly β-cyclocitral-induced gene expression is independent of the nuclear-encoded, plastid-localized EXECUTER 1 protein (Wagner et al., 2004; Ramel et al., 2012) that was reported to initiate $^1O_2$-mediated light stress response (Kim et al., 2012). This suggests

that high $^1O_2$ levels induce programmed cell death via EXCUTER 1 (Wagner et al., 2004) whilst low $^1O_2$ leads to stress acclimation via β-cyclocitral (Ramel et al., 2012) or other mechanisms (Alboresi et al., 2011). Recent work suggests β-cyclocitral-induced stress acclimation is salicylic acid (SA)-dependent: β-cyclocitral up-regulates SA concentration under excess light, thus inhibiting ROS accumulation in the chloroplast (Lv et al., 2015). β-cyclocitral also regulates the nuclear localisation of nonexpressor of pathogenesis-related gene 1 (*NPR 1*) via SA accumulation, subsequently inducing *GST5* (*gluthathione-S-tranferase 5*) and *GST13*, genes involved in β-cyclocitral-induced stress acclimation response (Ramel et al., 2012; Lv et al., 2015).

The identification of β-cyclocitral and DHA as photooxidative stress signals has shed new light on the transduction of $^1O_2$ signaling from chloroplast to nucleus. As a highly reactive molecule with short half-life, $^1O_2$ is unlikely to be a signalling compound. β-cyclocitral and DHA however, are lipid-soluble and thus could be membrane-permeable chloroplastic signals (Ramel et al., 2013a). There may be other β-carotene oxidative cleavage products that may also regulate $^1O_2$-responsive genes (Havaux, 2014).

1.5.5 Subcellular compartmentalisation regulates apocarotenoid production

Carotenoid localisation and apocarotenoid transport are important for apocarotenoid production (Shumskaya and Wurtzel, 2013), however, the controlling mechanisms are enigmatic. Not surprisingly most CCDs are plastid-localised, allowing access to carotenoid substrates. Within the plastid, suborganellar compartments such as plastoglobuli (PG) can function as sites of apocarotenoid production using carotenoid intermediates under specific developmental conditions. It has been shown that PGs are dynamic in composition (Lichtenthaler, 1968) and that PG participate in carotenoid metabolism. Interestingly, proteomic analysis has identified several enzymes of the carotenoid biosynthetic pathway inside PG including ZDS, lycopene β-cyclase (Ytterberg et al., 2006) and CCD4 (Huang et al., 2009). Moreover recent studies suggest that the stability of CCD4 in PG may be regulated by phosphorylation (Lundquist et al., 2013). This scenario opens the possibility that production of specific apocarotenoids occur in response to phosphorylation-mediated stimuli.

In contrast, CCD1 is cytosol-localised (Auldridge et al., 2006). How does CCD1 access

carotenoid substrates? Simkin and colleagues found tomato CCD1 enzymes are associated with chloroplast outer chloroplast membrane where carotenoid cleavage might occur (Simkin et al., 2004a). A similar mechanism has been proposed for CsCCD2, which is also cytosolic (Frusciante et al., 2014). However, many researchers have found CCD1 mRNA expression and carotenoid levels do not correlate (Ibdah et al., 2006; Ilg et al., 2010; Lashbrooke et al., 2013). This would suggest CCD1-mediated cleavage is controlled by other factors or other levels of regulation might operate including translational or post-translational regulation. Thus, the significance of cytosolic CCD enzymes associating with outer chloroplast membranes will require future analyses.

Organellar processes may also control CCD1 substrate access. Hemifused-membranes at plastid-endoplasmic reticulum (ER) contact sites may also allow interorganellar enzymatic activity (Mehrshahi et al., 2014). Another interesting hypothesis suggests stromules are involved in apocarotenoid transport; stromules and CCDs are affected by similar environmental cues and stromules are also thought important for subcellular organelle communication (Kwok and Hanson, 2004).

Another possibility is that CCD1 enzymes might only cleave apocarotenoids generated by other CCDs, capable of diffusing out of the plastid. MtCCD7 produces the C_{27} apocarotenoid substrate/s for MtCCD1 in mycorrhizal roots, for example (Floss et al., 2008). In other instances, perhaps CCD1 cleaves carotenoid substrates leaked into the cytosol under particular conditions, such as plastid degradation during fruit ripening. The observed increases in CCD1 expression in the fruits of many species, and the concurrent increases in fruit volatile emission, support this hypothesis (Mathieu et al., 2005; Ibdah et al., 2006; Kato et al., 2006; Garcia-Limones et al., 2008; Yahyaa et al., 2015). The broad substrate specificity of fruit-specific CCD1 enzymes, such as SlCCD1b, also support the notion of CCD1 'indiscriminately' cleaving leaked carotenoids (Ilg et al., 2014). Carotenoid leakage from plastids might also happen during insect attack, as suggested by Vogel (Vogel et al., 2008), with carotenoids then cleaved to produce insect-repellent compounds. This theory concurs with the observation that CCD1 overexpression can reduce crucifer beetle attack (Wei et al., 2011). A similar mechanism may help mitigate pathogen attack since many apocarotenoids seem to possess antimicrobial and antifungal properties (Utama et al., 2002). In light of these uncertainties, we propose that existing *in vitro* and *in bacterio* results need to be

complemented by *in planta* measurements of apocarotenoids.

1.5.6 Concluding Remarks and Future Perspectives

Plant carotenoid cleavage products are an exciting class of compounds whose biochemistry and functions are still largely unexplored. The big questions are summarized in the Outstanding Questions Box and are further discussed below.

While many apocarotenoids have been identified, those which possess ACS functions are unknown and it is also likely that many ACSs remain unidentified. Furthermore, ACSs 1-3 may represent groups of compounds, not 3 distinct compounds. In this regard genomic and chemical genetic techniques may help. For example, studies involving suppression of a specific CCD could narrow down the field of candidate apocarotenoids (McCourt and Desveaux, 2010) responsible for a specific function or signal. Targeted chemical screens may also uncover *in planta* apocarotenoid signals.

Beyond ABA and strigolactone, little is known about the genes responsible for post-CCD apocarotenoid modification and transport. How are apocarotenoids transported between sites of synthesis and action? What *are* the sites of action: stroma, cytosol or nucleus? Research into CCD1 suggests apocarotenoid biosynthesis spans multiple cellular locations (Tan et al., 2003; Simkin et al., 2004a) so there must be an active transport mechanism (Figure 1.4).

We also need to integrate our understanding of apocarotenoid chemistry with current knowledge of carotenoid biosynthesis. Studies suggest carotenoid biosynthetic enzymes exist in metabolons (Shumskaya and Wurtzel, 2013) and plants may alter metabolon composition during different developmental stages or in response to specific signals, and thus carotenoids produced. It is possible that the involvement of CCDs in specific carotenoid metabolons could explain how specific apocarotenoids are formed despite *in vitro* CCD substrate promiscuity. Inclusion of particular isoforms in these complexes might also provide a source of variability in the type of apocarotenoid produced. But, studying metabolons, protein-protein and protein-metabolite interactions remains a challenge. Utilisation of super-resolution fluorescence microscopy, allowing single molecule localization and characterisation (Schermelleh et al., 2010), and cryo-electron tomography (CryoET) to determine dynamic single-molecule structure (Zhang and Ren, 2012) could aid future study of apocarotenoid production by metabolons and subsequent transport within and out of plastids.

Apocarotenoid signal-perception is another important area for research. Apocarotenoids could theoretically bind to enzymes, transcription factors or even RNA sequences (e.g. riboswitches (Verhounig et al., 2010)) to exert regulatory effects. Affinity chromatography with apocarotenoids as bait could isolate apocarotenoid-binding proteins, transporters or RNA targets: proteomics and next-generation sequencing would then aid in their identification. Apocarotenoid analogues with fluorescent or affinity moieties (Khan et al., 2013) could also reveal interacting enzymes; a similar approach helped find strigolactone receptors (Prandi et al., 2013).

We anticipate much more will be discovered about apocarotenoid biology, biochemistry, function and formation, yielding new insights into how plants utilise this class of compounds.

Outstanding Questions

Genomic and chemical genetic strategies will help us to discover new bio-active apocarotenoids, and the pathways involved in their production and transport. Researchers will need to consider how apocarotenoid and carotenoid production is co-ordinated. Furthermore, we do not know how or where apocarotenoids are perceived by plants, and how downstream responses are mediated. New transcriptomics, biochemical, genetic and proteomics techniques will help to address the following key questions.

- How are apocarotenoids produced and how is their production regulated?
- Do CCDs interact with carotenogenic enzymes in a metabolon complex to facilitate the production of specific apocarotenoids?
- Which apocarotenoids possess biological function(s)?
- Are apocarotenoids transported and perceived within and between cells?
- How are apocarotenoids perceived and how do they regulate biological processes?

1.6 Aim of thesis

Reportedly the *ccr2* mutant accumulates poly-*cis* carotenes and lacks PLB (Park et al., 2002) in etiolated seedlings, in correlation this mutant shows a yellowing phenotype in newly emerged leaf tissues when grown under 8-h to 10-h photoperiods, indicating impaired chloroplast biogenesis. We speculate the accumulated poly-*cis* carotenes or likely their cleavage products apocarotenoids may play regulatory roles in skoto- and photo-morphogenesis via retrograde

signals dubbed ACSs in this thesis. To study the nature of the speculated ACSs, we performed forward genetic study by generating ethyl methanesulfonate (EMS) mutagenized *ccr2* and screening for double mutants that restored leaf greening. Through next generation sequencing (NGS) we identified causal mutations in revertants of *ccr2* (*rccr2*), followed by characterization of the mutated genes that may link apocarotenoids to plastid development. Using a combination of molecular and cellular technologies and bioinformatics approaches we aim to examine the ACSs that regulate etioplast development and chloroplast biogenesis, as well as to study other mechanisms leading to the reversion of *ccr2* yellowing phenotype especially if they are related to plastid development and the fine-tuning of carotenoid biosynthetic pathway.

The main content of following chapters is summarised as below:

- Chapter 2 of the thesis describes the materials and methods used in the present study. Although chapters 4 and 5 are written in the format of manuscripts to submit to *Plant Cell* and *Plant Physiology*, respectively, their "materials and methods" sections are combined into chapter 2 to avoid duplication.
- Chapter 3 describes the screening of *rccr2* and identification of causal mutations in each *rccr2* lines by NGS. In chapter 3, I also discuss the potential connection of some candidate genes to the regulation of plastid development by ACSs.
- In chapter 4, I study the *ccr2 ziso*-155 and *ccr2 det1*-154 double mutants and describe an ACS, namely ACS2, that is possibly derived from *cis*-carotenoids. ACS2 acts downstream of DET1 to regulate plastid development by affecting POR protein levels.
- In chapter 5, I discovered that mutations in PSY, the entry-point enzyme of carotenoid biosynthesis, supressed ACS2. The suppression of ACS2 was caused by reduced PSY activity and protein levels but not due to altered localization.
- In chapter 6, I make final discussion and present future perspectives.

Chapter 2: Materials and methods

2.1 Plant materials and growth conditions

2.1.1 Plant materials

The *Arabidopsis thaliana* ecotype Columbia (Col-0) and ecotype Landsberg erecta (Ler-0) were used as wild-type controls in this thesis. The Arabidopsis *ccr2* mutant, carrying a G-to-A mutation in *crtiso* gene at the start of intron 9 that leads to mis-splicing, was in Col-0 background and subjected to EMS mutagenesis to generate revertants of *ccr2* (*rccr2*). The *ccr2* mutant was crossed to Ler-0 followed by six rounds of backcross and screening for *ccr2* phenotypes to generate *ccr2* mutant in Ler-0 background (*Lccr2*). *Lccr2* was used as parent to cross to *rccr2* in preparation of F2 plants for Next Generation Sequencing (NGS); *ccr2* and Col-0 were also used as parents.

2.1.2 Soil-based growth

For soil grown plants, seeds were sown on soil with the following composition: Seed Raising Mix (Debco, NSW Australia) with 3 g of Osmocote Exact Mini (Scotts, NSW Australia) supplemented into 1 L of soil and the mixture was treated with 500 mL 0.3% (v/v) Azamax (Organic Crop Protectants, NSW Australia) solutions. Seeds were then stratified for 3 d at 4°C in the dark and covered with plastic hood or cling wrap to retain moisture, prior to transferring to an environmentally controlled growth chamber set to 21°C and illuminated by approximately 120 $\mu mol.m^{-2}.s^{-1}$ of fluorescent lighting. The plastic hood or cling wrap was removed 3 d after the seeds germinated. Unless otherwise stated, plants were grown in a 16-h photoperiod.

Photoperiod shift assays were performed by shifting three-week old plants grown under a 16-h photoperiod to a shorter 10-h one for one week and newly emerged leaf tissues were scored as displaying either the yellow true leaf (YTL) or green true leaf (GTL) phenotypes. To score floral meristem termination phenotypes, plants were grown under a 10-h photoperiod after shifting from 16 h until flowering stage and photographed.

2.1.3 Medium-based growth

For artificially grown seedlings in this research, full strength Murashige and Skoog (MS; GibcoBRL, MD USA) medium was used and it consists of 4.33 $g.L^{-1}$ MS salts with vitamins and 0.5% (or 0.8% for root assays) phytagel (Sigma-Aldrich, MO USA), with pH adjusted to 5.8 with 1 M KOH. Seeds were surface-sterilised for 3 h under chlorine gas by mixing 99 mL bleach (sodium hypochlorite solution, Pelikan Artline, NSW Australia) with 1 mL 36% hydrochloric acid (Ajax Finechem, NSW Australia) in a sealed five-litre container at a fume cupboard, followed by washing seeds twice with 70% (v/v) ethanol and twice with autoclaved MilliQ water. Seeds were then resuspended in autoclaved 0.1% agarose (AMRESCO, OH USA) and sown on the MS plates. The plates were sealed with 3M micropore tape (Carolina Biological, NC USA) and placed in dark at 4°C to stratify the seeds for 2 d, before exposed to light under the growth conditions described in the previous section. All washing and sowing procedures were carried out in a biosafety cabinet (Bio-Cabinets, VIC Australia) to minimise contamination. To inhibit CCD activities in etiolated seedlings, D15 (Sergeant et al., 2009) was dissolved in ethanol and added to MS medium by a 1:1000 dilution of the stock to reach a final concentration of 100 μM (Van Norman et al., 2014). Inhibition of PDS activity in etiolated seedlings was performed by adding norflurazon (Sigma-Aldrich) (Simkin et al., 2000) to MS medium at a final concentration of 20 μM.

Seed derived calli (SDC) were generated as previously described (Mathur and Koncz, 1998). Briefly, 5 mg surface-sterilized seeds were plated onto a 90 mm petri dish containing 40 mL of SDC medium (4.33 $g.L^{-1}$ MS basal salts (GibcoBRL), pH 5.8, 3% w/v sucrose, 0.1% v/v Gamborg B5 vitamins (Sigma-Aldrich), 0.5 $mg.L^{-1}$ 2,4-D, 2 $mg.L^{-1}$ indole-3-acetic acid (Sigma-Aldrich), 0.5 $mg.L^{-1}$ 2-isopentenyladenine (Sigma-Aldrich), 0.5% w/v phytagel). Seeds were germinated for 5 d under 16-h photoperiod and incubated for 16 d in dark before harvesting tissues for HPLC analysis. Callus treated with norflurazon were transferred onto the same medium containing 1 $\mu mol.L^{-1}$ norflurazon prior to etiolation. Norflurazon was dissolved in 100% ethanol to make a 1 $mmol.L^{-1}$ stock and diluted as appropriate in SDC medium.

The etiolated seedling greening experiments were performed by germinating stratified seeds in dark at 21°C for 4 d and then de-etiolating seedlings by exposing them to continuous fluorescent illumination of 80 $\mu mol.m^{-2}.s^{-1}$ for 3 d at 21°C. Twenty seedling tissues were then harvested for chlorophyll measurements at 12 h intervals starting from exposure to light.

For hypocotyl experiments, following etiolation for 4 d representative seedlings were photographed under an Olympus SZX16 microscope (Olympus, Tokyo Japan) to depict the apical hook (WT and *ccr2*) or open cotyledon (*ccr2 det1-154*). The length of the hypocotyl was scored using Image J (Schneider et al., 2012).

For root experiments, eleven individual seeds were sowed on a 12-cm square plate and germinated at 21°C under a 16-h photoperiod after stratification. Root length was scored for 11 d at 24 h intervals and plates were scanned using an Epson Perfection V700 scanner (Seiko Epson Corporation, Najano Japan) on day 11.

2.2 Microbial strains and growth conditions

Escherichia coli DH5a strain was normally used for plasmid propagation, except for plasmids expressing *ccdB* gene the DB3.1 resistant *E. coli* strain was used. Both DH5a and DB3.1 strains were originally obtained as chemical-competent stocks from New England BioLabs (MA USA) and ThermoFisher Scientific (MA USA), respectively, and were propagated and maintained in our lab. TOP 10 chemical competent *E. coli* cells (ThermoFisher Scientific) were used for GGPP or phytoene synthesis when transformed with artificial chromosome pAC-GGPPipi or pAC-PHYT, respectively. *E. coli* strain BL21 (DE3), propagated in our lab and used for the expression of recombinant proteins, was a gift from Dr. June Liu (Australian Department of Agriculture and Water Resources). Agrobacterium GV3101 strain (gift from Dr. Anthony Millar, The Australian National University) was used as plasmid carrier in Agrobacterium-mediated transformation of Arabidopsis.

All *E. coli* and Agrobacterium strains were cultured in sterile Luria-Bertani broth (LB broth, ThermoFisher Scientific) that contains 10 $g.L^{-1}$ peptone 140, 5 $g.L^{-1}$ yeast extract and 5 $g.L^{-1}$ NaCl, at 37°C and 28°C, respectively. Solid LB medium containing 1.2% agar was used for plate-based culture of *E. coli* and agrobacterium strains.

2.3 Revertant screening and identification of casual mutations

2.3.1 Revertant screening

ccr2 seeds were mutagenized using ethyl-methane sulfonate (EMS; Sigma-Aldrich) and a

mapping population established as previously described (Kim et al., 2006; Weigel and Glazebrook, 2006). Briefly, 1 g seeds (about 50,000) were incubated in a 50 mL Falcon tube with 25 volumes of 0.2% (v/v) EMS for 15 h on a rotator. EMS solution was then tipped off and seeds were washed 7 times in 25 mL sterile milli-Q water for 5 min followed by incubating seeds in water for 1 h as the last wash. Seeds were resuspended in 0.1% agarose and sowed in soil to grow M1 plants. M2 Seeds were collected from pools of 5-10 M1 plants and greater than 40,000 M2 seedlings from 30 pools in total were screened for the Green True Leaf (GTL) phenotype. Among the preliminary 194 EMS-mutagenized *ccr2* lines identified, 25 successfully produced a GTL phenotype at varying degrees, which were named as revertants of *ccr2* (*rccr2*). Lutein level and xanthophyll composition were examined in all rccr2 lines using HPLC to confirm a reduced level of lutein and a similar xanthophyll composition to *ccr2*. *rccr2* lines were backcrossed to Ler-0, the *ccr2* parent and Ler-0 carrying *ccr2* mutation (*Lccr2*); segregating F2 homozygous population was generated under a 10-h photoperiod. An equal area of leaf tissue from 30-78 F2 homozygous *rccr2* plants displaying a clear GTL phenotype and reduced lutein level was pooled for DNA extraction.

2.3.2 Plant imaging

Arabidopsis plant leaf colour and rosette area in pixel unit were measured using the Scanalyzer imaging system (LemnaTec GmbH, Aachen Germany). Images of plants were acquired from a top view on a digital camera and processed using LemnaTec Bonit HTS software. The proportion of the plants which appear yellow was calculated via dividing the number of 'yellow' pixels by the total number of pixels in each plant. In addition to Scanalyzer, photography of plants was also performed using the Lumix DMCFZ5 camera (Panasonic, Osaka Japan).

2.3.3 Genomic DNA extraction and library preparation

Fifty to one hundred milligrams of Arabidopsis leaf tissue was frozen in liquid nitrogen and ground to fine powder using a TissueLyser® (QIAGEN, Hilden Germany). Genomic DNA was extracted using the DNeasy Plant Mini Kit (QIAGEN) and eluted in 70 µL of sterile milli-Q water. The concentration of Genomic DNA was measured using a ND-1000 spectrophotometer (NanoDrop Technologies, DE USA) with NanoDrop software version 3.5.2. The measurements were taken at 260 nm (OD_{260}) and converted to concentration using the Beer-Lambert

equation where 1 OD is considered as 50 µg.mL^{-1} for double stranded DNA. The purity of DNA samples is examined using OD_{260}/OD_{280} ratio where a ratio of 1.8 indicates pure DNA.

One microgram of genomic DNA was sheared using the M220 Focused-Ultrasonicator (Covaris, MA USA) with the following settings: sample volume 50 µL, temperature 7°C, peak incident power 75 W, duty factor 10%, cycles per burst 200, treatment time 195 S. Physically sheared DNA was quality-controlled using MultiNA Microchip Electrophoresis System (Shimadzu, Kyoto Japan) to verify the targeted peak at about 200bp. DNA libraries were prepared using NEBNext® Ultra™ DNA Library Prep Kit (New England Biolabs, MA USA) and size selected (~320 bp) using AMPure XP Beads (Beckman Coulter, CA USA). Quality control of libraries was performed using a 2100 Bioanalyzer (Agilent Technologies, CA USA), followed by dilution of libraries to an equal concentration of 10 nmol.L^{-1} and checking the concentration again using Qubit 2.0 Fluorometre (ThermoFisher Scientific) and Qubit DS DNA HS Assay Kit (ThermoFisher Scientific). Libraries were then pooled and paired end next-generation sequencing (NGS) was performed using the Illumina HiSEQ1500.

2.3.4 Sequencing data analysis

The total number of reads ranged between 29-45 million representing approximately 22-35 times genome coverage. After sequencing, the raw reads were assessed for quality using the FastQC software (http://www.bioinformatics.babraham.ac.uk/projects/fastqc/), and subjected to trimming of illumina adapters and filtering of low quality reads with Adapter Removal programme (Lindgreen, 2012). The reads were mapped to the A. thaliana (TAIR9) genome with BWA mapper (Li and Durbin, 2009). The resultant BWA alignment files were converted to sorted bam files using the samtools v0.1.18 package (Li et al., 2009a) and was used as input for the subsequent SNP calling analyses.

The SNPs were called and analysed further on both the parent and mutant lines using NGM pipeline (Austin et al., 2011) and SHOREmap (Schneeberger et al., 2009). For the NGM pipeline, the SNPs called using samtools (v0.1.16) as instructed and processed into '.emap' files using a script provided on the NGM website. The .emap files were uploaded to the NGM web-portal to assess SNPs with associated discordant chastity values. To identify mutant specific SNPs, Parental line SNPs-filtered for EMS changes and homozygous SNPs were defined based on the discordant chastity metric. For SHOREmap, the SHORE software (Ossowski et al., 2008) was

used to align the reads (implementing BWA) and called the SNPs (Hartwig et al., 2012). SHOREmap backcross was then implemented to calculate mutant allele frequencies and filter out parent SNPs and defined the EMS mutational changes. Where appropriate, custom scripts were used to identify mutant specific, EMS SNPs, to filter out parent SNPs and annotate the region of interest.

The localization of SNPs and InDels were based on the annotation of gene models provided by TAIR database (http://www.arabidopsis.org/). The polymorphisms in the gene region and other genome regions were annotated as genic and intergenic, respectively. The genic polymorphisms were classified as CDS (coding sequences), UTR (untranslated regions), introns and splice site junctions according to their localization. SNPs in the CDS were further separated into synonymous and non-synonymous amino substitution. The GO/PFAM annotation data were further used to functionally annotate each gene.

2.3.5 Verification of mutations by Sanger sequencing

Phusion proof-reading polymerase (New England Biolabs) was used to amplify the DNA fragments that need to be sequenced to verify the mutation identified in NGS. PCR was carried out using 200 ng genomic DNA diluted to 2 µL or cDNA mixture as template, 1 X Phusion High Fidelity buffer, 0.5 µL of 10mmol.L^{-1} dNTP mix, 1.25 µL of each primer (10 µmol.L^{-1}), 0.5 units Phusion polymerase and 14.75 µL nuclease-free water to a final volume of 25 µL. Thermocycling conditions were 98°C for 30 s; 30 cycles at 98°C for 10 s, annealing temperatures depending on primers for 30 s and 72°C cycle for 20 s; final extension at 72°C for 5 min. Primers are listed in Table 2.1.

One percent agarose gels were prepared and run in 0.5 X TBE (44.5 mmol.L^{-1} Tris base, 44.5 mmol.L^{-1} Boric acid, 1 mmol.L^{-1} EDTA pH 8.0) to check the quality of PCR products; 1.5 mmol.L^{-1} ethidium bromide added to the gel to visualise DNA. Two microliters of PCR products were mixed with 1 µL of 6 X loading buffer (New England Biolabs) and 3 µL nuclease-free water, and were loaded along with 100 bp DNA molecular marker (New England Biolabs) to the gel. TBE Gels were run at 200 V for 20 min followed by visualisation using the GelDoc System UV transilluminator (Fisher Biotech, WA USA). All PCR products displayed a single band with expected molecular size on an agarose gel, and 100 ng of each product was sent to Biomolecular Resource Facilities at The Australian National University for Sanger sequencing

to verify mutations on genomic DNA.

For the verification of mutations that cause altered splicing, reverse transcriptase polymerase chain reaction (RT-PCR) was used to generate cDNA mixture from Arabidopsis total RNA and to amplify target sequences. Total RNA was extracted from Arabidopsis leaf tissue using Trizol reagent (Thermo Fisher Scientific). Fifty milligrams of leaf tissue was ground using a TissueLyser® (QIAGEN) at 25 sec^{-1} for 2 min, and 1 mL of Trizol reagent was added to each tube. Tubes were incubated at room temperature for 5 min and 200 µL of chloroform was added to each tube, followed by vigorously shaking all tubes and incubation at room temperature for 3 min. After centrifugation at 14,000× g for 10 min at 4°C, 500 µL of upper aqueous phase was transferred to a new tube and chloroform extraction was repeat once. An equal volume of 100% cold isopropanol was added to 380 µL of upper aqueous phase, mixed by inverting the tubes and incubated at -20°C for 2 h. After centrifugation 20,000× g for 20 min at 4°C, supernatant was removed with pipette and 1 mL of 75% ethanol was added to wash the pellet, followed by centrifugation at room temperature for 3 min at 7,500× g. Supernatant was thoroughly removed and tubes were air dried at room temperature until pellets started to become translucent. RNA pellets were dissolved by adding 50 µL of nuclease free water and incubation at room temperature for 5 min, and were stored at -80°C. Five to ten micrograms of extracted total RNA was treated by 2 U of TURBO DNase (Thermo Fisher Scientific) at 37°C for 30 min, and RNA was recovered using 1.8 × Agencourt RNAClean XP magnetic beads (Beckman Coulter). The concentration of RNA was measured by loading 2 µL of each sample to LabChip DS (PerkinElmer, MA USA) and considering 1 OD is as 40 $\mu g.mL^{-1}$.

First strand cDNA synthesis was performed using SuperScript™ III Reverse Transcriptase kit (ThermoFisher Scientific). Briefly, 1 µg of DNase-treated and beads-cleaned total RNA in a volume of 5 µL, 1 µL of oligo$(dT)_{20}$ (50 $\mu mol.L^{-1}$), 1 µL of dNTP mix (10 $mmol.L^{-1}$) was mixed with sterile milli-Q water to 13 µL, heated to 65°C for 5 min and incubated on ice for 2 min. The contents were then mixed with 4 µL of 5 × First-Strand Buffer, 1 µL of 100 $mmol.L^{-1}$ DTT, 40 units of RNaseOUT™ and 1 µL of SuperScript™ III Reverse Transcriptase. Following incubation at 25°C for 5 min and that at 50°C for 60 min, the reaction was inactivated by heating at 70°C for 15 min. Two microliters of synthesised cDNA was then used for PCR amplification using Phusion proof-reading polymerase (New England Biolabs) in a total reaction volume of 25 µL. Thermocycling conditions were the same as used for the

amplification of genomic DNA, and for all PCR products a single band of expected molecular size was achieve by optimizing annealing temperatures. Primers are listed in Table 2.2.

Amplified cDNA fragments were cloned using NEB PCR cloning kit (New England Biolabs) following manufacturer's instructions. Three microliters of cDNA was mixed with 1 µL linearized pMiniT vector, 1 µL sterile milli-Q water and 5 µL Cloning Master Mix, and incubated at 25°C for 15 min followed by 2 min on ice. Two microliters of completed ligation reaction was added to 50 µL NEB 10 beta competent *E. coli* cells (New England Biolabs) and incubated on ice for 20 minutes followed by heat shock at 42°C for 2 min. The contents were incubated on ice for 5 min before mixed with 950 µL SOC medium and incubated at 37°C for 1 h. For each ligation 50 µL was spread on a LB plate with ampicillin (100 $mg.L^{-1}$) followed by incubation at 37°C overnight.

Ten colonies were picked for each transformation and cultured overnight in 5 mL LB medium with 100 $mg.L^{-1}$ ampicillin. Plasmid extraction was carried out with QIAprep® Miniprep kit (QIAGEN) following the manufacturer's instructions. For each colony 100 ng plasmid DNA was sent to Biomolecular Resource Facilities for Sanger sequencing.

Table 2.1 Sequencing primers used in this study.

Name	Sequence	Description
PSY4F PSY4R	CTCTGTCTTATCTTACTTCC TAAACCCTTCCTCTTCTC	Forward and reverse primers for sequencing PCR products amplified from genomic DNA to verify the point mutation on exon 4 of the *psy-4* allele in *rccr2*[4]
PSY90F PSY90R	ACCGGTTTCTTGATTCACA TTCCACTTTCCTCTCGCT	Forward and reverse primers for sequencing PCR products amplified from genomic DNA to verify the point mutation on exon 5 of the *psy-90* allele in *rccr2*[90]
PSY130F PSY130R	GAACACCAAGCATCCAAA GTCTCGAAATGGCTGCAA	Forward and reverse primers for sequencing PCR products amplified from genomic DNA to verify the point mutation on exon 3 of the *psy-130* allele in *rccr2*[130]
PSY145F PSY145R	GGTCTTCTTCTTATGACC CATCACTTTATCCTACAA	Forward and reverse primers for sequencing PCR products amplified from genomic DNA to verify the point mutation at exon 2/intron 3 junction of the *psy-145* allele in *rccr2*[145]
DET1-154F DET1-154R	GGATTGATGCAGTTGACAG GTATCAGTTCAATGTAAC	Forward and reverse primers for sequencing PCR products amplified from genomic DNA to verify the point mutation at exon 4/intron 4 junction of the of the *det1*-154 allele in *rccr2*[154]
ZISO155F ZISO155R	TGTGCTGATGTAATGGGTG CGTGTTTTGTTTGCTGGAATC	Forward and reverse primers for sequencing PCR products amplified from genomic DNA to verify the point mutation on exon 3 of the *ziso-155* allele in *rccr2*[155]
pMiniT-F pMiniT-R	ACCTGCCAACCAAAGCGAGAACAA TCAGGGTTATTGTCTCATGAGCGG	Forward and reverse primers for sequencing the RT-PCR products amplified from splicing variants in in *rccr2*[145] or *rccr2*[154] and cloned into pMiniT vector

Table 2.2 Cloning primers used in this study.

Name	Sequence	Description
PSY145FC PSY145RC	CTTTGCTTATGACACCCG CAGAATATCGACCGGGTATC	Forward and reverse primers for cloning a 221-bp wild type *PSY* cDNA fragment or a 762-bp cDNA fragment from the *psy-145* splicing variant containing intron 3
DET1-154FC DET1-154RC	CAATGATGAGTCAAGATAAG TTACCCCACCGTCTACAC	Forward and reverse primers for cloning a 321-bp wild type *DET1* cDNA fragment containing exon 3, 4 and 5 or a 249-bp cDNA fragment from the *det1-154* splicing variant lacking exon 4
PSY-yeastF PSY-yeastR	TCTTTTGTAAGGAACCGAAGTAG TATCGATAGTCTTGAACTTGAAG	Forward and reverse primers for cloning wild type *PSY* and mutants into the yeast split ubiquitin system

2.4 Generation of transgenic plants

2.4.1 Plasmid construction

Plasmid pEarley-ZISO was designed to overexpress ZISO using the CaMV35S promoter. A full length wild type *ZISO* cDNA coding region was chemically synthesised (Thermo Fisher Scientific) and cloned into the intermediate vector pDONR221. Next, using gateway homologous recombination the *ZISO* cDNA was cloned into pEarleyGate100 vector (Earley et al., 2006) and sequenced to confirm cloning junctions. Similarly, pEarley-PSY and pEarley-DET1 were designed to overexpress full length wild type *PSY* and *DET1* cDNA, respectively, using the CaMV35S promoter in pEarleyGate100. Gateway cloning was carried out by Thermo Fisher Scientific and the constructs were propagated at our lab. All constructs were verified in the lab again by Sanger sequencing and restriction enzyme digestion.

2.4.2 Agrobacterium-mediated transformation of Arabidopsis via floral dipping

To make electrocompetent Agrobacterium cells, Agrobacterium strain GV3101 was streaked onto a plate containing LB medium, 1.2% agar, 25 $mg.L^{-1}$ Rifampicin and 25 $mg.L^{-1}$ Gentamicin. The plate was incubated for 1-3 d at 28°C until colonies formed. Single colonies were inoculated in 3 mL LB medium containing both antibiotics and grown at 28°C for 24 h with constant shaking at 200 rpm. The small culture was then diluted by 100-fold in LB medium with both antibiotics and grown at 28°C with constant shaking at 250 rpm until OD_{600} reached a value between 0.6-0.8. The culture was incubated on ice for 10 min and cells were harvested by centrifugation at 4,000× g for 10 min at 4°C. Agrobacterium cells were washed 3 times with cold sterile milli-Q water the volume of which was equal to that of the LB culture. Cells were then resuspended in 1/2 volume of cold sterile 10% (v/v) glycerol and pelleted again. The pellet was resuspended in 1/100 volume of cold 10% glycerol and 50 µL aliquots were made for the stock of electrocompetent Agrobacterium cells.

Ten nanograms of plasmid DNA in 1 µL sterile milli-Q water was added to 50 µL electrocompetent Agrobacterium cells and gently mixed. Cells and plasmid DNA were transferred to a chilled cuvette (Bio-Rad, CA USA) and electroporation was done with the following parameters: 1.8 kV, 25 µF and 400 Ω. One millilitre of LB medium without antibiotics

was immediately added to the cuvette, mixed by pipetting and transferred to an Eppendorf tube which was subsequently incubated at 28°C for 1 h. The cells (100 µL) were spread on a LB plate containing 25 $mg.L^{-1}$ Rifampicin, 25 $mg.L^{-1}$ Gentamicin and 50 $mg.L^{-1}$ Kanamycin and cultured at 28°C for 1-3 d until colonies formed. Single colonies were cultured in 5 mL LB medium containing all three antibiotics and plasmid DNA was extracted from 2.5 mL LB culture using QIAprep® Miniprep kit (QIAGEN). Plasmids were verified by restriction enzyme digestion before the remaining 2.5 mL culture was inoculated into 250 mL LB medium containing 25 $mg.L^{-1}$ Gentamicin and 50 $mg.L^{-1}$ Kanamycin, followed by growth at 28°C for 16 h with constant shaking at 250 rpm. Agrobacterium cells were pelleted by centrifugation at 4,000× g for 10 min at 4°C, and resuspended in 50 mL infiltration buffer (5% w/v Sucrose and 0.03% v/v Silwet L-77). Resuspended Agrobacterium cells were dropped onto each floral buds of Arabidopsis plants followed by incubating plants in dark at 21°C for 16 h. Plants were then grown under normal conditions as described earlier in this chapter until seeds were harvested for screening. The *rccr2*^{155} EMS mutant line was transformed with pEarley-ZISO; mutant line *rccr2*^{4}, *rccr2*^{90} and *rccr2*^{130} were transformed with pEarley-PSY and *rccr2*^{154} with pEarley-DET1. At least 10 independent transgenic lines were generated for each transformation and selected by spraying seedlings grown on soil with 50 mg/L of glufosinate-ammonium salt.

2.5 Pigments measurement

2.5.1 HPLC-based carotenoid analysis

Carotenoids from Arabidopsis leaf, root and 7-d old etiolated seedlings was quantified by HPLC as previously described. Frozen tissues of 3-5 biological replicates from each treatment condition were ground to fine powder using a Qiagen TissueLyser®. Pigments were isolated under green safe light with 400 µL of carotenoid extraction buffer (60% v/v ethyl acetate and 40% v/v acetone) and partitioned into the ethyl acetate layer by adding 320 µL of H_2O. The carotenoid-containing organic phase was separated via centrifugation and analysed by reverse phase HPLC (Agilent 1200 Series) using either the GraceSmart (4-µm, 4.6 × 250-mm column; Alltech) or Allsphere (OD2 Column 5-µm, 4.6 x 250-mm; Grace Davison) C_{18} columns. An ethyl acetate gradient of acetonitrile, milli-Q water, and triethylamine (9:1:0.01) with a flow rate of 1 mL/min separated carotenoids based upon retention time relative to known standards and their absorbance spectra at 440 nm (xanthophylls and some *cis*-carotenes), 340 nm

(phytofluene) and 286 nm (phytoene). Quantification of individual pigments was performed by integrating peak area on the chromatogram to nanomolar units using standard curves and was normalized against fresh weight (milligrams).

HPLC analysis and quantification of SDC was performed at the lab of Prof Ralf Welsch (Faculty of Biology II, University of Freiburg) as previously described (Welsch et al., 2008). For saponification, extracts were mixed with 4 mL of ethanol, 120 µL KOH (1 $g.mL^{-1}$) added, vortexed for 20 sec, heated for 10 min at 85°C and cooled on ice. Six millilitres of 1% (w/v) NaCl solution was added, vortexed and carotenoids were extracted twice with 2 mL of petroleum ether:diethyl ether (PE:DE, 2:1, v/v).

To examine the phytoene levels in yeast alongside split ubiquitin and β-galactosidase activity assays, yeast cells were lysed by sonication in 2 mL of 100% acetone on ice (30 cycles of 10 s on /10 s off). Lysates were centrifuged at 15,000× g for 10 min at 4°C and the following extraction of phytoene and HPLC analysis were performed as per described for SDC at the lab of Prof Ralf Welsch.

2.5.2 Protochlorophyllide quantification

Protochlorophyllides (Pchlides) were extracted and measured using published methods (Kolossov and Rebeiz, 2003) with modifications. Around 100 mg of 7-d old etiolated Arabidopsis seedlings were harvested under dim-green safe light, frozen in liquid nitrogen and ground to fine powder using a TissueLyser® (QIAGEN) at 25 sec^{-1} for 2 min. Two milliliters of 80% acetone pre-chilled to -20°C was added to each sample and the mixture was briefly homogenized. After centrifugation at 18,000× g for 10 min at 1°C, supernatant was split to 2×1 mL for Pchlides and protein extraction. Fully esterified tetrapyrroles were extracted from the acetone extracts with equal volume followed by 1/3 volume of hexane. Pchlides remained in the hexane-extracted acetone residue (HEAR) were used for fluorescence measurement using a TECAN M1000PRO plate reader (Tecan Group, Männedorf Switzerland) and net fluorescence were determined as previously described (Rebeiz, 2002). Pchlides in HEAR fraction were then transferred to diethyl ether by adding 200 µL diethyl ether, 60 µL saturated NaCl and 15 µL 0.37 M KH_2PO_4 at pH 7.7, followed by 100 µL diethyl ether only. The absorbance of Pchlides in diethyl ether was measured with TECAN M1000PRO (Tecan Group) and concentration was determined as described before (Rebeiz, 2002) to cross check the fluorescence measurements.

Protein extraction was performed using 80% acetone and 10% TCA; protein concentration was measured with Bradford reagent (Bio-Rad) and used to normalize the net fluorescence and concentration of Pchlides.

2.5.3 Chlorophyll concentration measurement

Total chlorophyll was measured as described previously (Porra et al., 1989) with minor modifications. Briefly, 20 seedlings of each samples were put in a 1.5 mL centrifuge tube with a 3.175 mm steel ball, frozen in liquid nitrogen for 5 min and homogenised in a TissueLyser® (QIAGEN) for 2 min at 25 s^{-1}. Homogenised tissue was rigorously resuspended in 300 µL of extraction buffer (80% acetone and 2.5 $mmol.L^{-1}$ NaH_2PO_4, pH 7.4), incubated at 4°C in dark for 15 min and centrifuged at 20,800× g for 10 min. Two hundred and fifty microliters of supernatant was transferred to a NUNC 96-well plate (Thermo Fisher Scientific) and measurements of A647, A664 and A750 were obtained using an iMark Microplate Absorbance Reader (Thermo Fisher Scientific). Total chlorophyll of each extraction was determined using the following equation modified from (Porra, 2002): (Chl a + Chl b) (µg) = (17.76 × (A647-A750) + 7.34 × (A664-A750)) × 0.895 × 0.25.

2.6 RNA library construction and differential gene expression analysis

2.6.1 RNA extraction and library construction

Total RNA was extracted from Arabidopsis leaf tissues grown under 8-h photoperiod or etiolated seedlings grown in dark for 7 d by TRIzol Reagent. RNA was treated with TURBO DNase and recovered with Agencourt RNAClean XP magnetic beads. The concentration was then determined using LabChip DS. The quality of RNA was examined by LabChip GXII (PerkinElmer) and samples with a quality score greater than 7.0 were used to construct RNA libraries. Libraries were constructed from 1 µg DNase-treated total RNA using Illumina TruSeq Stranded mRNA Library Prep Kit (Illumina, CA USA) followed by size selection (~280 bp) using AMPure XP Beads (Beckman Coulter). Quality control of RNA libraries was performed using LabChip GXII (PerkinElmer), followed by dilution of libraries to an equal concentration of 10 $nmol.L^{-1}$ and checking the concentration again using a Qubit DS DNA HS Assay Kit (ThermoFisher Scientific). Libraries were then pooled and pair-end sequenced by Illumina

HiSEQ2000. On average 15 million reads were obtained from sequencing each library and 21,365-23,840 mRNA transcripts were identified.

2.6.2 Data analysis

After sequencing, quality control was performed with FASTQC v.0.11.2 (Andrews), adapters removed using scythe v.0.991 with flags -p 0.01 for the prior (Buffalo), reads quality trimmed with sickle v.1.33 with flags q 20 (quality threshold) -l 20 (minimum read length after trimming) (Najoshi), aligned to the Arabidopsis genome (TAIR10) using the subjunc v.1.4.6 aligner with -u and -H flags to report only reads with a single, unambiguous best mapping location (Liao et al., 2014), and the number of reads mapping per gene was summarised using featureCounts v. 1.4.6 with flags -s 2, -P and -c to map reverse stranded and discard read pairs mapping to different chromosomes (Liao et al., 2014).

Statistical testing for relative gene expression was performed in R using edgeR v.3.4.2 (Robinson and Smyth, 2007, 2008; Robinson et al., 2010; Robinson and Oshlack, 2010; McCarthy et al., 2012), voom (Law et al., 2014) in the limma package 3.20.1 (Smyth, 2004, 2005). Transcripts were considered differentially expressed where fold change greater than 2 and FDR adjusted $P < 0.05$. The bioinformatics analysis pipeline from fastq to summarised counts per gene is available https:// github.com/pedrocrisp/NGS-pipelines.

2.7 Quantitative reverse transcriptase polymerase chain reaction (qRT-PCR)

Plant tissues were collected and snap-frozen in liquid nitrogen then physically disrupted by QIAGEN TissueLyser® at 25 sec^{-1} for 1 min. The total RNA was extracted from the fine powder of plant tissue using Spectrum™ Plant Total RNA kit (Sigma-Aldrich) included an on-column DNase I treatment according to the manufacturer's protocol. Isolated samples were quantified using LabChip DS (PerkinElmer) prior to the cDNA synthesis. First strand cDNA synthesis was performed using 1 µg total RNA, Oligo dT18 primer and Transcriptor First Strand cDNA synthesis kit (Roche, Basel, Switzerland) according to manufacturer's instructions. The relative transcript abundance was quantified using LightCycler 480 (Roche). The qRT-PCR was performed with mixture of 2 µL of primer mix (2 µM from each Forward and Reverse primer), 1 µL 1/10 diluted cDNA template, 5 µL LightCycler 480 SYBR Green I Master mix and sterile

milli-Q water up to the total volume of 10 µL. For each sample, three technical replicates for each of one to three biological replicates were tested. The relative gene expression levels were calculated by using relative quantification (Target Eff Ct(Wt-target)/Reference Eff Ct(Wt-target)) and fit point analysis (Pfaffl, 2001). Protein Phosphatase 2A (At1g13320) gene was used as house-keeper reference control for all experiments (Czechowski et al., 2005). In cases where absolute qualification is needed, cloning plasmids carrying wild type transcript or splicing variant is used as reference to generate a standard curve and optimize qPCR protocols. All primer sequences are listed in Table 2.3.

2.8 Transmission electron microscopy

Cotyledons from 5-d old etiolated seedlings were harvested in dim-green safe light and fixed overnight in primary fixation buffer (2.5% Glutaraldehyde, and 4% paraformaldehyde in 0.1 M phosphate buffer pH 7.2) under vacuum, post-fixed in 1% osmium tetraoxide for 1 h, followed by an ethanol series: 50%, 70%, 80%, 90%, 95% and 3 × 100% for 10 min each. After dehydration, samples were incubated in epon araldite (resin):ethanol at 1:2, 1:1 and 2:1 for 30 min each, then 3 times in 100% resin for 2 h. Samples were then transferred to fresh resin and hardened under nitrogen stream at 60°C for 2 days, followed by sectioning of samples using Leica EM UC7 ultramicrotome (Leica Microsystems, Wetzlar, Germany). Sections were placed on copper grids, stained with 5% uranyl acetate, washed thoroughly with distilled water, dried, and imaged with H7100FA transmission electron microscope (Hitachi, Pleasanton, CA) at 100 kV. For each of the dark-grown-seedling samples, prolamellar bodies were counted from 12 fields on 3 grids.

Table 2.3 qRT-PCR primers used in this study.

Name	Sequence	Description
PSY145eFq PSY145eRq	GGCAATCTACGGTAAGTTAC GCAACTGTATCAGCGAGA	Forward and reverse primers for testing wild type *PSY* transcript without intron 3 (162bp)
PSY145iFq PSY145iRq	CCAATGGTTGAAGAGCTG CAGCTTCAACTTCTCTTG	Forward and reverse primers for testing *psy-145* splicing variant containing intron 3 (155bp)
DET1-154Fq DET1-154Rq	ATCTTCAGGGAGATTTGGAATGAA GGATGATGATCAGCACTTCTTGTT	Forward and reverse primers for testing *det1-154* splicing of exon 4 (194bp/125bp)
PP2AFq PP2ARq	CTTCGTGCAGTATCGCTTCTC ATTGGAGAGCTTGATTTGCG	Forward and reverse primers for testing Protein Phosphatase 2A House Keeper
PORAFq PORARq	TTTCGGAGCAAAGCAAAGC TTTGTGACTGATGGAGTTGAAG	Forward and reverse primers for testing gene encoding Protochlorophyllide Oxidoreductase A
PORBFq PORBRq	CCCTTCAAAGCGTCTCATC AATCTCCTCCATCAATCATAGC	Forward and reverse primers for testing gene encoding Protochlorophyllide Oxidoreductase B
PORCFq PORCRq	ACCATCAAGGAACAGAGAAGAC CTAAACCTAAACCAGACGAAGC	Forward and reverse primers for testing gene encoding Protochlorophyllide Oxidoreductase C

2.9 Protein localisation using green fluorescent protein (GFP) tagging

2.9.1 Plasmid construction

Full length coding regions of wild type Arabidopsis PSY protein, mutants identified in this study, reported *Zea mays* PSY variants ZmPSY1-$N_{168}T_{257}$, ZmPSY1-$N_{168}P_{257}$ (Shumskaya et al., 2012) and their equivalents in Arabidopsis AtPSY-$N_{181}T_{270}$ and AtPSY-$N_{181}P_{270}$ were chemically synthesized by Thermo Fisher Scientific and cloned into the intermediate vector pDONR221, followed by gateway cloning to pDEST15-CGFP vector (Gift from Professor James Whalen, La Trobe University) to construct pCGFP-AtPSY-WT, pCGFP-AtPSY4, pCGFP-AtPSY90, pCGFP-AtPSY130, pCGFP-ZmPSY-NT, pCGFP-ZmPSY-NP, pCGFP-AtPSY-NT and pCGFP-AtPSY-NP.

2.9.2 Protoplast isolation and transient expression of GFP-fusion PSY protein

To isolate etiolated or green Arabidopsis protoplasts, 200 mg of etiolated or green cotyledons were harvested under green safe light and treated in a 9-mm Petri dish with an enzyme solution (0.5% cellulase, 0.05% pectinase, 600 mmol.L^{-1} mannitol, 10 mmol.L^{-1} $CaCl_2$ and 20 mmol.L^{-1} MES pH 5.6) at 21°C for 6 h with gentle shaking, followed by shaking vigorously for 3 min. The protoplasts were collected through a 60-µm nylon filter and washed 3 times with 20 mL cold washing buffer (600 mmol.L^{-1} mannitol, 10 mmol.L^{-1} $CaCl_2$ and 20 mmol.L^{-1} MES pH 5.6), by centrifugation at 120× g for 5 min and resuspending the pellet. The number of protoplasts per mL was determined using a haemocytometer. In 150 µL of 600 mmol.L^{-1} mannitol containing 10 mmol.L^{-1} $CaCl_2$, 10 µg of one PSY-CGFP plasmid and equal amount of SSU-RFP plasmid (Gift from Dr. Yan Wang, La Trobe University) were both added to 10^6 protoplasts and mixed gently for 5 s. Five hundred microliters of 40% polyethylene glycol 6000 solution (in 500 mmol.L^{-1} mannitol and 100 mmol.L^{-1} $Ca(NO_3)_2$) was added and the contents were mixed gently for 15 s, followed by dilution with 4.5 mL mannitol/MES solution (500 mmol.L^{-1} mannitol, 15 mmol.L^{-1} $MgCl_2$ and 0.1% MES pH 5.6) and incubation at 21°C for 20 min. The protoplasts were pelleted by centrifugation at 120× g and washed with 600 mmol.L^{-1} mannitol and 10 mmol.L^{-1} $CaCl_2$, followed by incubation for 16 h at 25°C in dark. The

protoplasts were subjected to confocal microscopy and western blot using isolated stromal and membrane fractions.

2.9.3 Confocal microscopy

The expression of PSY-GFP fusion proteins was visualised using Leica TCS SP2 Laser Scanning Confocal Microscope (Leica Microsystems) with an excitation at 460/480 nm and fluorescence was detected at 495 nm to 540 nm, while RFP was detected at 570 nm to 625 nm with the excitation at 535/555 nm. An HC PL APO 40x/1.10 water immersion objective was used for all images.

2.10 *In vitro* and *in vivo* enzymatic assays of phytoene synthase

2.10.1 Vector design

Coding regions of wild type Arabidopsis PSY and mutants identified in this study were codon-optimised and cloned into pRSETA (ThermoFisher Scientific) through restriction sites *Xho* I and *Eco*R I that were attached respectively to the 5'- and 3'-end of the chemically synthesized sequences. Following the prediction of chloroplast-targeting peptide of PSY on ChloroP 1.1 Server (http://www.cbs.dtu.dk/services/ChloroP/), 55 codons at the 5'-end of *PSY* gene, exclusive of start codon, were deleted from the designed coding sequences. Codon optimisation was done using the GeneOptimizer portal of ThermoFisher Scientific https://www.thermofisher.com/au/en/home/life-science/cloning/gene-synthesis/geneart-gene-synthesis/geneoptimizer.html). To facilitate the purification of recombinant PSY without additional tags, sequence "GAAAATCTGTATTTTCAGGGT" that encodes TEV protease (Tobacco Etch Virus nuclear-inclusion-a endopeptidase) was inserted between *Xho* I site and start codon. Chemical synthesis and cloning were carried out by ThermoFisher Scientific, and the plasmids were verified by sequencing and restriction enzyme digestion in our lab. pRSET-PSY-WT, pRSET-PSY4, pRSET-PSY90 and pRSET-PSY130 were transformed to *E. coli* strain DH5α for propagation, followed by transforming BL21 (DE3) strain for the expression of recombinant PSY.

2.10.2 Transformation

Competent DH5α and BL21 (DE3) cells were made following a simplified protocol. *E. coli*

strains were streaked on LB plates containing no antibiotics and single colonies were inoculated in 5 mL of LB. Following an overnight culture at 37°C, cells were diluted by 100-fold in LB medium and cultured at 37°C with constant shaking at 250 rpm until OD_{600} reached 0.4-0.6. The LB culture was incubated on ice for 20 min and cells were pelleted by centrifugation at 4,000× g for 10 min at 4°C. Cell pelleted were washed once with 1/2 volume of cold 100 $mmol.L^{-1}$ $CaCl_2$ and resuspended in 1/100 volume of 100 $mmol.L^{-1}$ $CaCl_2$. The resuspended chemical competent cells in a 50-µL aliquot were then mix with 100 ng plasmid DNA and incubated on ice for 30 min, followed by heat shock at 42°C for 90 s and incubation on ice for 2 min. The mix of competent cells and plasmid DNA was diluted by 500 µL LB medium and incubated at 37°C for 45 min. Cells (100 µL) were then spread on an LB plate containing 100 $mg.L^{-1}$ Ampicillin and incubated for 14 h at 37°C. Single colonies were inoculated and cultured overnight at 37°C for the extraction of plasmid DNA if in DH5α strain, or for the expression of recombinant PSY if in BL21 (DE3).

2.10.3 Induction and verification of the expression of recombinant PSY protein

For induction, overnight small cultures were diluted 100-fold in fresh LB medium containing 100 $mg.L^{-1}$ Ampicillin and grown at 37°C to mid-log phase ($OD6_{00}$=0.5-0.7). Induction was initiated by the addition of 0.5 $mmol.L^{-1}$ IPTG (Isopropyl β-D-1-thiogalactopyranoside, final concentration) and constant shaking at 28°C. Cells were harvested after 4-h induction by centrifugation at 5,000× g and washed once in 1/2 culture volume of phosphate-buffered saline (PBS). Cells were resuspended in 1/20 culture volume of lysis buffer (100 $mmol.L^{-1}$ Tris.HCl pH 7.0, 5 $mmol.L^{-1}$ EDTA, 5 $mmol.L^{-1}$ DTT), and disrupted by lysozyme treatment (200 $mg.L^{-1}$) for 20 min at 30°C followed by sonication on ice (50-100 cycles of 10 s on /10 s off). The soluble and insoluble (inclusion body) fractions were separated by centrifugation at 22,000× g for 1 h at 4°C, and the insoluble fraction was washed 3 times with 1/20 culture volume of wash buffer (100 $mmol.L^{-1}$ Tris.HCl pH 7.0, 5 $mmol.L^{-1}$ EDTA, 5 $mmol.L^{-1}$ DTT, 2$mmol.L^{-1}$ urea and 2% w/v Triton X-100) and once with wash buffer without Triton X-100, centrifuging at 22,000× g for 30 min at 4°C to clarify the suspension. Recombinant PSY in the inclusion bodies was extracted from washed pellets using 1/100 culture volume of extraction buffer (50 $mmol.L^{-1}$ Tris.HCl pH 7.0, 5 $mmol.L^{-1}$ EDTA, 5 $mmol.L^{-1}$ DTT and 8 $mol.L^{-1}$ guanidine.HCl),

and was diluted by 5-fold before loaded to a Bolt 17-well 4% – 12% Bis-Tris Plus gel (Thermo Fisher Scientific). To examine the expression of recombinant PSY in both soluble fraction and inclusion bodies, 10 µL of each sample was mixed with equal volume of 2× LDS buffer and heated for 10 min at 70°C followed by incubation on ice for 3 min. The gel was run for 42 min at 165 volt after 20 µL of each treated protein sample was loaded; gel was stained with GelCode® Blue Safe Protein Stain (ThermoFisher Scientific) to visualise protein bands.

2.10.4 Purification and identification of recombinant proteins from soluble fraction

In a typical preparation of recombinant PSY protein from soluble fraction, *E. coli* cells were harvested following induction by centrifugation at 5,000× g. The pellets were washed with cold PBS and resuspended in 50 mL buffer A (50 mmol.L^{-1} NaH_2PO_4, 20 mmol.L^{-1} imidazole, 1 mol.L^{-1} NaCl, pH 7.4), and lysed by lysozyme treatment and sonication on ice as described in the above section. After centrifugation at 22,000× g for 30 min at 4°C, the supernatant that contained the soluble fraction was loaded onto a Pierce 5-ml Ni-NTA column (ThermoFisher Scientific) that had been equilibrated with buffer A. The column was washed with 25 mL buffer A that contained 40 mmol.L^{-1} imidazole and then with buffer A that contained 60 mmol.L^{-1} imidazole. Protein was eluted using an appropriate volume of buffer A that contained 200 mmol.L^{-1} imidazole, 10 µL of which was subjected to gel electrophoresis (detailed above) and western blot with anti-PSY polyclonal antibody as per described in the corresponding section of this chapter. Buffer exchange to TEV digestion buffer (50 mmol.L^{-1} Tris.HCl pH 8.0, 150 mmol.L^{-1} NaCl, 20 mmol.L^{-1} KCl, 2 mmol.L^{-1} β-mercaptoethanol) was carried out using a Pierce desalting spin column (ThermoFisher Scientific). The column was equilibrated with 400 µL TEV digestion buffer three times and 100 µL purified recombinant protein was loaded with 20 µL TEV digestion buffer to improve recovery percentage. Protein samples were collected by centrifuging the column at 1,500× g for 2 min. Protein samples were pooled after buffer exchange and concentration was determined using Bradford reagent (Bio-Rad), followed by digesting 500 µL of protein using TEV (TEV:protein = 1:8) at 4°C for 14 h. A Pierce 5-ml Ni-NTA column (ThermoFisher Scientific) was equilibrated with TEV digestion buffer and TEV-cleaved recombinant PSY was loaded, followed by eluting 4 times the recombinant protein with 100 µL digestion buffer each. The concentration of TEV-cleaved and purified recombinant PSY

protein was determined again before *in vitro* enzymatic assays.

2.10.5 *In vitro* activity assay of recombinant PSY

Artificial chromosome pAC-GGPPipi, a gift from Dr. Nazia Nisar (Department of Agriculture and Water Resources) and propagated in our lab, was verified by restriction enzyme digestion and transformed to TOP 10 chemical competent cells as previously described in this chapter. After spreading the cells on LB plates containing 25 $mg.L^{-1}$ chloramphenicol and incubation for 14 h at 37°C followed by 6 d at room temperature, single colonies were inoculated to 20 mL chloramphenicol-containing LB medium and cultured at 28°C for 18 h to synthesise GGPP in *E. coli*. The same colonies were also inoculated and cultured in LB medium with 25 $mg.L^{-1}$ chloramphenicol at 37°C for 14 h to extract artificial chromosome followed by verification. TOP 10 strain carrying pAC-PHYT was used as a positive control to verify the absorbance peek of phytoene in HPLC.

Cells were harvested by centrifugation at 12,000× g for 10 min at 4°C, and 1 g of cells (wet weight) were resuspended in 2 mL of enzyme assay buffer (100 $mmol.L^{-1}$ Tris.HCl pH 7.6, 10 $mmol.L^{-1}$ $MgCl_2$, 2 $mmol.L^{-1}$ $MnCl_2$, 1$mmol.L^{-1}$ 3,3',3''-phosphanetriyltripropanoic acid, 20% v/v glycerol and 0.08% v/v Tween 80). Cells were lysed by sonication (20 cycles of 10 s on /10 s off) on ice, followed by centrifugation at 20,000× g for 30 min at 4°C. To the supernatant 5 µg of purified recombinant PSY protein was added, followed by incubation at 20°C in dark for 20 min. At a 4-min interval, 200 µL aliquots were withdraw and the reaction was stopped by adding EDTA (500 $mmol.L^{-1}$ stock pH 8.0) to a final concentration of 50 $mmol.L^{-1}$. Assays were extracted by adding 260 µL carotenoid extraction buffer and partitioning phytoene into ethyl acetate phase. The extractions were dried under nitrogen stream in dark, resuspended in 100 µL ethyl acetate and subjected to HPLC as described previously in this chapter.

2.10.6 *In vitro* activity assay of endogenous Arabidopsis PSY

The immunoprecipitation of endogenous PSY was performed using P-PER® Plant Protein Extraction Kit and Pierce Co-Immunoprecipitation kit (both from ThermoFisher Scientific) following manufacturer's instructions and is summarised below.

For total protein extraction, 160 mg leaf tissue from a 25-d old Arabidopsis plant grown under 16-h photoperiod was homogenised in 3.5 mL P-PER® Working Solution containing 20 µL Halt™ Protease Inhibitor Cocktail (ThermoFisher Scientific). Following centrifugation at 3,500×

g for 5 min, the lower aqueous layer containing total protein was recovered for the immunoprecipitation of PSY which is described in the corresponding sections in this chapter. Five micrograms of endogenous PSY co-immunoprecipitate (with binding proteins) was subjected to enzymatic activity assay as described in the above section for recombinant PSY.

2.10.7 *In vivo* PSY activity assay

In vivo PSY activity was examining by measuring phytoene levels in norflurazon-treated Arabidopsis SDC. Generation of SDC and HPLC analysis were carried out as previously described in this chapter.

2.11 Split Ubiquitin System

Split-ubiquitin and β-galactosidase activity assays were carried out at our collaborators' lab (Prof. Ralf Welsch) The cDNA sequences of wild type *AtPSY* gene and mutants were amplified from constructs pCGFP-AtPSY-WT, pCGFP-AtPSY4, pCGFP-AtPSY90 and pCGFP-AtPSY130 by PCR using Phusion proof-reading polymerase (New England Biolabs) and the primers listed in Table 2.2. Coding sequences were truncated and the 56 codons encoding a predicted chloroplast-targeting signal were deleted from the 5'-end of *PSY* gene. The cDNA sequences of Arabidopsis *OR* and *GGPS11* genes were designed (with chloroplast-targeting peptides removed) and amplified at our collaborators' lab. The truncated cDNA sequences of *AtPSY*, *AtOR* and *AtGGPPS11* were cloned to make Cub- or Nub-fusion constructs which were then transformed into yeast strain THY.AP5 (Cub) or THY.AP4 (Nub). Yeast strains carrying Cub fusions were mated with strains carrying Cub fusions and the resulting diploid cells were grown on synthetic complete medium lacking leucine and tryptophane (-LW). Interaction growth tests were performed with overnight cultures spotted on fully selective medium (-LWAH), in a series of 1:10 dilutions with a starting OD_{600} of 2 after grown for about 2 d at 29°C. To reduce background activation of reporter genes and visualize different interaction strengths, methionine was added to the medium suppressing the expression of Cub-fusion proteins (+Met; 150 µmol.L^{-1} and 1 mmol.L^{-1}). Control combinations with empty Cub- or Nub-expressing vectors were included in the experiments.

For β-galactosidase activity assays, yeast cells were pelleted from 250 µL overnight culture in complete medium and resuspended in 650 µL assay buffer (100 mmol.L^{-1} HEPES.KOH pH 7.0, 150 mmol.L^{-1} NaCl, 2 mmol.L^{-1} $MgCl_2$, and 1% w/v BSA), followed by adding 50 µL chloroform

and 50 µL 0.1% (w/v) SDS and vortex for 1 min. Enzymatic reactions were started by adding 125 µL of 4 $mg.mL^{-1}$ *ortho*-nitrophenyl-β-galactoside in the assay buffer. Following an incubation at 30°C until the mixture turned visibly yellow, reactions were stopped by adding 400 µL of 1 $mol.L^{-1}$ Na_2CO_3. Reactions were then centrifuged for 5 min at 20,000× g and OD_{420} was measured to determine the concentration of *ortho*-nitrophenol (oNP) in the supernatant. B-galactosidase activity was calculated as nmol $oNP.min^{-1}.OD_{600}^{-1}$, using the molar extinction coefficient:oNP = 3300 $g.L^{-1}.mol^{-1}$. All β-galactosidase activity assays were performed in triplicate.

2.12 Western blot, immunoprecipitation and enzyme-linked immunosorbent assay

2.12.1 Isolation of stromal and membrane fractions from Arabidopsis etioplasts

Two hundred micrograms of etiolated Arabidopsis seedlings (7-d old) were ground manually using a sterile plastic mini-pestle in a 5-mL Eppendorf tube with 1.2 mL isolation buffer (330 $mmol.L^{-1}$ D-sorbitol, 20 $mmol.L^{-1}$ MOPS, 13 $mmol.L^{-1}$ Tris, 3 mmol $MgCl_2$ and 0.1% w/v BSA, pH 7.5). One gram of homogenised seedlings were combined and filtered through 40-micron nylon mesh (Shanghai Blotting Cloth, Shanghai China). The homogenate was centrifuged at room temperature for 1 min at 250× g, followed by centrifugation at 4°C for 7 min at 2,000× g. To isolate intact etioplasts, the pellet was resuspended in 10 mL isolation buffer and layered on 40% (w/v) Percoll® (Sigma-Aldrich) followed by centrifugation at 2,000× g for 5 min at 4°C. The Percoll® layer was removed and the etioplast pellet was washed twice with 5 mL isolation buffer. Etiolated protoplasts transiently expressing PSY-GFP fusion proteins were also resuspended in 10 mL isolation buffer following the same protocol to isolate intact etioplasts. Etioplasts were then resuspended in 600 µL hypotonic buffer containing 10 $mmol.L^{-1}$ Tris.HCl pH 7.0 and 4 $mmol.L^{-1}$ $MgCl_2$ by vortex for 30 s and then centrifuged at 12,000× g for 10 min. The pellet (total membranes) was resuspended in 600 µL µL hypotonic buffer; 10 µL supernatant (stroma) or 10 µL resuspended membranes was treated with equal volume of 2× LDS buffer and subjected to denatured protein gel electrophoresis, followed by western blot using anti-PSY or anti-GFP antibody.

For isolation of prototthylakoids from PLBs, etioplasts were isolated as described above and resuspended in 5 mL hypotonic buffer for a 10-min lysis on ice. PLBs were pelleted through centrifugation at 3,000× g for 15 min at 4°C and resuspended in 5 mL hypotonic buffer. Following an ultrasonic bath treatment (Model Fx 10, Unisonics, NSW Australia) for 3× 3 min with 1-min intervals on ice, the suspension was layered on a sucrose step gradient (15 mL of 1 mol.L^{-1} sucrose under 10 mL of 600 mmol.L^{-1} sucrose in hypotonic buffer) and centrifuged at 4°C for 3 h at 75,000× g. Protothylakoids accumulating at the interface of the gradient were collected, diluted with equal volume of hypotonic buffer and concentrated by ultracentrifugation at 125,000× g for 1 h at 4°C; the protothylakoids which pelleted below the gradient were harvested and combined with the fraction collected from the interface. The combined protothylakoid fractions were resuspended in 600 µL hypotonic buffer and 10 µL of each sample was used for western blot.

2.12.2 Protein extraction and western blot

Fifty to one hundred milligrams of etiolated Arabidopsis seedlings (7-d old) were harvested under dim-green safe light and frozen in liquid nitrogen; around 100 mg green leaf tissues of 25-d old plants were harvested under normal light and frozen in liquid nitrogen. Tissues were ground to fine powder using a QIAGEN TissueLyser® at 25 sec^{-1} for 1 min. Total protein was extracted by adding 1 mL extraction solution (10% Trichloroacetic acid, TCA and 0.07% Dithiothreitol, DTT in 100% Acetone) and incubating at -80°C overnight. Protein pellets formed by centrifugation at 15,000× g and 4°C for 15 min were washed twice using Acetone contain 0.07% DTT. Pellets were re-suspended in 100 µL – 200 µL solubilisation buffer (9 mol.L^{-1} Urea, 4% CHAPS, 1% DTT and 35 mmol.L^{-1} Tris Base), sonicated and incubated at room temperature overnight. Samples were centrifuged at 15,000× g and room temperature for 15 min and the concentration of protein in supernatant was measured using Bradford reagent (Bio-Rad).

The concentration of protein in each sample was adjusted to 2 µg.$µL^{-1}$ by mixing with solubilisation buffer. For western blot using anti-POR antibody (Agrisera Antibodies, Vännäs SWEDEN, AS05067), 5 µg total protein of each sample was heated for 10 min at 70°C in 1× LDS buffer (Thermo Fisher Scientific) and loaded to a Bolt 17-well 4% – 12% Bis-Tris Plus gel (Thermo Fisher Scientific); to examine DET1 protein levels using western blot, 10 µg total protein of each sample was loaded to the gel; to examine recombinant PSY protein from *E. coli* cell lysates, endogenous PSY from stromal or membrane fractions of Arabidopsis

etioplasts or PSY-GFP fusion protein transiently expressed in etioplasts, 10 µL of each sample was used for gel electrophoresis; to examine endogenous PSY or OR protein levels in Arabidopsis leaf tissues, 10 µg total protein of each sample was used for gel electrophoresis; to detect OR protein from co-immunoprecipitation, 10 µL of PSY co-immunoprecipitate was loaded to the gel. The gel was run for 38 min at 165 volt and proteins were transfer to a PVDF membrane (Bio-Rad) using a Bio-Rad Trans-Blot® Turbo™ Transfer System. PVDF membranes were blocked in 1× TBST buffer containing 5% skim milk powder at 4°C overnight, and then incubated with anti-POR polyclonal antibody (1:2000), anti-PSY polyclonal antibody (1:1000, Agrisera Antibodies AS163991), anti-OR polyclonal antibody (1:1000, gift from Prof. Li Li, College of Agriculture and Life Sciences, Cornell University) or anti-GFP polyclonal antibody (1:2500, Agrisera Antibodies AS152987) for 2 h at room temperature. Before an overnight incubation of a PVDF membrane with anti-DET1 polyclonal antibody (1:1000, Agrisera Antibodies AS153082), the membrane was blocked at room temperature for 2 h. PVDF membranes were then washed 3 × 10 min at room temperature with 20 ml of 1× TBST buffer and incubated with HRP-conjugated Goat anti-Rabbit IgG (1:2500, Agrisera Antibodies AS09602) at room temperature for 90 min. The membranes were washed another 3 times and covered by 1.5 mL of ECL™ Prime Western Blotting Detection Reagent (GE Healthcare Life Sciences, PA USA). Following an incubation of 5 min in dark, the membranes were subjected to a FUSION Pulse Chemiluminescence/ Fluorescence Imaging System (Fisher Biotech, WA Australia) to visualize and record the bands. As an internal reference to examine proteins attracted from Arabidopsis plants, PVDF membranes were re-probed using anti-Actin polyclonal antibody (1:3000, Agrisera Antibodies AS132640) and HRP-conjugated Goat anti-Rabbit IgG (1:2500, Agrisera Antibodies), followed by visualization of the bands. Semi-quantification of bands from western blot was performed using Image J (Schneider et al., 2012).

2.12.3 Immunoprecipitation and co-immunoprecipitation

Immunoprecipitation was performed with Pierce Co-Immunoprecipitation Kit (ThermoFisher Scientific), according to the manufacturer's instructions. Briefly, 20 µg of anti-PSY antibody in 200 µL 1× coupling buffer was coupled to 50 µL of AminoLink Plus coupling resin by adding 3 µL sodium cyanoborohydride solution and incubating the reaction on a rotator at room temperature for 2 h. The resin was washed with 200 µL 1× coupling buffer followed by 200 µL

quenching buffer. Another 3 µL sodium cyanoborohydride solution and 200 µL quenching buffer were added to the resin and incubated for 15 min. The resin was then washed twice with 200 µL 1× coupling buffer and 6 times with 150 µL washing solution.

About 2 mL of total protein extracted from 160 mg Arabidopsis leaf tissue were pre-cleared with 160 µL of control agarose resin and then incubated with 50 µL antibody-coupled AminoLink Plus resin overnight at 4°C. Three to four 500-µL aliquots were loaded onto a spin column one by one and centrifuged at 1000× g for 1 min. The column was washed 3 times with 200 µL wash buffer and proteins were eluted with 100 µL elution buffer, followed by adding 5 µL of 1 $mol.L^{-1}$ Tris (pH 9.5) to neutralise the eluent. Immunoprecipitation with normal rabbit IgG (Agrisera Antibodies AS101545) was included as a negative control for the specificity of anti-PSY antibody.

2.12.4 Enzyme-linked immunosorbent assay

All enzyme-linked immunosorbent assays (ELISAs) were carried out in Clear Flat-Bottom Immuno 96-well plates (ThermoFisher Scientific Catalog# 655061), and to each well all reagents were added at a volume of 50 µL. Plates were coated with Arabidopsis total protein (20 $\mu g.mL^{-1}$) diluted in carbonate buffer (pH 9.6) at 4°C overnight, followed by washing the plates 3 times with PBST (PBS with 0.05% v/v Triton X-100, pH 7.4). Plates were then blocked for 1 h at room temperature with 5% skim milk powder in PBS-TY buffer (PBS with 0.05% v/v Triton X-100 and 1% w/v yeast extract, pH7.4) followed by washing the plates 3 times with PBST. Plates were then incubated with anti-PSY (1 $\mu g.mL^{-1}$, Agrisera Antibodies AS163991) or anti-OR (1 $\mu g.mL^{-1}$, gift from Prof. Li Li), washed and incubated with HRP-conjugated Goat anti-Rabbit IgG (0.4 $\mu g.mL^{-1}$, Agrisera Antibodies AS09602). All antibodies were diluted in PBS-TY buffer and all incubations were performed at 37°C for 1 h. After each incubation, plates were washed 3 times with PBST by shaking at 150 rpm for 5 min at room temperature.

After antibody incubations and washing the plates, substrate solution containing 0.5 $mg.mL^{-1}$ O-phenylenediamine dihydrochloride (Sigma-Aldrich) in phosphate-citrate buffer (pH 5.0) and 0.02% (v/v) H_2O_2 was added and incubated for 5 min at room temperature. The reactions were stopped with 50 µL of 2$mol.L^{-1}$ H_2SO_4, and the absorbance at 492 nm was measured on a TECAN M1000PRO plate reader (Tecan Group). Solubilisation buffer diluted in carbonate buffer was used as blank control and a serial dilution of purified recombinant PSY protein in

carbonate buffer was used as positive control. All ELISAs were done in triplicates.

2.13 Statistical analysis

Analysis of variance (ANOVA) was performed to test for significant ($P < 0.05$) differences between three or more sample groups and one-way ANOVA was used for a single independent variable. In cases where two independent variables were involved in the analyses, two-way ANOVA was carried out. In ANOVA analyses, post-hoc Tukey's Honestly Significant Difference (HSD) tests were also performed and Tukey groups were generated. Sigma Plot version 11.0 (Systat Software, IL USA) or SPSS version 22.0 (IBM Software, NY USA) was used for statistical analyses in the present study.

Chapter 3: Identification of genes regulating plastid development in the *ccr2* mutant

3.1 Introduction

Depending upon the environment, the developmental program that a newly germinated seedling adopts can be skotomorphogenesis in the dark or photomorphogenesis in the light. Young seedlings undergoing skotomorphogenesis have elongated hypocotyls, unopened apical hooks and closed cotyledons (Josse and Halliday, 2008) (Figure 3.1A). Phytochrome interacting factors (PIFs) accumulate in dark and promote skotomorphogenesis by regulating around 10% of gene in the genome, including the repression of photosynthesis associated nuclear genes (*PhANG*s) (Leivar et al., 2008; Leivar and Monte, 2014). HY5, a positive regulator of photomorphogenesis, is degraded by COP1 associated with CCD complex (COP10/DET1/DDB1) in dark and hence photomorphogenic development is repressed (Osterlund et al., 2000b; Osterlund et al., 2000a; Saijo et al., 2003) (Figure 3.1B). In the cotyledons of a dark-grown seedling, proplastids differentiate into etioplasts which exhibit a characteristic paracrystalline membrane structure known as prolamellar body (PLB) (Solymosi and Schoefs, 2010; Pogson and Albrecht, 2011). PLBs contain protochlorophyllide (Pchlide), a precursor of chlorophyll bound to protochlorophyllide oxidoreductase (POR), NADPH, lipids, a few proteins and usually two carotenoids: violaxanthin and lutein that are essential for photoprotection and light harvesting in a "future" chloroplast (Pogson and Albrecht, 2011).

Upon illumination, etiolated seedlings proceed with photomorphogenesis (or deetiolation) and the apical hook and cotyledons are opened (Figure 3.1A) (Pogson and Albrecht, 2011; Rudowska et al., 2012). COP1 and PIFs are deactivated in light through interaction with active phytochrome B (phytochrome B-Pfr) (Yi and Deng, 2005; Leivar et al., 2008) and HY5 promotes photomorphogenic development by positively regulating *PhANG*s (Lee et al., 2007) (Figure 3.1B). During photomorphogenesis, etioplasts differentiate into chloroplasts and the membrane structures of PLBs are transformed into grana and stroma thylakoids (Adam et al., 2011). Alternatively, a proplastid directly differentiates into a chloroplast in the light (Sakamoto et al.,

2008). In angiosperms, light induces the enzyme activity of POR that converts Pchlide to chlorophyllide *a*, which is subsequently converted to chlorophyll *a* and *b* (Forreiter and Apel, 1993). Due to up-regulation of *PhANG*s, proteins involved in photosynthesis, especially thylakoid proteins, are rapidly synthesized upon illumination (von Zychlinski et al., 2005; Kleffmann et al., 2007), and a coordination between the biosynthesis of pigments and the import of pigment-binding proteins is required for the formation of photosynthetic complexes on thylakoids. Hence, the biosynthesis of carotenoids and chlorophylls is tightly regulated during chloroplast development as they are essential for the assembly of photosynthetic system and photoprotection.

Plastid development is largely under nuclear control which is referred to as anterograde control (Leon et al., 1998; Richly and Leister, 2004; Cui et al., 2006). However, the coordination of plastid development and gene expression is also mediated by retrograde control, in which the signals produced in a plastid are transduced to nucleus and regulate nuclear gene expression (Woodson and Chory, 2008; Pogson and Albrecht, 2011; Estavillo et al., 2012; Chi et al., 2013; Chan et al., 2016). Carotenoids are essential components of a PLB during skotomorphogenesis and protect a newly generated chloroplast from being photo-bleached once a seedling is switched to photomorphogenic development. It has hence been hypothesized that carotenoids or their derivatives can trigger retrograde signals, regulating plastid development and fine-tuning carotenoid biosynthesis (Hou et al., 2016) (Figure 3.2). Although in recent studies, apocarotenoids, the cleavage products of carotenoids, were found to regulate leaf and root development and act as photooxidative stress signals (Ramel et al., 2012; Avendano-Vazquez et al., 2014; Van Norman et al., 2014), the regulatory roles of apocarotenoids in plastid development have remained unclear.

The *ccr2* (*carotenoid and chloroplast regulation 2*) mutant displays altered skotomorphogenesis and all etioplasts contain no PLB in dark-grown seedlings. Consequently, the seedlings show delayed greening when illuminated. While *ccr2* plants grown under 16-h photoperiod are green, newly emerged leaf tissues from *ccr2* plants grown under 8-h photoperiod contain impaired chloroplasts and display a distinctive yellowing phenotype, indicating altered

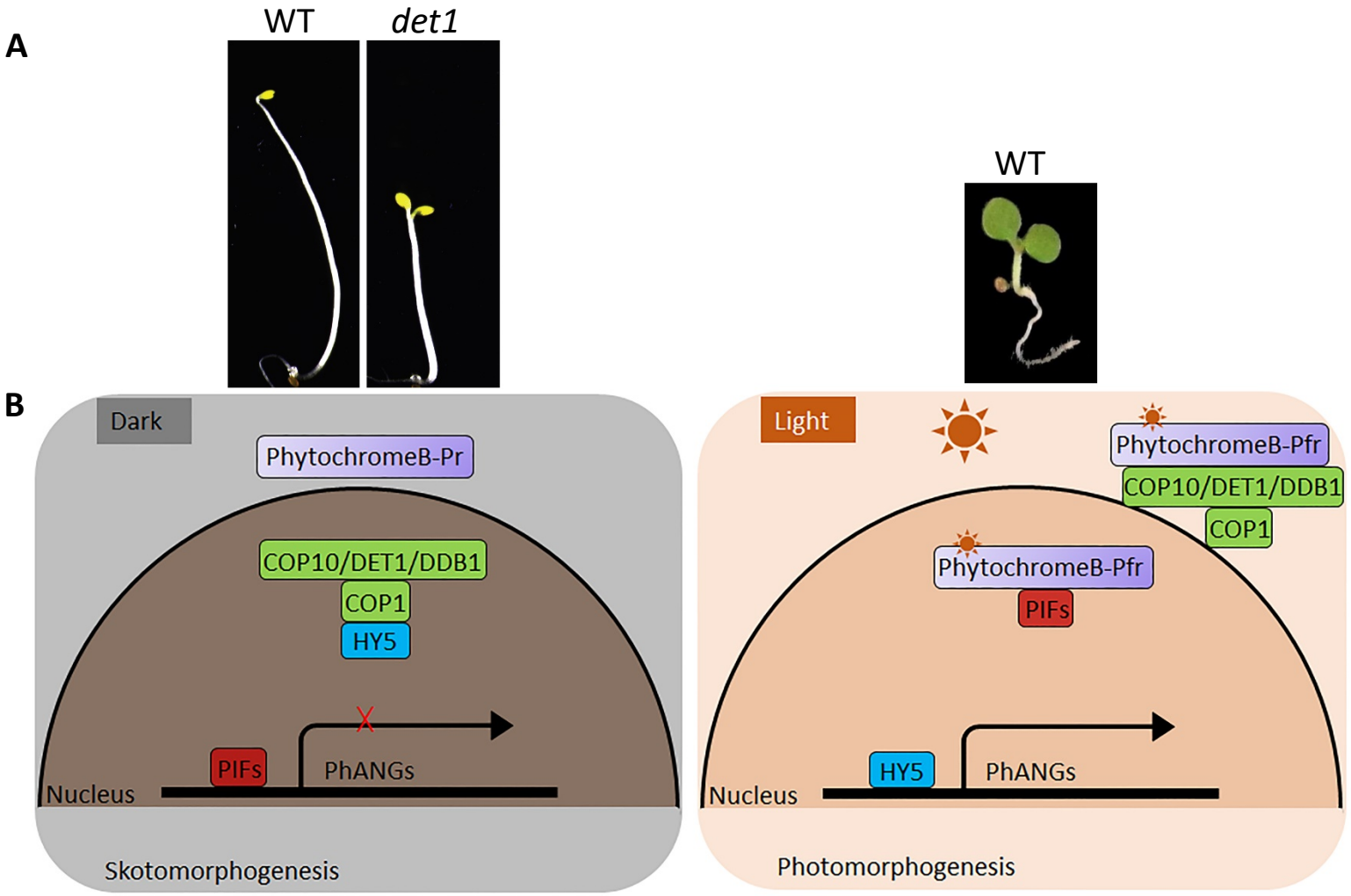

Figure 3.1 Plant development and regulation of gene expression in dark and light. A. Plants accumulate carotenoids but not chlorophylls in dark, consequently the cotyledons display a yellow colour. Wilde type Arabidopsis seedlings (WT) grown in dark have elongated hypocotyl, unopened apical hook and closed cotyledons, while a *det1* mutant has short hypocotyl, opened apical hook and opened cotyledons. In light, a wild type Arabidopsis seedling synthesizes chlorophylls and has short hypocotyl, no apical hook and opened cotyledons. B. In dark, the CDD complex (COP10/DET1/DDB1) aids in COP1-mediated degradation of HY5 and PIFs repress the expression of *PhANG*s (photosynthesis associated nuclear genes) by its promoter-binding activity. In light, phytochrome B is activated to Pfr form that deactivates the CCD complex and interacts with PIFs. Following light activation of phytochrome B, PIFs are phosphorylated and targeted for proteolytic degradation. HY5 promotes photomorphogenesis by positively regulating *PhANG*s.

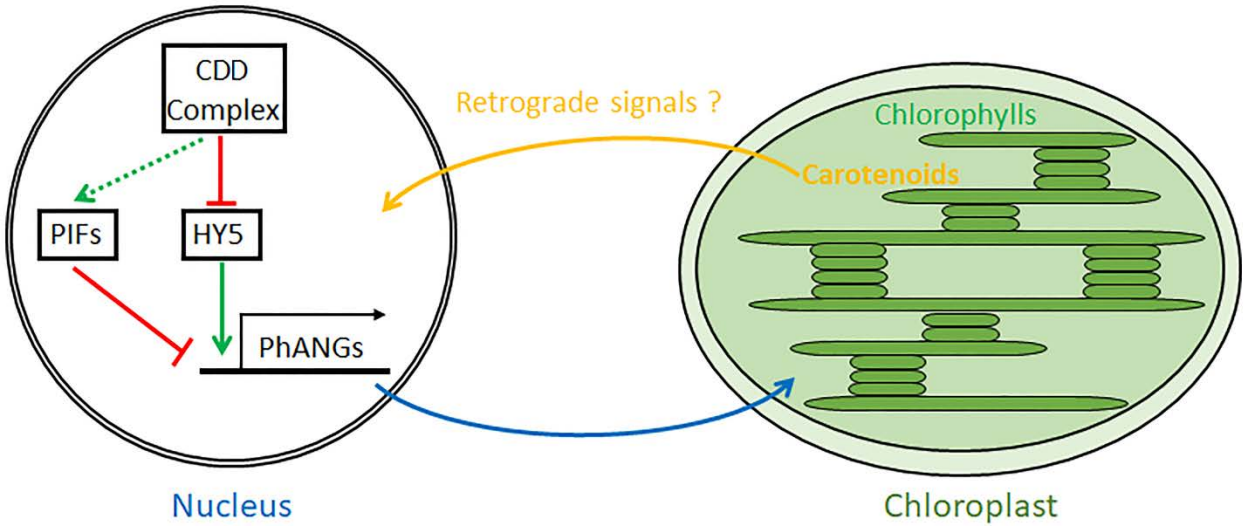

Figure 3.2 A schematic model speculates that carotenoids may trigger retrograde signals modulating photosynthesis associated nuclear genes (*PhANG*s) expression and subsequently regulating chloroplast development.

photomorphogenesis (Park et al., 2002). Due to loss of function of carotenoid isomerase (CRTISO), *ccr2* accumulates *cis*-configured carotenoids (Park et al., 2002), which suggests the mutant to be a model in studying the functions of carotenoid-derived signals in plastid development.

To elucidate the carotenoid-derived retrograde signals that regulate plastid development, we performed forward genetics study in which 180 EMS mutant lines were generated in a *ccr2* background and 26 of them reverted the *ccr2* leaf yellowing phenotype under 8-h photoperiod. The revertants of *ccr2* were named as *rccr2* lines. We then performed Next-Generation Sequencing (NGS) of the 26 *rccr2* lines to identify the causal mutations in each line and studied the functions of mutated genes which link carotenoid-derived signals to plastid development.

3.2 Results

3.2.1 Phenotypes of the *ccr2* mutant

In comparison to wild type Arabidopsis plants (WT), the *ccr2* mutant showed a distinctive yellowing phenotype in newly developed leaf tissue undergoing cell differentiation when it is grown under a short 8-h photoperiod (Figure 3.3A). The leaf-yellowing phenotype was reproduced by shifting 3-week old *ccr2* plants from a 16-h photoperiod to 8 h (Figure 3.3B). While

the newly emerged leaf tissue remained yellow, the mature leaf sectors of *ccr2* appeared green. Irrespective of photoperiods and shifts, the rosette leafs from WT were green (Figure 3.3A and B). The percentage of yellow leaf area in a *ccr2* plant was about 12-fold higher than WT when measured using the Scanalyzer imaging system (Figure 3.4A). Accordingly, the total chlorophyll level in the yellow sectors of *ccr2* leaves was reduced by more than 2-fold compared to WT rosette leaves, while that in the mature green leaves of *ccr2* displayed no significant difference to WT (Figure 3.4B). Consistent with the reduction of chlorophyll levels in *ccr2* yellow leaf (YL) sectors, total carotenoid content was significantly reduced due to lower levels of neoxanthin, lutein and β-carotene, although antheraxanthin and zeaxanthin were increased. In the mature green leaves (GL) of *ccr2*, total carotenoid content was about 2-fold higher than in YL; in both YL and GL of *ccr2*, lutein levels were significantly lower than in WT leaves, which was identified as another typical *ccr2* phenotype in addition to leaf yellowing (Table 3.1 and Figure 3.5). In *ccr2* YL, transmission electron microscopy (TEM) showed abnormal chloroplasts lack thylakoid and grana stacks, indicating impaired plastid membrane structures in comparison to that in WT rosette leaves (see Figure 4.1E in Chapter 4). Reportedly the cotyledon greening of *ccr2* is delayed in comparison to WT (Park et al., 2002), etiolated Arabidopsis seedlings were hence exposed to continuous white light (80 $\mu mol.m^{-2}.s^{-1}$) and chlorophyll levels were measured at 12-h intervals after illumination. Compared to WT seedlings, *ccr2* displayed severely reduced chlorophyll biosynthesis (Figure 3.6, data shown at 24-h intervals) and its total chlorophyll content was only about 50% of WT level after 72 h of illumination. A G-A mutation in *crtiso* gene leads to loss-of-function of carotenoid isomerase (CRTISO) in *ccr2* (Park et al., 2002), and consequently the accumulation of *cis*-carotenoids that are synthesized upstream of CRTISO in the carotenogenic pathway was observed in etiolated seedlings using HPLC analyses, whereas none of these *cis*-isomers was detectable in WT seedlings (Table 3.2).

Compared to WT, *ccr2* also displayed terminated primary floral meristem and altered floral architecture, producing a stunted floral architecture that failed to produce healthy siliques with viable seed (Figure 3.7A and B), and the root length of *ccr2* is also severely reduced (Figure 3.8)

3.2.2 Characterization of revertants of *ccr2* (*rccr2*)

To elucidate the nature of the speculated carotenoid-derived retrograde signals in *ccr2* that lead to impaired plastid development, a forward genetic screen was performed by growing the M2 generation seedlings of EMS-mutagenized *ccr2* under a 10-h photoperiod and 26 clear revertants of *ccr2* (*rccr2*) were identified. All 26 *rccr2* lines showed a complete reversion of the leaf yellowing phenotype of *ccr2* under a 10-h photoperiod and displayed newly emerged green leaves similar in colour to that of WT (Figure 3.4A).

Consistent with the greening in newly emerged leaf tissues, the chlorophyll content of all *rccr2* lines was similar to WT (Figure 3.4B). Although in most *rccr2* lines the biosynthesis of chlorophyll during cotyledon greening showed no significant differences to WT, 6 lines displayed delayed greening which resembled *ccr2* (Figure 3.6), suggesting that in those lines only leaf greening but not cotyledon greening was restored. Leaf tissues of all *rccr2* lines contained reduced lutein (Figure 3.5) and a total carotenoid level similar to GL of *ccr2*, although individual carotenoid levels varied (Table 3.1 and discussed in 3.3); the *cis*-carotenoid profiles of *rccr2*^{4}, *rccr2*^{74}, *rccr2*^{90}, *rccr2*^{130}, *rccr2*^{145}, *rccr2*^{154} and *rccr2*^{155} were altered when compared to *ccr2* (Table 3.2), indicating that carotenoid biosynthesis was affected by the EMS-introduced mutations in those *rccr2* lines, whereas the rest 19 lines possessed similar *cis*-carotenoid profiles to *ccr2*. None of the 26 *rccr2* lines reverted floral meristem termination and reduced root length that were observed in *ccr2* (Figures 3.7B and 3.8). In summary, all *rccr2* lines showed reversion in the leaf-yellowing phenotype normally displayed by *ccr2* plants grown under a shorter photoperiod, and all but a few *rccr2* lines showed normal cotyledon greening following deetiolation. Therefore, our *rccr2* screen specifically targeted phenotypes related to plastid development, and not root or reproductive development.

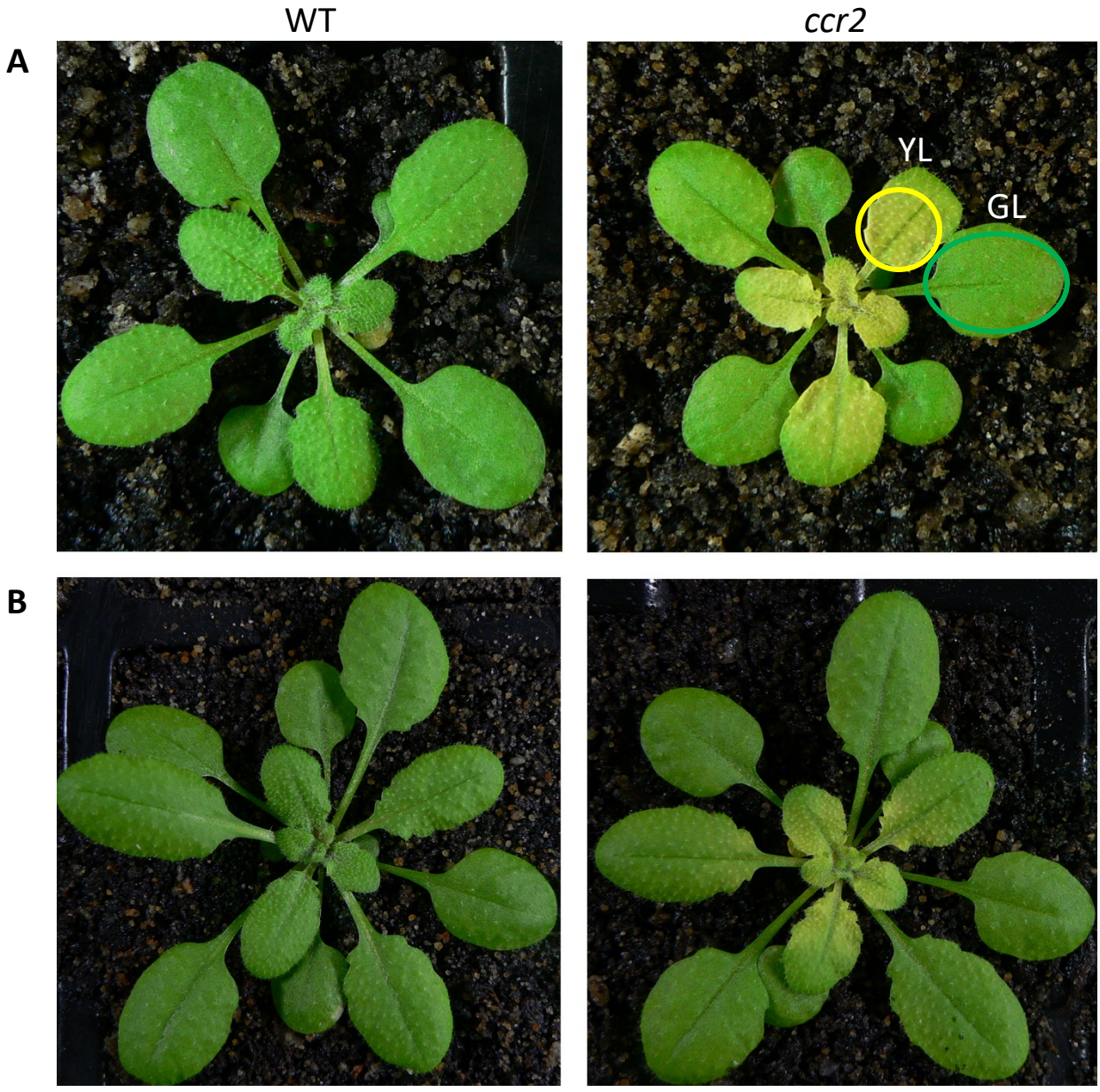

Figure 3.3 The *ccr2* mutant has a yellowing phenotype in newly emerged leaf tissues. A. Three-week old WT and *ccr2* plants growing under an 8-h photoperiod. In *ccr2*, newly formed leaf tissues are yellow (YL, yellow circle) and mature leaf tissues are green (GL, green circle). B. Three-week old plants were shifted from 16-h to 8-h photoperiod for one week. Irrespective of photoperiod and shifts, WT has green true leaves.

Figure 3.4A

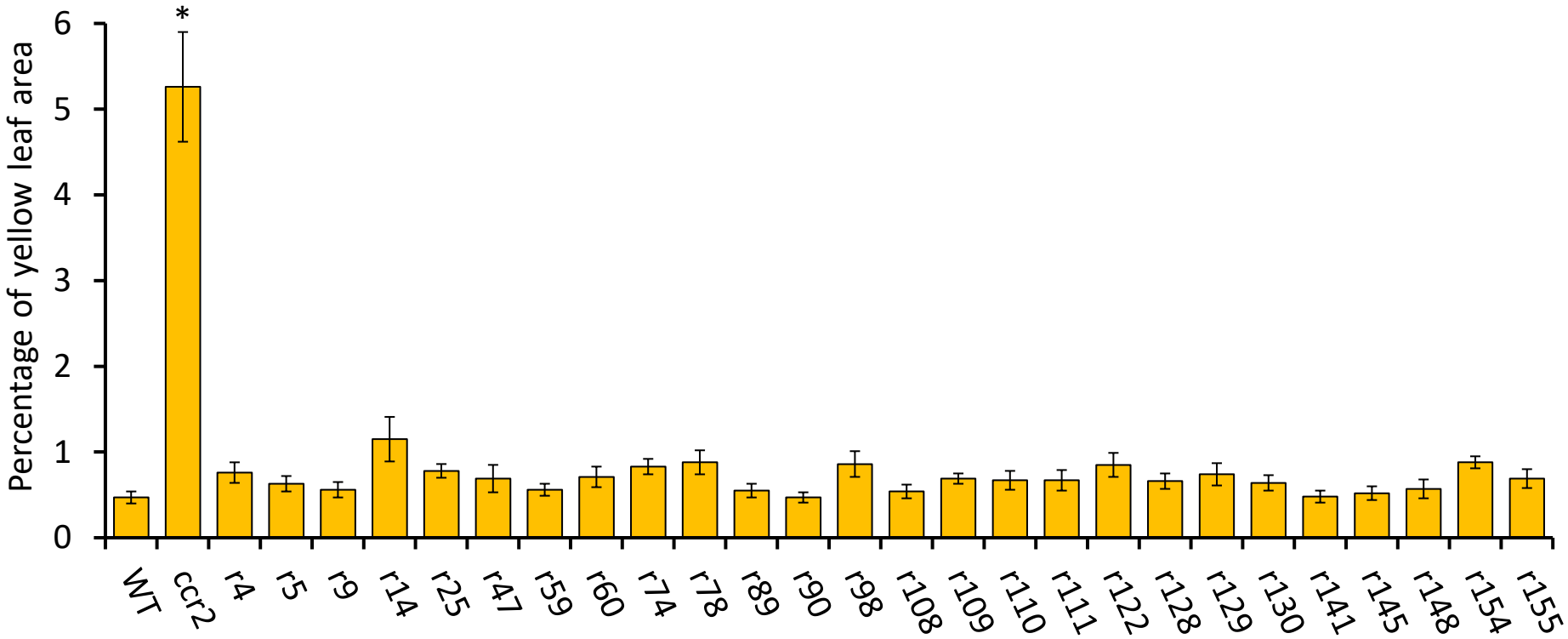
Percentage of yellow leaf area
0
1
2
3
4
5
6
*
WT
ccr2
r4
r5
r9
r14
r25
r47
r59
r60
r74
r78
r89
r90
r98
r108
r109
r110
r111
r122
r128
r129
r130
r141
r145
r148
r154
r155

Figure 3.4B

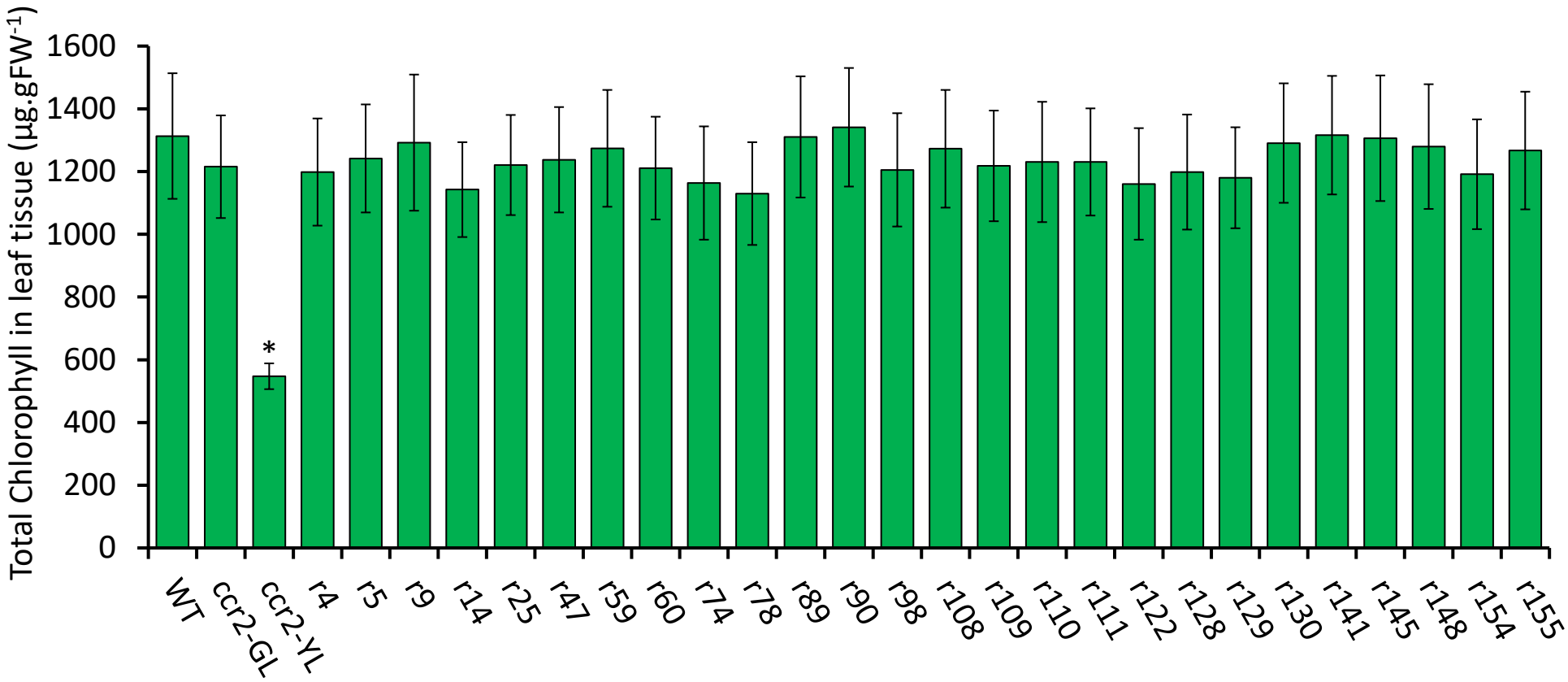

Figure 3.4 The *ccr2* mutant has increased yellow leaf area and reduced leaf chlorophyll content compared to WT, and *rccr2* (revertant of *ccr2*) lines reverted the phenotypes. All plants were grown under an 8-h photoperiod. A. Percentage of yellow leaf area of WT, *ccr2* and all *rccr2* lines. *rccr2* is abbreviated to "*r*" in the charts, e.g. *r*4 is the abbreviation of *rccr2*^{4}. B. Total chlorophyll in leaf tissue of WT, *ccr2* and all *rccr2* lines, showing that chlorophyll content is significantly reduced in *ccr2* yellow leaf tissue. Values were averaged from five biological replicates and error bars denote standard error. * *P*<0.05 in one-way ANOVA.

Table 3.1 Carotenoid levels (µg.gFW^{-1}) in the leaves of WT, *ccr2* and *rccr2* lines grown under an 8-h photoperiod

	WT	*ccr2* (YL)	*ccr2* (GL)	*rccr2*^{4}	*rccr2*^{5}	*rccr2*^{9}	*rccr2*^{14}	*rccr2*^{25}	*rccr2*^{47}	*rccr2*^{59}	*rccr2*^{60}	*rccr2*^{74}	*rccr2*^{78}	*rccr2*^{89}
Neo	30.63 b ±2.54	12.58 a ±0.92	27.60 b ±2.96	28.45 b ±1.79	27.00 b ±2.23	28.25 b ±1.56	28.59 b ±2.27	28.32 b ±2.69	25.82 b ±1.37	26.98 b ±1.65	24.52 b ±1.46	25.88 b ±2.14	29.85 b ±1.98	27.38 b ±1.84
Viol	45.57 a ±3.61	42.39 a ±2.86	66.92 b ±5.54	65.17 b ±3.67	67.14 b ±4.82	65.33 b ±6.02	70.62 b ±4.62	64.79 b ±3.99	62.57 b ±4.15	68.26 b ±4.20	62.73 b ±5.18	64.52 b ±3.76	85.93 d ±6.73	82.50cd ±5.22
Anth	1.92 a ±0.09	11.68 c ±1.07	10.51 c ±0.64	11.08 c ±0.73	12.45 c ±0.81	11.01 c ±0.75	17.81cd ±1.43	11.28 c ±1.02	15.69cd ±1.16	11.90 c ±0.89	11.64 c ±0.73	11.26 c ±1.04	9.15bc ±0.61	9.89bc ±0.58
Lut	113.60d ±9.52	23.86 a ±1.96	42.60 c ±3.78	43.86 c ±2.89	39.78 c ±2.13	41.57 c ±3.79	33.65bc ±2.22	40.63 c ±3.64	42.56 c ±3.51	39.84 c ±1.90	40.70 c ±3.05	47.63 c ±3.37	45.62 c ±2.96	43.76 c ±2.76
Zea	0.00 a ±0.00	5.68 e ±0.32	2.27 c ±0.18	2.09 c ±0.16	3.96 cd ±0.21	2.99 cd ±0.20	4.54 d ±0.40	2.32 c ±0.15	2.65 c ±0.17	2.19 c ±0.18	2.11 c ±0.18	2.54 c ±0.14	6.32 e ±0.36	4.08 d ±0.30
β-Car	64.32 d ±4.34	21.44 a ±1.73	61.64 d ±4.27	67.42de ±3.46	60.27 d ±4.02	62.54 d ±3.85	52.43bd ±4.23	62.25 d ±3.05	61.83 d ±4.19	60.76 d ±4.56	58.04cd ±5.10	58.27cd ±2.89	46.23 b ±2.02	45.67 b ±3.61
Total	256.04b ±20.10	117.63a ±8.86	211.54b ±17.37	218.07b ±12.70	210.60b ±14.22	211.69b ±16.17	207.64b ±15.17	209.59b ±14.54	211.12b ±14.55	209.93b ±13.38	199.74b ±15.70	210.10b ±13.34	223.10b ±14.66	213.28b ±14.31

Continue Table 3.1

	rccr2^{90}	*rccr2*^{98}	*rccr2*^{108}	*rccr2*^{109}	*rccr2*^{110}	*rccr2*^{111}	*rccr2*^{122}	*rccr2*^{128}	*rccr2*^{129}	*rccr2*^{130}	*rccr2*^{141}	*rccr2*^{145}	*rccr2*^{148}	*rccr2*^{154}	*rccr2*^{155}
Neo	29.29 b ±1.47	29.87 b ±1.66	25.74 b ±1.52	26.54 b ±2.12	25.78 b ±1.94	24.96 b ±1.76	27.45 b ±1.87	26.48 b ±1.26	26.52 b ±1.55	28.65 b ±2.00	26.34 b ±1.72	27.50 b ±1.84	25.63 b ±1.32	25.02 b ±1.25	28.15 b ±1.49
Viol	62.53 b ±4.33	61.64 b ±5.15	63.18 b ±3.82	62.73 b ±4.51	64.53 b ±3.09	67.58 b ±3.77	68.25 b ±4.02	62.16 b ±4.81	68.79 b ±3.97	72.23bc ±5.30	68.31 b ±4.02	61.75 b ±4.74	78.06cd ±5.69	48.17 a ±3.68	64.27 b ±4.62
Anth	16.24cd ±1.18	12.65c ±0.63	15.65cd ±0.87	15.42cd ±1.22	20.05 d ±1.85	15.27cd ±0.84	10.34 c ±0.61	11.09 c ±0.76	9.88 bc ±0.63	21.11 d ±1.86	16.19cd ±1.20	14.73cd ±0.78	13.86bd ±0.87	7.88 ac ±0.39	16.82cd ±1.14
Lut	42.51 c ±3.45	48.52 c ±3.17	46.76 c ±2.98	42.15 c ±3.56	43.58 c ±3.41	39.56 c ±2.58	44.34 c ±2.25	45.38 c ±3.50	46.23 c ±2.79	34.85bc ±2.87	40.05 c ±3.41	33.69bc ±3.28	34.57bc ±2.04	41.81 c ±3.66	43.43 c ±3.62
Zea	3.78 cd ±0.24	1.69 bc ±0.12	2.27 c ±0.16	1.12 b ±0.09	1.10 b ±0.08	4.62 d ±0.17	2.18 c ±0.17	2.83 cd ±0.14	2.27 c ±0.13	4.45 d ±0.35	5.24 de ±0.36	4.46 d ±0.28	4.54 d ±0.36	1.46 bc ±0.09	0.91 b ±0.03
β-Car	59.99 d ±3.78	66.91 d ±4.85	57.83cd ±4.16	63.36 d ±4.79	57.56cd ±3.56	63.20 d ±4.23	60.77 d ±5.78	54.56bd ±4.03	58.94cd ±3.52	64.39 d ±3.71	55.77bd ±2.90	60.01 d ±4.32	56.79cd ±4.07	73.59 e ±5.64	58.79cd ±2.65
Total	214.34b ±14.45	221.28b ±15.58	211.43b ±13.51	211.32b ±16.29	212.60b ±13.93	215.19b ±13.35	213.33b ±14.70	202.50b ±14.50	212.63b ±12.59	225.68b ±16.09	211.90b ±13.61	202.14b ±15.24	213.45b ±14.35	197.93b ±14.71	212.37b ±13.55

Neo: Neoxanthin; Viol: Violaxanthin; Anth: Antheraxanthin; Lut: Lutein; Zea: Zeaxanthin; β-Car: β-Carotene. Letters denote post-hoc Tukey groups from a one-way ANOVA test.

Table 3.2 *cis*-carotenoid levels (μg.gFW^{-1}) in etiolated seedlings (7-d old) of WT, *ccr2* and *rccr2* lines

	WT	*ccr2*	*rccr2*^{4}	*rccr2*^{5}	*rccr2*^{9}	*rccr2*^{14}	*rccr2*^{25}	*rccr2*^{47}	*rccr2*^{59}	*rccr2*^{60}	*rccr2*^{74}	*rccr2*^{78}	*rccr2*^{89}	*rccr2*^{90}
Phytoene	0.00 ±0.00	6.94 ±0.42	1.26* ±0.07	6.63 ±0.36	7.26 ±0.50	6.97 ±0.38	6.88 ±0.31	6.20 ±0.25	6.90 ±0.49	7.51 ±0.57	4.82* ±0.32	7.28 ±0.63	6.87 ±0.44	0.92* ±0.06
Phytofluene	0.00 ±0.00	4.68 ±0.28	1.72* ±0.09	4.45 ±0.32	4.85 ±0.25	4.73 ±0.34	4.53 ±0.30	4.25 ±0.40	4.72 ±0.29	5.03 ±0.38	3.51* ±0.29	4.93 ±0.41	4.58 ±0.37	1.24* ±0.05
ζ-Carotene	0.00 ±0.00	10.07 ±0.76	2.60* ±0.15	9.77 ±0.89	10.64 ±0.73	10.11 ±0.84	9.86 ±0.77	9.23 ±0.81	10.24 ±0.64	10.96 ±0.92	4.79* ±0.36	10.56 ±0.85	9.82 ±0.67	1.43* ±0.08
Neurosporene	0.00 ±0.00	3.55 ±0.22	2.58* ±0.14	3.48 ±0.18	3.78 ±0.15	3.42 ±0.15	3.50 ±0.16	3.27 ±0.27	3.48 ±0.24	3.92 ±0.18	2.60* ±0.15	3.85 ±0.21	3.46 ±0.23	1.66* ±0.09
Prolycopene	0.00 ±0.00	4.98 ±0.37	3.87* ±0.24	5.14 ±0.29	5.19 ±0.46	4.91 ±0.38	4.75 ±0.38	4.61 ±0.25	4.89 ±0.41	5.45 ±0.36	3.96* ±0.28	4.30 ±0.34	4.75 ±0.26	2.58* ±0.11

Continue Table 3.2

	rccr2^{98}	*rccr2*^{108}	*rccr2*^{109}	*rccr2*^{110}	*rccr2*^{111}	*rccr2*^{122}	*rccr2*^{128}	*rccr2*^{129}	*rccr2*^{130}	*rccr2*^{141}	*rccr2*^{145}	*rccr2*^{148}	*rccr2*^{154}	*rccr2*^{155}
Phytoene	7.17 ±0.66	6.80 ±0.45	6.86 ±0.54	7.20 ±0.58	7.26 ±0.53	6.99 ±0.41	6.58 ±0.34	6.64 ±0.47	1.37* ±0.07	7.30 ±0.56	2.11* ±0.14	6.76 ±0.51	6.12 ±0.60	7.55 ±0.69
Phytofluene	4.79 ±0.33	4.50 ±0.28	4.61 ±0.41	4.92 ±0.32	4.96 ±0.35	4.66 ±0.46	4.39 ±0.27	4.47 ±0.38	1.20* ±0.08	5.12 ±0.25	1.75* ±0.09	4.83 ±0.36	4.03 ±0.37	6.17* ±0.48
ζ-Carotene	10.36 ±0.95	9.83 ±0.76	9.90 ±0.77	10.47 ±0.68	10.57 ±0.90	10.04 ±0.74	9.76 ±0.59	9.76 ±0.63	2.89* ±0.18	11.00 ±1.06	4.48* ±0.35	9.85 ±0.51	9.24 ±0.80	3.68* ±0.24
Neurosporene	3.64 ±0.25	3.44 ±0.31	3.43 ±0.27	3.74 ±0.32	3.72 ±0.32	3.63 ±0.26	3.70 ±0.33	3.76 ±0.30	2.14* ±0.17	3.91 ±0.19	3.10 ±0.25	3.32 ±0.22	3.25 ±0.24	0.00* ±0.00
Prolycopene	4.81 ±0.36	4.85 ±0.40	4.85 ±0.29	5.13 ±0.42	5.22 ±0.41	4.91 ±0.37	4.73 ±0.35	4.72 ±0.28	3.06* ±0.19	5.44 ±0.27	4.76 ±0.43	4.78 ±0.35	3.46* ±0.45	0.00* ±0.00

*Difference is significant when compared to *ccr2*, *P*<0.05 in one-way ANOVA. ζ-Carotene: tri-*cis*-ζ-carotene and di-*cis*-ζ-carotene; Neurosporene: tri-*cis*-neurosporene; Prolycopene: tetra-*cis*-lycopene.

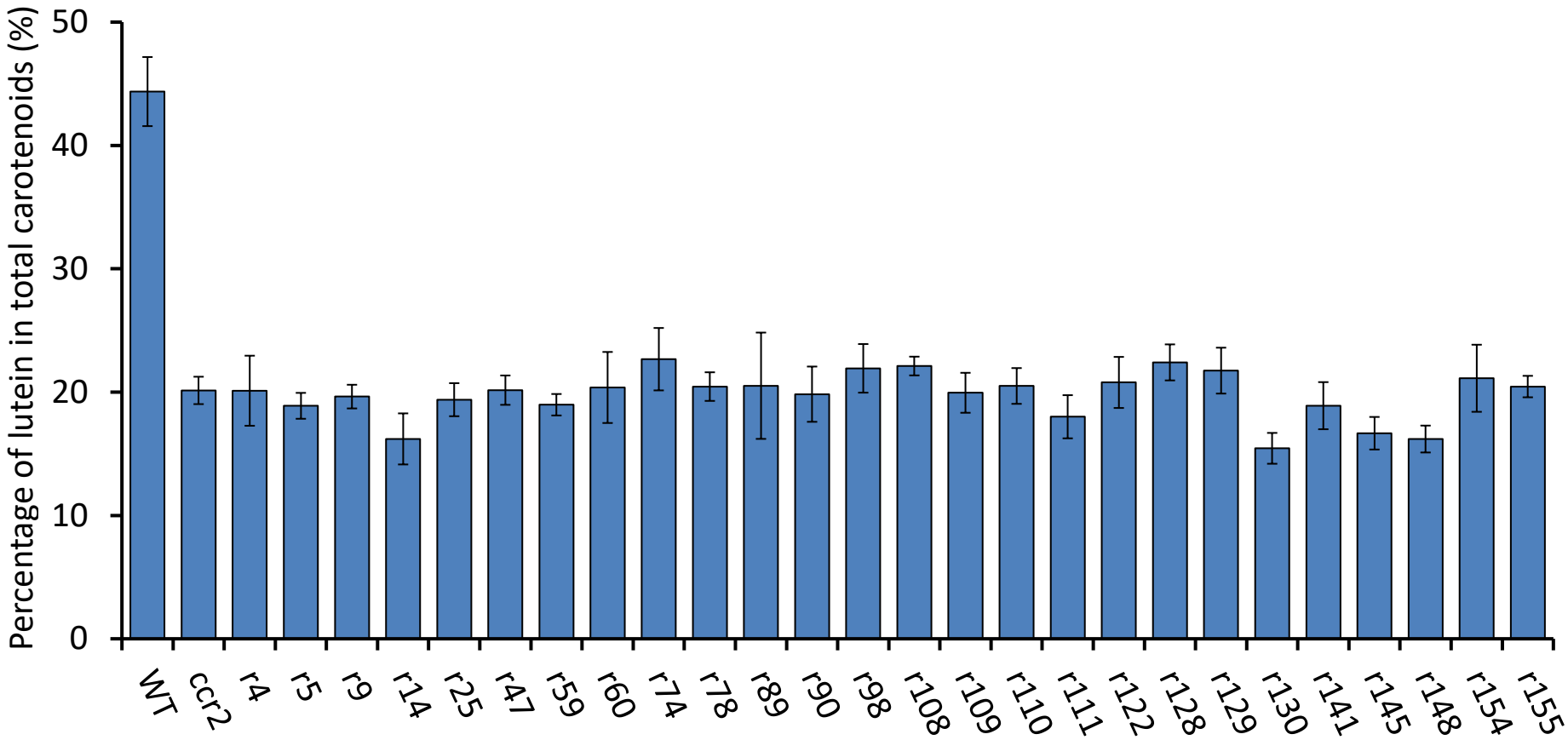

Figure 3.5 *ccr2* and all *rccr2* lines displayed reduced levels of lutein in comparison to WT. All plants were grown under an 8-h photoperiod. The yellow and green leaf tissues of *ccr2* both have reduced lutein levels and only that of green leaf tissue is shown in this figure. Values were averaged from at least three biological replicates and error bars denote standard error.

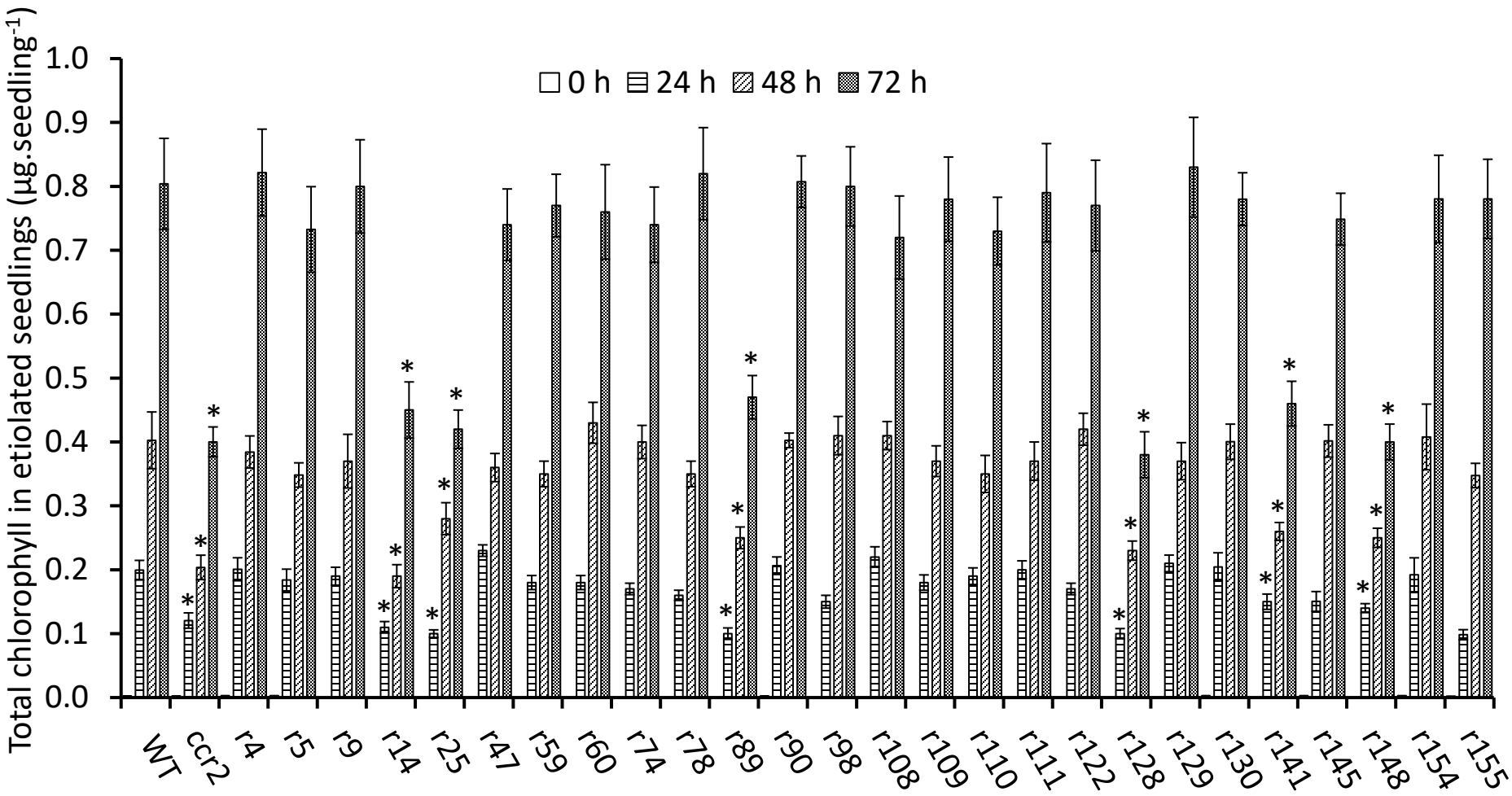

Figure 3.6 Total chlorophyll levels in cotyledons following de-etiolation. *ccr2* and six *rccr2* lines showed delayed greening compared to WT. WT, *ccr2*, and all *rccr2* lines were grown in darkness for 4 d, exposed to continuous white light and chlorophyll was measured at 12-h intervals. Chlorophyll levels at 0 h, 24 h, 48 h and 72 h are shown in the figure. *P<0.05 in one-way ANOVA. Each value was averaged from 20 seedlings and error bars denote standard error.

Figure 3.7A

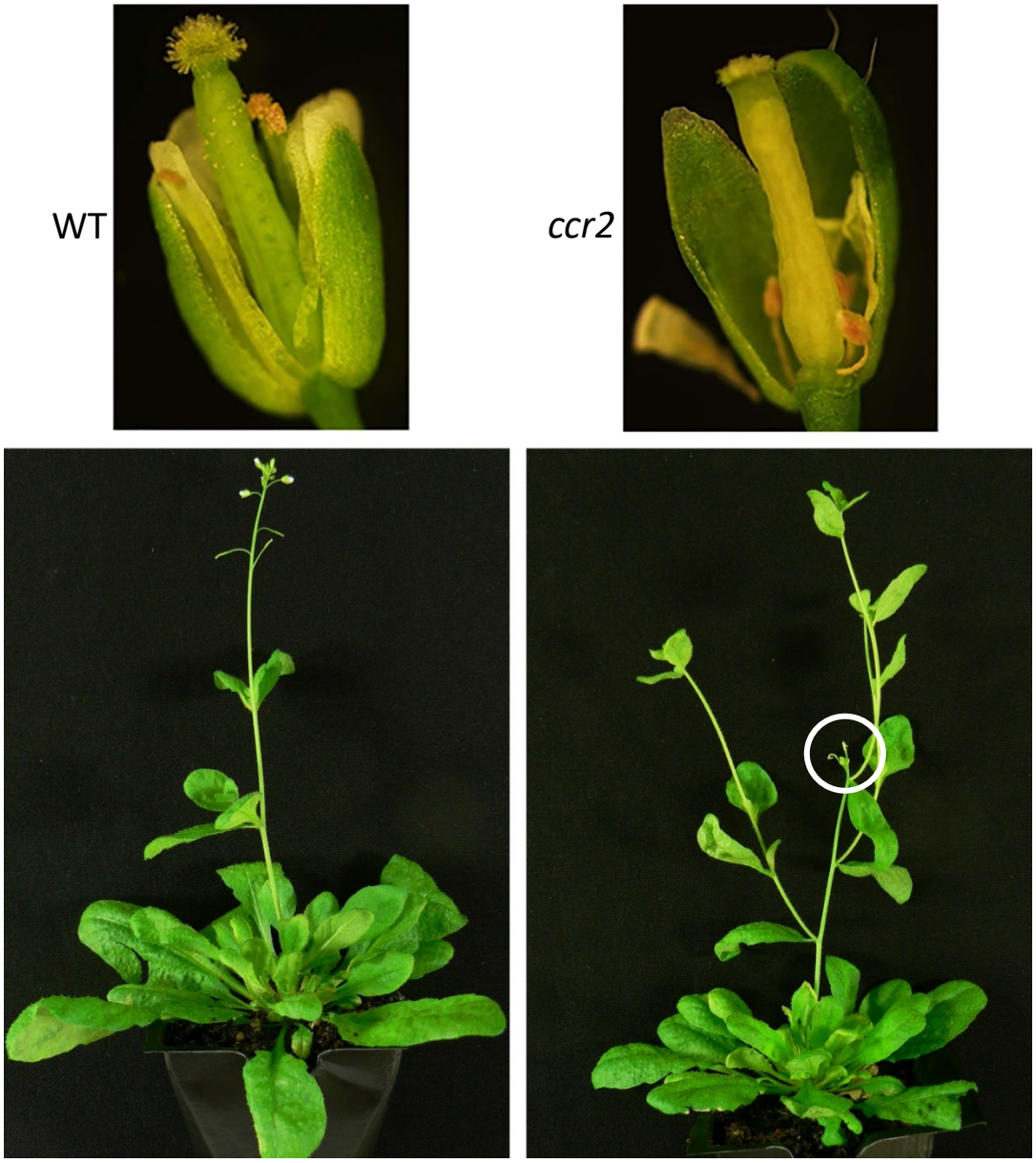

Figure 3.7B

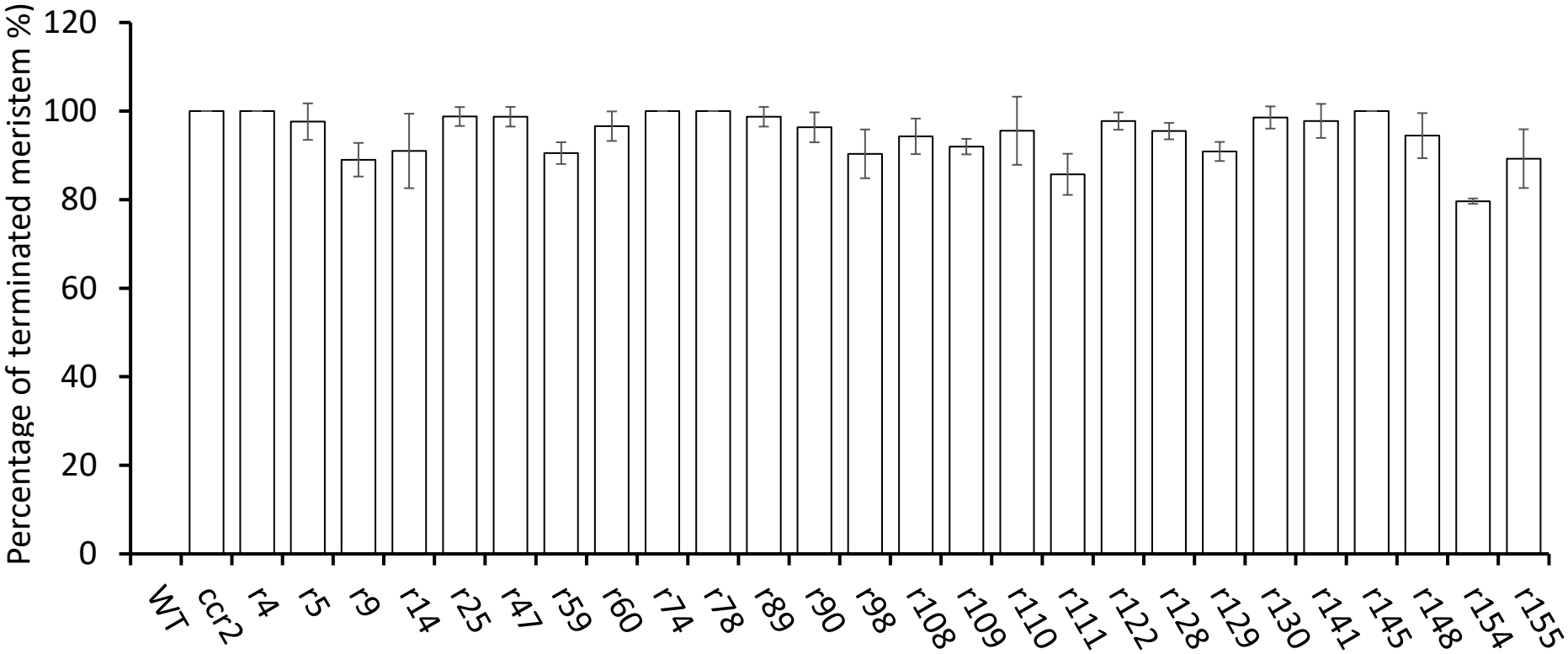

Figure 3.7 The *ccr2* mutant has terminated primary floral meristem and altered floral architecture and no *rccr2* lines reverted those phenotypes. Five-week old plants were shifted from 16-h to 8-h photoperiod and scored for floral phenotypes. A. *ccr2* showed floral meristem termination (lower, marked by a white circle) and altered floral architecture (upper) compared to WT. B. None of the 26 *rccr2* lines reverted the floral phenotypes of *ccr2*. For each genotype, three groups each containing 10 representative plants were scored and values were averaged from the three groups. Error bars denote standard error.

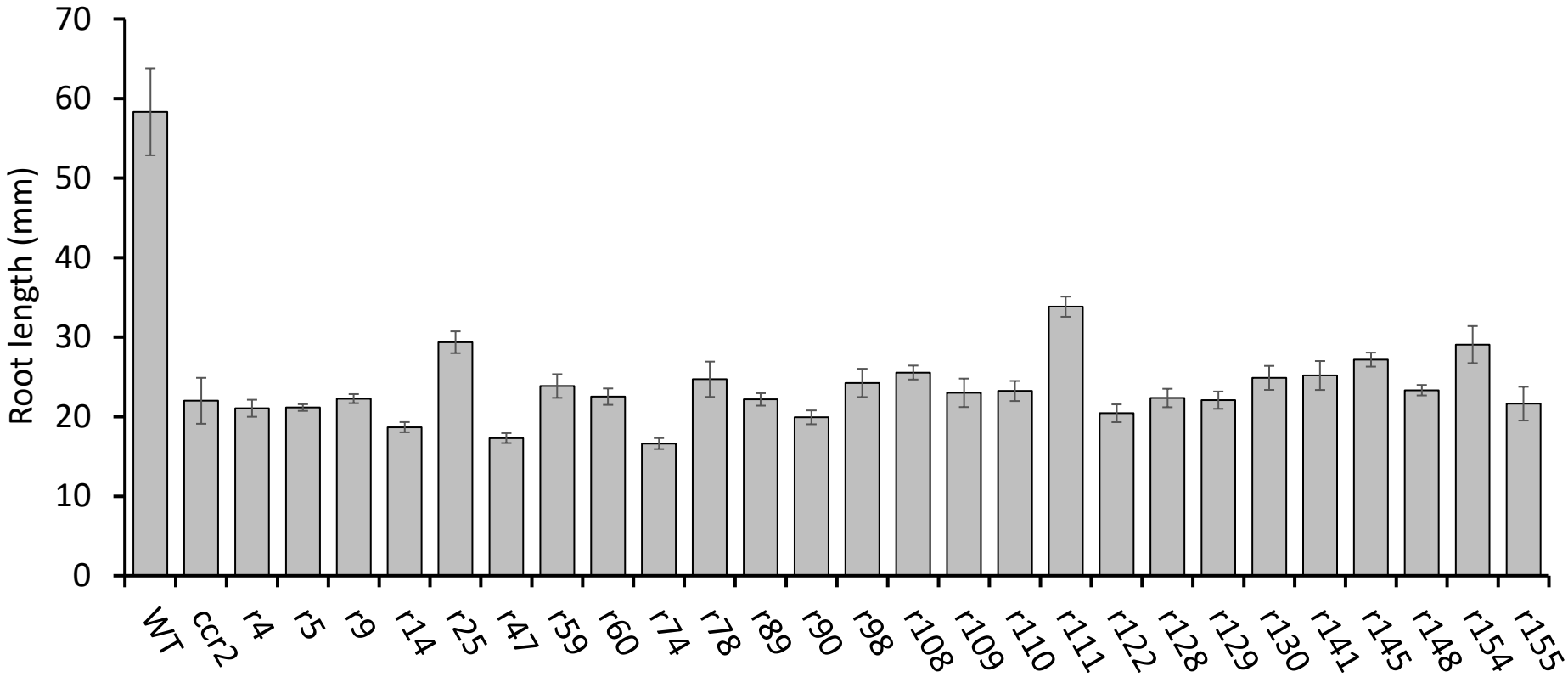

Figure 3.8 The *ccr2* mutant and all *rccr2* lines displayed significantly reduced root length compared to WT. Seedlings of WT, *ccr2* and all 26 *rccr2* lines were grown on MS medium containing 0.8% phytagel under a 16-h photoperiod. Root length was scored for 11 d at 24-h intervals and that of the final day is shown in the figure. For each genotype, values were averaged from 15-30 seedlings. One-way ANOVA was performed to compare between means; $P < 0.05$ was set as statistically significant. Error bars denote standard error.

3.2.3 Identification of causal mutations by next generation sequencing

rccr2 lines were backcrossed to Ler-0 and the *ccr2* parent in both Columbia (*ccr2*^{Col}) and Landsberg (*ccr2*^{Ler}) background (Table 3.3), and NGS technologies were used to sequence the genomic DNA from a segregating homozygous F_2 mapping population for each of the 26 *rccr2* lines. Homozygous F_2 plants were screened first by observing the leaf greening phenotype under a 10-h photoperiod and the F_2 populations of all *rccr2* lines displayed a segregation ratio of close to 1:3 (Green:Yellow) or 13:3 when backcrossed to Ler-0, suggesting the causal mutations to be recessive. Carotenoid levels of the plants with green true leaves were then analyzed by HPLC, using reduced lutein as an indication of homozygous *ccr2* mutation; for the *rccr2* lines that were backcrossed to Ler-0, F_2 plants with green true leaves but displaying similar morphological traits of rosette to Ler-0 (Passardi et al., 2007) were removed from the population before HPLC was performed. In each segregating F_2 population, plants showing both green true leaves under 10-h photoperiod and reduced lutein in carotenoid profile were used to generate a mapping pool for NGS and most pools consisted of more than 30 homozygous plants (Table 3.3).

Through NGS of all 26 *rccr2* lines, 2.8×10^7 to 4.6×10^7 reads were obtained for each F_2 mapping population, which accounted for 21-34 times of genome coverage (Table 3.3). A scoring system (Table 3.4) was utilized to assess the SNPs (Single Nucleotide Polymorphisms) identified by NGS, grading chastity, BLOSUN (BLOcks SUbstitution Matrix) (Henikoff and Henikoff, 1992) and function of mutated genes from 0 to 5 (Table 3.4). In addition, we aligned SNPs from different mapping populations of a same *rccr2* line, and highlighted homozygous mutations in "SNP deserts" of the same pattern across different mapping pools. For each *rccr2* line, a mutation with the highest score across mapping populations was deemed as the most likely causal mutation and is listed in Table 3.5 with a brief description of its reported functions. The mutated genes identified by NGS encode enzymes in the carotenoid biosynthesis pathway (e.g. PSY), proteins that are involved in chloroplast development (e.g. FtsH protease 11), proteins that are involved in photomorphogenesis (e.g. Deetiolated1), receptor or transporter proteins (e.g. glutamate receptors), protein-protein interacting factors (e.g. AtOR-like protein) or other proteins/enzymes that play regulatory roles in cell signaling (Table 3.5).

Table 3.3 General NGS information of each *rccr2* line

rccr2 lines	Crossed to	*F_2 segregation (Green : Yellow)	$^{\Delta}F_2$ plants with reduced lutein	F_2 plants sequenced	Number of reads	Genome coverage
rccr2^{4}	*ccr2*^{Ler}	181 : 526	51 (of 51)	23	34872415	26
rccr2^{4}	*ccr2*^{Col}	154 : 479	56 (of 56)	47	29638570	22
rccr2^{4}	Ler-0	1208 : 254	105 (of 434)	86	42695174	32
rccr2^{5}	*ccr2*^{Ler}	122 : 348	70 (of 70)	52	38542197	29
rccr2^{5}	*ccr2*^{Col}	205 : 621	64 (of 64)	52	31678210	24
rccr2^{9}	*ccr2*^{Ler}	137 : 405	39 (of 39)	24	28463216	21
rccr2^{9}	*ccr2*^{Col}	213 : 652	56 (of 56)	50	43189652	33
rccr2^{9}	Ler-0	837 : 185	83 (of 340)	74	32385428	24
rccr2^{14}	*ccr2*^{Col}	110 : 306	102 (of 102)	87	36474631	28
rccr2^{14}	Ler-0	908 : 198	50 (of 223)	30	40627654	31
rccr2^{25}	*ccr2*^{Col}	89 : 274	52 (of 52)	52	38459220	29
rccr2^{47}	*ccr2*^{Col}	75 : 229	34 (of 34)	22	27664523	21
rccr2^{59}	*ccr2*^{Col}	66 : 202	66 (of 66)	60	30587650	23
rccr2^{60}	Ler-0	1052 : 253	14 (of 210)	11	29487299	22
rccr2^{74}	*ccr2*^{Col}	128 : 397	60 (of 60)	60	36382030	27
rccr2^{78}	*ccr2*^{Col}	66 : 211	28 (of 28)	24	34562788	26
rccr2^{89}	*ccr2*^{Col}	183 : 525	77 (of 77)	60	42006587	32
rccr2^{90}	*ccr2*^{Col}	92 : 256	80 (of 80)	60	35746581	27
rccr2^{90}	Ler-0	836 : 200	65 (of 192)	41	42872313	32
rccr2^{98}	*ccr2*^{Col}	81 : 233	48 (of 48)	33	37675209	28
rccr2^{98}	Ler-0	1362 : 324	36 (of 244)	11	40536780	31
rccr2^{108}	*ccr2*^{Ler}	64 : 195	38 (of 38)	31	39204375	30
rccr2^{108}	Ler-0	1118 : 267	15 (of 180)	11	29631054	22
rccr2^{109}	*ccr2*^{Col}	146: 458	76 (of 76)	62	45653892	34
rccr2^{109}	Ler-0	1535 : 338	52 (of 255)	36	36824310	28
rccr2^{110}	Ler-0	894 : 219	35 (of 238)	32	33687903	25
rccr2^{111}	Ler-0	924 : 206	31 (of 176)	22	41547695	31
rccr2^{122}	*ccr2*^{Col}	77 : 244	53 (of 53)	45	28176506	21
rccr2^{128}	*ccr2*^{Ler}	125 : 356	42 (of 42)	37	27653812	21
rccr2^{129}	*ccr2*^{Ler}	109 : 342	45 (of 45)	37	33472109	25
rccr2^{130}	*ccr2*^{Ler}	86 : 239	30 (of 30)	26	42496122	32
rccr2^{130}	*ccr2*^{Col}	152 : 460	56 (of 560	47	35191132	27
rccr2^{141}	*ccr2*^{Ler}	92 : 293	90 (of 90)	76	36854718	28
rccr2^{141}	*ccr2*^{Col}	176 : 517	84 (of 84)	68	37832344	29
rccr2^{145}	*ccr2*^{Ler}	214 : 628	91 (of 91)	72	45392220	34
rccr2^{145}	*ccr2*^{Col}	167 : 523	85 (of 85)	78	39665451	30
rccr2^{148}	*ccr2*^{Col}	190 : 554	89 (of 89)	76	44069575	33
rccr2^{154}	*ccr2*^{Ler}	53 : 178	44 (of 44)	40	40041378	30
rccr2^{155}	*ccr2*^{Ler}	96 : 278	93 (of 93)	76	36715977	28
rccr2^{155}	*ccr2*^{Col}	85 : 261	85 (of 85)	65	39770795	30

*Green: plants with green true leaves under a 10-h photoperiod; Yellow: plants with yellow true leaves under the same photoperiod. $^{\Delta}$F2 plants with green true leaves were subjected to HPLC to screen for homozygous *ccr2* mutation that led to reduced lutein.

Table 3.4 The scoring system used in this study to evaluate SNPs identified by NGS

Score	Chastity	BLOSUM*	Function of mutated genes
5	≥ 0.95	-10 and -9	Directly involved in carotenoid biosynthesis or plastid development
4	0.92 – 0.94	-8 and -7	Involved in plant development or stress responses
3	0.9 – 0.91	-6 and -5	Encoding kinases, phosphatases or transcription factors
2	0.85 – 0.89	-4 and -3	Encoding other signalling factors that regulate gene expression
1	0.80 – 0.84	-2 and -1	Encoding other proteins or RNAs that regulate gene expression
0	< 0.80	≥ 0	Encoding other proteins with known or unknown functions

*An SNP is scored as 5 if it leads to an altered splice site and consequently changed ORF or a premature stop codon, and scored as 3 if the altered splice site results in an inserted intron or a deleted exon which does not change the ORF. Those scores substitute BLOSUM.

Table 3.5 Possible causal mutations identified in each *rccr2* line using NGS

rccr2 lines	SNP position	Chastity			Base change	Location in the gene	Amino acid change	Accession	Description of the gene product
		×*ccr2*^{Ler}	×*ccr2*^{Col}	×Ler-0					
rccr2^{4}	5660555	0.83	0.88	0.98	C→T	CDS	M→I	At5g17230	Phytoene synthase (PSY), the entry point enzyme of carotenoid biosynthesis.
rccr2^{5}	5660555	0.67	0.9	$^{\Delta}$NS	C→T	CDS	M→I	At5g17230	Phytoene synthase (PSY), the entry point enzyme of carotenoid biosynthesis.
rccr2^{9}	11613547	1	1	0.93	C→T	CDS	Q→*	At1g32230	Radical-Induced Cell Death1 (RCD1), belonging to WWE protein-protein interaction domain protein family.
rccr2^{14}	21567149	0.97	0.87	NS	C→T	CDS	G→E	At5g53170	FtsH protease 11 (FtsH11), involved in high temperature adaptation processes in chloroplast development.
rccr2^{25}	3621275	NS	0.89	NS	G→A	CDS	V→M	At2g08986	Unknown protein that has 30201 Blast hits to 17322 proteins in 780 species.
rccr2^{47}	18326605	NS	0.85	NS	G→A	CDS	G→S	At4g39400	BRI1, a leucine-rich receptor-like protein kinase family protein.
rccr2^{59}	1853804	NS	1	NS	C→T	CDS	G→R	At5g06130	AtOR-Like protein that interacts directly with the PSY and acts as a positive posttranscriptional regulator.
rccr2^{60}	3959350	NS	NS	0.96	G→A	Splice site	No	At1g11730	Galactosyltransferase family protein. Galactosyltransferases are involved in galactolipid biosynthesis and located on the outer membrane of chloroplast envelope.
rccr2^{74}	1855210	NS	0.93	NS	G→A	CDS	Q→*	At5g06130	AtOR-Like protein that interacts directly with the PSY and acts as a positive posttranscriptional regulator.
rccr2^{78}	2961614	NS	1	NS	G→A	CDS	D→N	At4g05612	Unknown protein
rccr2^{89}	6148606	NS	0.967	NS	C→T	CDS	W→*	At5g18525	Protein serine/threonine kinase and/or protein tyrosine kinase that potentially regulates cell proliferation/development, and contains WD40 repeat domain.
rccr2^{90}	5660151	NS	0.96	0.68	C→T	CDS	A→T	At5g17230	Phytoene synthase (PSY), the entry point enzyme of carotenoid biosynthesis.

rccr2 lines	SNP position	Chastity			Base change	Location in the gene	Amino acid change	Accession	Description of the gene product
		×*ccr2*^{Ler}	×*ccr2*^{Col}	×Ler-0					
rccr2^{98}	8260848	NS	1	0.83	C→T	Splice site	No	At5g24280	Gamma-irradiation and mitomycin c induced 1 (GMI1) that is involved in damaged DNA repair via homologous recombination.
rccr2^{108}	4633530	0.95	NS	0.90	G→A	CDS	S→F	At5g14370	CCT motif family protein. CIA 2, a CCT motif-containing protein, is a transcription factor that upregulates chloroplast translocon genes.
rccr2^{109}	3716106	NS	0.92	0.89	C→T	CDS	W→*	At5g11570	Major facilitator superfamily (MFS) protein that has membrane transporter activity.
rccr2^{110} *rccr2*^{111}	2937753	NS	NS	1	G→A	CDS	A→V	At1g09100	RPT5B, 26S proteasome AAA-ATPase subunit. In dark, Arabidopsis COP1 interacts with transcription factors such as HY5 and triggers their degradation via the 26S proteasome.
rccr2^{122}	□ND	NS	Het	NS	ND	ND	ND	ND	ND
rccr2^{128}	22614671	0.95	NS	NS	C→T	CDS	E→K	At1g61310	LRR and NB-ARC domains-containing disease resistance protein.
rccr2^{129}	ND	Het	NS	NS	ND	ND	ND	ND	ND
rccr2^{130}	5660938	0.97	1	NS	G→A	CDS	P→S	At5g17230	Phytoene synthase (PSY), the entry point enzyme of carotenoid biosynthesis.
rccr2^{141}	19616865	1	1	NS	G→A	CDS	W→*	At5g48400	Glutamate-like receptor 1.2 (GLR1.2); plant GLRs function as cation channels and are implicated in light signaling.
rccr2^{145}	5661514	0.87	0.94	NS	C→T	Splice site	No	At5g17230	Phytoene synthase (PSY), the entry point enzyme of carotenoid biosynthesis.
rccr2^{148}	19620864	NS	0.95	NS	G→A	CDS	A→T	At5g48410	Glutamate-like receptor 1.3 (GLR1.3); plant GLRs function as cation channels and are implicated in light signaling.
rccr2^{154}	6347991	1	NS	NS	G→A	Splice site	No	At4g10180	De-etiolated1 (DET1) is a repressor of photomorphogenic gene expression.
rccr2^{155}	3606630	0.92	0.98	NS	C→T	CDS	W→*	At1g10830	15-*cis*-zeta-carotene isomerase (ZISO), an isomerase in carotenoid biosynthetic pathway.

[Δ]NS: Not Sequenced; [□]ND: No Data; Het: all alleles are heterozygous or no SNP desert.

3.3 Discussion

Altogether, 18 candidate genes were identified by NGS of the 26 revertants. Here I briefly discuss these candidate genes with known functions. In chapters 4 and 5, I undertake a detailed analysis of the reversion of the *ccr2* leaf-yellowing phenotype due to lesions in *PSY*, *ZISO* and *DET1*.

3.3.1 Characterization of *ccr2* and *rccr2*

In *ccr2* YL, the percentage composition of zeaxanthin and antheraxanthin was significantly increased (Figure 3.1), probably suggesting a greater demand of photo-protective pigments in the violaxanthin cycle (Niyogi et al., 1998; Jahns et al., 2009) when the leaf tissue contains impaired chloroplasts. Interestingly, the composition of violaxanthin was enhanced in *ccr2* GL to a higher level than in WT and remained at high levels in all *rccr2* lines. Furthermore, the levels of zeaxanthin and antheraxanthin were still significantly higher in *rccr2* lines than in WT, and other major carotenoids in leaf tissue of *rccr2* lines remained mostly at similar levels to *ccr2* GL, including *rccr2* lines carrying mutated genes encoding carotenogenic enzymes (PSY and ZISO) and PSY-interacting protein AtOR-like (Figure 3.1). We hence propose that the leaf yellowing phenotype was reverted via mechanisms other than simply restoring carotenoid composition to wild type levels, and that altered chloroplast development in *ccr2* is possibly due to carotenoid-derived retrograde signals the production or perception of which is repressed in *rccr2* lines. Consistently, unlike WT all *rccr2* lines accumulated *cis*-carotenoids, although the composition in some lines was different to that in *ccr2* (Table 3.2). The difference in *cis*-carotenoid levels could suggest that there is a threshold level of *cis*-carotenoids required to produce a carotenoid-derived retrograde signal.

Unlike that in leaf tissue, chlorophyll biosynthesis in cotyledons of some *rccr2* lines was not restored to wild type levels (Figures 3.4B and 3.6). The absence of PLB in *ccr2* etioplasts correlates with delayed greening in cotyledons upon illumination (Park et al., 2002). Therefore, cotyledon greening at wild type levels may suggest restored PLB formation in *rccr2* lines, and delayed cotyledon greening possibly suggest that those *rccr2* lines lack PLB formation, arguing for different mechanisms to restore chlorophyll levels in leaves.

In the present forward genetics study, *rccr2* lines were only screened by observing the reversion of leaf yellowing (Figure 3.4A and B), intriguingly floral meristem termination and root length phenotypes of *ccr2* were not reverted (Figures 3.7 and 3.8), suggesting that separate signals or mechanisms may lead to those phenotypes.

3.3.2 Mutations in *PSY*, *OR* and *ZISO*

In this study, I identified four mutant alleles of *PSY, rccr2*^{4}, *rccr2*^{90}, *rccr2*^{130} and *rccrr2*^{145}, using NGS; EMS mutations led to single amino acid changes in *psy*-4, *psy*-90 and *psy*-130, and an altered slice site in *psy*-145 (Table 3.5). As the entry point enzyme of carotenoid biosynthesis, PSY controls carbon flux into the pathway (Cazzonelli and Pogson, 2010). Therefore, altered activity of PSY exerts profound effects on carotenoid profile (Ducreux et al., 2005; Fraser et al., 2007; Maass et al., 2009; Welsch et al., 2010; Cao et al., 2012), probably including *cis*-carotenoid levels, and may subsequently affect the proposed carotenoid-derived signals that regulate chloroplast development. In addition to affecting the activity of PSY, single amino acid changes were reported to have dramatic effects on its localization (Shumskaya et al., 2012). PSY has been proposed to form a metabolon with other enzymes in the carotenoid pathway (Shumskaya and Wurtzel, 2013), and changed localization of the entry point enzyme may affect the function of this biosynthetic machinery of carotenoids. All four *rccr2* lines carrying mutated *psy* displayed altered *cis*-carotenoid profiles in etiolated seedlings, while carotenoid content in leaf tissue were similar to that of *ccr2* (Tables 3.1 and 3.2), suggesting the speculated retrograde signals in *ccr2* to be triggered by *cis*-carotenoids. It has been established that basic helix-loop-helix (bHLH) transcription factors PIF1, PIF3, PIF3 and PIF5 repress the expression of *PSY* gene in dark and that during photomorphogenesis light-triggered degradation of PIFs derepresses *PSY* expression and promotes carotenoid biosynthesis (Toledo-Ortiz et al., 2010). Also involved in photomorphogenesis, gibberellin (GA)-regulated DELLA proteins derepress *PSY* expression in cotyledons by repressing the transcriptional activity of PIFs (Cheminant et al., 2011). Taken together, the expression and function of *PSY* is closely linked to photomorphogenesis and multiple alleles of *PSY* identified in this study likely contain causal mutations of the reverted chloroplast development.

Arabidopsis ORANGE (AtOR) and AtOR-like, plastid-localized proteins that contain a DnaJ cysteine-rich zinc finger domain, physically interact with PSY and regulate its protein levels, acting as major posttranslational regulators (Zhou et al., 2015). Altered protein levels of PSY may also affect carotenoid content and carotenoid-derived signals. Interestingly two alleles of *AtOR-like* (At5g06130) were identified in the present study; EMS mutations introduced a single amino acid change in *rccr2*^{59} and a premature stop codon in *rccr2*^{74} (Table 3.5). *Ator-like*-74 led to significant changes in *cis*-carotenoid profile compared to *ccr2*, whereas a*tor-like*-59 showed no significant effect on *cis*-carotenoid levels (Table 3.2), probably due to a less severe change in the AtOR-like protein. It has been reported that cauliflower (*Brassica oleracea*) OR protein (BoOR) affects carotenoid accumulation by regulating chromoplast differentiation and carotenoid storage sink (Lu et al., 2006; Lopez et al., 2008b; Li et al., 2012). However, OR exerts no effects on leaf carotenoid composition (Li et al., 2001); in agreement with previous reports, no clear changes of carotenoid content were observed in leaves of the two *rccr2* lines carrying mutated a*tor-like* alleles (Table 3.1).

ZISO, a carotenoid isomerase that was characterized in Arabidopsis in 2010 (Chen et al., 2010), catalyzes the conversion of tri-*cis*-ζ-carotene at the 15-*cis* double bond to form di-*cis*-ζ-carotene. The Arabidopsis *ccr2* mutant accumulates neurosporene isomers and tetra-*cis*-lycopene that were proposed to prevent the formation of PLB thereby perturbing plastid development and delaying the greening of etiolated seedlings upon illumination (Park et al., 2002; Cuttriss et al., 2007). *rccr2*^{155} lacks those *cis*-carotenes due to a mutated *ZISO* (*ziso*-155) with a premature stop codon, and ζ-carotene was reduced as the formation of di-*cis*-ζ-carotene is blocked in this mutant (Tables 3.2 and 3.5). I hence hypothesize that mutated *ZISO* and consequently changed *cis*-carotenoid composition in *rccr2*^{155} lead to the restoration of leaf greening. It has remained to be investigated if *cis*-carotenoids trigger retrograde signals or just structurally prevent PLB formation. However, 19 other *rccr2* lines possessed similar *cis*-carotenoid composition to *ccr2* while still showed restoration of leaf greening (Figure 3.4 A and B; Table 3.2), which is in agreement with retrograde signals playing regulatory roles in chloroplast development.

3.3.3 Mutations in *DET1*, *RPT5B* and *GLK1*

DET1 and COP1 are among the first identified photomorphogenesis repressors (Deng et al., 1992; Pepper et al., 1994). COP1 is a Ub E3 ligase (E3 ubiquitin ligase) that act as a key repressor in the light signaling pathway, mediating the degradation of transcription factors involved in photomorphogenesis by the Ub-proteasome system (Deng et al., 1992; Yi and Deng, 2005); DET1 forms the CDD complex with DDB1 (Damaged DNA Binding protein 1) and COP10, aiding in COP1-mediated protein degradation (Schroeder et al., 2002; Yanagawa et al., 2004). The repression of CDD complex by light-activated photoreceptors such as phyB-Pfr allows the accumulation of photomorphogenesis-promoting transcription factors and the initiation of photomorphogenic development of a plant seedling (Yi and Deng, 2005). Reportedly, DET1 regulates protein levels of PIFs by physically interacting with and stabilizing those factors, and thereby represses photomorphogenesis (Dong et al., 2014; Shi et al., 2015). DET1 was also suggested to negatively regulate protein abundance of DELLA and act in the CDD complex which targets long hypocotyl in far-red 1 (HFR1) for degradation (Li et al., 2015; Shi et al., 2015). I identified a mutated *DET1* gene from *rccr2*^{154} and the mutation introduced an altered splice site (Table 3.5) which may presumably affect the function of DET1 protein and hence promote photomorphogenesis. Suppression of *DET1* gene expression was shown to result in elevated carotenoid biosynthesis in plants including tomato and canola (*Brassica napus*) (Davuluri et al., 2005; Wei et al., 2009; Enfissi et al., 2010), in line with which leaf carotenoid content and *cis*-carotenoid composition in etiolated seedlings were both altered in *rccr2*^{154} (Tables 3.1 and 3.2). More interestingly, a significant reduction of tetra-*cis*-lycopene was associated with *det1*-154 in this revertant line, which is consistent with the hypothesis that tetra-*cis*-lycopene many be among the carotenoids that trigger the retrograde signals in *ccr2*.

Following the interaction with COP1, transcription factors such HY5 are degraded by the 26S Ub-proteasome system of which RPT5B is an AAA-ATPase subunit (Yi and Deng, 2005; Guyon-Debast et al., 2010). *RPT5B* was mutated in *rccr2*^{110} and *rccr2*^{111}, which is likely associated with promoted photomorphogenesis and restoration of leaf greening in those *rccr2* lines. Notably, an SNP was located in *AtGLK1* (Arabidopsis Golden2-like 1, At2g20570) in *rccr2*^{108}, although being heterozygous. In Arabidopsis, a double knockout mutant *glk1 glk2* displayed reduced

transcription of *PhANG*s and perturbed chloroplast development (Fitter et al., 2002). Given the roles of *GLK* family in the transcriptional regulation of chloroplast biogenesis (Kobayashi and Masuda, 2016), the mutated *AtGLK1* in *rccr2*^{108} may need further investigation.

3.3.4 Mutation in *FtsH*

FtsHs (filamentation temperature sensitive) are a well-characterized family of membrane-bound and ATP-depended metalloproteases. Seventeen *FtsH* family genes have been discovered in Arabidopsis, and 12 of them encode FtsHs, the rest five encoding FtsHi proteins which lack the zinc-binding site required for proteolytic activity and are protease-inactive (Wagner et al., 2012; Nishimura et al., 2016). Eight of the 12 FtsHs and five FtsHi proteins are targeted to chloroplasts and FtsH11 is localized in both chloroplasts and mitochondria (Urantowka et al., 2005; Ferro et al., 2010). Multiple roles have been attributed to FtsHs in chloroplasts, including thylakoid biogenesis and degradation of damaged photosynthetic proteins (Ostersetzer and Adam, 1997; Chen et al., 2000; Bailey et al., 2002; Sakamoto et al., 2003). Interestingly, *FtsH1* gene expression was found to be induced by phytochrome A during photomorphogenesis (Tepperman et al., 2001). It has been suggested that the dual-targeted FtsH11 is crucial in the thermotolerance of Arabidopsis and that in the leaves of *ftsh11* photosynthetic capacity was dramatically reduced at 30°C (Chen et al., 2006). *ftsh11* growing under a prolonged photoperiod or continuous light displayed bleached phenotypes, suggesting that FtsH11 plays an essential role in chloroplast structure and function during growth under long photoperiods (Wagner et al., 2016). *rccr2*^{14} showed variegated leaves when grown under a 16-h photoperiod while no variegation was observed under 8 h (Figure 3.9), in correlation with the variegation phenotype carotenoid composition was altered in leaf tissue, displaying increased antheraxanthin and reduced β-Carotene and lutein (Table 3.1). *Ftsh11*-14 carries an EMS mutation that results in a G→E amino acid substitution, which may affect the function of FtsH11 protease (Table 3.5). However, how a mutated FtsH11 reverted the leaf yellowing phenotype in *ccr2* remains to be elucidated. The chlorophyll biosynthesis in *rccr2*^{14} during cotyledon greening was not restored to wild type levels, suggesting that PLB formation during skotomorphogenesis was not restored in this revertant line.

Figure 3.9 *rccr2*^{14} displays variegated leaves under a 16-h photoperiod. Twenty plants were grown under an 8-h photoperiod for 25 d. Plants were then split into two groups and one group was shifted to 16 h, the other group remaining under 8 h; both groups were photographed 10 d after the shift.

3.3.5 Mutations in *GLRs*

Mutations in two genes that encode glutamate-like receptor homologous 1.2 (AtGLR1.2, At5g48400) and AtGLR1.3 (At5g48410) were identified by NGS from *rccr2*^{141} and *rccr2*^{148}, respectively (Table 3.5). Plant GLRs are homologous of mammalian ionotropic glutamate receptors (iGluRs) (Price et al., 2012). In Arabidopsis AtGLR 3.4 was found to be an amino acid-gated channel inducing cytosolic calcium peaks (Vincill et al., 2012); multiple members of the 20 AtGLRs that have been discovered so far are hence speculated to be amino acid-activated channels (Chiu et al., 1999; Price et al., 2012). Previous reports have suggested that plant GLRs are involved in a wide range of biological processes, which was reviewed comprehensively (Price et al., 2012). Of particular interest to this study is the involvement of plant GLRs in signaling that regulates chloroplast development. Mammalian iGluR inhibitor DNQX (6,7-dinitroquinoxaline-2,3-(1*H*,4*H*)-dione) and iGluR agonist BMAA (S(+)-β-methyl-α,β-diaminopropionicacid), both induced hypocotyl elongation and reduced chlorophyll levels in light grown Arabidopsis seedlings, whereas dark grown seedlings were unaffected, indicating regulatory roles of AtGLRs that are specific to light signaling; it seemed that the regulation of

light signaling by AtGLRs can be positive or negative (Lam et al., 1998; Brenner et al., 2000). AtGLR3.4 was found to be localised in chloroplasts and T-DNA insertions in this plant GLR negatively affected photosynthetic phenotypes (Teardo et al., 2011). When etiolated seedling of *rccr2*^{141} and *rccr2*^{148} were exposed to continuous light the cotyledons showed delayed greening resembling *ccr2* (Figure 3.6), indicating that the restoration of leaf greening was due to affected light signaling and that plastid development in dark-grown seedling might not be restored. Given the amino acid-channeling activities of plant GLRs, I also propose that the perception or transduction but not production of the speculated retrograde signals was affected in the two *rccr2* lines.

Chapter 4: A *cis*-carotenoid derived apocarotenoid posttranscriptionally regulates protochlorophyllide oxidoreductase and prolamellar body formation during skotomorphogenesis

This chapter has been written as a manuscript to be submitted to *Plant Cell* and hence follows the submission guidelines of the journal. The main text is formatted according to the journal's instructions, and supplemental tables and figures are attached to the end of the chapter. However, to facilitate the examiners' review, figures and legends are embedded to the main text instead of being individual files; figures are formatted as instructed by the journal but not scaled to the journal's required size. References of this manuscript have been incorporated into thesis references at the end of thesis.

A *cis*-carotenoid derived apocarotenoid posttranscriptionally regulates protochlorophyllide oxidoreductase and prolamellar body formation during skotomorphogenesis

[1]Xin Hou, [2]Christopher I Cazzonelli, [2]Yagiz Alagoz, [1]John Rivers, [1]Jacinta Watkins, [2]Rishi Aryal, [2]Namraj Dhami, [1]Marri Shashikanth, [3]Jiwon Lee and [1]Barry J Pogson

Affiliations:

[1] Australian Research Council Centre of Excellence in Plant Energy Biology, College of Medicine, Biology and Environment, Research School of Biology, The Australian National University, Canberra, ACT 2601, Australia.

[2]Hawkesbury Institute for the Environment, University of Western Sydney, Hawkesbury Campus, Bourke Street, Richmond, NSW AUSTRALIA 2753

[3]Centre for Advanced Microscopy, The Australian National University, Canberra, ACT 2601, Australia

Corresponding Authors: Barry J Pogson (barry.pogson@anu.edu.au)
Christopher I Cazzonelli (c.cazzonelli@westernsydney.edu.au)

The author(s) responsible for distribution of materials integral to the findings presented in this article in accordance with the policy described in the Instructions for Authors (www.plantcell.org) are: Barry Pogson (barry.pogson@anu.edu.au) and/or Christopher Cazzonelli (c.cazzonelli@westernsydney.edu.au)

Running Title: *cis*-carotenoid control of plastid development and photomorphogenesis

Key words: *cis*-carotenoid, apocarotenoid, photoperiod, light, plastid, etioplast, chloroplast, prolamellar body, epistasis, photomorphogenesis

ABBREVIATIONS

ccr	*carotenoid and chloroplast regulation*
rccr2	revertant of *ccr2*
DAG	Days after germination
YL	yellow leaf
GL	green leaf
ACS	Apocarotenoid signal
NFZ	Norflurazon

ABSTRACT

cis-carotenoids produced early in the carotenoid pathway may serve as substrates for the production of novel apocarotenoid signals (ACS) that regulate nuclear gene expression, metabolic homeostasis and leaf development. When and where they accumulate and what physiological functions they may serve in higher plants remain unclear. *cis*-carotenoids are not easily detected in most plant tissues, except in the absence of carotenoid isomerase (CRTISO) activity when photoisomerisation rate-limits the isomerisation of tetra-*cis* to all-*trans*-lycopene. *crtiso* mutants display different virescent phenotypes in different species and here we demonstrate a physiological link to *cis*-carotenoid accumulation. The accumulation of *cis*-carotenoids in Arabidopsis *crtiso* mutant (*ccr2*) tissues was observed in plant tissues grown under extended darkness (i.e. shorter photoperiod) and coincided with a perturbation in chloroplast development that caused leaf yellowing. A forward genetic screen identified an epistatic interaction between the ζ-carotene isomerase (*ziso*) and *ccr2* which could restore plastid development, and revealed that di-*cis*-ζ-carotene, tri-*cis*-neurosporene and tetra-*cis*-lycopene are likely substrates for the generation of an ACS, named ASC2. Transcriptomics analysis of *ccr2 ziso* mutant tissues impaired in plastid development revealed that photosynthesis associated nuclear gene expression (*PhANG*) was activated through the down-regulation of genes involved in repressing photomorphogenesis. We identified an alternative splice mutant of *det1,* a repressor of photomorphogenesis, which could restore PLB formation and cotyledon greening following de-etiolation in *ccr2*. Chemical inhibition of carotenoid cleavage dioxygenase activity provided evidence that ACS2 posttranscriptionally maintains protochlorophyllide oxidoreductase protein levels acting downstream of DET1 to control PLB formation and plastid development.

INTRODUCTION

Carotenoids are a diverse group of hydrophobic isoprenoid pigments controlling numerous biological processes in photosynthetic organisms and facilitate animal health (Cazzonelli, 2011; Baranski and Cazzonelli, 2016). In addition to providing plant flowers, fruits and seeds with distinct colours, carotenoids have essential roles in light harvesting, photomorphogenesis and photoprotection (Howitt and Pogson, 2006; Baranski and Cazzonelli, 2016). Carotenoids also serve as substrates necessary for the biosynthesis of plant phytohormones, apocarotenoid derived volatiles that attract pollinating insects or zoochoric animals, and signalling metabolites that control various aspects including plastid communications, gene expression, plant growth, physiology and development (Hou et al., 2016). The mechanisms by which environmental perturbations impact carotenoid production, storage and degradation remain largely unknown.

In higher plants, carotenoid biosynthesis is initiated by the condensation of two molecules of geranylgeranyl diphosphate to form phytoene, which is catalysed by the rate-limiting enzyme phytoene synthase (PSY) (von Lintig et al., 1997; Li et al., 2008b; Rodriguez-Villalon et al., 2009a; Welsch et al., 2010; Zhou et al., 2015). Next, phytoene desaturase (PDS), ζ-carotene desaturases (ZDS), ζ-carotene isomerase (ZISO) and *cis*-*trans*-carotene isomerase (CRTISO) convert the colourless phytoene into the pinkish-red coloured all-*trans*-lycopene (Bartley et al., 1999; Isaacson et al., 2002; Park et al., 2002; Dong et al., 2007; Chen et al., 2010; Yu et al., 2011; Baranski and Cazzonelli, 2016). The carotenoid biosynthetic pathway branches after lycopene to produce alpha or beta-carotenes, their derivatives distinguished by different cyclic end groups. The addition of β-ring and ε-type rings are catalysed by lycopene β-cyclase (β-LCY) and lycopene ε-cyclase (ε-LCY), respectively (Cunningham et al., 1993; Cunningham et al., 1996; Pecker et al., 1996; Ronen et al., 1999). α-carotene and β-carotene are further hydroxylated to produce the oxygenated carotenoids called xanthophylls (e.g. lutein, violaxanthin and zeaxanthin), which comprise the most abundant carotenoid pigments found in all green photosynthetic leaves.

After a decade of advancement in understanding the biosynthetic enzymes, the next frontier is to discover the mechanisms that regulate carotenoid biosynthesis, organelle accumulation and storage, as well the formation, release and disposal of their breakdown products (Cazzonelli and Pogson, 2010; Havaux, 2014). Carotenoid enzymes and pigments are localised

in the plastid, whereas the genes are encoded in the nucleus. Some degree of retrograde and/or anterograde signalling between the plastid and nucleus is therefore necessary to coordinate the production of carotenoids, downstream phytohormones and apocarotenoid signalling metabolites (Chi et al., 2013). In plants, carotenoids serve as substrates in the production of at least two hormones: abs*cis*ic acid (ABA) and strigolactones (SLs). Such carotenoid-derived signalling molecules affect the synthesis of colour, flavour, root-mycorrhizal interactions and developmental processes (McQuinn et al., 2015; Walter et al., 2015). The Carotenoid Cleavage Dioxygenase/Nine-*cis*-epoxy-carotenoid Dioxygenase (CCD/NCED) family have been demonstrated to cleave carotenoids to yield apocarotenoid signalling metabolites (Hou et al., 2016). Members of the CCD family have different substrate preference, and contribute to the turnover of carotenoids with a high degree of enzymatic cleavage specificity in plant tissues (Walter and Strack, 2011; Harrison and Bugg, 2014). There are nine members of the CCD family in Arabidopsis. Five CCDs make up the NCED sub-group and are exclusively involved in cleavage of violaxanthin and neoxanthin to form ABA (Tan et al., 2003). Of the other four, CCD1 and CCD4 have roles in carotenoid degradation; CCD7 and CCD8 (also known as MAX3 and MAX4) are involved in strigolactone biosynthesis. These four enzymes however, have been shown via *in vitro* assays to cleave a variety of carotenoids, including the *cis*-carotenoids (Bruno et al., 2016; Hou et al., 2016).

Non-enzymatic oxidative cleavage of carotenoids can also produce apocarotenoid metabolites by photooxidation reactions mediated by singlet oxygen ($^1O_2$) the main reactive oxygen species (ROS) or through co-oxidation mediated via enzymes such as lipoxygenases and peroxidases (Leenhardt et al., 2006a; Gonzalez-Perez et al., 2011). A variety of β-apocarotenoid oxidation and/or enzymatic cleavage products such as β-carotene 5,8-endoperoxide, geranylacetone, pseudoionone β-cyclocitral, β-carotene-5,6-epoxide and β-ionone have also been linked to signalling processes (Havaux, 1998; Yamauchi et al., 1998; Simkin et al., 2008; Bradbury et al., 2012; Ramel et al., 2012). However, only β-cyclocitral has been demonstrated to function in protecting plant cells against high-light stress responses by repressing genes through the chloroplast to nucleus signal transduction pathways that moderate development, growth and biogenesis of cellular components (Havaux, 2014).

An exciting hunt is on for *cis*-carotenoid derived metabolites produced in the upper part of the pathway that may function as signalling metabolites (Kachanovsky et al., 2012; Fantini et

al., 2013; Avendano-Vazquez et al., 2014; Alvarez et al., 2016). While the identity of any ACS derived from the *cis*-carotenoids formed in the early part of the biosynthesis pathway remains unknown and the cis-carotenoid substrates undefined, there is sufficient evidence to support their roles in mediating chloroplast to nuclear communication by controlling nuclear gene expression. For example, accumulation of ζ-carotene and/or phytofluene in the Arabidopsis *clb5/zds* (chloroplast biogenesis-5/ζ-carotene desaturase) mutant altered chloroplast to nuclear communications and expression of nuclear encoded genes involved in early chloroplast development, photosynthetic activity and carotenoid biosynthesis. Whilst *zds* mutants produced an abnormal needle-like leaf abnormality, fluridone, a PDS inhibitor, and the *ccd4 clb5* double mutant rescued the *clb5* phenotype, providing evidence for a novel *cis*-carotenoid derived ACS metabolite (Avendano-Vazquez et al., 2014). A metabolon regulatory loop was proposed in tomato fruit that can sense the levels of *cis*-carotenoid accumulation, their derivatives or the enzymes themselves revealing a poly-*cis*-carotene metabolic branch leading to the biosynthesis of all-*trans*-ζ-carotene (Fantini et al., 2013). An ACS metabolite derived from tetra-*cis*-lycopene and/or tri-*cis*-neurosporene was reported in tomato and implicated in the metabolic feedback-regulation of *PSY1* transcription, linking the organellar metabolic status to overall plant development (Kachanovsky et al., 2012). The 5' untranslated region (5'UTR) of a splice variant of the Arabidopsis *PSY* mRNA was reported to control translational activities in response to high carotenoid pathway fluxes, providing a potential mechanism by which an ACS may regulate the carotenoid pathway in a flux-dependent manner (Alvarez et al., 2016). Collectively, these evidences highlight potentially new functions for *cis*-carotenoids in controlling physiological processes and responses to environmental perturbations.

The identification of a *cis*-carotenoid derived signalling metabolite has proved difficult due to mutations in early stages of carotenoid biosynthesis being either lethal (*psy*, *pds* and *zds*) or affecting leaf chlorophyll production by an unknown manner (*ziso* and *crtiso*). For instance, the maize *y9*/*ziso* mutant shows a pale-green zebra-striping pattern in leaves of field grown individuals, appearing as lighter green and less vigorous compared to wild type maize plants. The Arabidopsis (*ziso*) mutant exhibited a delayed greening when exposed to light that was influenced by environmental factors (Li et al., 2007; Chen et al., 2010). Similarly, the *crtiso* mutants in Arabidopsis, tomato, melon and rice show varying degrees of unexplained leaf yellowing or delayed leaf greening (Isaacson et al., 2002; Park et al., 2002; Chai et al., 2011;

Galpaz et al., 2013). The Arabidopsis *ccr2/crtiso* mutant accumulates neurosporene isomers and poly-*cis*-lycopene, which was proposed to structurally prevent prolamellar body formation (PLB) thereby perturbing plastid development and delaying the greening of de-etiolated *ccr2* seedlings exposed to continuous light (Park et al., 2002; Cuttriss et al., 2007). The prolamellar body is a crystalline agglomeration of protochlorophyllide (Pchlide), Pchlide oxidoreductase and fragments of prothylakoid membranes that provides the structural framework for the incipient photosynthetic apparatus (Sundqvist and Dahlin, 1997). Intriguingly, the leaves of the light-grown *zebra/crtiso* rice mutant exhibit a characteristic 'zebra' phenotype and decreased level of lutein, which becomes more severe under high light intensity (Chai et al., 2011). In the *tangerine*/*crtiso* tomato mutant, newly developed leaves manifest yellow accumulating prolycopene and its precursors before turning light green eventually maturing as dark green foliage, again highlighting an effect of carotenoid biosynthesis on chloroplast development (Isaacson et al., 2002). Finally, the *yofi*/*crtiso* melon mutant caused yellowish seedlings to develop to young 'yellow–green' plantlets, while the mature plant is green with 'yellow–green' shoot apical meristems and young leaves (Galpaz et al., 2013). The *crtiso* loss-of-function mutants show altered composition of the downstream xanthophyll pigments, in particularly reduced lutein, and a massive accumulation of upstream *cis*-carotenoids (Isaacson et al., 2002; Park et al., 2002). The *ziso* and *crtiso* isomerase mutants can both affect *cis*-carotenoid accumulation and plastid development, but exactly if, which and how *cis*-carotenoids are responsible for the aforementioned physiological changes displayed by the isomerase mutants remain unclear.

We describe how an environmental cue such as light can cause phenotypic variation in the carotenoid isomerase mutant. Extended darkness and shorter photoperiods causes the accumulation of *cis*-carotenoids in newly emerged leaf tissues of *ccr2* that impair PLB formation and plastid development, thereby delaying cotyledon and leaf greening. An epistatic interaction between the *ziso* and *crtiso* restored plastid development and identified di-cis-ζ-carotene, neurosporene and/or tetra-*cis*-lycopene as candidate substrates for biosynthesis of an apocarotenoid signal. We provide chemical and genetic evidence that the apocarotenoid signal acts downstream of *det1* to post-transcriptionally upregulate POR protein levels and PLB formation thereby linking *cis*-carotenoid signalling to the control of skotomorphogenesis.

RESULTS

Photoperiod affects plastid differentiation and leaf development

The carotenoid isomerase mutants display different leaf pigmentation phenotypes in different species. Why are there different leaf pigmentation phenotypes among different species and what causes this leaf colour variegation? To address this, we investigated if the quantity of light affects leaf pigment levels and hence plastid development. Growing *ccr2* plants at a light intensity of 50 µmol.m^{-2}.s^{-1} under a 16-h photoperiod did not cause any obvious changes in morphology or leaf colour (Supplemental Figure 1A). Next, we reduced the photoperiod to 12 h and immature leaves from *ccr2* rosettes emerged slightly pale green in comparison to WT. To accentuate this finding, plants were grown under an 8-h photoperiod with a light intensity at 150 µmol.m^{-2}.s^{-1} and immature newly emerged leaves from *ccr2* appeared bright yellow in comparison to WT (Supplemental Figure 1B). With age the yellow leaf (YL) phenotype became less obvious and green leaves (GL) appeared (Supplemental Figure 1C). Irrespective of photoperiod, the chlorophyll levels in rosette leaves from WT were not significantly different, however, the newly emerged leaves from *ccr2* plants grown under a shorter 8-h photoperiod showed a substantial reduction in total chlorophyll (Supplemental Figure 1D). Therefore, by reducing the photoperiod we were able to replicate previous reports describing a leaf colour variegation phenotype for *crtiso* mutants in different plants (Isaacson et al., 2002; Chai et al., 2011).

Next, we demonstrated that day length affects plastid development in newly emerged leaf tissues undergoing cellular differentiation. We were able to replicate the YL phenotype by shifting three-week old *ccr2* plants from a long 16-h to shorter 8-h photoperiod (Figure 1A-B). The newly emerged leaves of *ccr2* appeared bright yellow, while leaves that developed under a 16-h photoperiod remained green, similar to wild type (Figure 1B). Consistent with the phenotype the yellow leaf sectors of *ccr2* displayed a 2.4-fold reduction in total chlorophyll levels, while mature green leaf sectors formed prior to the photoperiod shift had chlorophyll levels similar to that of WT (Figure 1C). The chlorophyll a/b as well as carotenoid/chlorophyll ratios were not significantly different (Figure 1C). Consistent with the reduction in chlorophyll, total carotenoid content in yellow leaf sectors of *ccr2* was reduced due to lower levels of lutein, β-carotene and neoxanthin (Figure 1D). The percentage composition of zeaxanthin and

antheraxanthin was significantly enhanced in yellow leaf sectors, perhaps reflecting a greater demand to enhance photo-protective pigments (Supplemental Figure 1E). But why would a shorter photoperiod in the absence of CRTISO activity cause leaf yellowing and reduce pigmentation? To address this, we used transmission electron microscopy (TEM) to demonstrate that the yellow *ccr2* leaf sectors contained poorly differentiated chloroplasts lacking membrane structures (e.g. well-formed thylakoid and grana stacks) when compared to green leaf tissues from WT (Figure 1E). Therefore, we concluded that a shorter photoperiod alters plastid development during cellular differentiation in emerging immature leaves of *ccr2*.

A shorter photoperiod promotes *cis*-carotenoid accumulation and alters plastid differentiation

We next investigated the relationship between photoperiod, perturbations in carotenogenesis and plastid development. Green leaf tissues from the Arabidopsis *ccr2* mutant have an altered proportion of β-xanthophylls at the expense of less lutein, yet plants grown under a longer photoperiod show normal plastid development (Park et al., 2002). This raised a question: does reducing the photoperiod limit the photoisomerisation of poly-cis-lycopene to all-trans-lycopene thereby altering lutein, ABA and/or strigolactone biosynthesis? To address this *ccr2*, *lycopene epsilon cyclase* (*lut2; lutein deficient 2*), *zeaxanthin epoxidase* (*aba1-3; aba deficient 1*) and *carotenoid cleavage dioxygenase 8* (*max 4*; *more axillary branching 4*) mutants were shifted from a 16-h to 8-h photoperiod (Figure 2A). *ccr2* showed a clear leaf-yellowing phenotype, while the other mutants produced green leaves similar to that of WT. Therefore, we could not attribute the yellow leaf colour to a reduction in lutein or signalling processes induced through a perturbation of strigolactone or ABA biosynthesis.

Next, we tested if the *ccr2* yellow leaf phenotype was linked to the accumulation of *cis*-carotenoids in the upper part of the pathway prior to lycopene formation. Mutations in *PSY, PDS* and *ZDS* cause leaf bleaching and are not viable in soil. Alternatively, *carotenoid*

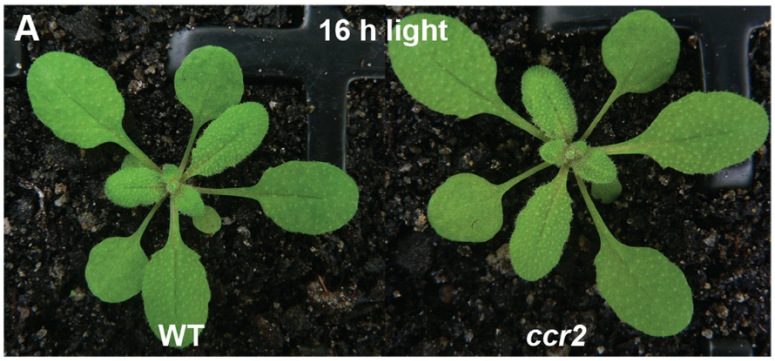

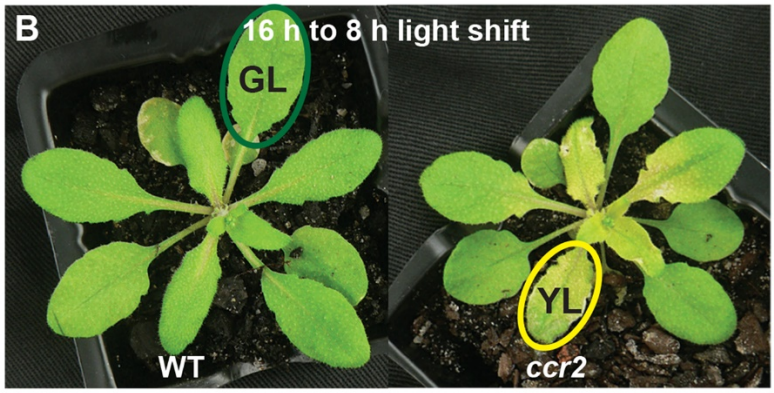

C

Genotype	Leaf	TChl (mol/gfw)	Chl a/b	TCar/TChl
WT	Green	1659 (+/-165)	2.7	0.26
ccr2	Green	1411 (+/-66)	2.8	0.24
ccr2	Yellow	586 (+/-27)*	2.7	0.28

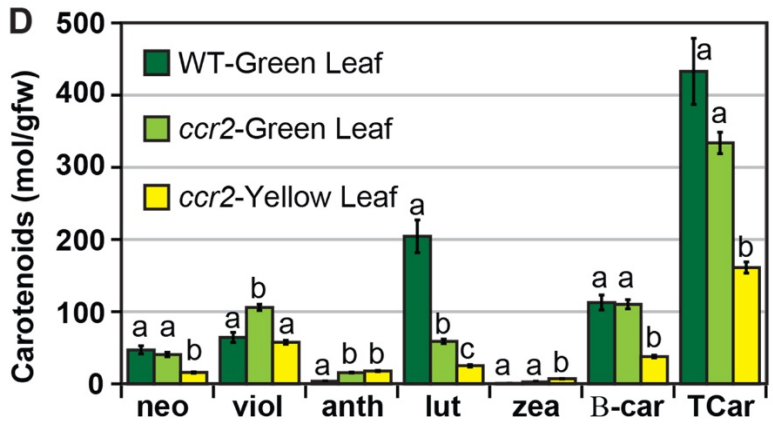

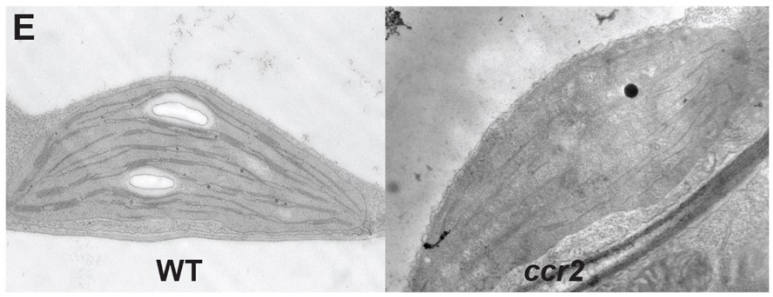

Figure 1. A shorter photoperiod alters plastid development and pigmentation in *ccr2*. (A) Three-week old wild type (WT) and *ccr2* plants growing under a 16-h photoperiod. **(B)** Three-week old plants were shifted from 16-h to 8-h photoperiod for one week and newly formed yellow leaves (YL; yellow outline) emerged from *ccr2*, while green leaves (GL; green outline)

emerged from WT. **(C)** Average chlorophyll levels and pigment ratios in green (WT and *ccr2*) and yellow (*ccr2*) leaves formed one week after a photoperiod shift from 16 to 8 h. Standard error is shown for TChl (n= single leaf from five plants). Star denotes significant differences (*t*-test, $P < 0.05$). **(D)** Absolute carotenoid levels in green (WT and *ccr2*) and yellow (*ccr2*) leaves formed one week after a photoperiod light shift from 16 to 8 h. Values represent average and standard error bars are displayed (n= single leaf from five plants). Lettering denotes significance (*t*-test, $P < 0.05$). Neoxanthin (neo), violaxanthin (viol), antheraxanthin (anth), lutein (lutein), zeaxanthin (zea), β-car (β-carotene), Total Chlorophyll A+B (TChl), Chlorophyll a/b ratio (Chl a/b), Total carotenoids (TCar). **(E)** Transmission electron micrograph images showing a chloroplast with grana stacks from WT green leaf sectors compared to a typical deformed plastid representative from yellow leaf sectors of *ccr2*. Images and values are representative of multiple experimental and biological repetitions.

chloroplast regulator 1 (ccr1 or otherwise known as *sdg8*; *set domain group 8*) and *ζ-carotene isomerase* (*ziso*) mutants are viable and accumulate *cis*-carotenoid molecules in dark-grown etiolated tissues (Cazzonelli et al., 2009b; Chen et al., 2010). Indeed, both *ccr1* and *ziso* displayed a partial yellow leaf phenotype near the zone of cellular differentiation (e.g. petiole-leaf margin). However, unlike *ccr2* the maturing leaf tissues green up rapidly making it harder to distinguish from that of WT (Figure 2A). The overexpression of the native *CRTISO* gene under control of the CaMV35S promoter in *ccr2* and *ccr1* mutant backgrounds successfully prevented the yellow leaf phenotype from appearing in newly emerged immature leaf tissues. Therefore, carotenoid mutants capable of accumulating *cis*-carotenoids can show an altered plastid development when grown under a shorter photoperiod.

This raised a question: does a shorter photoperiod lead to the accumulation of *cis-carotenoid*s in newly emerged leaf tissues of *ccr2* displaying alterations in plastid development? Firstly, we tested if an extended dark period (6 days) would force the accumulation of *cis*-carotenoids in mature (3 weeks) rosette leaf tissues. Indeed, the adult WT leaves appeared pale green having detectable levels of phytofluene and phytoene, while *ccr2* leaves were notably yellow having clearly discernible quantities of *cis*-lycopene, neurosporene isomers, ζ-carotene, phytofluene and phytoene (Figure 2B). We next shifted three-week old WT and *ccr2* plants from a 16-h to 8-h photoperiod and the yellow sectors from newly emerged *ccr2* leaves accumulated detectable levels of *cis*-lycopene, neurosporene isomers, ζ-carotene, phytofluene and phytoene (Figure 2C). Interestingly, even when plants were grown under a 16-h photoperiod we could detect traces of phytofluene and phytoene in floral buds as well as immature rosette leaves from *ccr2*, but not WT (Figure 2D). In addition, a higher ratio of phytofluene and

phytoene relative to β-carotene was observed in newly emerged *ccr2* tissues, which coincided with a lower percentage of lutein, yet higher percentages of zeaxanthin, antheraxanthin and violaxanthin when compared to older more mature tissues (Supplemental Table 1). This led us to suspect that phytoene and phytofluene were not involved in signalling plastid development as they accumulate in tissues exposed to a 16-h photoperiod that showed normal plastid development. In contrast, *cis*-lycopene, neurosporene isomers and di-*cis*-ζ-carotene were not detected in immature *ccr2* leaf tissues from plants grown under a 16-h photoperiod and are hence more likely to be candidates signalling a perturbation in plastid development (Figure 2D).

To investigate if these *cis*-carotenoids generate a graft transmissible signal, we performed reciprocal hypocotyl grafts between *ccr2* and *max4* (*ccd8*). *max4* was chosen due to having a clearly visible shoot branching phenotype and other than strigolactone, was not expected to impact apocarotenoid biosynthesis. Numerous successful grafts showed that the *ccr2* scion always produced immature yellow leaves when grown under a shorter photoperiod (Figure 2E). This confirmed that the impaired plastid development in *ccr2* was unlikely due to a root transmissible signal. Collectively, our findings demonstrate that a shorter photoperiod most likely limits photoisomerisation in newly emerged leaf tissues of *ccr2* undergoing cellular differentiation leading to the accumulation of *cis*-carotenoids that impair plastid differentiation. The question remains: is it really a *cis*-carotenoid and how does it signal a perturbation in plastid development?

Mutagenesis by way of a forward genetics screen restores plastid development in *ccr2*

We hypothesized that a *cis*-carotenoid derived apocarotenoid signal could perturb chloroplast differentiation, thereby affecting organelle and/or cellular signaling processes leading to the yellowing of newly emerged leaf tissues. Because we could not make use of the homozygous lethal *pds*, *psy* and *zds* mutants, we undertook a forward genetics screen. *ccr2* seeds were mutagenized using ethyl-methane sulfonate (EMS) grown and seeds collected from pools of 5-10 M_1 plants. Approximately 40,000 M_2 seedlings from 30 stocks of pooled seeds were screened for the emergence of immature green rosette leaves when grown under a 10-h photoperiod. Initially, 194 EMS-mutagenized revertant *ccr2* (*rccr2*) lines were identified.

However, only 26 reproducibly displayed green immature leaves in response to a photoperiod shift as exemplified by r*ccr2*^{154} and r*ccr2*^{155} (Figure 3A). Leaf tissues of all *rccr2* lines contained reduced lutein and a xanthophyll composition similar to *ccr2* (Figure 3B). When grown under a shorter photoperiod *rccr2* lines produced greener rosettes with less yellow colour compared to *ccr2* and chlorophyll levels were similar to WT (Figure 3C-D).

In order to establish a segregating population for next generation mapping (NGM) of genetic mutations responsible for restoring plastid development in *ccr2*, *rccr2* lines were backcrossed to the original *ccr2* parent (Col-0) and/or a *ccr2* line established in the Landsberg erecta background (*Lccr2*). *rccr2* lines contained a recessive trait associated with the emergence of green leaf tissues when grown under a shorter photoperiod (e.g. r*ccr2*^{154} and r*ccr2*^{155}; Figure 3E). Next generation sequencing (NGS) technologies were used to deep sequence the genomic DNA (gDNA) from leaves of homozygous (M_2) plants and through using a NGM approach we identified non-recombinant deserts in chromosome 1 (360,5576 bp) and chromosome 4 (6,346,463 bp) for both r*ccr2*^{155} and r*ccr2*^{154}, respectively (Figure 3F-G). Both non-recombinant deserts contained SNPs displaying a discordant chastity value of approximately 1.0 representing the actual causal mutation of interest (Austin et al., 2011). Herein we next describe the detailed identification and characterisation of r*ccr2*^{155} and r*ccr2*^{154} as well as define their role in restoring plastid development in *ccr2*.

An epistatic interaction between *ziso* and *ccr2* revealed specific cis-carotenoids perturb PLB formation

rccr2^{155} lacked recombination at the bottom arm of chromosome 1 surrounding a single nucleotide polymorphism (G-A mutation at 3606630 bp) within exon 3 of the *ZISO* gene (639 bp of mRNA), hereafter referred as *ccr2 ziso-155* (Figure 4A). This polymorphism caused a premature stop codon leading to a truncated ZISO protein (212 instead of 367 amino acids). A double mutant generated by crossing *ccr2* with *ziso1-4* (*ccr2 ziso1-4*) confirmed the loss-of-function in *ziso* can restore plastid development in newly emerged immature leaves of *ccr2*. The overexpression of the functional *ZISO* cDNA fragment in *ccr2 ziso-155* restored the leaf-yellowing phenotype displayed by *ccr2* plants grown under an 8-h photoperiod (Figure 4B). Carotenoid analysis of immature leaf tissues of *ccr2 ziso-155* revealed reduced lutein and xanthophyll composition similar to *ccr2*, indicating that the complementation of the YL was

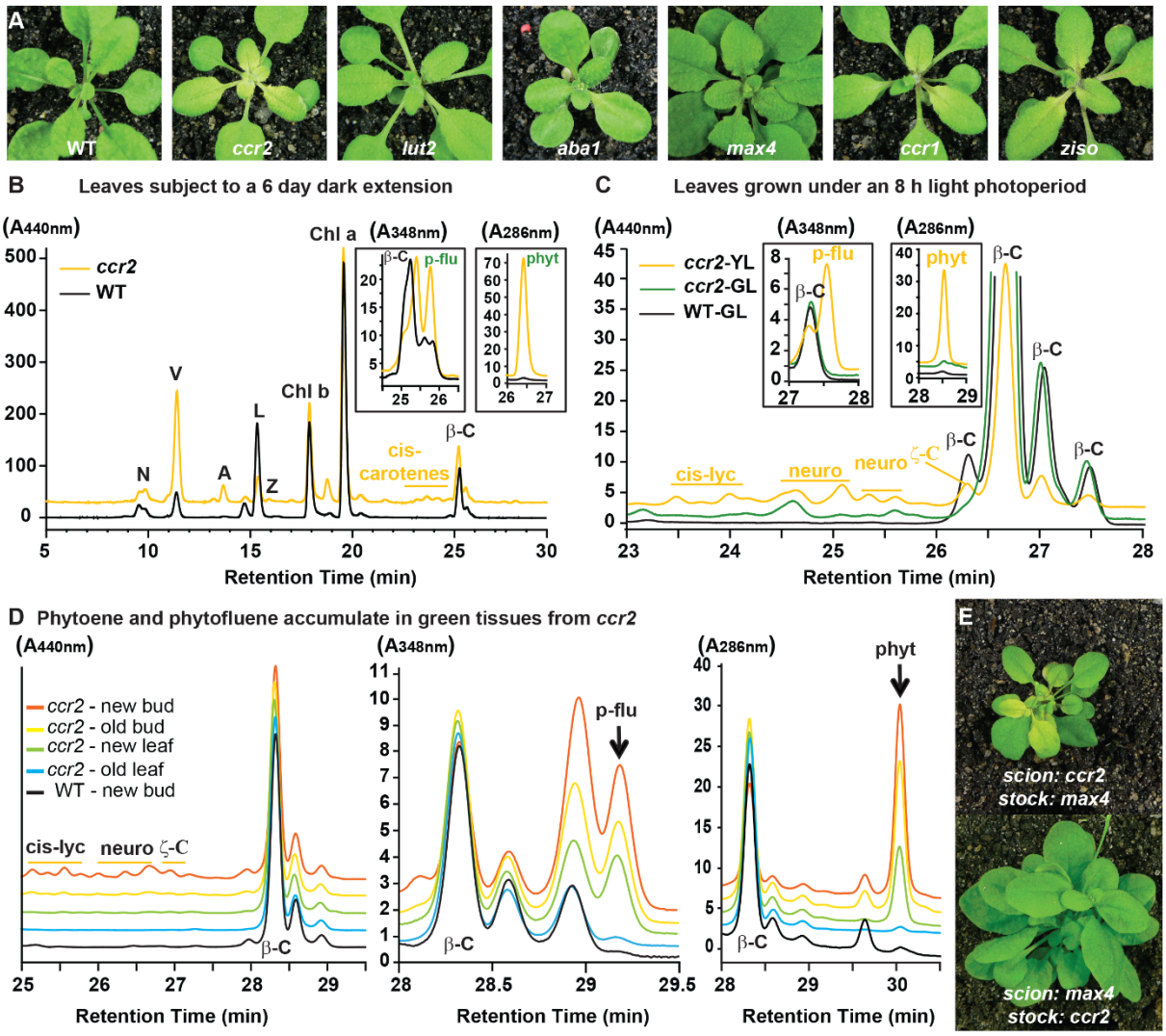

Figure 2. Altered plastid development in *ccr2* is linked with *cis*-carotenoid accumulation and not to a perturbation in ABA or strigolactone. (A) Mutants that perturb the levels of lutein, ABA, strigolactone (SL) and accumulate *cis*-carotenoids (*ccr2*, *ccr1* and *ziso*) were grown for 2 weeks in a 16-h photoperiod and then shifted to a shorter 8-h photoperiod for one week. Representative images showing newly emerged immature leaves from multiple experimental and biological repetitions (n > 20 plants per line) are displayed. Genetic alleles tested include Col-0 (WT), *ccr2* (carotenoid isomerase), *lut2* (epsilon lycopene cyclase), *aba1-3* (zeaxanthin epoxidase), *max4/ccd8* (carotenoid cleavage dioxygenase 8), *ccr1* (set domain group 8) and *ziso* (ζ-carotene isomerase). **(B)** Carotenoid profiles of rosette leaves from three-week-old plants grown under 16-h photoperiod and subjected to a constant dark extension for 6 days. **(C)** Carotenoid profiles of three-week-old rosette leaves from plants grown under constant 8-h photoperiod. **(D)** Carotenoid profiles of old (mature) and new (immature) floral buds and rosette leaves harvested four weeks after germination. Carotenoid profile traces of various tissue extracts from wild type (WT) and *ccr2* are shown at wavelengths close to the absorption maxima of A440 (all xanthophylls, *cis*-lycopene, neurosporene and ζ-carotene) as well as A348 (phytofluene) and A286 (phytoene). violaxanthin/neoxanthin isomers (V/N), violaxanthin (V), antheraxanthin (A), lutein (L), *poly-cis*-lycopene (*cis*-Lyc), tri-*cis*-neurosporene (neuro), ζ-carotene (ζ-C), β-carotene (β-C), lycopene (lyc), phytofluene (p-flu), phytoene (phyt), neurosporene isomers (neuro-iso). HPLC traces are representative of multiple leaves from

multiple experimental repetitions. **(E)** Reciprocal hypocotyl grafts between *ccr2* and *max4* were performed on plant grown under 16-h photoperiod and after two weeks shifted to 8-h photoperiod. Representative images of multiple grafts are displayed.

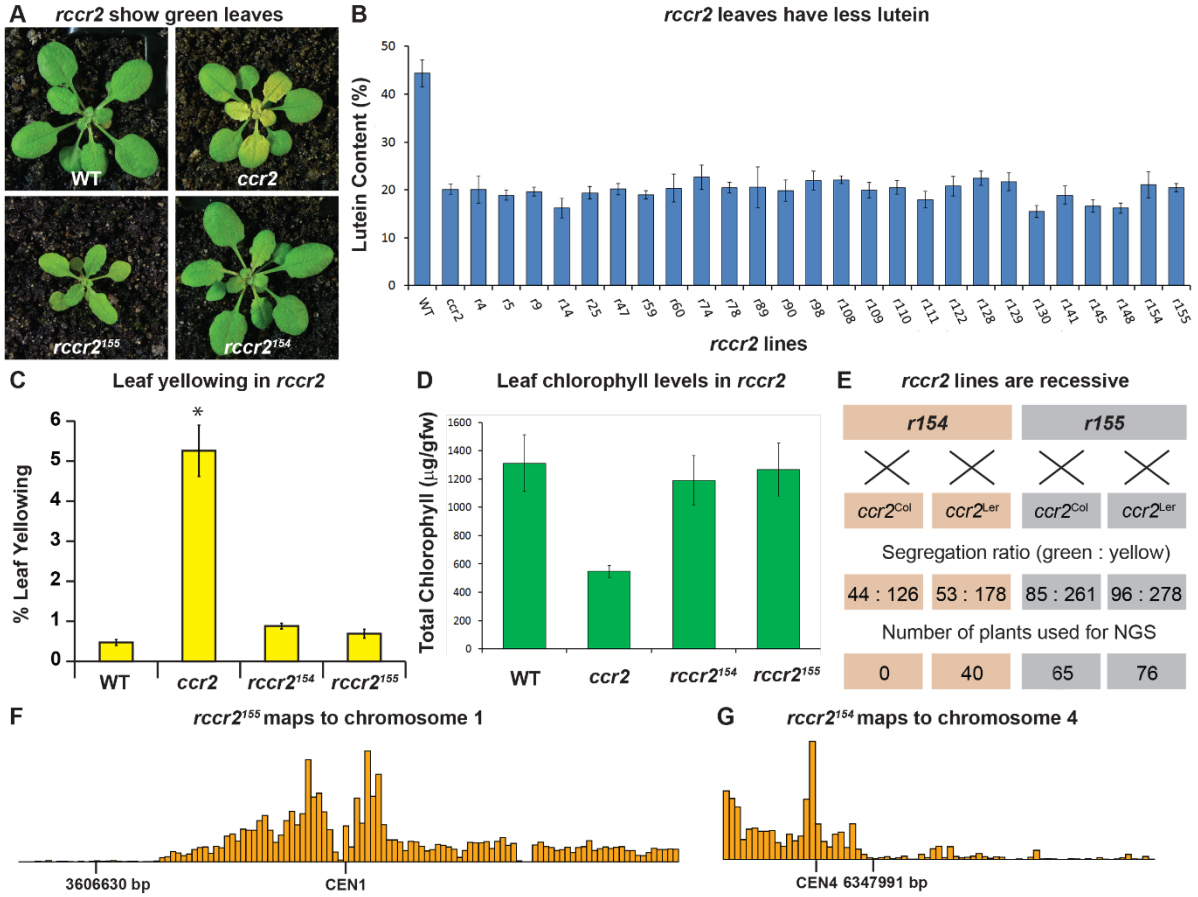

Figure 3. A forward genetics screen identifies revertant lines of *ccr2* having reduced lutein and normal chlorophyll accumulation when grown under a shorter photoperiod. (A) Representative images of *rccr2*^{155} and *rccr2*^{154} rosettes one week after shifting two-week old plants from 16-h to 8-h photoperiod. **(B)** Percentage lutein relative to total carotenoids in immature leaves from WT, *ccr2* and *rccr2* lines. **(C)** Percentage rosette leaf yellowing in WT, *ccr2*, *rccr2*^{154} and *rccr2*^{155} rosettes as quantified using a Lemnatec Scanalyser and software. **(D)** Total chlorophyll content in immature rosette leaves from WT, *ccr2*, *rccr2*^{154} and *rccr2*^{155}. **(E)** Segregation ratios of *rccr2*^{154} and *rccr2*^{155} after backcrossing to the *ccr2* parent from both Columbia (Col-0) and Landsberg erecta (Ler) ecotypes. **(F)** and **(G)** Next generation sequencing of pooled leaf gDNA from a segregating population of *rccr2*^{155} **(F)** and *rccr2*^{154} **(G)** plants revealed less recombination surrounding SNPs at 3606630 bp and 6347991 bp, respectively. Error bars denote standard error and stars reveal statistical significance (*t*-test, $P < 0.05$).

not due to a change in xanthophyll levels (Figure 3B). The epistatic nature between *ziso* and *crtiso* revealed that a specific *cis*-carotenoid downstream of *ZISO* activity perturbed plastid development.

But which of the *cis*-carotenoids is the substrate to produce an ACS (named ACS2) that

perturbs plastid development? Analysis of the *cis*-carotenoid profile in etiolated seedling tissues showed that *ccr2 ziso1-4* had an identical carotenoid profile to that of *ziso* in that it could only accumulate 9,15,9'-tri-*cis*-ζ-carotene, phytofluene and phytoene (Figure 4C). In contrast, *ccr2* accumulated lower levels of these three compounds, yet higher quantities of 9, 9'-di-*cis* ζ-carotene, 7,9,9'-tri-*cis*-neurosporene, 9'-*cis*-neurosporene and 7,9,9',7'-tetra-*cis*-lycopene, all of which were undetectable in the *ccr2 ziso1-4* and *ccr2 ziso-155* mutants (Figure 4C). Therefore, *ziso* blocks the biosynthesis of neurosporene isomers, tetra-*cis*-lycopene and 9, 9'-di-*cis* ζ-carotene under shorter photoperiods, which they themselves or their cleavage products appear to be able to disrupt plastid development in *ccr2* when grown under shorter photoperiods.

How are the specific *cis*-carotenoids disrupting chlorophyll biosynthesis? To answer this question, we examined the plastid structures in WT, *ccr2*, *ziso* and *ccr2 ziso-155* in etiolated cotyledons. As expected all WT cotyledons contained etioplasts having a PLB membrane aggregation of semi-crystalline lattices of branched tubules arranged in geometric patterns (Figure 4D), while *ccr2* lacked the formation of a PLB in all sections examined (Supplemental Table 2). We observed 65% of *ziso* etioplasts contained PLBs (Figure 4D, Supplemental Table 2), which is not surprising given that *ziso* mutants show a partial leaf-yellowing phenotype (Figure 2A). Intriguingly, the majority (>94%) of etioplasts examined from *ccr2 ziso-155* and *ccr2 ziso1-4* contained a PLB (Supplemental Table 2). These data indicate that specific *cis*-carotenoids downstream of *ziso* can perturb PLB formation in dark grown seedlings. This raised a question of whether these *cis*-carotenoids may also affect chloroplast development following deetiolation?

Cotyledon greening of deetiolated seedlings revealed a significant delay in chlorophyll biosynthesis for both *ccr2* and *ziso1-4* when compared to WT after 24, 48 and 72 h of continuous white light (Figure 4E). The reduced levels of chlorophyll in *ziso* were not as severe as *ccr2*, keeping consistent with *ziso* showing a slight yellowing phenotype in comparison to *ccr2* at the margins of newly emerged leaf tissues exposed to shorter photoperiod (Figure 2A). Cotyledons of the *ccr2 ziso-155* and *ccr2 ziso1-4* double mutants accumulated levels of

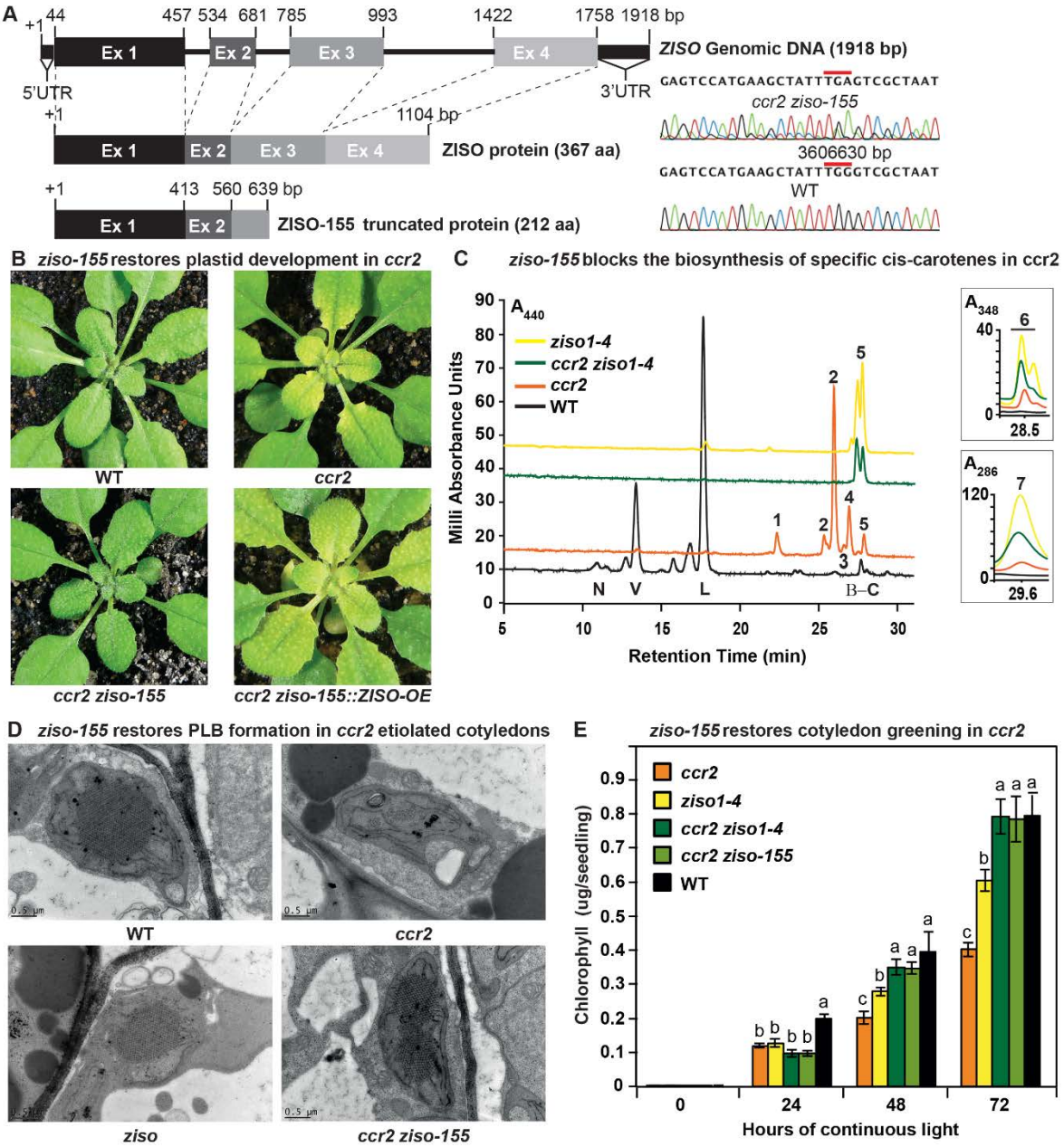

Figure 4. *ziso* alters cis-carotenoid profile to restore PLB formation, plastid development and cotyledon greening in *ccr2*. (A) Schematic structure of the wild type *ZISO* gDNA, ZISO protein and the truncated version of the *ZISO-155* genomic sequence. *ccr2 ziso-155* contains a G->A mutation in AT1G10830 (3606630 bp) as confirmed by Sanger sequencing that results in a premature stop codon (TGA) in exon 3. **(B)** Rosette images of WT, *ccr2*, *ccr2 ziso-155*, and *ccr2 ziso-155::ZISO-OE* showing leaf pigmentations in newly emerged leaves following a photoperiod shift assay. Images are representative of 84/89 T_4 generation *ccr2 ziso-155* plants and multiple plants from six independent lines of c*cr2 ziso-155::ZISO-OE*. **(C)** Carotenoid profiles of dark grown cotyledons from WT, *ccr2*, *ziso1-4*, and *ccr2 ziso1-4* etiolated seedlings. Wavelengths close to the absorption maxima of A440 (ζ-carotene isomers), A348 (phytofluene; insert) and A286 (phytoene; insert) are shown. Neoxanthin (N); violaxanthin (V); lutein(L), β-carotene (β-C). *cis*-lycopene isomers (1 and 2) neurosporene (3); 7,9,9‘-tri-*cis*-neurosporene (4) ζ-carotene (5), phytofluene (6), phytoene (7). **(D)** Transmission electron micrographs of a representative etioplast from five-day-old dark grown cotyledons. The etioplasts of WT, *ziso* and *ccr2 ziso-155* show well-developed PLBs, while *ccr2* does not have any. Images are

representative of more than 15 plastids from at least five TEM sections. **(E)** Total chlorophyll levels in cotyledons following de-etiolation. WT, *ccr2*, *ziso1-4*, *ccr2 ziso-155*, and *ccr2 ziso1-4* were grown in darkness for five days, exposed to continuous white light and chlorophyll measured at 0 24, 48 and 72 h. Letters denote statistical analysis by ANOVA with a post-hoc Tukey test (n > 20 seedlings). Error bars denote standard error.

chlorophyll similar to that of WT, 48 and 72 h following deetiolation (Figure 4E). Since the PLB is required to carry the precursor pigment for chlorophyll, and chloroplasts in cotyledons differentiate mostly from etioplasts, we conclude that a specific *cis*-carotenoid produced in *ccr2* prevents PLB formation during skotomorphogenesis, which perturbs plastid development during photomorphogenesis.

The activation of photosynthesis associated nuclear gene expression restores PLB formation in *ccr2*

Next, we searched for molecular mechanisms by which specific *cis*-carotenoids might perturb PLB formation in *ccr2* and how *ccr2 ziso-155* might restore plastid development. We performed transcriptome analysis on dark-grown etiolated seedlings (ES) and immature rosette leaf tissues from WT, *ccr2* and *ccr2 ziso-155* plants grown under a shorter photoperiod. The immature leaves from *ccr2* were clearly yellow and impaired in plastid development, while immature leaves from WT and *ccr2 ziso-155* were green. Irrespective of the tissue type, there were 2- to 4-fold less differentially expressed genes in *ccr2* (ES;191 and JL;1217) when compared to *ccr2 ziso-155* (ES;385 and JL;5550) (Supplemental Table 3 and 4). Gene ontology (GO) analysis of the miss-regulated genes in both *ccr2* tissue types showed enrichment in metabolic, photosynthetic and abiotic stress responsive processes. In comparison, there was a different enrichment of differentially expressed genes in etiolated tissues of *ccr2 ziso-155,* being mostly involved in responses to hormones, while in immature leaves, the majority of genes appeared to be involved in the regulation of biological process and in particularly chromatin organization.

We searched for differentially expressed genes in *ccr2* common to both etiolated seedlings and leaf tissues (green or otherwise) and noticed a striking downregulation of *PhANGs* (e.g. *HY5*, *DXS*, *CLB6*, *GUN5*, *LHCB1*, *LHCB2* and *RBCS*) and upregulation of photomorphogenesis associated nuclear genes (*PhMoANG*s) (e.g. *DET1*, *COP1* and *PIF3*) (Supplemental Table 5). GO

analysis of the 27 differentially expressed genes in both *ccr2* tissue types showed a significant enrichment in pigment metabolic processes associated with photosynthesis, as well as the positive regulation of biological processes. It is not unusual to observe the miss-expression of *RBCS*, *LHCB* and *CAB1* in mutants having impaired plastid development and altered pigmentation (Ruckle et al., 2007; Woodson et al., 2011). The up-regulation of *COP1/FUS*, *DET1* and *PIF3* in *ccr2* was intriguing and perhaps indicated a level of feedback regulation due to the down-regulation of *PhANGs* and absence of a PLB.

Next, we searched for differentially expressed genes in *ccr2* that were contra-regulated in the *ccr2 ziso-155* mutant background (Supplemental Table 5). Interestingly, of the 27 genes miss-expressed in both tissue types of *ccr2*, 20 were significantly attenuated or contra-regulated in *ccr2 ziso-155* leading to the downregulation of *PhMoANG*s and upregulation of *PhANG*s (Supplemental Table 6). Again, genes involved in biological processes linking photosynthesis, responsiveness to light stimulation and functions in metabolic processes to cellular components such as the chloroplast were pronounced. In particular, there was a clear repression of the *DET1, COP1* and *PIF3* negative regulators of photomorphogenesis as well as the upregulation of *HY5*, a positive regulator of *PhANG*s. This finding is consistent with the fact that genes miss-expressed in *ccr2 ziso-155* leaf tissues were enriched in chromatin modifying processes and DET1 via interaction with DDM1 has been shown to control chromatin processes that in turn regulate *PhANG* expression(Lau and Deng, 2012). Analysis of genes miss-expressed in the *det1* mutant also showed the down-regulation of *PIF3*, and up-regulation of some *PhANGs* (Supplemental Table 6). In summary, our transcriptomics analysis links the accumulation of *cis*-carotenoids to gene regulatory mechanisms that control photosynthesis and photomorphogenesis associated nuclear gene expression.

Activation of photomorphogenesis by *det1*-154 restores plastid development in *ccr2*

Next, we searched for *rccr2* lines that could provide evidence to link *cis*-carotenoid signalling to photomorphogenesis. *rccr2*^{154} was mapped to a mutation in deetiolated 1 (*det1*), hereafter referred as *ccr2 det1-154*, which restored plastid development in immature *ccr2* leaves (Figure 3). Sequencing of the *det1* gDNA identified a G to A point mutation at the end of exon 4 that caused the alternative splicing of exon 4, thereby producing a 69 bp shorter *DET1* transcript

length (Figure 5A; Supplemental Figure 2A). The splicing of exon 4 removed a 23 amino acid open reading frame which is predicted to have homology to a six-hairpin glycosidase-like domain that may catalyse the transfer of sugar moieties from activated donor molecules to specific acceptor molecules (Campbell et al., 1997). Quantitative PCR confirmed that the shorter *DET1-154* transcript (spliced and missing exon 4) was highly enriched (approx. 200-fold) in *ccr2 det1-154*, while the normal *DET1-154* transcript (contains exon 4) was repressed in *ccr2 det1-154* (Supplemental Figure 2B). The above ground phenotypes of *ccr2 det1-154* were consistent with *det1-1* (Chory et al., 1989) showing smaller pale green rosette with a shorter floral stem height and reduced fertility (Supplemental Figure 2C). The overexpression the full length *DET1* transcript (*CaMV35s::DET1-OE)* in *ccr2 det1-154* restored the yellowing phenotype in *ccr2* leaves from plants grown under an 8-h photoperiod (Figure 5B). Therefore, alternative splicing of *det1* and removal of exon 4 appears sufficient to restore plastid development in *ccr2* leaves grown under a shorter photoperiod.

We next investigated how *det1-154* can restore plastid development in *ccr2*. TEM confirmed that the dark-grown cotyledons from etiolated *ccr2 det1-154* seedlings showed PLBs in 69% of etioplasts examined during skotomorphogenesis (Supplemental Table 2, Supplemental Figure 2D). Unlike *ccr2 ziso-155* which blocked the biosynthesis of specific *cis*-carotenoids attributed to blocking PLB formation (Figure 4C), *ccr2 det1-154* accumulated *cis*-lycopene and neurosporene isomers as well as ζ-carotenoid, although the composition of those *cis*-carotenoids was altered (Figure 5C; unpublished data in Table 3.2 of Chapter 3), revealing that *det1-154* restores PLB formation by an alternative mechanism. Interestingly, the activation of photomorphogenesis in *ccr2* by *det1-154*, as evident by etiolated seedlings having characteristic *det1-1* phenotypes such as a shorter hypocotyl, no apical hook and open cotyledons (Figure 5D), agrees with our transcriptomic data whereby *ccr2 ziso-155* lead to a repression of *det1* and activation of *PhANG*s (Supplemental Table 6). As expected the presence of a PLB in *ccr2 det1-154* dark grown seedlings enabled cotyledons to green normally following deetiolation (Figure 5E). Therefore, we can conclude that *ccr2* produces a *cis*-carotenoid derived signal that prevents PLB formation during skotomorphogenesis, yet displays no obvious phenotypes of photomophogenic mutants (Table 1). However, upon activation of photomorphogenesis by *det1-154* in *ccr2*, the PLB becomes restored even in the presence of all detectable *cis*-carotenoids. In conclusion, *ccr2* and *det1* have different signaling mechanisms controlling PLB formation during skotomorphogenesis.

Table 1. A cis-carotenoid derived ACS acts downstream of DET1 to control skotomorphogenesis

Germplasm	Hypocotyl Length		Apical Hook	Cotyledons	PLB	cis-carotenes
WT	normal	13.4 ± 0.2	yes	closed	yes (100%)	no
ccr2	normal	13.8 ± 0.2	yes	closed	no (0%)	yes
ccr2 det1-154	shorter	*8.3 ± 0.2	no	open	yes (69%)	yes

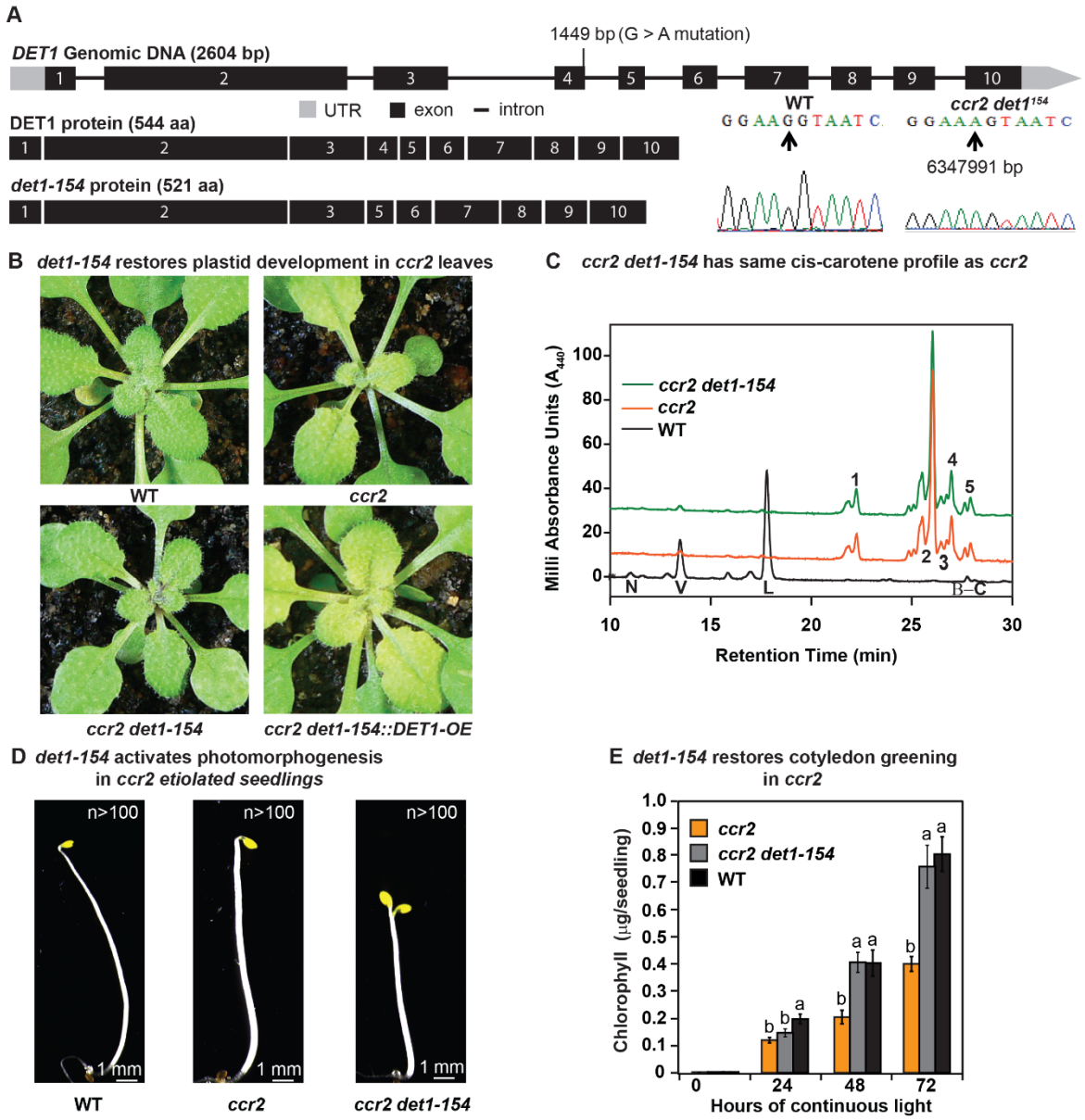

Figure 5. *det1* restores PLB formation, plastid development and cotyledon greening in *ccr2*. **(A)** Schematic structure of the wild type *DET1* gDNA, DET1 protein, SNP confirmation and alternative spliced *DET1-154* protein. A G->A mutation at the end of exon 4 (1,449 bp) of AT4G10180 (6,347,991 bp) was confirmed by sanger sequencing that leads to the skipping of exon 4 (69 bp). The *DET1-154* splice variant produces a shorter protein (521 aa). Exon 4 comprises exactly 23 amino acids containing homology to the six-hairpin glycosidase-like (IPR008928) domain. **(B)** Rosette images of WT, *ccr2*, *ccr2 det1-154*, and *ccr2 det1-154::DET1-OE* showing leaf pigmentations in newly emerged leaves following a 16-h to 8-h photoperiod shift assay. Images are representative of 122/149 T_1 generation *ccr2 det1-154* plants from

twelve independent lines surviving Basta herbicide selection after being transformed with pEARLEY::DET1-OE. **(C)** Carotenoid profiles of dark grown cotyledons from WT, *ccr2*, and *ccr2 det1-154* etiolated seedlings. Wavelengths close to the absorption maxima of A440 (ζ-carotene isomers) show neoxanthin (N); violaxanthin (V); lutein (L), β-carotene (β-C) in WT and *cis*-lycopene isomers (1 and 2) neurosporene (3), 7,9,9'-tri-*cis*-neurosporene (4) and ζ-carotene (5) in *ccr2 det1-154*. **(D)** Etiolated seedling morphology of WT, *ccr2* and *ccr2 det1-154*. Seedlings were grown in the dark for four days on MS media without sucrose. Representative images (>100 seedlings from independent experiments) depict a typical apical hook for WT and *ccr2*, and shorter hypocotyl with open cotyledons for *ccr2 det1-154*. **(E)** Chlorophyll levels in cotyledons following de-etiolation. *ccr2*, *det1-154* and WT were etiolated for 5 days in darkness and thereafter exposed to continuous white light. Chlorophyll measurements were taken at 0 24, 48 and 72 h after deetiolation. Letters denote statistical analysis by ANOVA with a post-hoc Tukey test (n > 20 seedlings). Error bars denote standard error.

D15 inhibition of carotenoid cleavage activity reveals a *cis*-carotenoid derived apocarotenoid signal controls PLB formation

A question remained as to whether the accumulation of specific *cis*-carotenoids lead to the production of ACS2? *cis*-carotenoids are hydrophobic metabolites and oxidative cleavage by enzymatic activity would be likely necessary to enable a plastid–derived *cis*-carotenoid to become a mobile ACS that could somehow regulate PLB formation. We initially crossed *ccr2* to carotenoid cleavage dioxygenase loss-of-function mutants; *ccd1*, *ccd4*, *ccd7* (*max3*) and *ccd8* (*max4*) and tested if plants exposed to a shorter photoperiod would revert the leaf-yellowing phenotype characteristic of *ccr2*. We analysed more than 10 plants for each of the *ccr2 ccd* double mutant lines and observed a perturbation in plastid development in >93% of plants, each displaying clearly visible yellow leaves similar to *ccr2* (Supplemental Figure 3A-B). We concluded that no single *ccd* mutant was sufficient to block the production of any *cis*-carotenoid derived ACS metabolite, however there is a degree of functional redundancy among family members, as well as multiple cleavage activities and substrate promiscuity (Hou et al., 2016).

To address this challenge, we decided to utilise the aryl-C3N hydroxamic acid compound, D15, a good inhibitor of 9,10 cleavage enzymes (CCD) rather than 11,12 cleavage enzymes (NCED) (Van Norman et al., 2014). Exogenous application of D15 to nodes in Arabidopsis yielded strigolactone deficient phenotypes (from MAX3 and MAX4 inhibition), but not ABA-deficient symptoms (Sergeant et al., 2009). D15 is not soluble in water and does not easily penetrate

leaf tissues but seedling roots can absorb D15 from MS media (Sergeant et al., 2009; Van Norman et al., 2014). Therefore, using TEM we imaged etioplasts from dark grown WT and *ccr2* etiolated seedling tissues treated with D15. The majority (86%) of *ccr2* etioplasts displayed a PLB, whilst in control treatments *ccr2* etioplasts showed no discernible PLB (Figure 6A; Supplemental Table 2). D15 had no significant effect on PLB formation in *ziso1-4*, which was still slightly perturbed (Supplemental Table 2). These data indicate that ACS2, derived from a specific *cis*-carotenoid produced downstream of *ziso*, appears to be controlling PLB formation in *ccr2*.

Previously, it was thought that a *cis*-carotenoid produced by *ccr2* was structurally perturbing PLB formation as PChlide levels were normal (Park et al., 2002) and blocking carotenoid biosynthesis using norflurazon (NFZ) treatment was sufficient to rescue PLB formation (Cuttriss et al., 2007). The PChlide levels in WT and *ccr2* after D15 treatment were similar, despite the presence of *cis*-carotenoids and a PLB in *ccr2* (Figure 6B). As expected etiolated *ccr2* seedlings grown on D15-treated MS media accumulated chlorophyll in cotyledons within 24 h of continuous light treatment following deetiolation in a manner similar to WT (Figure 6C). Therefore, a normal PLB is necessary to promote the re-greening of cotyledons and *ccr2* perturbs PLB formation independent of PChlide biosynthesis. In conclusion, chemical inhibition of CCD activity using D15 provides new evidence for the existence of an apocarotenoid likely derived from cleavage of a *cis*-carotenoid downstream of di-cis-ζ-carotene at the 9,10 position, that plays a regulatory role in the earliest steps of PLB formation during skotomorphogenesis and hence plastid development during deetiolation.

ACS2 posttranscriptionally up-regulates POR protein levels when transcript levels are low

Then what is the mechanism by which ACS2 controls PLB formation during skotomorphogenesis? To address this, we examined the effect of D15 on POR protein and transcript levels in WT, *ccr2* and *ccr2 det1-154* etiolated seedlings. We firstly quantified PORA/B protein levels in dark grown seedlings treated with or without D15 and compared the

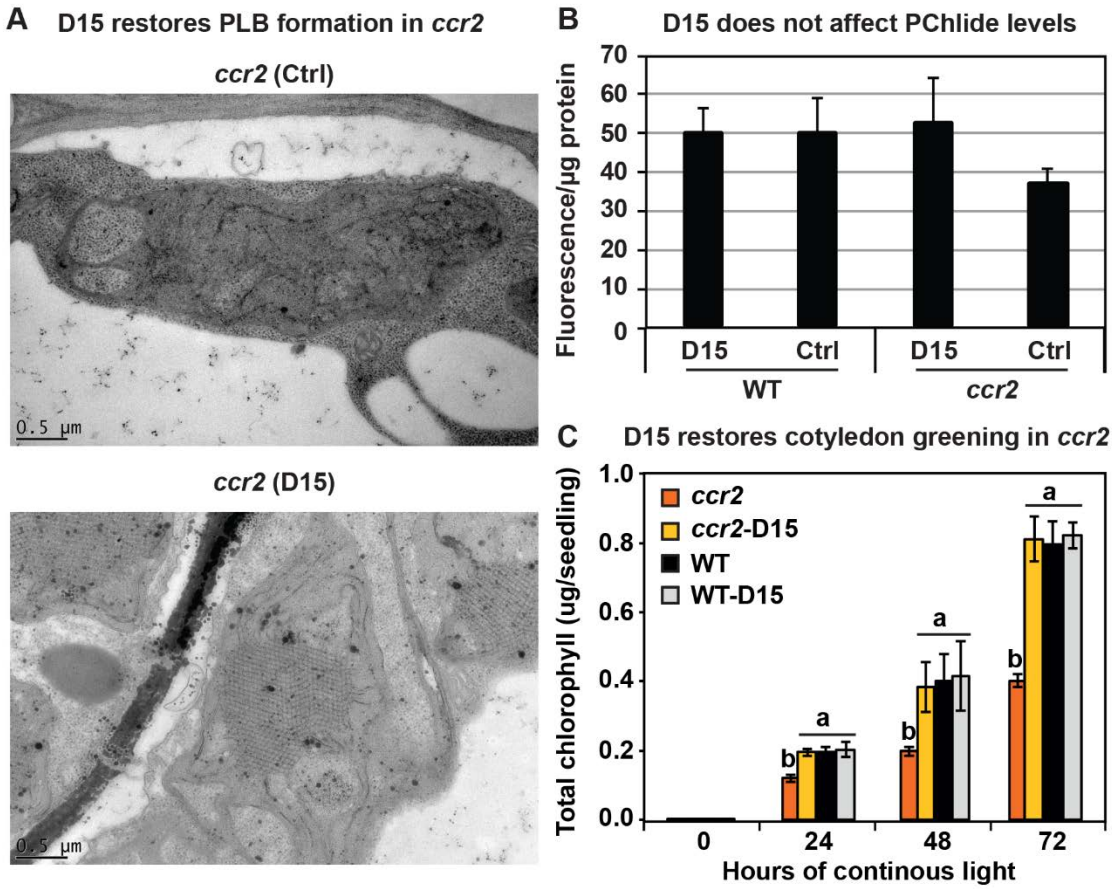

Figure 6. The carotenoid cleavage inhibitor, D15, restores PLB formation in etiolated *ccr2* seedlings and cotyledon greening following deetiolation. (A) Transmission electron micrographs of a representative etioplast from five-day-old dark grown cotyledons reveal a well-developed PLB in *ccr2* treated with the carotenoid cleavage inhibitor D15, but not in *ccr2* treated with ethanol only (control; ctrl). **(B)** Pchlide levels in Wild Type (WT) and *ccr2* treated +/- D15. Fluorescence was measured at 638 nm and 675 nm with an excitation at 440 nm. Net fluorescence of Pchlide was calculated and normalised to protein content. **(C)** D15 restores chlorophyll accumulation in *ccr2* de-etiolated seedlings exposed to continuous light. Twenty seedlings from each of three biological replicates were harvested for chlorophyll determination in every 12 h under continuous light. Ethanol-only was included as a control treatment to dissolve the D15. Statistical analysis was by ANOVA with a post-hoc Tukey test (n = 20 seedlings).

band intensity relative to the actin control protein (molecular weight of 41.6 kD) (Figure 7A-B). The Arabidopsis PORA/B proteins were detected in Arabidopsis as a single immunoreactive signal (PORA; 37 kDa, and PORB; 36 kD) (Sperling et al., 1998; Park et al., 2002; Paddock et al., 2012) (Figure 7A). The POR levels were not significantly different in WT following D15 treatment. A subtle yet significant increase in POR was observed in *ccr2* and D15 treatment reduced POR back to WT levels highlighting a likely role for ACS2 in regulating POR protein levels (Figure 7A-B). This was exemplified by a substantial 80% reduction in POR protein levels

in *ccr2 det1-154* following D15 treatment, and is in agreement with previous studies that protein and transcript levels of POR were dramatically reduced in a *det1* mutant (Sperling et al., 1998). Therefore, it seems that ACS2 acts downstream of *det1* to control POR protein levels. We next examined if ACS2 regulates POR protein levels at the transcriptional and/or posttranslational level? PORA and PORB mRNA and protein levels are present at relatively high levels in etiolated seedlings, becoming down-regulated upon exposure to white light induced photomorphogenesis (Armstrong et al., 1995) and were previously shown to be down-regulated in *det1* and *cop1* mutants (Sperling et al., 1998). PORA has been described as the major enzyme required for chlorophyll production (Paddock et al., 2010). We quantified transcript levels of *PORA* and *PORB* transcripts and while we observed a slight reduction in response to D15 treatment of WT etiolated seedlings, there was a striking repression of *PORA* and *PORB* in *ccr2 det1-154* irrespective of D15 treatment. Collectively, our evidence has identified that ACS2 acts downstream of DET1 to posttranscriptionally regulate PORA and PORB protein levels, despite having negligible effects on POR transcript levels (Figure 7C).

DISCUSSION

Seasonal photoperiods link *cis*-carotenoids to leaf yellowing and altered plastid development

Determining a function for *cis*-carotenoids has been challenging as apart from some fruits (e.g. tomato and melon) and mutant etiolated tissues (Isaacson et al., 2002; Park et al., 2002), *cis*-carotenoids tend not to accumulate at detectable levels in photosynthetic tissues. *cis*-carotenoids may be more than just a by-product from inefficient carotenoid biosynthesis, as several reports now link their accumulation to the control of *PSY* gene expression and epistasis in tomato colour (Kachanovsky et al., 2012), 5'UTR mediated translational control of PSY protein abundance (Kachanovsky et al., 2012; Alvarez et al., 2016), and leaf development in Arabidopsis(Avendano-Vazquez et al., 2014). These reports highlight that *cis*-carotenoids as signals themselves or as substrates for apocarotenoid biosynthesis may control development, organelle signaling and molecular feedback regulation. However, determining a physiological function for *cis*-carotenoid accumulation *in planta* has been confounded as it is unknown which prevailing environmental condition can facilitate their accumulation in a tissue-specific manner. Interestingly, carotenoid isomerase mutants from different plant species all share a

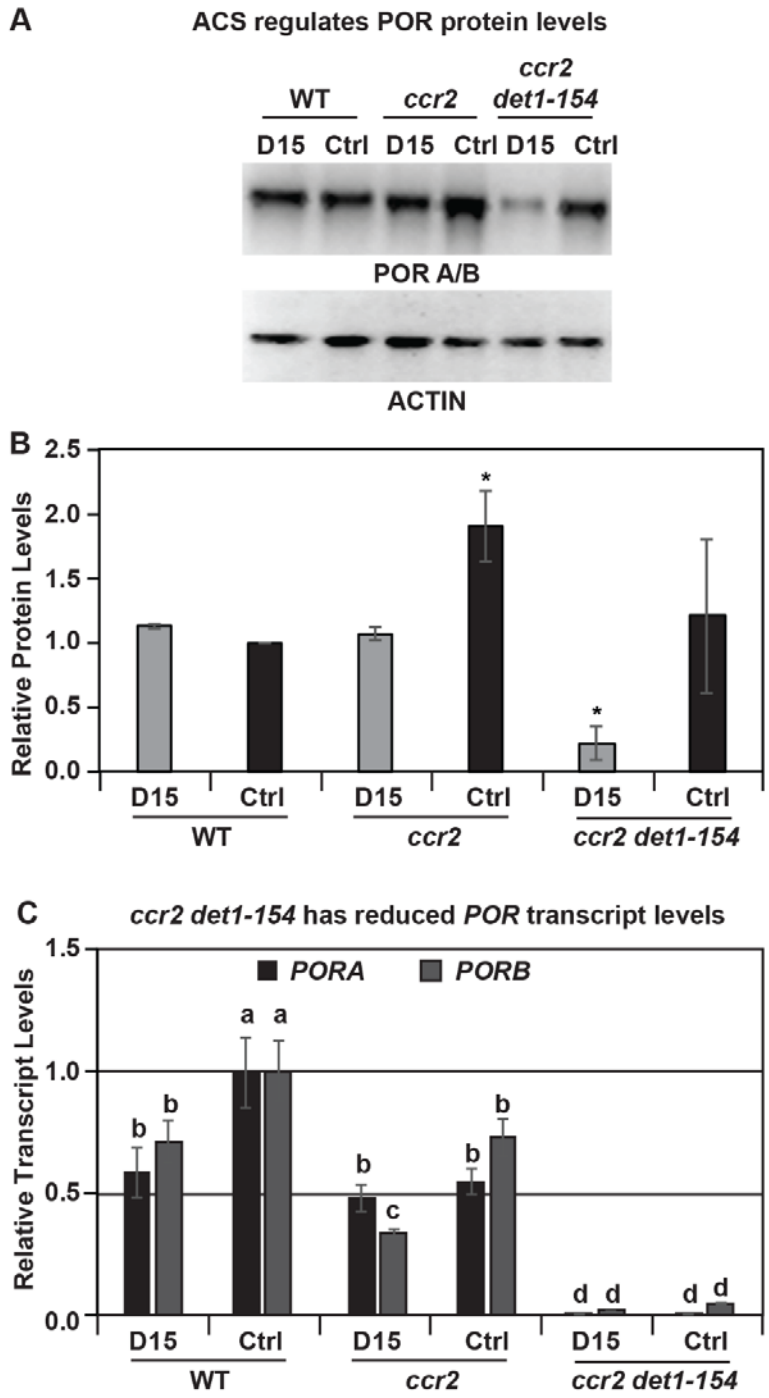

Figure 7. Chemical inhibition of CCD activity identifies a *ccr2* generated apocarotenoid signal that acts downstream of *det1-154* to post-transcriptionally regulate POR protein levels. (A) Representative image of a western blot showing POR and Actin protein levels. Proteins were extracted from WT, *ccr2* and *ccr2 det1-154* etiolated seedlings grown on MS media (Ctrl) or media containing D15. **(B)** Quantification of the average of three biological western blots normalised against actin as a protein loading control. ImageJ was used to quantify bands and statistical analysis performed using a two-way ANOVA with post-hoc Tukey test. Stars signify significant differences. Error bars represent standard error (n=3). **(C)** Transcript levels of *PORA* and *PORB* in WT, *ccr2* and *ccr2 det1-154* etiolated seedlings growing on control (Ctrl) MS media or containing D15. Statistical analysis was confirmed by ANOVA (Two-Factor With Replication) followed by with a post-hoc test. Error bars represent standard error.

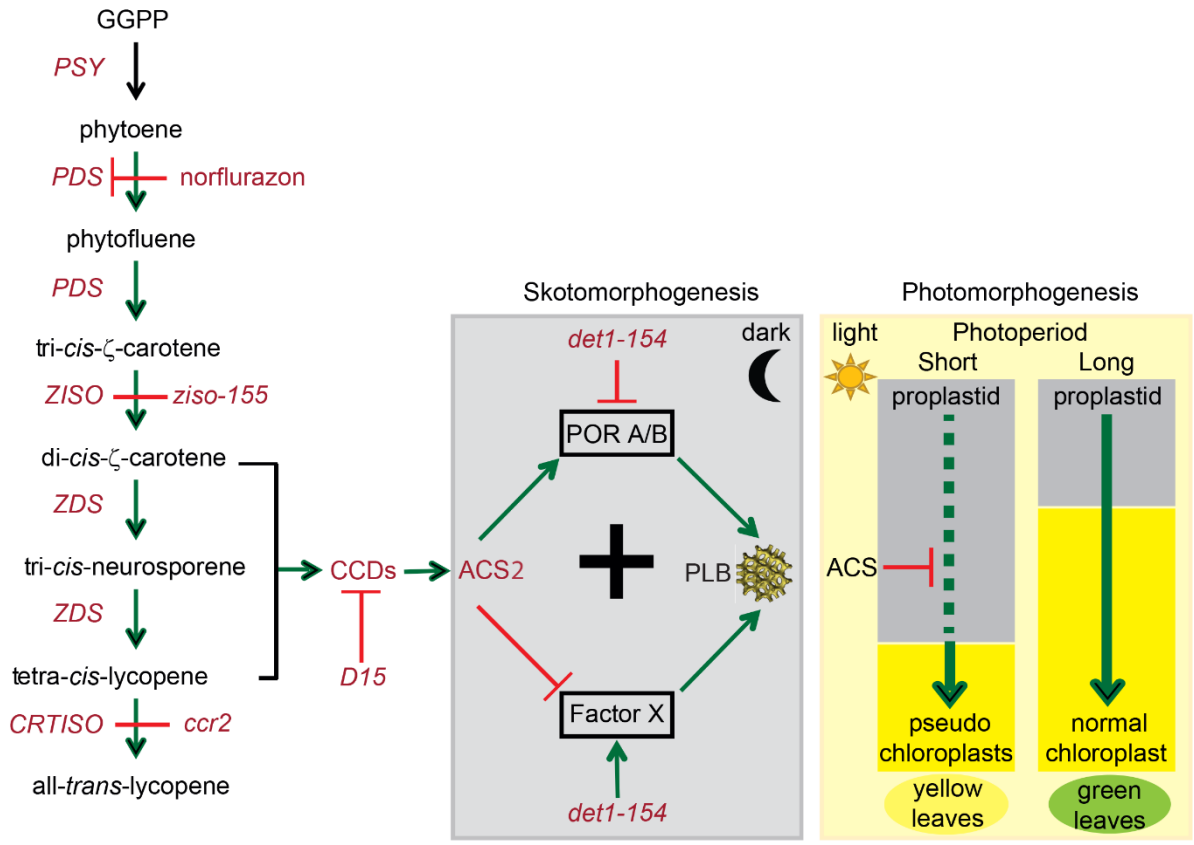

Figure 8. Model describing how ACS2 affects PLB formation during skotomorphogenesis and chloroplast biogenesis during photomorphogenesis. In the dark, *ccr2* accumulates specific poly-*cis*-carotenes that generate ACS2 via CCD activity. During skotomorphogenesis, production of ACS2 post-transcriptionally enhances POR protein translation to maintain PChlide levels, yet ACS2 also inhibits "Factor X" required for PLB formation. Factor X might represent a retrograde signal, hormone, gene and/or protein. NFZ and *ziso-155* block the biosynthesis of di-*cis*-ζ-carotene, neurosporene isomers and tetra-*cis*-lycopene, which are likely substrates for the biosynthesis of ACS2. Chemical inhibition of CCD activity by D15 blocks the production of the ACS2. The *det1-154* splice mutant activates photomorphogenesis and *PhANG*s thereby promoting PLB formation, chloroplast development and chlorophyll biosynthesis in newly emerged leaves grown under a shorter photoperiod. Green lines represent positive regulation and red lines represent negative inhibition. PSY, phytoene synthase; PDS, phytoene desaturase, ZDS, ζ-carotene desaturase; ZISO, ζ-carotene isomerase; CRTISO, carotenoid isomerase; *det1-154*, Deetiolated1; D15, inhibitor of CCD activity; CCD, carotenoid cleavage dioxygenase; *ccr2*, *CRTISO* mutant.

leaf phenotype consisting of yellow and green transition sectors, that become prominent depending upon the growth season. We have taken advantage of using the Arabidopsis *crtiso* mutant (Park et al., 2002), known to accumulate *cis*-carotenoid species in dark-grown etiolated tissues, to identify which photosynthetic tissues accumulate *cis*-carotenoids and determine the seasonal factor causes leaf yellowing.

Here we demonstrate that photoperiod and hence the duration of darkness, is one major contributing factor that can enhance *cis*-carotenoid accumulation in photosynthetic tissues. Newly developed floral buds and leaves from *ccr2* accumulated trace levels of phytoene and phytofluene when plants were grown under a long photoperiod (Figure 2B and D). However, high levels of these *cis*-carotenoids as well as ζ-carotene, neurosporene isomers and tetra-cis-lycopene accumulated when plants were exposed to a shorter photoperiod or extended darkness (Figure 2C). This could be explained by a higher *PSY* promoter activity resulting in a build-up of non-metabolized intermediates during higher phytoene flux in younger tissues (Welsch et al., 2003). The accumulation of *cis*-carotenoids in tissues undergoing rapid cell division (apical meristems) and cellular meiosis (pollen grain in floral bud) is mirrored by a stronger expression pattern for *CRTISO* in these tissues (Cazzonelli et al., 2010). Perhaps the higher abundance of *cis*-carotenoids in younger tissues reflects a role for themselves or their apocarotenoid derivatives in cellular programming events (Cazzonelli et al., 2009b). Nonetheless, it is clear that CRTISO activity must be strictly controlled in newly developing tissues to maintain *cis*-carotenoid levels and hence maintain carotenoid flux through to the epsilon- and beta-carotenoid branches in the pathway**.**

In Arabidopsis, the accumulation of *cis*-carotenoids during skotomorphogenesis caused the absence of a PLB to form in etioplasts, thereby delaying cotyledon greening following deetiolation (Park et al., 2002). Arabidopsis rosette leaves that emerged from *ccr2* plants grown under a shorter photoperiod contained yellow and green leaf transition sectors with cells containing pseudo-chloroplasts (Figure 1A-C and E), reminiscent of a virescent phenotype described for other plant species, defective in *CRTISO* activity. The altered plastid development in *ccr2* was not attributed to a block in lutein, strigolactone, ABA or alteration in xanthophyll composition, and furthermore the leaf-yellowing phenotype was not graft transmissible (Figure 1D; Figure 2A and E; Supplemental Figure 1E). Since the *ccr2 ziso-155* double mutant can limit the biosynthesis of specific *cis*-carotenoids (e.g. ζ-carotene, neurosporene isomers and tetra-cis-lycopene) and restore plastid development in greening leaves as well cotyledons following de-etiolation (Figure 3A, C-D; Figure 4B-C, E), we reasoned that the yellowing phenotype was linked to the accumulation of specific *cis*-carotenoids. In the rice *zebra2/crtiso* mutant the leaf-yellowing phenotype was attributed to the photoperiodic accumulation of tetra-*cis*-lycopene and the simultaneous generation of singlet oxygen (Han et al., 2012). Yellow leaf tissues impaired in plastid development would be

expected to accumulate singlet oxygen. However, leaf yellowing is not always linked to seasonal photoperiod changes or *cis*-carotenoid accumulation and it seems likely that in this case the impairment in plastid development manifests in the production of singlet oxygen. Therefore, we concluded that the shorter photoperiod and extended darkness enhance the accumulation of specific *cis*-carotenoids causing a perturbation in plastid development from which the generation of singlet oxygen manifests causing leaf yellowing.

Extended dark limits photoisomerisation causing specific *cis*-carotenoids to accumulate

This raised the question of how a shorter photoperiod might cause the accumulation of *cis*-carotenoids and which cis-carotenoids perturb plastid development? There are two isomerase reactions during cis-carotenoid biosynthesis, tri-*cis*-ζ-carotene to di-*cis*-ζ-carotene and tetra-*cis*-lycopene to all-*trans*-lycopene mediated by ZISO and CRTISO, respectively (Masamoto et al., 2001; Giuliano et al., 2002; Park et al., 2002; Chen et al., 2010). Enzymatic isomerisation is necessary during skotomorphogenesis and in the absence of light. However, in both *ziso* and *crtiso* Arabidopsis mutants when photoperiod is sufficient the phenomena of photoisomerisation occurs, controlling *cis*-carotenoid accumulation. These two isomerase mutants do not share the same intensity of yellowing in newly emerged leaves. A moderately shorter photoperiod induces signs of leaf yellowing in *ccr2*, but not *ziso* (unpublished data). Under extended dark or very short photoperiods, *ccr2* leaves become strongly virescent, while *ziso* leaves display mild yellowing (Figure 2A). Similarly, *ziso* and *ccr2* etiolated cotyledons show different degrees of plastid development. During skotomophogenesis, *ziso* etioplasts produce normal PLBs in 66% of the cells observed, while *ccr2* does not produce any PLBs (Supplemental Table 2; Figure 4D). *ccr2* cotyledons show a severe delay in greening following deetiolation, while *ziso* cotyledons show only a partial delay in greening (Figure 4E). There are two plausible options: photoisomerisation of tri-*cis*-ζ-carotene to di-*cis*-ζ-carotene is more efficient than tetra-*cis*-lycopene to all-*trans*-lycopene under a reduced lighting duration, or a specific *cis*-carotenoid downstream of tri-*cis*-ζ-carotene perturbs plastid development thereby inducing leaf yellowing. Therefore, photoisomerisation can be rate-limiting depending upon the photoperiod and age of tissue, which affects the accumulation of specific *cis*-carotenoids that have a physiological function controlling plastid development.

We provided direct evidence through the epistatic interaction of *ZISO* and *CRTISO* that neurosporene and tetra-*cis*-lycopene isomers or maybe even 9, 9'-di-*cis* ζ-carotene are the specific *cis*-carotenoids that accumulate in tissues of *ccr2,* but not *ziso*, and perturb PLB formation thereby delaying cotyledon greening following de-etiolation (Figure 4C-E; Supplemental Table 2). Treatment of etiolated seedlings with NFZ restored PLB formation in *ccr2* etioplasts (Cuttriss et al., 2007), highlighting that phytoene accumulation, the absence of xanthophylls or an altered carotenoid composition were not the cause of the PLB perturbation observed in *ccr2*. The accumulation of neurosporene and its isomers in *ccr2* are in agreement with a previous finding where the silencing of *CRTISO* in tomato fruit tissues insensitive to photoisomerisation led to the accumulation of neurosporene isomers (Fantini et al., 2013). Both neurosporene and tetra-*cis*-lycopene isomers were implicated as potential substrates for cleavage into a signaling metabolite that controls PSY gene and/or protein expression levels (Kachanovsky et al., 2012; Alvarez et al., 2016). These *cis*-carotenoids can be found to accumulate in newly emerged yellow leaf tissues of *ccr2* plants growing under a shorter photoperiod (Figure 2C-D). It also seems reasonable that the loss-in-function of *ziso* also forced the accumulation of di-*cis*-ζ-carotene. Isomers of di-*cis*-ζ-carotene were described as products and/or substrates in the plant poly-*cis*-carotenoid biosynthetic pathway to lycopene (Breitenbach and Sandmann, 2005) and are implicated in controlling leaf development (Avendano-Vazquez et al., 2014). We did not observe any obvious effect of a shorter photoperiod on *ccr2* rosette leaf development. Therefore, we conclude that di-*cis*-ζ-carotene, neurosporene and tetra-*cis*-lycopene or their isomers are the candidate *cis*-carotenoids accumulating in *ccr2* that perturb thylakoid membrane integrity and the lattice like formation of the PLB in the *ccr2* mutant.

ACS2 regulates nuclear gene expression and plastid development

Although there is strong evidence to implicate the existence of *cis*-carotenoid derived apocarotenoid signaling metabolites having regulatory functions, they are yet to be characterised (Hou et al., 2016). It would appear that the *cis*-carotenoids themselves are not membrane bound structural regulators of PLB formation as previously proposed (Park et al., 2002), rather they are substrates for a apocarotenoid signal? The chemical inhibition of CCD activity by D15 restored PLB formation in *ccr2* etioplasts, despite the accumulation of *cis*-carotenoids (Figure 6; Supplemental Table 2). While D15 did not affect PChlide levels in WT or

ccr2, it did reduce POR protein levels in etiolated cotyledons from *ccr2*. Therefore, *ccr2* appears to make an a cellular mobile retrograde apocarotenoid signal. It was previously shown that the *CCD4* mutant could rescue leaf development and the retrograde control over gene expression in *zds* mutants that accumulated di-*cis*-ζ-carotene, in addition to tri-*cis*-ζ-carotene and phytofluene (Avendano-Vazquez et al., 2014). The *ccr2 ccd4* double mutant did not restore plastid development (Supplemental Figure 3) allowing us to conclude that the ACS mediating the needle like leaf development in *zds/clb5* mutants is unlikely to be the same as that controlling plastid development in *ccr2*. The accumulation of tri-*cis*-neurosporene or 7,9,9′,7′-tetra-*cis*-lycopene were shown to be preferred substrates of *in vitro* CCD7 enzymatic cleavage at the 9,10 positions (Bruno et al., 2016). However, the loss-in-function of *ccd7* was not sufficient to restore plastid development in *ccr2*. Similarly, *ccd1* and *ccd8* were also not sufficient to restore plastid development in *ccr2*. Evidently, there could be redundancy among two or more CCDs in generating a *ccr2* derived ACS. Our future experiments will focus on testing this hypothesis and identifying the identity of ACS2.

Hypocotyl and floral meristem grafting studies demonstrated that *ccr2* was not generating a mobile signal that moved from root to shoot or from shoots to the floral meristem (Figure 2E). To assess its potential to control intracellular processes, we undertook in depth analysis of the transcriptome from dark grown etiolated and leaf tissues which had altered and restored plastid development. Interestingly *ccr2* lacking a PLB, displayed a transcript profile having a significant upregulation of genes involved in photomorphogenesis, which would lead to a down-regulation of *PhANG* gene expression (Supplemental Table 6). The restoration of the PLB in the *ccr2 ziso* double mutant conversely downregulated key gene involved in photomorphogenesis such as *DET1*, *PIF3* and *COP1*, which lead to the upregulation of *PhANG* expression and other genes involved in retrograde gene expression (Supplemental Table 6). This is consistent with photomorphogenesis mutants like *det1* regulating *PhANG* expression (Schroeder et al., 2002), and substantiates that a *cis*-carotenoid derived signal is involved in the control of plastid signalling pathways downstream of photomorphogenesis. The downregulation of expression of some *PhANG*s in *ccr2* was similarly observed in the *zds/clb5* mutant that accumulates phytofluene and ζ-carotene (Avendano-Vazquez et al., 2014). Mutants disrupting *cis*-carotenoid accumulation hence may have overlapping roles in disrupting plastid development. The down-regulation of *DET1*, *PIF3* and *COP1* in *ccr2 ziso* (Supplemental Table 6) revealed that the *cis*-carotenoid derived ACS2 targets the regulation

of genes involved in *PhMoANG* expression thereby playing a key role in controlling PLB formation during skotomorphogenesis. This raised the question as to what might be the key gene regulatory target of ACS2 and how it might control PLB formation during skotomorphogenesis.

ACS2 signals downstream of *DET1* to posttranscriptionally regulate POR

DET1 encodes a nuclear protein acting downstream from the phytochrome photoreceptors to regulate light driven seedling morphogenesis and *PhANG* expression (Schroeder et al., 2002). It has been suggested that *det1* up-regulates carotenoid levels and affects chromoplast development in tomato (Kilambi et al., 2013). A model has been proposed whereby DET1 and the chromatin regulator DDB1, negatively regulate the expression of hundreds of genes via chromatin interactions (Lau and Deng, 2012). DET1 interacts with COP1, to limit promoter access and transcription factor availability, respectively (Schroeder et al., 2002; Lau and Deng, 2012). In response to light stimulation during de-etiolation, the rapid down-regulation of *DET1*, leads to the repression of other *PhMoANG*s (e.g. *COP* and *PIF* genes) and up-regulation of *PhANG*s (Benvenuto et al., 2002). Whereas *det1* null alleles are lethal following germination, weaker alleles survive and exhibit various phenotypes as adults, including open cotyledons and shorter hypocotyls in dark grown seedlings as well as a pale coloured rosette and poor fertility in light grown plants (Chory et al., 1989). The transcriptomic profile of *ccr2 ziso-155* revealed some similarity to the *det1-1* mutant in terms of differentially expressed *PhANGs* as well as reduced *DET1* and *PIF3* levels, however it did not show any classical photomorphogenic phenotypes (Supplemental Table 6). The *ccr2 det1-154* splice mutant did however display *det1*-like phenotypes similar to those previously described (Figure 5D; Supplemental Figure 2C) (Chory et al., 1989). *det1-154* is a partial loss-of-function *det1* mutant allele producing a smaller peptide due to the alternative splicing that skips a highly conserved 4th fourth exon, that may play some important role in promoting genome wide chromatin interactions (Figure 5A; Supplemental Figure 2A-B). Intriguingly, *ccr2* restored PLB formation in *det1-154* (Supplemental Figure 2D) yet *det1-1*/*cop1* mutants do not contain a PLB nor do they generate normal levels of POR or PChlide (Sperling et al., 1998). This evidence leads us to hypothesise that *ccr2*, which does not have a PLB, yet contains normal POR and PChlide levels, was

providing a *cis*-derived apocarotenoid signal that could act downstream of *det1-154* to restore PLB formation. By this analogy, the presence of the *cis*-carotenoid itself would not be responsible for structurally perturbing the PLB formation as was originally proposed (Park et al., 2002) since *ccr2 det1-154* still contains *cis*-carotenoids. Therefore, the mechanisms by which *ccr2* perturbs PLB formation whilst having normal POR and Pchlide levels and how D15 restores PLB formation in *ccr2* remains a mystery open for future investigation. Perhaps, there is another ACS that regulates PLB formation directly or indirectly, which *det1-154* may be able to bypass, an area of research requiring further investigation beyond the scope of this work. What is clear is that *ccr2* generates ACS2 restoring PLB formation in *det1-154*.

Previous studies showed that PLB formation in *cop1* mutants could be restored by the overexpression of *PORA* (Sperling et al., 1998). Therefore, we reasoned that POR could be the downstream target of the *ccr2* generated ACS2. Indeed, we observed *ccr2* to enhance POR, although not to a significant extent (Figure 7A-B). The fact that D15 treated etiolated *ccr2* seedlings could reduce POR protein levels in *ccr2* back to wild type levels, yet have no effect on *POR* transcription provided evidence that some post-transcriptional feedback mechanism underpinned the regulation by ACS2 (Figure 7). The posttranscriptional regulation of PORA has been previously reported (Paik et al., 2012). The treatment of *ccr2 det1-154* with D15 was sufficient to block plastid development and POR protein levels, yet *POR* transcript levels remained unchanged and almost absent. Therefore, we propose that a *ccr2* derived *cis*-carotenoid cleavable by CCD activity generates ACS2 that moves out of the chloroplast to post-transcriptionally enhance POR protein levels even when *POR* transcript levels are barely detectable. So how and why might ACS2 regulate POR protein levels?

The negative effect of light on PORA is mediated at three different levels. 1) The *PORA* mRNA declines, 2) the plastids may lose their translational capacity or efficacy in their ability to import POR and/or, 3) PORA may become destabilised in illuminated seedlings (Sundqvist and Dahlin, 1997). POR possesses several features: it has a light-dependent catalytic activity; it can accumulate in plastids of dark-grown angiosperms (etioplasts) via binding to the Pchlide substrate, and the POR complex requires NADPH acts as a cofactor to form the PLBs (Masuda and Takamiya, 2004). NFZ was previously shown to rescue the PLB in *ccr2*, substantiating that ACS2 can prevent PLB formation, yet maintain wild type POR levels (Park et al., 2002; Cuttriss et al., 2007). Perhaps, the accumulation of *cis*-carotenoids under specific conditions when CRTISO activity or photoisomerisation are rate-limited (e.g. absence of SDG8; (Cazzonelli et

al., 2009b), aid the generation of ACS2 that suppresses PLB formation and plastid development, yet maintains higher levels of POR (Figure 7A-B) to help prime and/or slow chloroplast biogenesis until the environmental conditions become more favourable. Obviously photoperiod represents an environmental condition that triggers reproductive development and interestingly, the chromatin regulator SDG8, a major regulator of flowering time in Arabidopsis, is required for permissive expression of *CRTISO* (Cazzonelli et al., 2009a). PORA has been proposed to play a special role in the formation of POR ternary complexes containing photoactive Pchlide-F655, PLB assembly, and protection against photo-oxidative damage caused by non-photoactive Pchlide (Reinbothe et al., 1996). Indeed, our evidences clearly demonstrate that POR is the likely target of regulation by ACS2. Perhaps ACS2 perturbs the POR ternary complex or posttranscriptional regulation mediated by *det1*. Alternatively, ACS2 may prevent the import of POR protein into the chloroplast, affect POR activity and/or binding to the Pchlide substrate. The mechanism by which ACS2 posttranscriptionally regulates POR has become the focus of our future investigations. In conclusion, herein we provide new evidence that the *cis*-carotenoid derived ACS2 signals the nucleus in a retrograde manner to control PLB formation through the posttranscriptional regulation of POR protein levels during skotomorphogenesis and affects chloroplast biogenesis during photomorphogenesis (Figure 8).

METHODS

Please refer to chapter 2: Materials and Methods. All related methods have been included in chapter 2 and for submission. They will be slightly amended to meet the requirements of the journal.

SUPPORTING INFORMATION

Supplemental Table 1. Immature *ccr2* tissues have *cis*-carotenoids and altered xanthophyll composition.

Genotype	Tissue	Age	Percentage Xanthophyll Composition						Relative Ratio	
			Lutein	β-C	Zea	Anth	Viol	Neo	Phyt	p-flu
WT	Rosette Leaf	new	50	26	0.0	0.5	10	13	0.00	0.00
	Rosette Leaf	old	48	27	0.1	0.6	11	13	0.00	0.00
	Floral Bud	new	50	24	0.0	0.6	15	10	0.00	0.00
	Floral Bud	old	51	23	0.0	0.4	16	9	0.00	0.00
	Maximum SD		1	1	0.3	0.4	0	2	ND	ND
ccr2	Rosette Leaf	new	11	33	1.4	5.5	36	13	0.37	0.29
	Rosette Leaf	old	20	36	0.6	3.4	28	12	0.02	0.00
	Floral Bud	new	12	34	1.3	4.2	38	11	1.55	0.59
	Floral Bud	old	17	34	1.0	3.5	33	12	0.76	0.38
	Maximum SD		1.2	0.6	0.2	0.7	0.7	0.3	ND	ND

Percentage of individual carotenoid levels relative to the total carotenoid content. Ratios of phytoene and phytofluene are relative to β-carotene. Data represent the average and maximum standard deviation (SD) for two biological replicates. Similar results were observed in independent experiments. Greyed highlighted values represent notable differences in younger tissues. β-C; β-carotene, Zea; zeaxanthin, anth; antheraxanthin, Viol; violaxanthin, neo; neoxanthin, phyt; phytoene, p-flu; phytofluene. ND; not determined.

Supplemental Table 2. Supplemental Table 2. D15 and *ziso-155* restore PLBs in *ccr2* etiolated cotyledons.

Germplasm	Treatment	Number of etioplasts containing PLBs				
		Total	PLB	Ratio (%)	SE (%)	Tukey Groups
WT	H_2O	90	90	100	0.0	c
WT	EtOH	64	64	100	0.0	c
WT	D15	48	48	100	0.0	c
ccr2	H_2O	63	0	0	0.0	a
ccr2	EtOH	72	0	0	0.0	a
ccr2	D15	71	61	85	2.5	b
ziso1-4	H_2O	73	48	66	2.1	e
ziso1-4	D15	68	45	66	2.3	e
ccr2 ziso1-4	H_2O	63	59	94	5.5	c
ccr2 ziso-155	H_2O	79	76	95	5.0	c

PLB formation was examined in WT, *ccr2*, *ziso*, *ccr2 ziso* and *ccr2 ziso-155* cotyledons 9 DAG in the dark. D15 (CCD inhibitor), EtOH (control solvent for dissolving D15) and/or H_2O was added to the growth media.

Supplemental Table 3. Transcriptomic analysis of WT, *ccr2* and *ccr2 ziso-155* etiolated tissues. See the electronic attachment *Supplemental Table 3 in Chapter 4-HX PhD thesis.xlsx.*

Supplemental Table 4. Transcriptome analysis of WT, *ccr2* and *ccr2 ziso-155* immature leaf tissues. See the electronic attachment *Supplemental Table 4 in Chapter 4-HX PhD thesis.xlsx*.

Supplemental Table 5. Significantly expressed genes regulated in *ccr2* and contra-regulated *ccr2 ziso-155* that are common to both etiolated and immature leaf tissues. See the electronic attachment *Supplemental Table 5 in Chapter 4-HX PhD thesis.xlsx.*

Supplemental Table 6. Differentially expressed genes in etiolated seedlings & young leaves of *ccr2* that are contra-regulated in *ccr2 ziso*-155.

GENE ID	GENE	Protein Encoding Description	Etiolated Seedlings		Young Leaves		*det1*	NFZ	gun5 +NFZ	gun1 +NFZ	Gene Ontology Analysis			
			ccr2	*ziso-155*	ccr2	*ziso-155*					CP	PS	LR	MR
At1g09530	PIF3	Transcription factor interacts with photoreceptors and negatively regulates signalling	30	0.1	220	0.1	↓	NS	NS	NS			✓	✓
At4g10180	DET1/ FUS2	Encodes a nuclear-localized protein that acts as a repressor of photomorphogenesis	5.1	0.1	5.9	0.2	NS	NS	NS	NS			✓	✓
At3g19390		Granulin repeat cysteine protease family protein	4.4	NS	6.8	NS	NS	NS	NS	NS				✓
At5g13210		Unknown conserved expressed protein	3.8	NS	0.4	NS	↑	NS	NS	NS	✓			
At3g45730		Unknown expressed protein	2.8	NS	2.4	NS	NS	10.6	0.33	0.37				
At5g43500	ATARP9	Encodes an expressed protein similar to actin-related proteins	2.4	NS	2.2	NS	NS	NS	NS	NS				
At5g48240		Unknown expressed protein	2.1	NS	2.2	NS	NS	NS	NS	NS				✓
At2g32950	COP1/ FUS3	Repressor of photomorphogenesis and induces skotomorphogenesis in the dark	2.0	0.0	8.9	0.1	↑	NS	NS	NS			✓	✓
At5g11260	HY5	Transcription factor negatively regulated by COP1 and mutant shows ABA resistant phenotypes	0.5	8.1	0.3	8.4	NS	2.8	NS	NS			✓	✓
At4g02770	PSAD1	Expressed protein with similarity to photosystem I reaction center subunit II	0.5	NS	0.5	NS	↑	0.15	3.26	3.39	✓	✓		✓
At3g17070		Peroxidase family expressed protein	0.5	NS	0.5	NS	NS	NS	NS	NS				✓
At2g31751		Potential natural antisense gene, expressed protein	0.4	NS	0.5	NS	NS	NS	NS	NS				
At4g15560	CLA1/ DXS	1-deoxyxylulose 5-phosphate synthase activity involved in the MEP pathway	0.3	4.2	0.1	16.2	NS	0.42	NS	NS	✓		✓	✓
At4g34350	ISPH/ CLB6	4-hydroxy-3-methylbut-2-enyl diphosphate reductase involved in the MEP pathway	0.3	9.4	0.2	11	↑	NS	NS	NS	✓			✓
At1g24510	TCP-1	T-complex expressed protein 1 epsilon subunit	0.3	12.0	0.1	7.9	NS	NS	NS	NS				✓
At3g59010	PME35	Pectin methylesterase that regulates the cell wall mechanical strength	0.2	NS	0.4	NS	↓	NS	NS	NS				
At1g29930	CAB1/ LHCB1.3	Subunit of light-harvesting complex II (LHCII),which absorbs light and transfers energy to the photosynthetic reaction center	0.2	13	0.2	11	NS	NS	NS	NS	✓	✓		✓
At2g05070	LHCB2.2	Light-harvesting chlorophyll a/b-binding (LHC) protein that constitute the antenna system of the photosynthetic apparatus.	0.2	NS	0.2	NS	↑	NS	NS	NS	✓	✓		✓
At5g13630	GUN5/ CHLH	Magnesium chelatase involved in plastid-to-nucleus signal transduction.	0.2	17	0.2	20	↑	0.33	3.0	2.79	✓	✓		✓
At1g67090	RBCS1a	Member of the Rubisco small subunit (RBCS) multigene family and functions to yield sufficient Rubisco content for leaf photosynthetic capacity.	0.1	67	0.1	61	NS	NS	2.0	NS	✓	✓	✓	✓

Notes: NS; not significant, CP; chloroplast, PS; photosynthesis, LR; light response, MR; metabolic response.

Supplemental Figure 1.

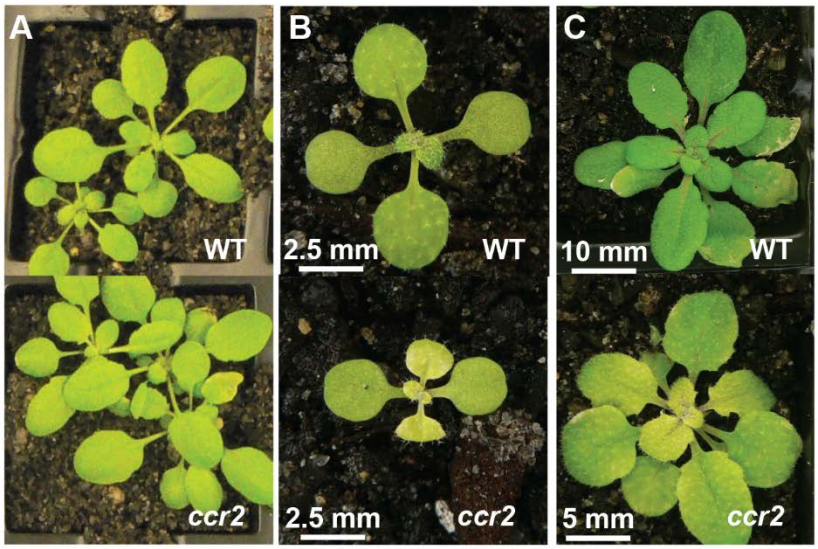

D

Tissue	Light (h)	Genotype	Total
Rosette Leaves	16	WT	$^{a}980 \pm 148$
	16	*ccr2*	$^{a}789 \pm 166$
	8	WT	$^{a}793 \pm 114$
	8	*ccr2*	$^{b}468 \pm 56$

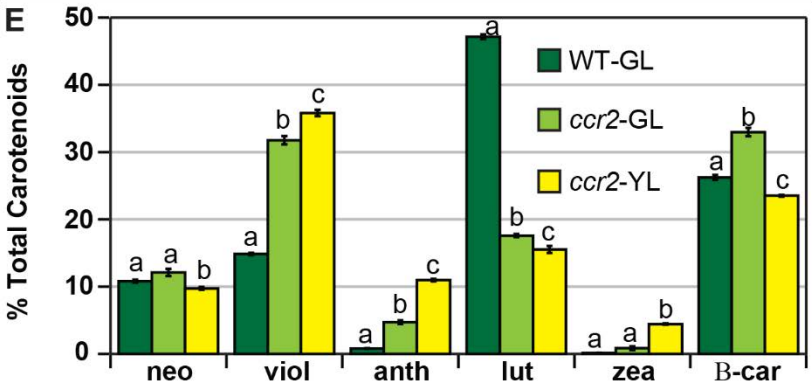

Supplemental Figure 1. A shorter photoperiod promotes leaf colour variegation affecting chlorophyll levels and carotenoid composition in *ccr2*. (A) WT and *ccr2* plants were grown under a 16-h photoperiod (50 µE light intensity) and representative images taken 14 DAG. **(B)** and **(C)** WT and *ccr2* plants were grown under a continuous 8-h photoperiod (150 µE light intensity) and representative images taken 14 and 21 DAG, respectively. **(D)** Chlorophyll content in immature leaves that recently emerged from WT and *ccr2* rosettes 14 DAG. Values represent the average and standard deviations of total chlorophyll content (mg/gfw) from a single leaf sector (n=2-7 plants). Lettering denotes significance (*t*-test, $P < 0.05$). **(E)** Percentage carotenoid composition (relative to total) in green (WT and *ccr2*) and yellow (*ccr2*) leaves formed one week after a photoperiod light shift from 16 to 8 h. Values represent average and standard error bars are displayed (n=single leaf from 5 plants). Lettering denotes significance (*t*-test, $P < 0.05$). Neoxanthin (neo), violaxanthin (viol), antheraxanthin (anth), lutein (lutein), zeaxanthin (zea), β-car (β-carotene), Green Leaf (GL), Yellow Leaf (YL).

Supplemental Figure 2.

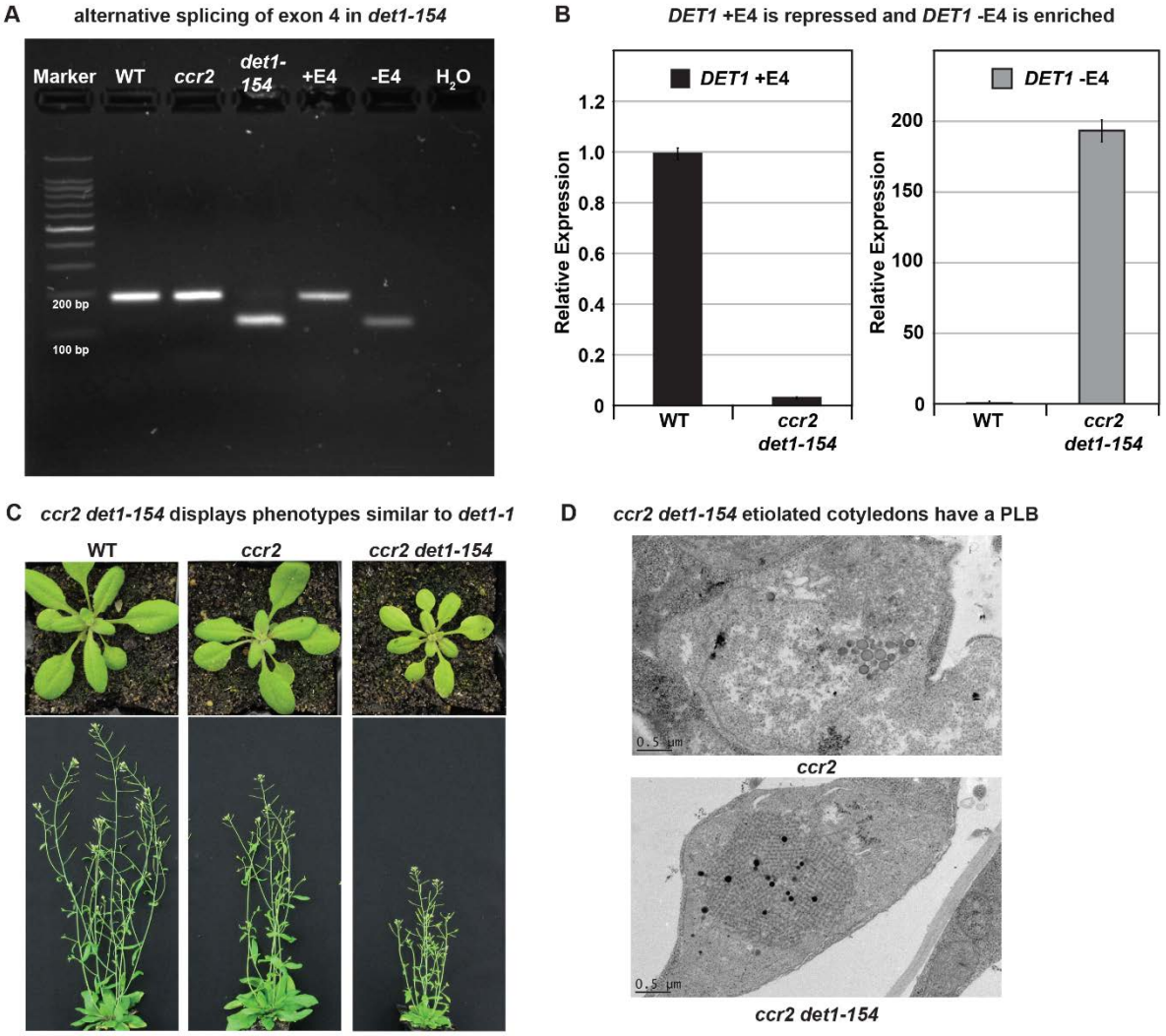

Supplemental Figure 2. Characterisation of *det1-154* splicing and mutant phenotypes. (A) Reverse transcription PCR confirms alternative splicing of exon 4 in *ccr2 det1-154* leaf tissues. Primers span exon 4 to amplify the spliced (125 bp; *ccr2 det1-154*) or unspliced (194 bp: WT and *ccr2*) amplicons. *DET1* complementary DNA was reverse transcribed from WT and *ccr2 det1-154* mRNA and cloned into TOPO vector to validate the unspliced (+E4; plus exon 4) and spliced (-E4; minus exon 4) amplicon transcript lengths, respectively. The H_2O lane serves as a negative control and the 100 bp ladder confirms fragment sizes. **(B)** Quantification of unspliced (+E4) and spliced (-E4) *DET1* mRNA transcript levels in WT and *ccr2 det1-154* leaf tissues, respectively. Standard error bars are shown (n=4). **(C)** *ccr2 det1-154* displays *det1* phenotypes, including a small pale green rosette, shorter floral architecture and partially sterility in comparison to WT and *ccr2*. **(D)** Transmission electron micrographs of a representative etioplast from five-day-old dark grown cotyledons showing a well-developed PLB in *ccr2 det1-154* compared to *ccr2*, which lacks a PLB.

Supplemental Figure 3.

A An 8 hr photoperiod causes yellowing in *ccr2 ccd* mutants

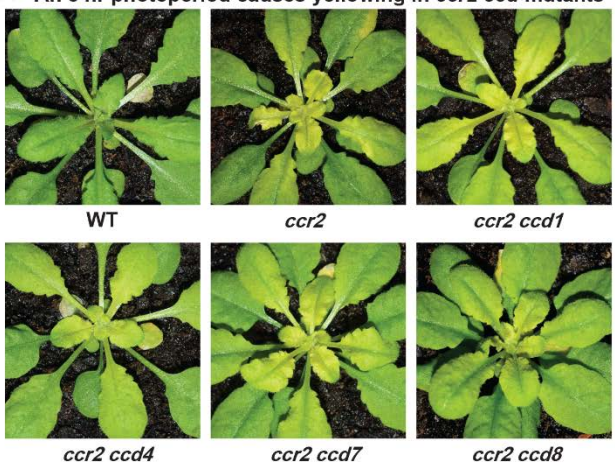

B Plastid development is unaffected in *ccr2 ccd* mutants

Genotype	Leaf Colour		Number of Plants
	Yellow	Green	
Col	0	10	10
ccr2	10	0	10
ccr2 ccd1	28	2	30
ccr2 ccd4	12	0	12
ccr2 max3	10	0	10
ccr2 max4	10	0	10

Supplemental Figure 3. The loss-of-function of single *CCDs* cannot restore PLB formation in *ccr2*. A photoperiod shift assay of WT, *ccr2* and F_3 homozygous double mutant lines of *ccr2 ccd1, ccr2 ccd4, ccr2 ccd7,* and *ccr2 ccd8* was performed by shifting three-weeks-old plants from 16-h to 8-h photoperiod until newly formed yellow leaves were clearly visible in *ccr2*. **(A)** Representative images of plants focusing on the immature leaves in the rosette. **(B)** Quantification of plastid development by scoring yellow leaf colouration among individual plants. Similar data was obtained from multiple independent experiments. Statistical analysis by ANOVA with post-hoc Tukey test showed no significant difference in the number of plants displaying a yellow leaf phenotype of *ccr2* compared to the *ccr2 ccd* double mutants.

Chapter 5: Mutations in Arabidopsis phytoene synthase suppress apocarotenoid signals and regulate chloroplast development

This chapter has been written as a manuscript to be submitted to the journal *Plant Physiology* and hence follows the submission guidelines of the journal. The main text is formatted according to the journal's instructions, and supplemental tables and figures are attached to the end of the chapter. However, to facilitate the examiners' review, figures and legends are embedded to the main text instead of being individual files; figures are formatted as instructed by the journal but not scaled to the journal's required size. References of this manuscript have been incorporated into references at the end of this thesis.

Mutations in Arabidopsis Phytoene Synthase Suppress Apocarotenoid Signals and Regulate Chloroplast Development

Xin Hou[a], Ralf Welsch[b], Christopher I. Cazzonelli[c], Yan Wang[d], James Whelan[d] and Barry J. Pogson[a,1]

[a] Australian Research Council Centre of Excellence in Plant Energy Biology, College of Medicine, Biology and Environment, Research School of Biology, The Australian National University, Canberra, ACT 2601, Australia.

[b]Faculty of Biology II, University of Freiburg, D79104 Freiburg, Germany

[c]Hawkesbury Institute for the Environment, University of Western Sydney, Hawkesbury Campus, Bourke Street, Richmond, NSW 2753, Australia

[d]School of Life Sciences, ARC Centre of Excellence in Plant Energy Biology, La Trobe University, VIC 3086, Australia

Running Title: Mutations in *AtPSY* Suppress Apocarotenoid Signals

SUMMARY

An enzyme in the carotenoid biosynthetic pathway affects carotenoid-derived retrograde signals, regulating chloroplast development.

FOOTNOTES

1 **Corresponding Author:** Barry J Pogson

Australian Research Council Centre of Excellence in Plant Energy Biology,
Research School of Biology, College of Science,
The Australian National University
Canberra, ACT 2601, Australia.
Email: barry.pogson@anu.edu.au
Telephone: +61-2-61255629

ABSTRACT

Phytoene synthase (PSY) is a major rate-controlling enzyme that catalyses the initial step of carotenoid biosynthesis and is hence under multi-level regulation. Alteration of *PSY* gene expression, protein levels or enzyme activity can exert profound effects on carotenoid composition and plant development. Here we show that four mutants of PSY: *psy*-4, *psy*-90, *psy*-130 and *psy*-145 reduced *cis*-carotenoids to levels below a threshold and suppressed apocarotenoid signal 2 (ACS2) which negatively regulates plastid development in *ccr2* (*carotenoid and chloroplast regulation 2*). The restoration of plastid development in the four *ccr2 psy* double mutants was caused by decreased PSY activity and reduced protein levels due to altered PSY-AtOR (ORANGE) interaction, but not by changed localization of PSY. This study reveals a novel role of PSY, modulating carotenoid-derived retrograde signals and regulating plastid development.

INTRODUCTION

Carotenoids are a large group of C_{40} isoprenoid compounds that are synthesized in all photosynthetic organisms and some non-photosynthetic organisms (Hirschberg, 2001; Maresca et al., 2008; Ruiz-Sola and Rodriguez-Concepcion, 2012; Nisar et al., 2015). Carotenoids exert numerous functions in higher plants. They are the basis for many pigments, scents in flowers, and aromas in fruits and attract animals and insects for pollination and seed dispersal. In chloroplasts, carotenoids stabilize membranes and serve as components of photosystems (PSs), protecting the photosynthetic apparatus from photooxidative damage [reviewed in (Nisar et al., 2015)]. Carotenoids are also precursors of the phytohormones abscisic acid (ABA) and strigolactone (SL) [reviewed in (Nambara and Marion-Poll, 2005; Xie et al., 2010)]. In etioplasts, carotenoids are required to form prolamellar bodies (PLBs), the characteristic paracrystalline membrane structure that defines etioplasts and accelerate photomorphogenesis upon illumination (Park et al., 2002; Rodriguez-Villalon et al., 2009b).

In the carotenoid biosynthetic pathway, phytoene synthase (PSY) catalyses the first committed step, the formation of phytoene from two geranylgeranyl diphosphate (GGPP) molecules (Misawa et al., 1994). Phytoene is then converted to all-*trans* lycopene in four steps catalysed by two desaturase, phytoene desaturase (PDS) and ζ-carotene desaturase (ZDS), and two *cis-trans* isomerases, 15-*cis*-ζ-carotene isomerase (ZISO) and carotenoid isomerase (CRTISO) (Isaacson et al., 2002; Park et al., 2002; Breitenbach and Sandmann, 2005; Li et al., 2007) (Figure 1). The *cis*-configured carotenoids formed between phytoene and all-*trans* lycopene or their cleavage products were proposed to trigger retrograde signals that regulate carotenoid biosynthesis and plant development (Kachanovsky et al., 2012; Avendano-Vazquez et al., 2014; Hou et al., 2016).

As the entry-point enzyme of carotenoid biosynthesis, PSY controls the carbon flux into the pathway (Figure 1). Therefore, altered *PSY* expression is often sufficient to affect carotenoid content in plants (Ducreux et al., 2005; Fraser et al., 2007; Maass et al., 2009; Welsch et al., 2010; Cao et al., 2012). Given the essential roles in carotenogenesis, PSY is highly regulated at both transcriptional and post-transcriptional levels. For example, the transcription of *PSY* is modulated by light signalling through multiple factors including phytochrome-interacting factors (PIFs) and gibberellin (GA)-regulated DELLA proteins (Toledo-Ortiz et al., 2010;

Cheminant et al., 2011). In Arabidopsis, the ORANGE protein (AtOR) was recently reported to regulate PSY post-transcriptionally, affecting its protein levels through physical interaction (Zhou et al., 2015). The localization of PSY was found to dramatically affect enzymatic activity (Welsch et al., 2000), and interestingly altered PSY activity by a single amino acid change also led to changed localization (Shumskaya et al., 2012).

In Arabidopsis, an apocarotenoid signal (ACS), named ACS2, was found to perturb plastid development, leading to a yellowing phenotype in newly emerged leaf tissue and delayed cotyledon greening in mutant *ccr2* (*carotenoid and chloroplast regulation 2*) (Park et al., 2002) (see chapter 4). ACS2 is likely generated from *cis*-carotenoids that are accumulated in *ccr2* under a short photoperiod due to the absence of CRTISO activity (Figure 1). ACS2 was proposed to act downstream of DET1 (Deetiolated 1), modulating photosynthesis associated nuclear gene expression (PhANG) and regulating PLB formation by maintaining protochlorophyllide oxidoreductase (POR) protein levels (see chapter 4).

Here we show that mutations in *PSY* supresses ACS2 and restores plastid development. A forward genetic screen identified four revertants of *ccr2* (*rccr2*) that carried mutations in *PSY* and displayed normal chloroplast biogenesis. Those mutations reduced the enzymatic activity of PSY, and thereby caused a reduction of the *cis*-carotenoids that were likely the substrates of ACS2. PSY proteins levels were also reduced due to altered interaction between PSY and AtOR, which consequently affected *cis*-carotenoid composition. The localization of PSY was not affected by the mutations. The present study demonstrates a novel role of PSY in the regulation of plastid development.

RESULTS

Mutations in *PSY* gene restore plastid development in *ccr2* mutant

To investigate the genes that are involved in the production and regulation of ACS, we performed forward genetics screening on the *ccr2* mutant in which ACS2 is triggered and regulates plastid development. Twenty-six EMS-mutagenized *ccr2* lines restored chloroplast development and reverted the leaf-yellowing phenotype (see chapter 4). Four of those *rccr2* lines, namely *rccr2*^{4}, *rccr2*^{90}, *rccr2*^{130} and *rccr2*^{145}, have mutations in *PSY* gene (Supplemental Table S1). Under a short 8-h photoperiod, all four *rccr2* lines displayed greening in newly developed leaf tissue similar to WT, while *ccr2* showed a clear yellowing phenotype (yellow

Figure 1

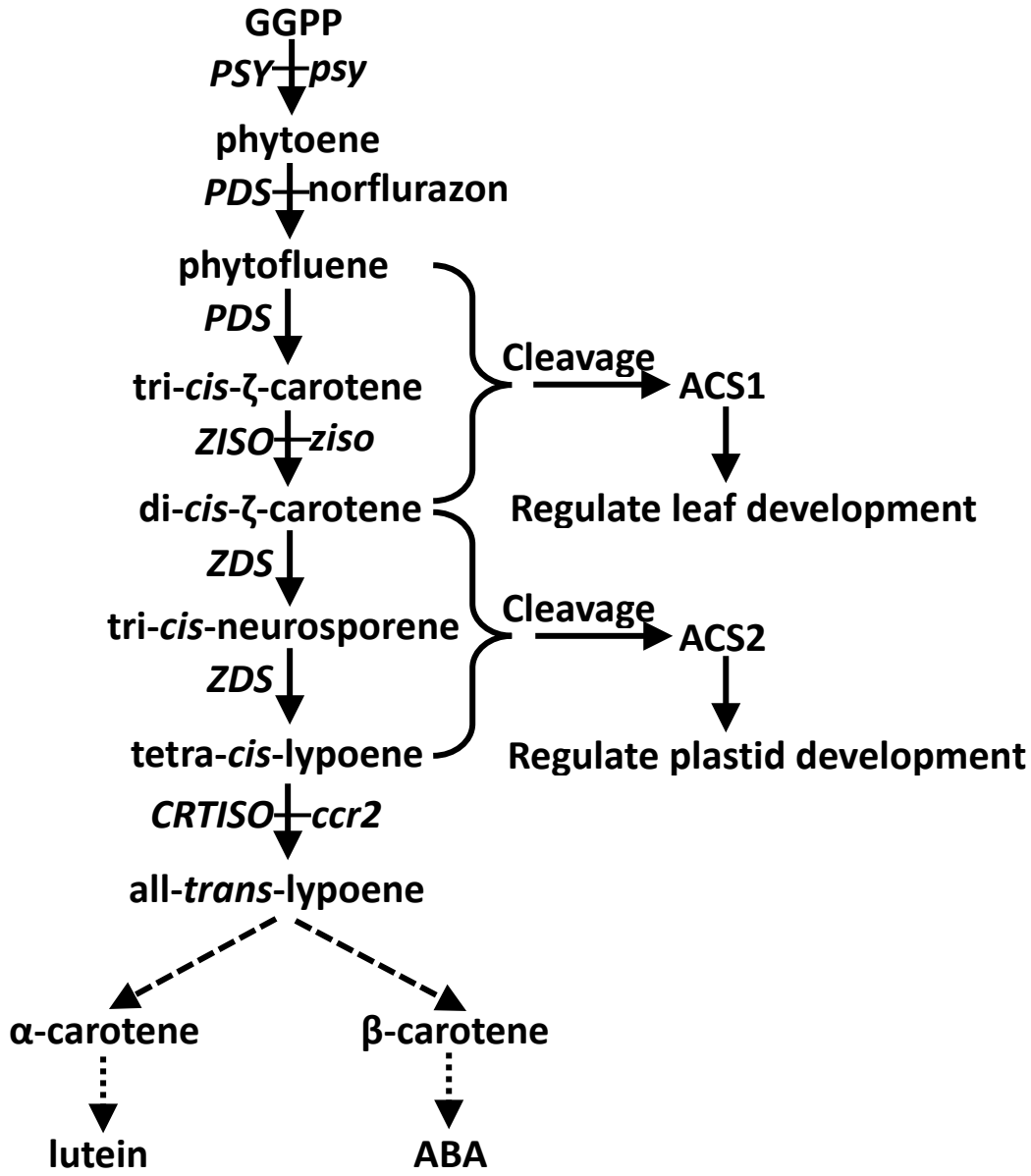

Figure 1: Simplified diagram of the carotenoid biosynthesis pathway. Genes encoding the catalysing enzymes of each step before all-*trans*-lycopene are labelled to the left of the pathway and mutants are labelled to the right. GGPP: geranylgeranyl diphosphate; PSY: phytoene synthase; PDS: phytoene desaturase; ZISO: 15-*cis*-ζ-carotene isomerase; ZDS: ζ-carotene desaturase; CRTISO: carotenoid isomerase. Norflurazon is an herbicide that inhibits PDS activity. ACS: apocarotenoid signal; ACS1: see (Avendano-Vazquez et al., 2014) and (Hou et al., 2016); ACS2: see Chapter 4.

leaf, YL) (Figure 2A and Supplemental Figure S1A). Consistent with this observation, the total chlorophyll content in the four *rccr2* lines was restored to WT levels, whereas that in *ccr2* YL was significantly reduced (Figure 2B). In dark-grown seedlings of the four *rccr2* lines PLB formation was restored and in correlation normal chlorophyll biosynthesis resembling WT was observed during deetiolation, while *ccr2* seedlings showed delayed greening upon illumination (Figure 2C, Supplemental Figure S1C and S1D). SNP (single nucleotide polymorphism) analysis revealed two G→A mutations at exons 4 and 5 of *PSY*, in *rccr2*^{4} and *rccr2*^{90} respectively, leading to M266I and A352T amino acid changes in PSY protein. In *rccr2*^{130}, a C→T mutation at exon 3 resulted in a substitution of P178 to S. Another G→A mutation found in *rccr2*^{145} was at exon 2/intron 3 border and created an alternative splice site which may retain intron 3 in the transcript, introducing a premature stop codon and leading to a truncated, non-functional protein. All mutations were confirmed by Sanger sequencing (Figure 3 and Supplemental Table S1). Quantitative RT-PCR showed that in *rccr2*^{145} the *psy*-145 transcript was present together with WT transcript, which was on average around 3-fold higher than the splicing variant (Supplemental Figure S2). When *rccr2*^{145} was grown in soil, an albino phenotype indicating impaired carotenoid biosynthesis was observed in about 20% seedlings of the population, which probably suggests that the percentage of *psy*-145 splicing variant varies in plants of a large population (Supplemental Figure S1B) (Bartley and Scolnik, 1995). Therefore, the four *rccr2* lines were confirmed to be *ccr2 psy* double mutants and mutations in *PSY* gene was correlated to the restoration of plastid development which is inhibited in *ccr2* by ACS2 (see chapter 4).

Mutated PSY versions supress ACS2 in *ccr2* by affecting c*is*-carotenoid composition

To confirm that the restoration of plastid development in *ccr2 psy* mutants was due to a mutated *PSY* gene and subsequently supressed ACS2, we overexpressed (OE) wild type *PSY* gene in the four double mutants, *ccr2* and WT. Interestingly all *ccr2 psy*::*PSY*-OE lines growing under 8-h photoperiod displayed yellowing in newly developed leaf tissue, similar to *ccr2* (Supplemental Figure S3A). In agreement with the yellowing phenotype, a significant reduction of total chlorophyll was observed in YL of *PSY*-OE lines compared to GL of WT or WT::*PSY*-OE (Supplemental Figure S3B). We examined the *cis*-carotenoids that were proposed

Figure 2

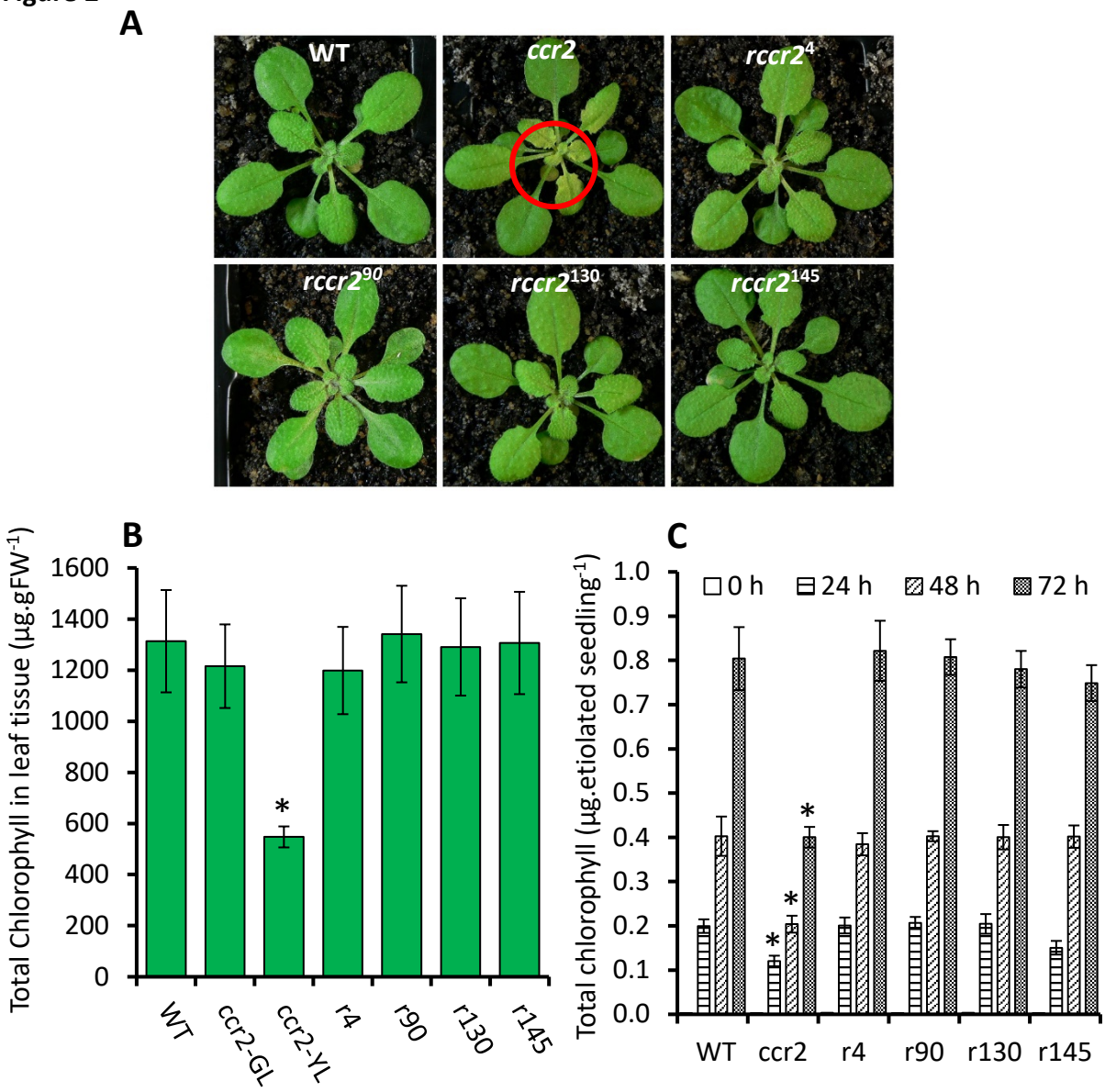

Figure 2: Mutated PSY restored chloroplast development in ccr2 leaves and cotyledon greening in etiolated seedlings. A, Three-week old WT and *ccr2* plants growing under 8-h photoperiod. In *ccr2*, newly developed leaf tissues were yellow (YL, red circle) while all leaves in WT were green (GL). B, Total chlorophyll in leaf tissue of WT, *ccr2* and *rccr2* lines carrying a mutated *PSY* gene, showing that chlorophyll content was significantly reduced in *ccr2* YL and restored to wild type levels in *rccr2* lines. Plants were grown under 8-h photoperiod. Values were averaged from five biological replicates and error bars denote standard error. C, Compared to WT, *ccr2* showed delayed greening, while *rccr2* lines carrying a mutated *PSY* gene restored cotyledon greening. Seedlings were grown in darkness for 4 d, exposed to continuous white light and chlorophyll was measured at 12-h intervals. Chlorophyll levels at 0 h, 24 h, 48 h and 72 h are shown in the figure. Each value was averaged from 20 seedlings. *rccr2* is abbreviated to "*r*" in the charts, e.g. *r*4 is the abbreviation of *rccr2*^{4}. A star denotes that difference is significant when compared to WT and $P<0.05$ in one-way ANOVA.

Figure 3

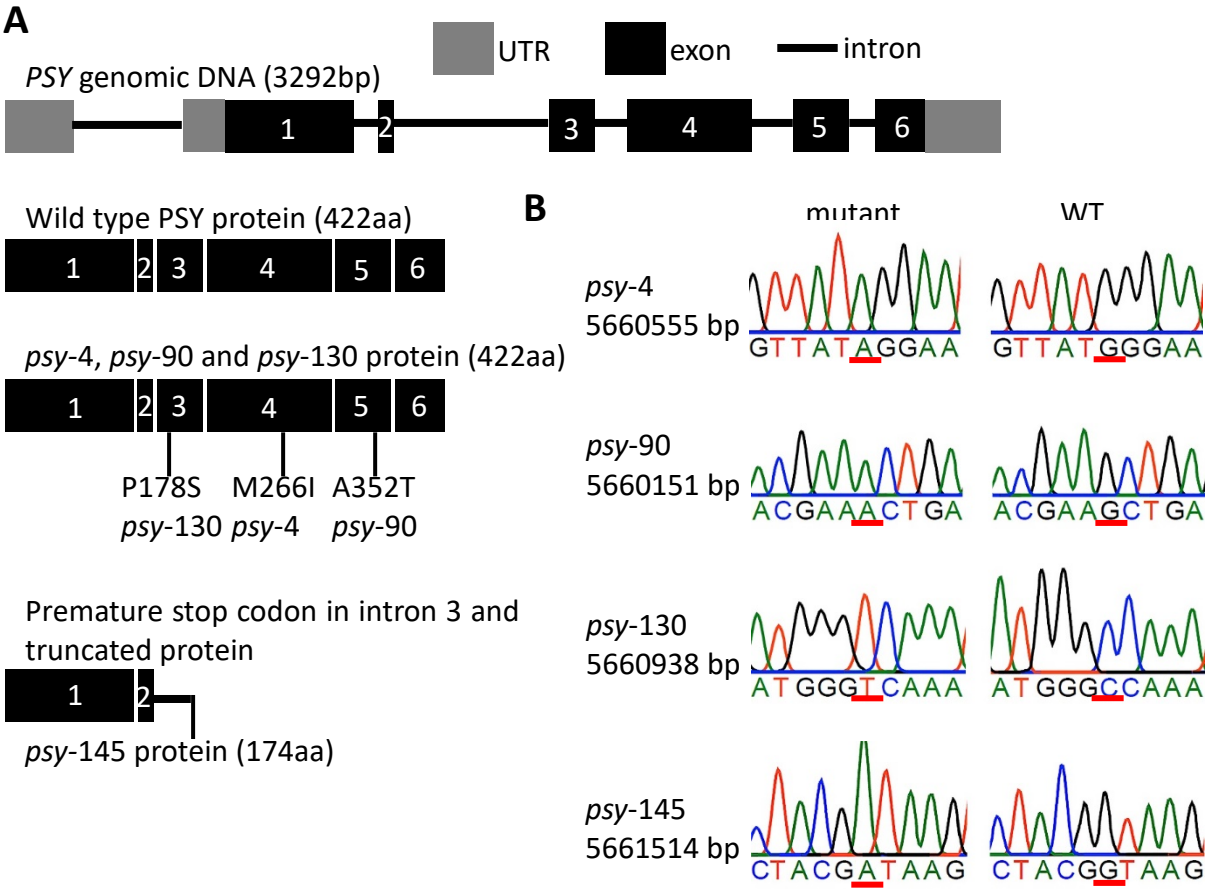

Figure 3: Mutations of *PSY* gene were identified by NGS from four *rccr2* lines. A, Schematic structure of wild type *PSY* gene genomic DNA, PSY protein and mutants in the four *ccr2 psy* lines. The point mutations in *psy*-4, *psy*-9 and *psy*-130 lead to amino changes, while in *psy*-145 a G→A mutation at the exon 2/intron 3 junction alters the splice site and intron 3 (541 bp) is hence retained in the transcript, introducing a premature stop codon and resulting in a truncated protein with 174 amino acids. B, The point mutations in *PSY* gene were confirmed by Sanger sequencing. Notably, in NGS data analysis mutations were annotated according to forward strand sequence in TAIR database, while the coding sequence of *PSY* is on complementary strand.

to trigger ACS2 in *ccr2* and were able to link the restoration of plastid development to altered levels of ACS2 precursors in the *ccr2 psy* mutants. In comparison to *ccr2*, the levels of *cis*-ζ-carotene (including tri-*cis*-ζ-carotene and di-*cis*-ζ-carotene) were significantly reduced in 7-d old etiolated seedlings of all *ccr2 psy* mutants. In *ccr2 psy*-4, *ccr2 psy*-90 and *ccr2 psy*-130, a clear reduction of tri-*cis*-neurosporene and tetra-*cis*-lycopene was also observed. Among the four double mutants, *ccr2 psy*-90 displayed the lowest levels of all *cis*-carotenoids measured. Associated with the leaf yellowing of all *ccr2 psy*::*PSY*-OE lines, the composition of the above

mentioned *cis*-carotenoids in those lines was similar to that in *ccr2* (Figure 4A). The *cis*-carotenoid profile in *ccr2* etiolated seedlings was not clearly affected by *PSY*-OE, and that in WT was undetectable with or without *PSY*-OE, although western blots confirmed that PSY protein levels were dramatically increased in all OE lines (Figure 4A and 4B). PSY protein levels were lower in *ccr2 psy* double mutants (Figure 4B) compared to WT and *ccr2*, and thereby were investigated further in this study.

The enzyme activity of PSY is reduced in *psy* mutants

Reduced *cis*-carotenoid levels and supressed ACS2 could be a consequence of altered activity or protein levels of PSY. We first examined the phytoene synthase activity of the four *psy* mutants. Seed-derived callus (SDC), illuminated for 5 d and grown in the dark for 2 weeks, was used to assay phytoene synthase activity *in vivo*. In a *ccr2* background, SDC accumulated *cis*-carotenoids in dark due to the loss of carotenoid isomerase function (Park et al., 2002), whereas WT displayed no detectable *cis*-carotenoids in SDC. Norflurazon treatment inhibits PDS and results in the accumulation of phytoene in dark, which is used to indicate phytoene synthase activity (Figure 5A and Supplemental Figure S4A).

In comparison to WT and *ccr2*, the phytoene synthase activity in all four *ccr2 psy* double mutants was reduced by 1.5- to 3-fold, and *psy*-90 synthesized the lowest amount of phytoene accounting for only around 30% of WT level. The biosynthesis of *cis*-carotenoids measured in this study was downregulated accordingly in the double mutants, while that of all-*trans*-lycopene, lutein, β-carotene and other xanthophylls was unaffected (Figure 5A and Supplemental Figure S4A). We next purified recombinant PSY variants expressed in *E. coli cells* and performed *in vitro* activity assays using cell lysate of a GGPP-producing *E. coli* strain as substrate (Cunningham and Gantt, 2007). Endogenous phytoene synthase was also purified from leaf tissue of WT, *ccr2* and *ccr2 psy* double mutants by immunoprecipitation and subjected to *in vitro* measurements of enzymatic activity. Consistent with *in vivo* activity assays, all purified *psy* mutants showed a significant reduction of phytoene production, with *psy*-90 displaying the lowest activity although not being as remarkable as observed *in vivo* using callus.

Figure 4

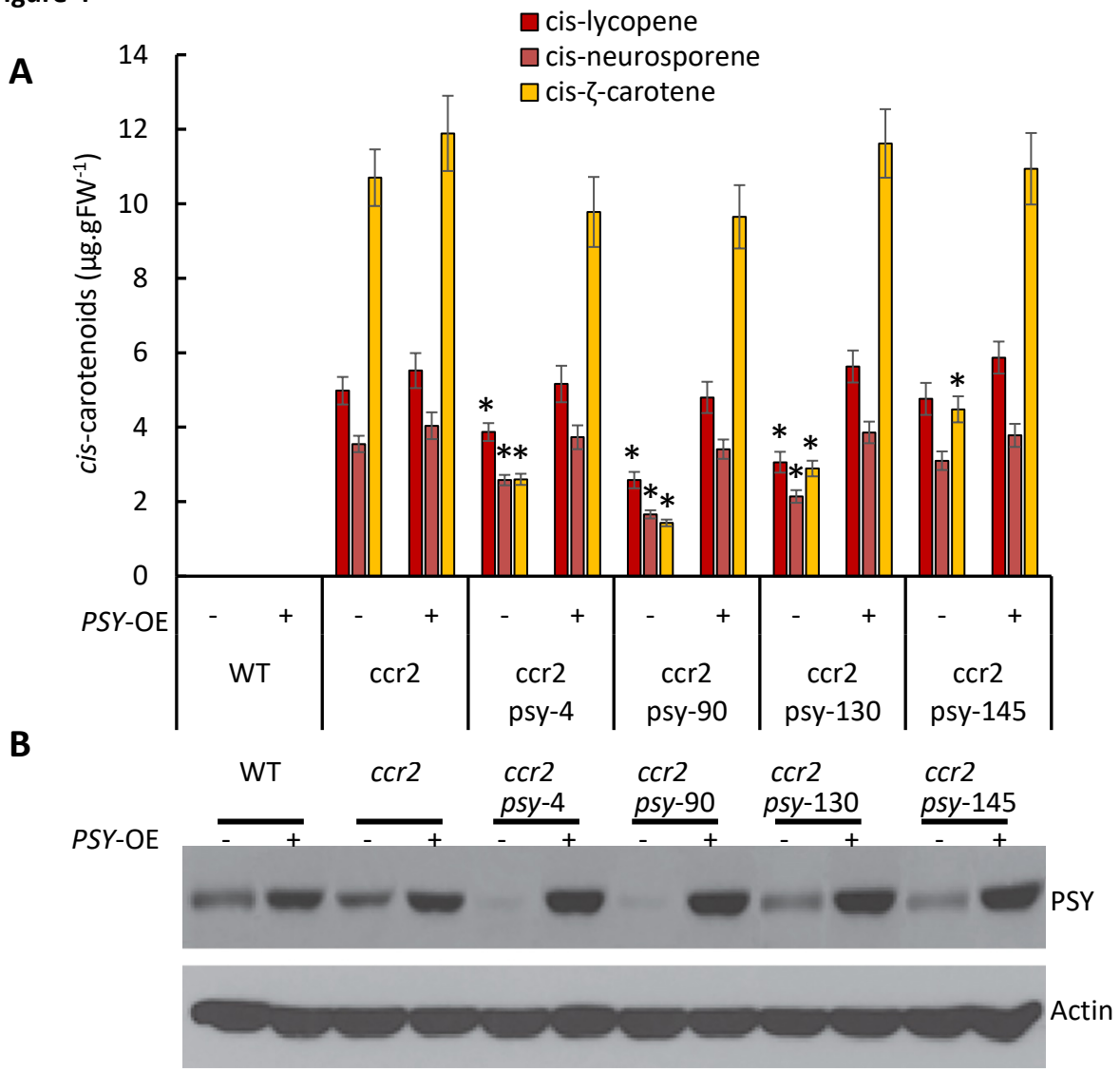

Figure 4: Mutations in PSY affected the composition of *cis*-carotenoids triggering ACS2. Wild type *PSY* gene was overexpressed using CMV35S promoter in WT, *ccr2*, *ccr2 psy*-4, *ccr2 psy*-90, *ccr2 psy*-130 and *ccr2 psy*-145. A, The *cis*-carotenoids that were proposed to trigger ACS2 in *ccr2* were reduced in *ccr2 psy* double mutants but similar to *ccr2* in the *PSY* overexpression lines (*PSY*-OE). Etiolated seedlings (7 d) were subjected to HPLC to measure *cis*-carotenoid levels. Three representative *PSY*-OE lines of each transformation were used in HPLC, with three replicates from each line. Error bars denote standard errors. *Difference is significant in comparison to *ccr2* ($P < 0.05$ in one-way ANOVA). C*is*-ζ-carotene: tri-*cis*-ζ-carotene and di-*cis*-ζ-carotene; *cis*-neurosporene: tri-*cis*-neurosporene; *cis*-lycopene: tetra-*cis*-lycopene. B, Western blots confirmed the overexpression of PSY protein in all OE lines. For each sample, 10 µg of total protein extracted from leaf tissues of 4-week old Arabidopsis plants was subjected to western blot using anti-PSY polyclonal antibody.

Figure 5

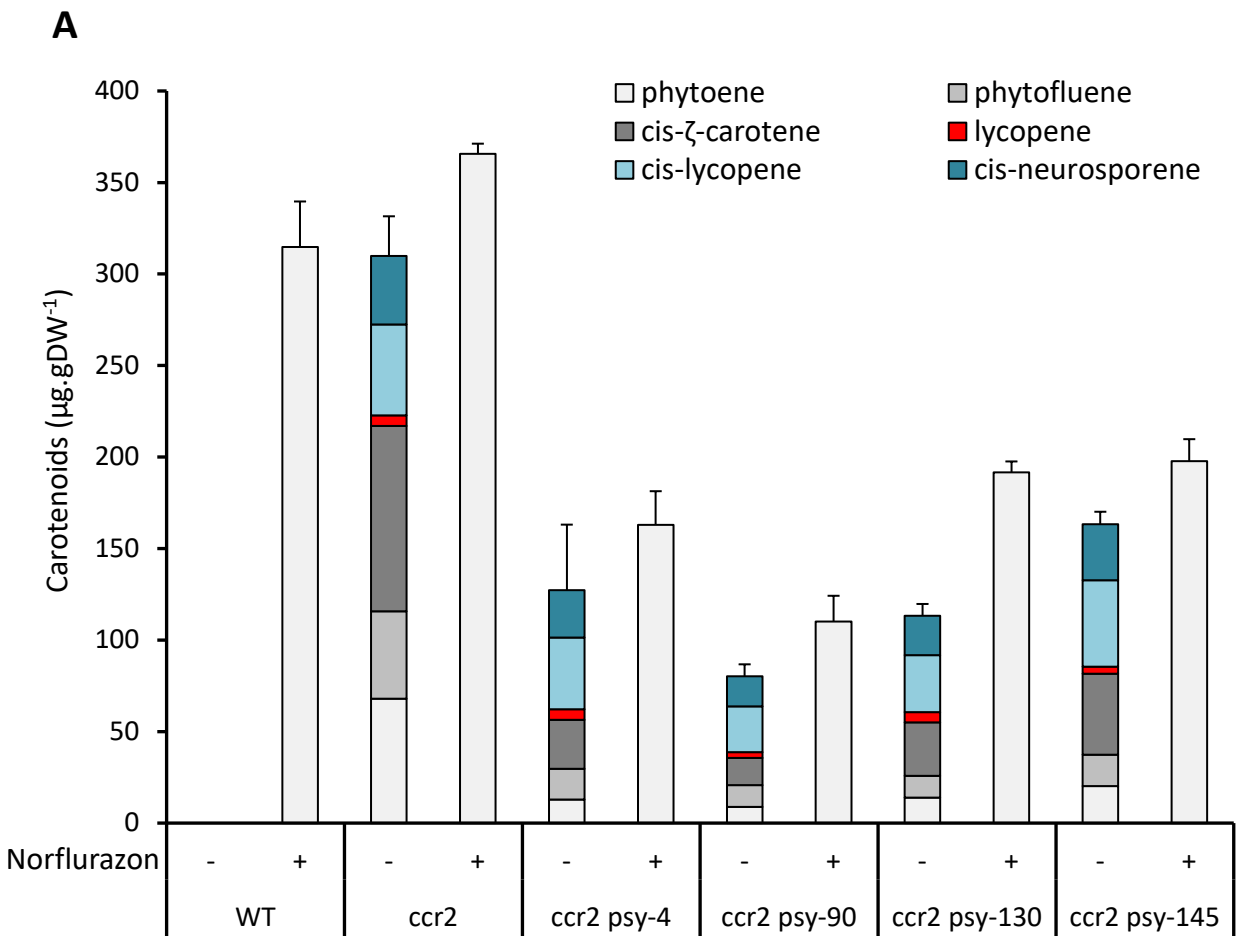
A
phytoene
phytofluene
cis-ζ-carotene
lycopene
cis-lycopene
cis-neurosporene
Carotenoids (µg.gDW-1)
400
350
300
250
200
150
100
50
0
Norflurazon
-
+
WT
ccr2
ccr2 psy-4
ccr2 psy-90
ccr2 psy-130
ccr2 psy-145

Figure 5

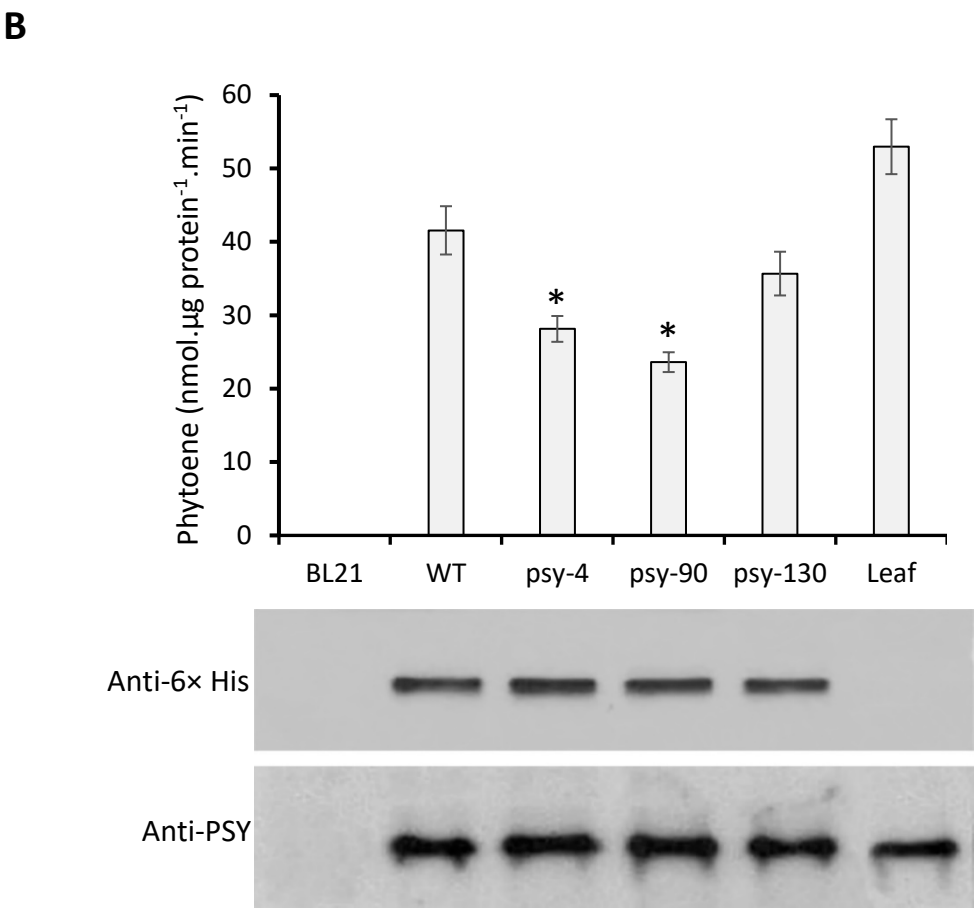

Figure 5: The enzymatic activity of PSY was reduced in *psy* mutants. A, *In vivo* PSY activity assays using seed-derived callus. Seeds were germinated directly on auxin-containing medium, illuminated for 5 d under 16-h photoperiod and etiolated for 2 weeks. For norflurazon treatment (+), callus were transferred onto the same medium containing 1 µmol.L^{-1} norflurazon prior to etiolation. Norflurazon inhibits PDS and leads to accumulation of phytoene, which is utilized to assay PSY activity. Carotenoids were quantified by HPLC. Data is shown as mean ± standard errors of three biological replicates. Lycopene: all-*trans*-lycopene. B, In vitro activity of recombinant WT PSY and mutants. Recombinant PSY protein was purified from *E. coli* cells expressing codon-optimized *PSY* gene or mutants. Five micrograms of recombinant PSY protein was subjected to an enzymatic activity assay which was then extracted using carotenoid extraction buffer before loaded for HPLC. Same amount of protein extracted from untransformed *E. coli* BL21 (DE3) cells was used as a negative control; endogenous PSY protein extracted from WT Arabidopsis leaf tissue was used a positive control. Enzyme activity was measured in triplicates and displayed as mean ± standard error. * Difference is significant in comparison to WT ($P < 0.05$ in one-way ANOVA). Western blots were done using anti-PSY and anti-6× His antibodies to confirm the expression and purification of recombinant PSY protein; five micrograms of each protein sample was loaded to the gel.

Mutations in PSY affect protein-protein interaction

Arabidopsis ORANGE protein (AtOR) was found to regulate PSY posttranscriptionally through physical interaction (Zhou et al., 2015). We reasoned that the mutations identified in *PSY* in this study might result in an alteration of PSY-AtOR protein interaction. A split ubiquitin system (SUS) based on yeast-two-hybrid (Y2H) was used to evaluate the protein-protein interaction between PSY and AtOR. A clear interaction was observed between wild type PSY and AtOR by growth in selective media and β-Galactosidase activity of yeast strains co-expressing different PSY versions fused to C-terminal ubiquitin moiety (Cub) and AtOR fused to N-terminal ubiquitin moiety (Nub). However, a significant suppression of the interaction was detected when *psy*-4 or *psy*-90 was fused to Cub, with *psy*-90 showing almost no interaction with AtOR (Figure 6A and 6B). To confirm reduced interaction between AtOR and PSY versions, we detected AtOR in PSY co-immunoprecipitates. Western blot using anti-OR antibody showed lower levels of AtOR that co-immunoprecipitated with *psy*-4 or *psy*-90, the later PSY version displaying dramatically reduced physical interaction with AtOR (Figure 6C).

We also tested the interaction between PSY versions and Arabidopsis GGPP synthase 11 (AtGGPPS11) which was proposed to be an essential interacting protein of PSY and required for the production phytoene (Ruiz-Sola et al., 2016). Interestingly, the protein-protein interaction between *psy*-90 and AtGGPPS11 was also negatively affected, although the other PSY versions showed normal interaction with AtGGPPS11 similar to that of wild type PSY (Figure 6A and 6B). In agreement with PSY activity assays, the production of phytoene in yeast cells expressing *psy*-90+AtGGPPS11 was almost abolished; *psy*-4 or *psy*-130 in combination with AtGGPPS11 produced significantly less phytoene (2-4 fold lower) in comparison to PSY-WT (Supplemental Figure S5).

Protein levels of PSY and OR are reduced in *psy* mutants

We next examined whether the suppressed PSY-AtOR interaction affected their protein levels. Western blots using total protein extracted from leaf tissues showed that PSY protein levels in *ccr2 psy*-4 and *ccr2 psy*-90 were clearly downregulated (Figure 7). We also measured PSY protein quantitatively using enzyme-linked immunosorbent assays (ELISAs), which confirmed the reduced levels of *psy*-4 and *psy*-90, by around 2-fold and 5-fold, respectively (Supplemental Figure S6). PSY and AtOR have been reported to exert mutual regulation to

each other (Zhou et al., 2015), we therefore also examined AtOR protein. The levels of AtOR protein were both reduced in *ccr2 psy*-4 and *ccr2 psy*-90 by 3- to 4-fold (Figure 7 and Supplemental Figure S6). ELISAs showed that AtOR was downregulated in *ccr2 psy*-145 while PSY protein levels were similar to that in WT (Supplemental Figure S6). A slight downregulation of PSY was also observed in *ccr2* (Supplemental Figure S6), which might be a result of ACS2 regulation or negative feedback by the accumulated *cis*-carotenoids.

The localization of PSY is not affected by the four mutations

The localization of the PSY enzyme can also be altered by a single amino acid change (Shumskaya et al., 2012), which may affect the assembly and localization of the carotenogenic metabolon (Bassard et al., 2012; Shumskaya and Wurtzel, 2013), resulting in altered carotenoid profiles and probably exerting effects on the production or transduction of ACSs. We therefore investigated whether the localization of the PSY versions identified in this study was changed. To observe the suborganellular localization of the PSY variants, we transiently expressed PSY-CGFP fusion proteins of PSY-WT or mutants in protoplasts which were isolated from wild type Arabidopsis leaf tissue. As a control, we also included *psy*-$N_{181}P_{270}$ (*psy*-NP), the Arabidopsis equivalent variant of ZmPSY-$N_{168}P_{257}$ that was reported to display an altered localization in chloroplasts and etioplasts. Surprisingly, we observed no significant difference among the localization of all PSY proteins in chloroplasts (Figure 8). We then repeated the transient expression in protoplasts isolated from cotyledons of Arabidopsis etiolated seedlings, followed by detecting PSY in PLB and stroma fractions of etioplasts. We confirmed that no mutants of PSY protein were localized differently (Supplemental Figure S7). It has been reported that PSY takes two topological forms: membrane-bound and stromal, and in agreement we detected endogenous PSY in both PLB and stroma fractions (Supplemental Figure S7). However, the transiently expressed PSY-CGFP fusion proteins seemed to only affect PSY levels in stroma (Supplemental Figure S7), which may explain the evenly distributed green fluorescence observed in chloroplasts in this study (Figure 8).

Figure 6

A

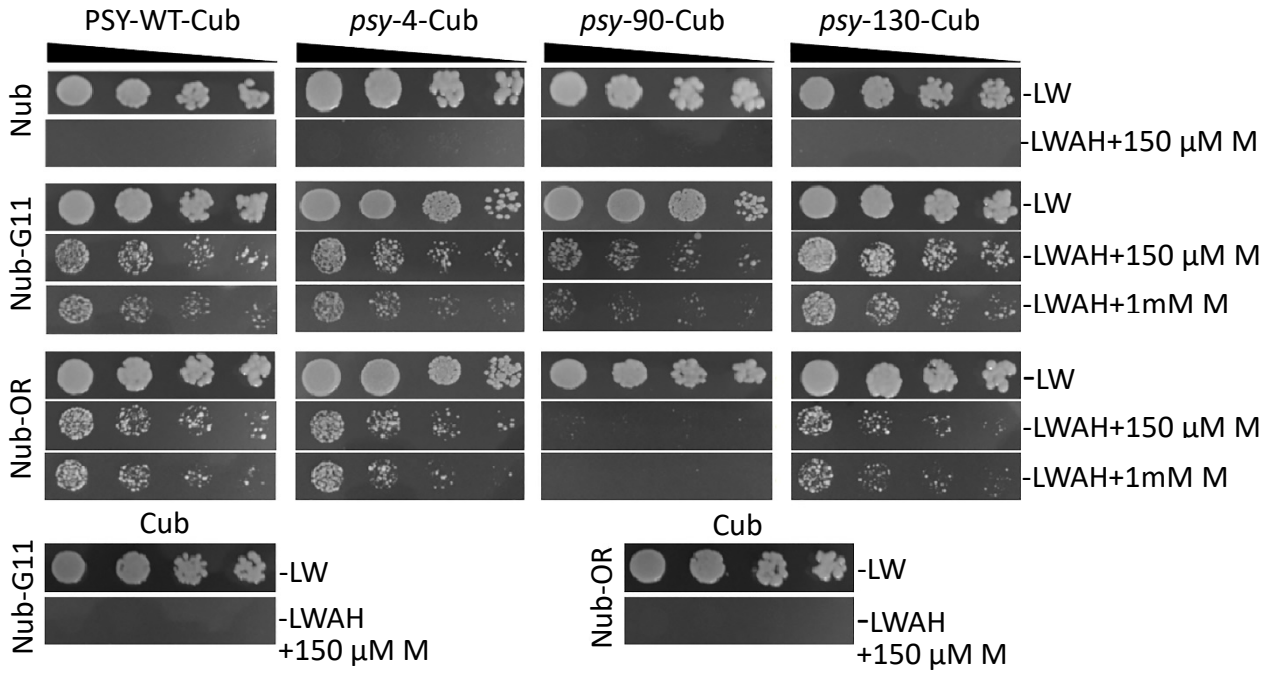
PSY-WT-Cub
psy-4-Cub
psy-90-Cub
psy-130-Cub
Nub
Nub-G11
Nub-OR
-LW
-LWAH+150 µM M
-LWAH+1mM M
Cub
Nub-G11
Nub-OR
-LW
-LWAH
+150 µM M

B

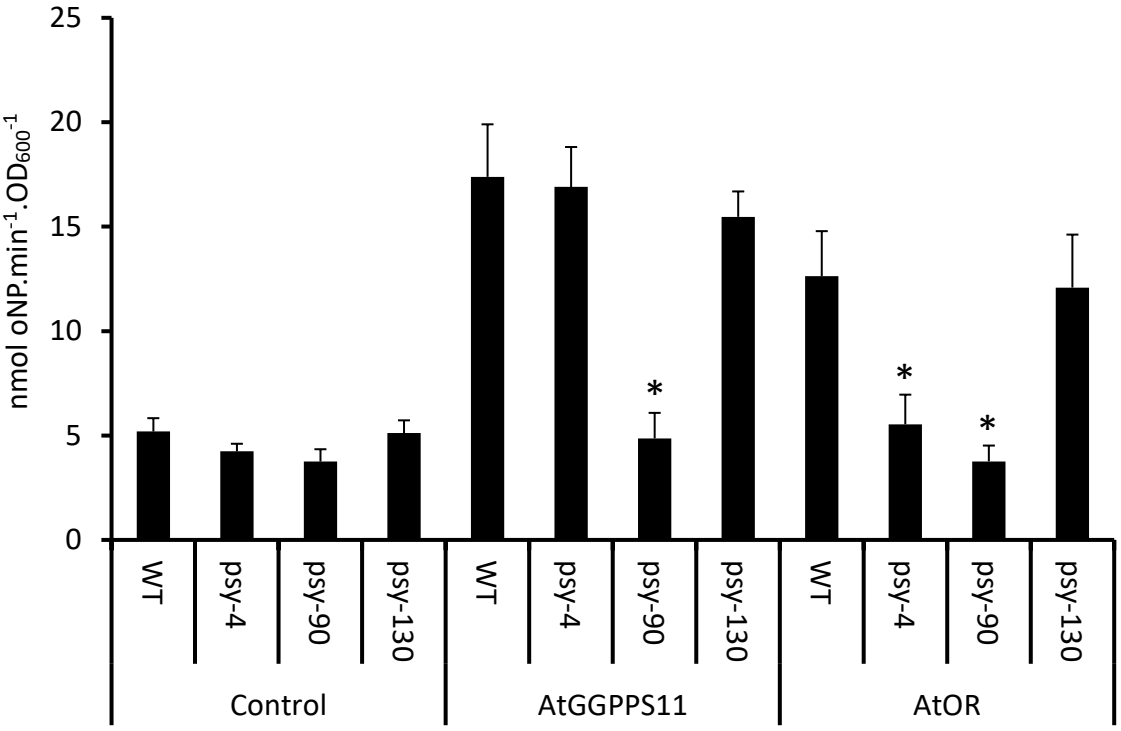
nmol oNP.min-1.OD600-1
25
20
15
10
5
0
WT
psy-4
psy-90
psy-130
Control
AtGGPPS11
AtOR
*

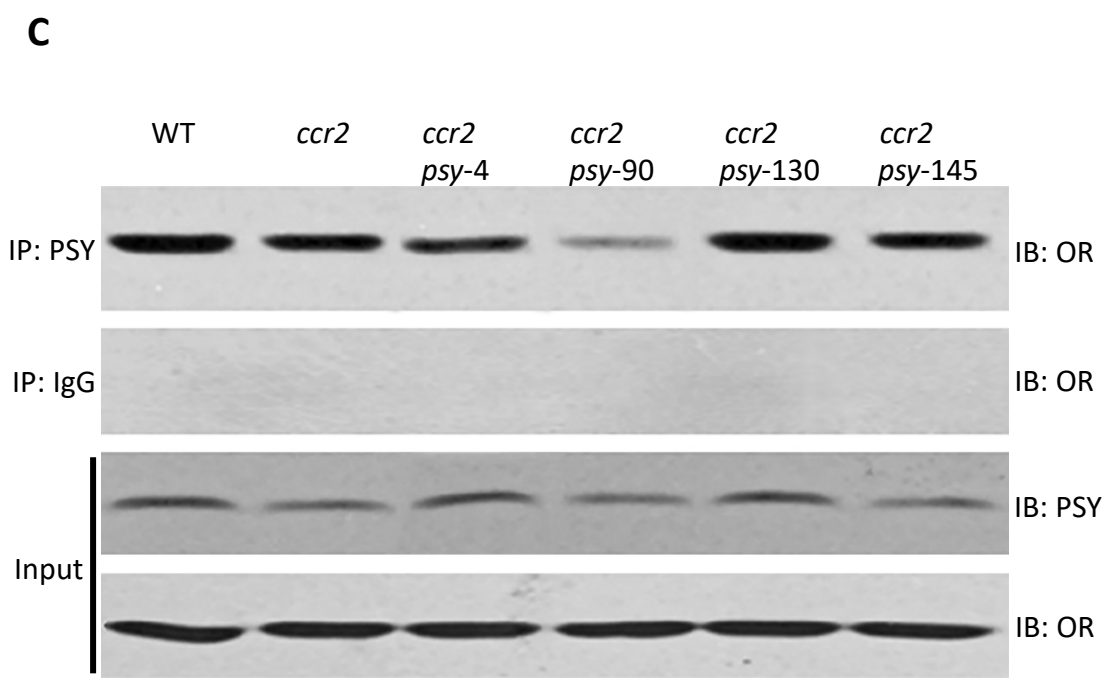

Figure 6: Mutations in PSY affected protein-protein interaction between PSY and OR and that between PSY and GGPPS11. A, Protein-protein interaction assays using split ubiquitin system. *PSY* gene versions fused to the C-terminal ubiquitin moiety (Cub) were co-expressed with AtOR (OR) and AtGGPPS11 (G11), respectively, fused to the N-terminal ubiquitin moiety (Nub). Yeasts were spotted onto either nonselective (-LW) or fully selective medium (-LWAH) in a series of 10-fold dilutions. In order to reduce background activation of reporter genes and visualize different interaction strengths, methionine (150 µmol.L^{-1} and 1 mmol.L^{-1}) was added to the media reducing expression of Cub fusion proteins (+150 µM M and +1mM M, respectively). Control combinations with empty Cub expressing vector are included below. B, β-Galactosidase activity of yeast strains co-expressing different PSY versions fused to Cub and AtOR or ArGGPPS11 fused with Nub or Nub only (Control), respectively. Enzyme activity was determined by oNPG assay and is given in nmol oNP.min^{-1}.OD_{600}^{-1}. Error bars indicate standard errors from three measurements. * Difference is significant ($P < 0.05$) in comparison to WT. C, Co-immunoprecipitation analysis of PSY and AtOR proteins. Equal amounts of total protein extracted from each leaf sample were immunoprecipitated using anti-PSY antibody or using normal rabbit IgG as a negative control. Ten microliters of immunoprecipitate was then subjected to western blot using anti-OR antibody. Fifty percent of protein before immunoprecipitation was kept for input, and was subjected to western blotting with anti-PSY and anti-OR antibodies. Experiments were done in triplicates and representative results are displayed.

Figure 7

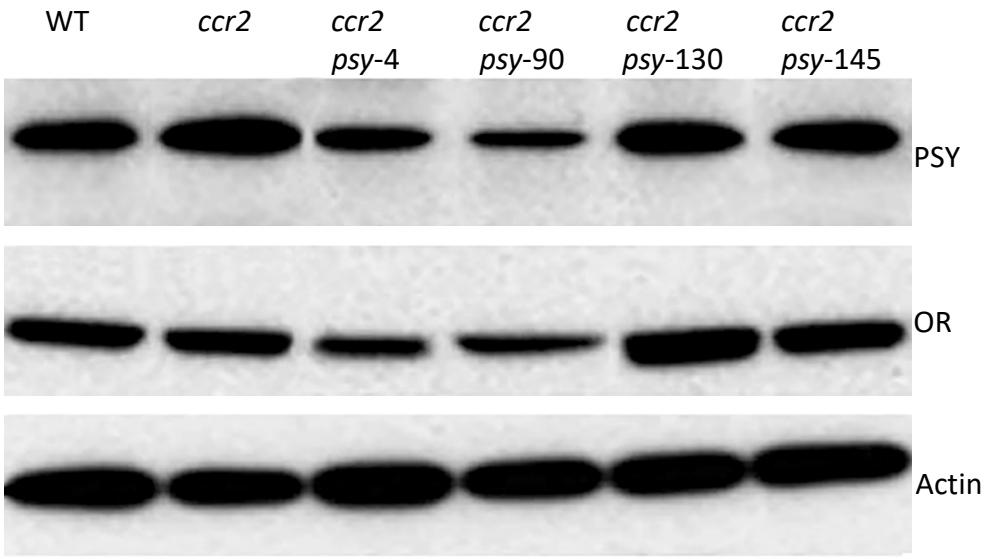

Figure 7: PSY and OR protein levels were both reduced in *psy* mutants. Ten micrograms of total protein extracted from leaf tissue of WT, *ccr2* or *ccr2 psy* mutants was used for western blot to determine protein levels of endogenous PSY and AtOR, with anti-PSY and anti-OR antibodies, respectively. Actin was included as an internal reference. Representative results from three replicates of each western blot are shown.

Figure 8

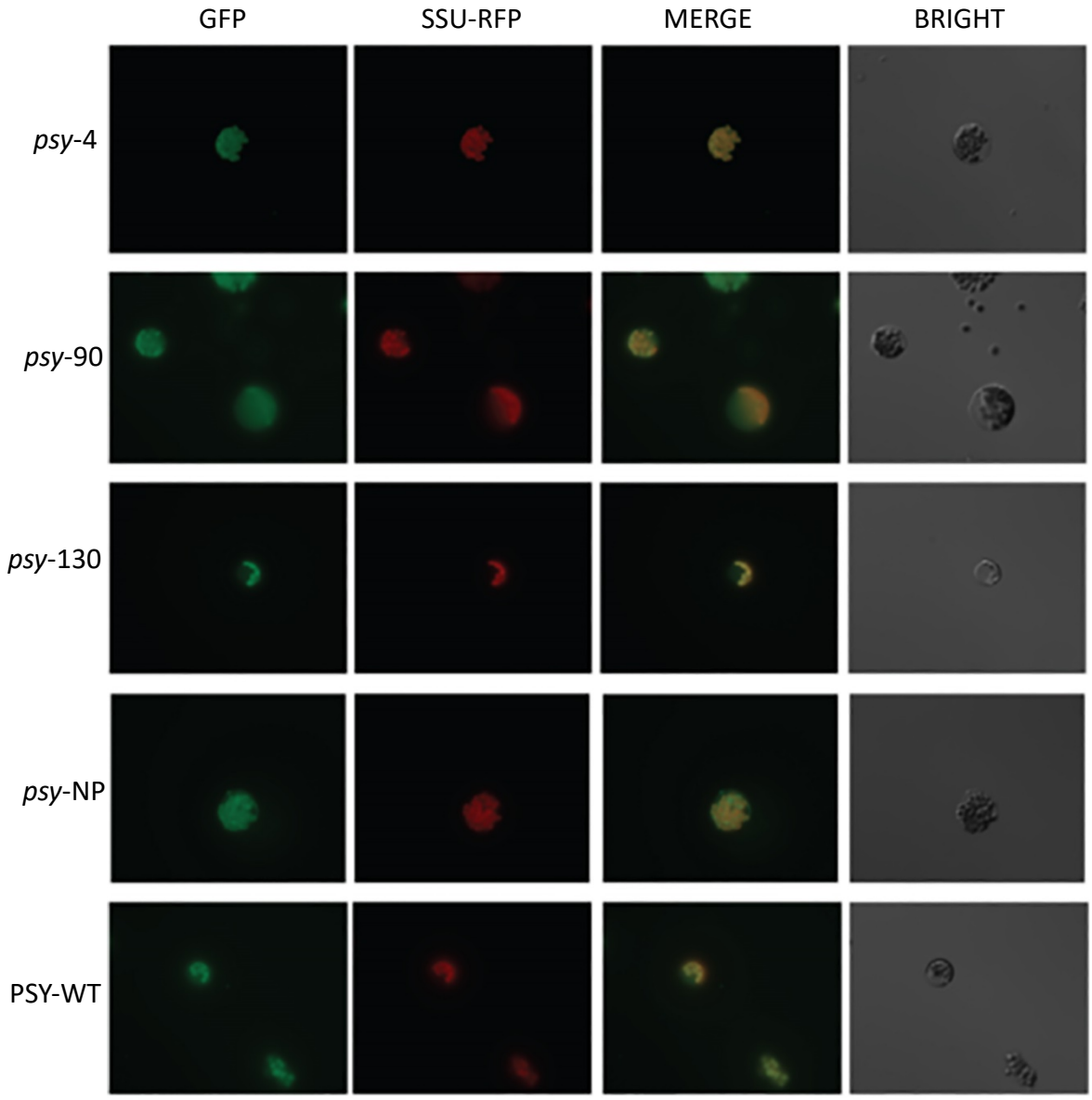

Figure 8: The localization of PSY was not altered in *psy* mutants. Protoplasts were isolated from green cotyledons of Arabidopsis seedlings and 10 µg of each PSY-CGFP plasmid with equal amount of SSU-RFP plasmid were incubated with 10^6 protoplasts. Following 16 h incubation in dark, protoplasts were subjected to confocal microscopy. BRIGHT: bright field; *psy*-NP: Arabidopsis PSY variant carrying Asn181 and Pro270.

DISCUSSION

PSY is a crucial enzyme regulating ACSs in plant

ACSs have been proposed to play regulatory roles throughout plant development (Kachanovsky et al., 2012; Ramel et al., 2012; Avendano-Vazquez et al., 2014; Van Norman et al., 2014; Hou et al., 2016). However, the factors that modulate the production and transduction of those carotenoid-derived signals have remained unclear. Since apocarotenoids are cleavage products of carotenoids (Walter and Strack, 2011; Havaux, 2014), carotenogenic enzymes may be essential in the modulation of ACSs. Here we show that PSY, the key enzyme in carotenoid biosynthetic pathway (Cazzonelli and Pogson, 2010), is a crucial factor that regulates the production of ACS2.

To investigate the production and regulatory roles of ACS2, we performed a forward genetics study and identified four point mutations in the *PSY* gene that reverted the leaf-yellowing phenotype of *ccr2* and restored PLB formation in etiolated seedlings (Figure 2 and Supplemental Figure S1). In the four *ccr2 psy* mutants, we found clear reduction of *cis*-ζ-carotene, tri-*cis*-neurosporene and tetra-*cis*-lycopene which were proposed to be accumulated and cleaved in *ccr2*, producing apocarotenoids and triggering ACS2 (Figure 4) (Chapter 4). Notably, those *cis*-carotenoids were still detectable in all *ccr2 psy* mutants, suggesting that a threshold of *cis*-carotenoid levels is required for the production of ACS2. The overexpression of wild type *PSY* gene in *ccr2 psy* double mutants restored the *cis*-carotenoid content to a similar level to *ccr2* (Figure 4) and in correlation a leaf-yellowing phenotype was observed in the overexpression lines (Supplemental Figure S3), indicating impaired chloroplast development in newly emerged leaf tissues (Chapter 4). We therefore could confirm that the PSY enzyme is crucial for the production of ACS2 that regulates plastid development. Reduction of the carotenoid biosynthetic flux resulted from a mutated version of *PSY* may supress ACS2 in *ccr2*.

As the entry-point enzyme of the carotenoid biosynthesis pathway (Ruiz-Sola and Rodriguez-Concepcion, 2012), PSY significantly affected *cis*-carotenoid content in this study. Interestingly, *cis*-carotenoids or *cis*-carotenoid-derived signals were also proposed to modulate *PSY* expression at transcriptional levels (Kachanovsky et al., 2012; Fantini et al., 2013). The complexity and mutual regulation in carotenoid-derived retrograde signals call for intensive

study.

Single amino acid changes alter PSY activity

Some single amino acid changes in PSY were reported to increase the enzyme's activity and upregulate carotenoid biosynthesis (Welsch et al., 2010; Shumskaya et al., 2012). In the present study, we observed clear reduction of PSY activity (Figures 4 and 5, Supplemental Figure S4). The $_{172}$DELVD$_{176}$ sequence of Arabidopsis PSY and the $_{298}$DVGED$_{302}$ sequence were predicted to form an active site together and bind phosphate groups of GGPP; the active site is conserved among isoprenoid synthases (Pandit et al., 2000; Shumskaya et al., 2012). The P178S mutation of *psy*-130 (Figure 3 and Supplemental Table S1) is between the $_{172}$DELVD$_{176}$ sequence and S$_{181}$ which was proposed to be an essential amino acid for the activity and localization of PSY (Shumskaya et al., 2012). Similarly, the M266I mutation in *psy*-4 (Figure 3 and Supplemental Table S1) is near $_{298}$DVGED$_{302}$ and P270 that was suggested to be another essential amino acid for PSY activity (Shumskaya et al., 2012). Although the A352T mutation of *psy*-90 (Figure 3 and Supplemental Table S1) is not close to the above active site or essential amino acid in protein sequence, it may interfere with the formation of a preferable structure of the PSY enzyme, which caused a more severe reduction of PSY activity and subsequently a dramatic drop of *cis*-carotenoid content (Figures 4 and 5, Supplemental Figure S4).

The mutation in *psy*-145 altered a splice site of the gene, therefore the splicing variant contained intron 3 which led to a truncated protein (Figure 3 and Supplemental Figure S2A). The complete loss of PSY activity in the truncated protein resulted in albino seedlings in a *ccr2 psy*-145 population (Figure S1B). However, most plants of the *ccr2 psy*-145 mutant would still possess a portion of functional PSY enzyme; in support of which the percentage composition of wild type *PSY* transcript on average was 2-fold higher than that of *psy*-145 splicing variant in the double mutant (Supplemental Figure S2B). *In vivo* activity assays of *ccr2 psy*-145 still displayed PSY activity (Figure 5A and Supplemental Figure S4A), and the immunoprecipitate of endogenous PSY from *ccr2 psy*-145 was also active (Supplemental Figure S4B), indicating that functional PSY was produced in the double mutant. The endogenous PSY protein immunoprecipitated from *ccr2 psy*-145 might contain both truncated *psy* and wild type enzyme, therefore a lower activity than that from *ccr2* or WT was observed (Figure 5B and Supplemental Figure S4B). In support of this, a band of non-truncated PSY protein (about 48 kD) was seen in western blots using anti-PSY antibody (Figure 6C and Figure 7).

We transiently expressed *psy*-4, *psy*-90 and *psy*-130 variants in chloroplasts and etioplasts, yet none of them displayed altered localisation (Figure 8) although reportedly a single amino acid change changed its localization through accumulation of crystalized carotenoids (Shumskaya et al., 2012). Notably, the three *psy* mutants carried reduced PSY activity in the present study, in contrast to the increase of PSY activity caused by a single amino acid change (Shumskaya et al., 2012). Interestingly, the amount of PSY in PLB fraction was not affected by transient expression of PSY-CGFP fusion proteins, although the amount in stroma was dramatically increased (Supplemental Figure S7). In line with our results, the active form of PSY is localized on membranes and stromal PSY seemed to be inactive; without a high level of interacting proteins, a large portion of overexpressed PSY might be present in stroma fraction and take the inactive form (Welsch et al., 2000; Zhou et al., 2015).

Protein-protein interaction is required for functional PSY

Using SUS, β-galactosidase activity assays and co-immunoprecipitation we found that the capacity of *psy*-4 and *psy*-90 to physically interact with AtOR was reduced in comparison to PSY-WT (Figure 6). The reduction in physical interaction resulted in reduced protein levels of both PSY and AtOR in the two mutants (Figure 7 and Supplemental Figure S6). The downregulation of PSY protein also accounted for reduced phytoene synthesis in SDC (Figure 5A and Supplemental Figure S4A). Furthermore, decreased AtOR protein levels might also negatively affect the recruitment of inactive PSY populations from stroma to membrane for activation, which consequently inhibited PSY activity (Zhou et al., 2015). In ELISAs, PSY levels in *ccr2 psy*-145 were not decreased while AtOR showed a slight reduction (Supplemental Figure S6), probably because that the truncated *psy*-145 still possessed immuno-reactivity to anti-PSY antibody yet lost interaction with AtOR.

In addition to PSY-AtOR interaction, *psy*-90 also showed reduction in PSY-AtGGPPS11 interaction (Figure 6A and 6B, Supplemental Figure S5). For the biosynthesis of carotenoids, a large enzyme complex was proposed to be formed, involving PSY and GGPPS (Camara, 1993; Cunningham and Gantt, 1998; Fraser et al., 2000; Shumskaya and Wurtzel, 2013). Within the metabolon, GGPPS may channel its product GGPP to PSY as substrate, and hence interaction with GGPPS is required for PSY activity (Ruiz-Sola et al., 2016). In yeast cells with *psy*-90+AtGGPPS11 combination, phytoene synthesis was almost abolished (Supplemental Figure S5), which supported the requirement of PSY-AtGGPPS11 interaction for PSY activity. The

A352T mutation in *psy*-90 seemed to suppress PSY-AtOR and PSY-AtGGPPS11 interaction and subsequently downregulate the protein levels and activity of PSY.

PSY links carotenoids to plastid development

The four mutated versions of *PSY* restored both PLB formation in etiolated seedlings and chloroplast biogenesis in leaf (Figure 2, Supplemental Figure S1A and C), suggesting those *psy* variants to affect both skotomorphogenesis and photomorphogenesis through the suppression of ACS2. In *ccr2*, ACS2 regulates plastid development partially via altering the protein levels of PIF3 and HY5 (Supplemental Figure S8). Taken together, the suppression of ACS2 in the four *ccr2 psy* double mutants affected plastid development possibly through modulating PIF3 and HY5. On the other hand, PIF family factors have been reported to regulate PSY expression in response to light signalling which controls chloroplast biogenesis and carotenoid biosynthesis (Toledo-Ortiz et al., 2010). Therefore, PSY acts as a hub that links carotenoid biosynthesis to plastid development.

MATERIAL AND METHODS

Please refer to chapter 2: Materials and Methods. All related methods have been included in chapter 2 and for submission they will be slightly amended to meet the requirements of the journal.

Accession Numbers

The Arabidopsis Genome Initiative locus number for the major gene discussed in this article is as following: *PSY* (At5g17230). The model of *PSY* gene is drawn from At5g17230.1.

Supplemental Material

Supplemental Tables

Supplemental Table S1: NGS information of the mutations in *PSY* gene in four *rccr2* lines

Supplemental Table S2: Primers used in this study

Supplemental Figures

Supplemental Figure S1: Mutations in *PSY* gene reverted the leaf-yellowing phenotype in *ccr2* and led to restoration of PLB formation in all *rccr2*^{psy} lines and albino phenotype in one line

Supplemental Figure S2: A single base pair change in *psy*-145 results in altered splicing in mRNA

Supplemental Figure S3: Overexpression of wild type *PSY* gene restored leaf yellowing in *ccr2 psy* double mutants

Supplemental Figure S4: *In vivo* and *in vitro* enzyme activity of PSY protein versions

Supplemental Figure S5: Phytoene produced in yeast cells with PSY+AtGGPPS11 combinations in split ubiquitin assays

Supplemental Figure S6: PSY and AtOR protein levels measured by enzyme-linked immunosorbent assays (ELISAs)

Supplemental Figure S7: PSY levels in PLB and stroma fractions of Arabidopsis etioplasts before and after the expression of PSY-GFP fusion protein

Supplemental Figure S8: ACS2 regulates protein levels of HY5 and PIF3 in *ccr2*

ACKNOWLEDGEMENTS

The Authors thank Dennis Schlossarek and Carmen Schubert (both from Faculty of Biology II, University of Freiburg, D79104 Freiburg, Germany) for their technical supports. We thank Jiwon Lee (Centre for Advanced Microscopy, The Australian National University, Canberra, ACT 2601, Australia) for technical supports in Transmission electron microscopy. We thank John Rivers, Dr Kai Xun Chan and Dr Ryan MacQuinn (Research School of Biology, The Australian National University) for helpful discussion.

Supplemental Table S1: NGS information of the mutations in *PSY* in four *rccr2* lines

***rccr2* lines**	**SNP position**	**Base change (Forward Strand)**	**Location in the gene**	**Amino acid change**
rccr2^{4}	5660555	C→T	CDS	M→I
rccr2^{90}	5660151	C→T	CDS	A→T
rccr2^{130}	5660938	G→A	CDS	P→S
rccr2^{145}	5661514	C→T	Splice site	Truncated protein

Supplemental Table S2: Primers used in this study

Name	Sequence	Accession
Sequencing		
PSY4F PSY4R	CTCTGTCTTATCTTACTTCC TAAACCCTTCCTCTTCTC	At5g17230
PSY90F PSY90R	ACCGGTTTCTTGATTCACA TTCCACTTTCCTCTCGCT	At5g17230
PSY130F PSY130R	GAACACCAAGCATCCAAA GTCTCGAAATGGCTGCAA	At5g17230
PSY145F PSY145R	GGTCTTCTTCTTATGACC CATCACTTTATCCTACAA	At5g17230
Cloning		
PSY145FC PSY145RC	CTTTGCTTATGACACCCG CAGAATATCGACCGGGTATC	At5g17230
qRT-PCR		
PSY145eFq PSY145eRq	GGCAATCTACGGTAAGTTAC GCAACTGTATCAGCGAGA	At5g17230
PSY145iFq PSY145iRq	CCAATGGTTGAAGAGCTG CAGCTTCAACTTCTCTTG	At5g17230
Yeast split ubiquitin system		
B1-PSY B2-PSY	B1-TCTTTTGTAAGGAACCGAAGTAG B2-TATCGATAGTCTTGAACTTGAAG	At5g17230
B1-AtOR B2-AtOR	B1-GCCGATAAATTCGCTTCCGGG B2-ATCGAAAGGGTCGATACGAGGATC	At5g61670
B1-AtGGPPS11 B2-AtGGPPS11	B1-TCTTCTTCCGTTGTTACAAAAG B2-GTTCTGTCTATAGGCAATGTAATT	At4g36810
B1 linker B2 linker	ACAAGTTTGTACAAAAAAGCAGGCTCTCCAACCACCATG TCCGCCACCACCAACCACTTTGTACAAGAAAGCTGGGTA	

SUPPLEMENTAL FIGURES

Supplemental Figure S1

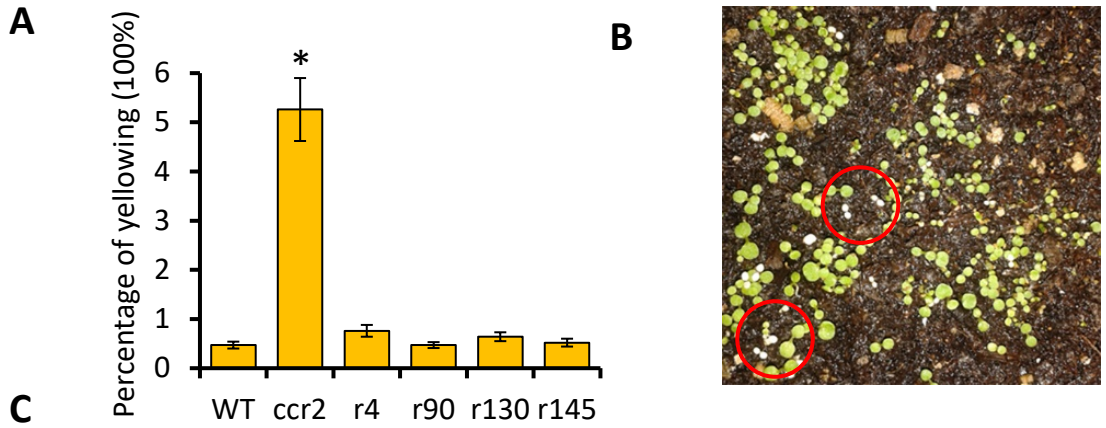

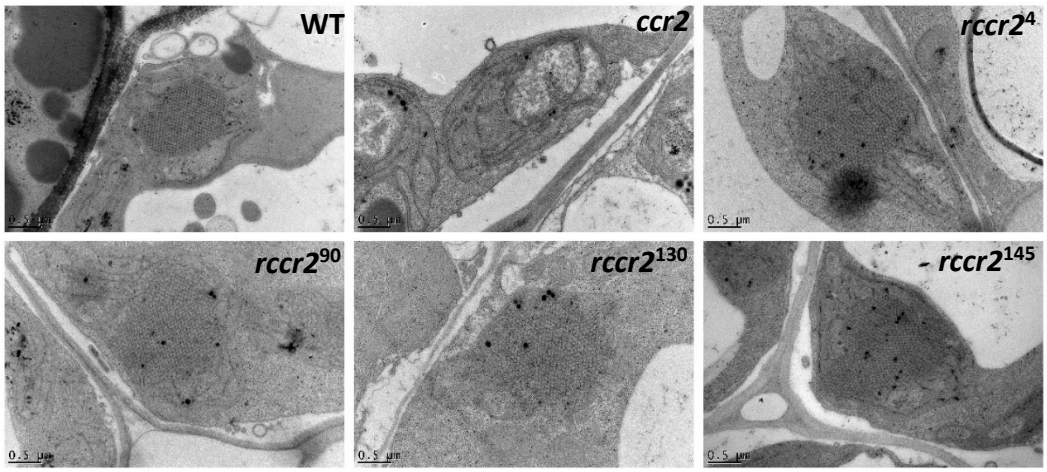

D

Germplasm	Ratio of etioplasts containing PLBs (%)	Tukey Groups
WT	100±0.0	a
ccr2	0±0.0	d
rccr2^{4}	95±2.3	ab
rccr2^{90}	100±0.0	a
rccr2^{130}	84±6.5	c
rccr2^{145}	92±2.6	bc

Supplemental Figure S1: Mutations in *PSY* reverted the leaf-yellowing phenotype in *ccr2* and led to restoration of PLB formation in all *rccr2*^{psy} lines and albino phenotype in one line. A, Percentage of yellow leaf area of WT, *ccr2* and *rccr2* lines carrying mutations in *PSY* gene. All plants were grown under 8-h photoperiod. *rccr2* is abbreviated to "*r*" in the charts, e.g. *r*4 is the abbreviation of *rccr2*^{4}. * Difference is significant in comparison to WT ($P < 0.05$ in one-way ANOVA). B, Albino seedlings of *rccr2*^{145} (red circle). Seedlings were grown under 16-h photoperiod. C, Transmission electron microscopy (TEM) images of a representative etioplast from 5-d old dark grown seedlings. The etioplasts of WT and *rccr2* lines carrying a mutated *PSY* gene showed well-developed prolamellar bodies (PLBs), while *ccr2* displayed complete absence of PLB formation. Images are representatives of more than 15 plastids from at least 5 TEM sections. D, Ratios of etioplasts containing PLBs. Letters denote post-hoc Tukey groups from a one-way ANOVA test.

Supplemental Figure S2

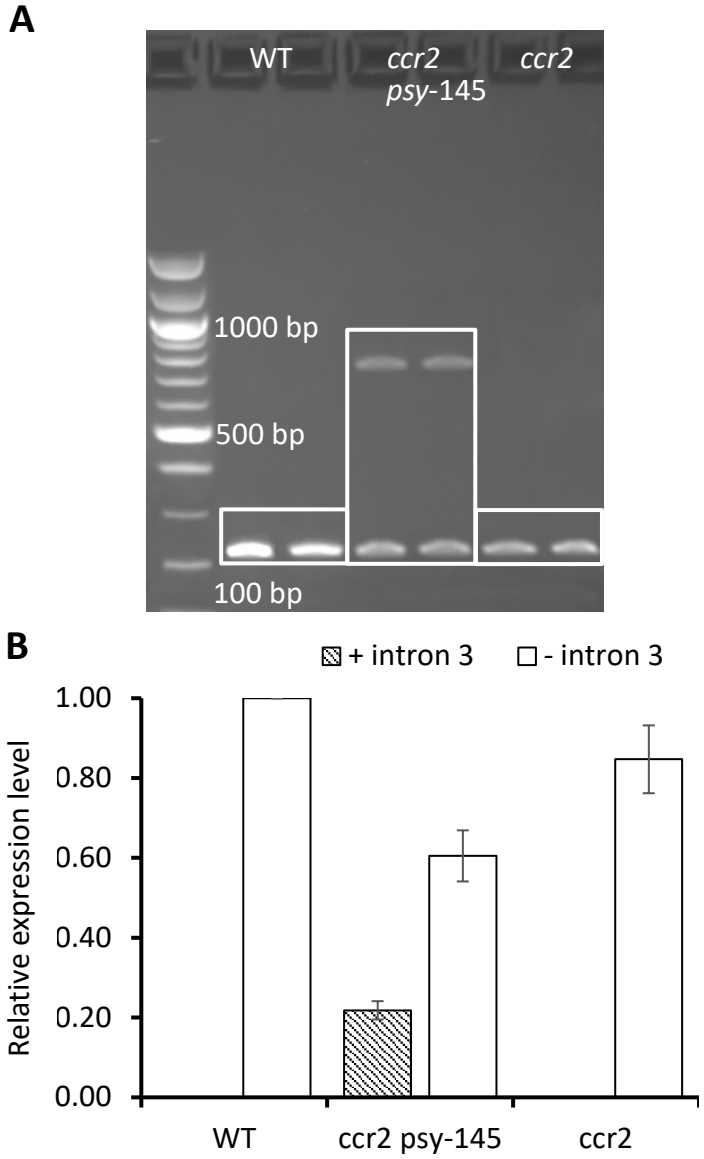

Supplemental Figure S2: A single base pair change in *psy-145* results in altered splicing in mRNA. A, Reverse transcription PCR (RT-PCR) confirms alternative splicing of intron 3 in *ccr2 psy*-145 leaf tissues. Exons 2 and 3 were partially amplified and products were run on a 1% agarose gel to examine the spliced (221 bp, WT and *ccr2*) or unspliced (762 bp, *ccr2 psy*-145) amplicons. The 100 bp ladder confirms fragment sizes. B, Quantitative RT-PCR (qRT-PCR) of partial *PSY* transcript of WT (-intron 3) and *psy*-145 (+intron 3) in WT, *ccr2 psy*-145 and *ccr2* leaf tissue. For *psy*-145, primers were designed to amplify a 162-bp product within intron 3; for WT, primers were designed to amplify part of exons 2 and 3 spanning intron 3, and qRT-PCR protocols were optimized to yield only the 155-bp product containing exon sequence but not the 696-bp fragment containing exons and intron 3, using cloning vectors carrying wild type *PSY* or *psy*-145 as reference. Standard error bars are shown (n=10). RNA levels were normalized to Protein Phosphatase 2A (AT1G13320) gene and displayed as fold change relative to *PSY* mRNA (-intron 3) in wild type Arabidopsis plants.

Supplemental Figure S3

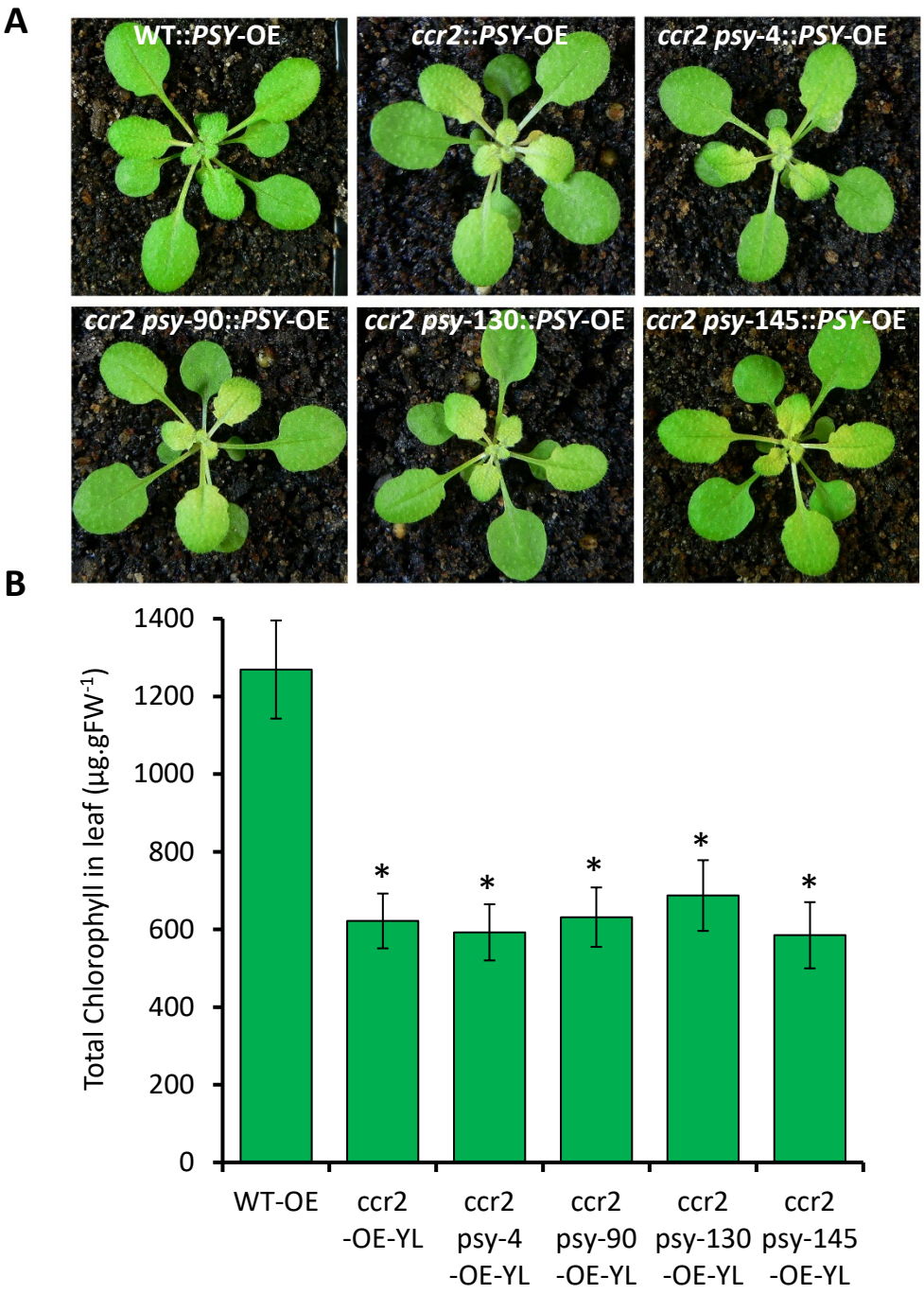

Supplemental Figure S3: Overexpression of wild type *PSY* gene restored leaf yellowing in *ccr2 psy* double mutants. A, Three-week old T4 generation transgenic plants growing under 8-h photoperiod. Rosette images show yellowing in newly developed leaf tissue except that of WT::*PSY*-OE. Images are representative of 50-100 T4 generation plants from five independent lines of PSY-OE. *PSY*-OE: *PSY* overexpression. B, Total chlorophyll in leaf tissue T4 generation transgenic plants, showing that chlorophyll content is significantly reduced yellow leaf (YL) tissue. Plants were grown under 8-h photoperiod. Values were averaged from five biological replicates and error bars denote standard error. *Difference is significant in comparison to WT-OE ($P < 0.05$ in one-way ANOVA).

Supplemental Figure S4

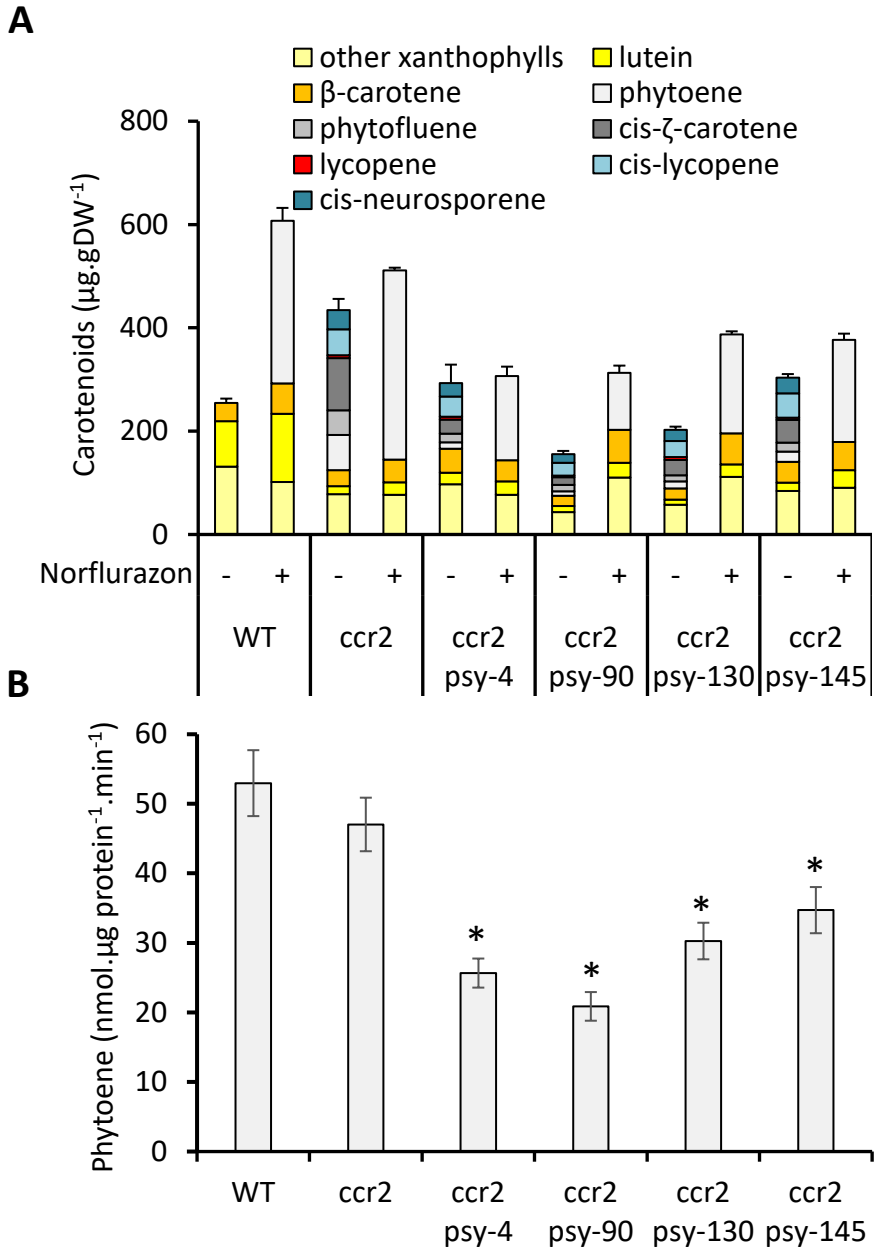

Supplemental Figure S4: *In vivo* and *in vitro* enzyme activity of PSY protein versions. A, All detectable carotenoids from seed-derived callus. Phytoene was accumulated when callus was treated with 1 µmol.L^{-1} norflurazon treatment (+); the amounts of phytoene accumulated were used to measure the enzyme activity of PSY protein versions. Carotenoids were quantified by HPLC and data is shown as mean ± standard errors of three biological replicates. B, *In vitro* activity of endogenous PSY (or *psy*) from WT, *ccr2* and *ccr2 psy* double mutants. Endogenous PSY protein or mutants were purified from leaf tissue of 25 d old Arabidopsis plants by immunoprecipitation and 5 µg of each was subjected to an enzymatic activity assay measuring the amount of phytoene produced. Experiments were done in triplicates and results are displayed as mean ± standard error. *Difference is significant in comparison to WT-OE ($P < 0.05$ in one-way ANOVA).

Supplemental Figure S5

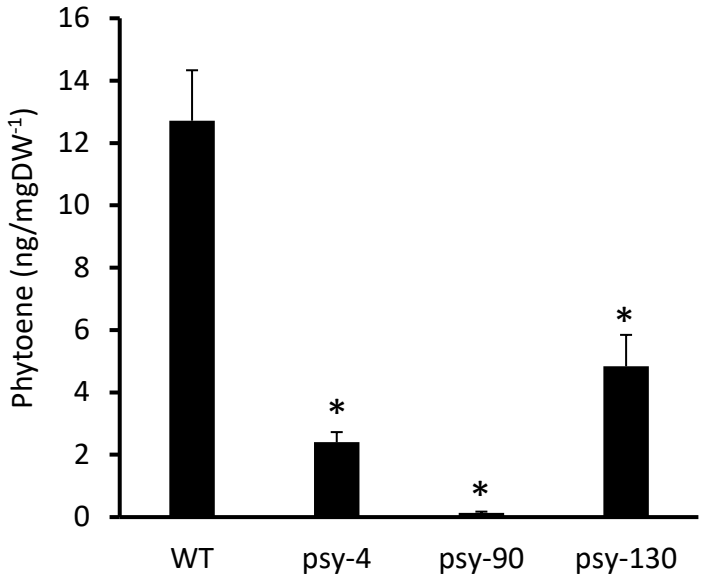

Supplemental Figure S5: Phytoene produced in yeast cells with PSY+AtGGPPS11 combinations in split ubiquitin assays. Phytoene levels were measured by HPLC. Error bars indicate standard errors from three measurements. *Difference is significant in comparison to WT ($P < 0.05$ in one-way ANOVA).

Supplemental Figure S6

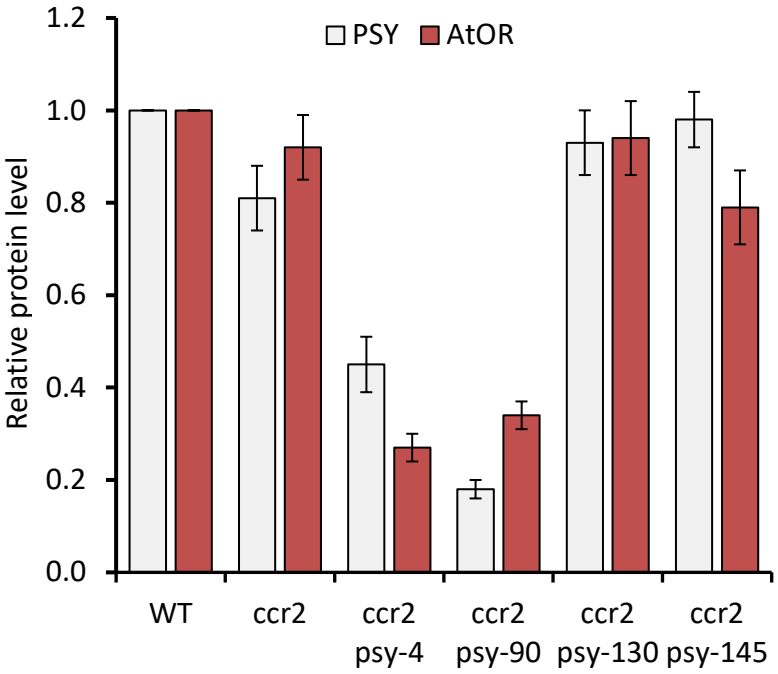

Supplemental Figure S6: PSY and AtOR protein levels measured by enzyme-linked immunosorbent assays (ELISAs). Each well was coated with total protein from Arabidopsis leaf tissue and then incubated with anti-PSY or anti-OR antibodies. Following the addition of substrate solution containing O-phenylenediamine dihydrochloride and H_2O_2 the absorbance was measured at 492 nm. All ELISAs were done in triplicates and values are shown as mean ± standard error.

Supplemental Figure S7

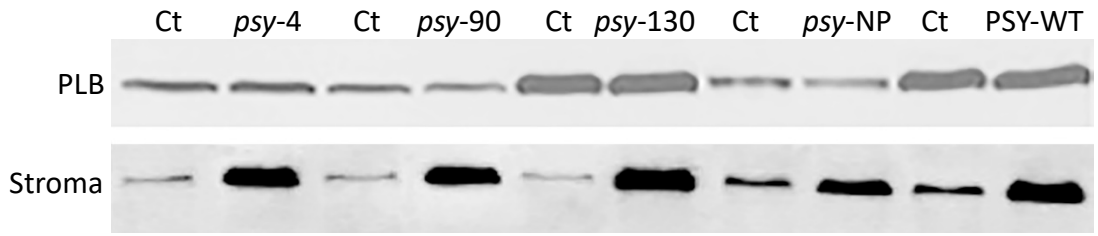

Supplemental Figure S7: PSY levels in PLB and stroma fractions of Arabidopsis etioplasts before and after the expression of PSY-GFP fusion protein. Protoplasts were isolated from cotyledons of etiolated WT Arabidopsis seedlings (7-d old) and incubated with a PSY-CGFP plasmid in dark for 16 h. Ten microliters of PLB or stroma fraction of etioplasts was subjected to western blot using anti-PSY antibody. Ct: control with no PSY-CGFP expression.

Supplemental Figure S8

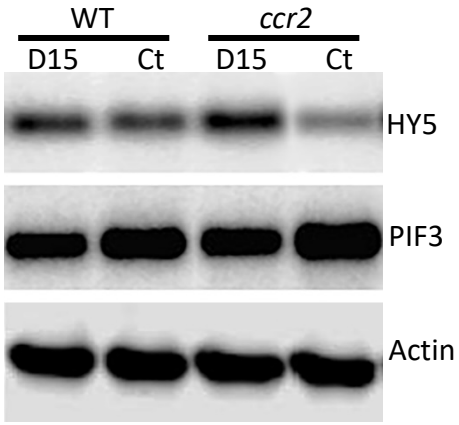

Supplemental Figure S8: ACS2 regulates proteins levels of HY5 and PIF3 in *ccr2*. The protein levels of HY5 was downregulated in *ccr2* but restored by D15 treatment. In contrast, PIF3 was upregulated in *ccr2* but reduced to wild type levels by D15 treatment. D15 (aryl-C3N hydroxamic acid compound) is an inhibitor of carotenoid cleavage dioxygenases (CCDs) and hence supresses the production of ACS2. HY5: Elongated Hypocotyl 5; PIF: Phytochrome-interacting Factor.

Chapter 6: Concluding remarks

In this thesis, I explored the nature of the proposed ACS which causes perturbed plastid development in *ccr2*. I identified a series of possible mutations from *rccr2* lines that reverted the *ccr2* leaf-yellowing phenotype, and confirmed causal lesions in three genes, *PSY*, *ZISO* and *DET1*. By examining double mutants *ccr2 ziso* and *ccr2 det1*, I elucidated the regulation of plastid development by a retrograde signal named ACS2 which acts downstream of DET1 to affect POR protein levels. I then studied the mechanisms of the suppression of ACS2 by mutations in *PSY*. The following content is to summarise the present study and discuss future perspectives in addition to those mentioned in section 1.5 of chapter 1.

6.1 Different mechanisms are involved to regulate ACS2 in *rccr2* lines

In the present study, I identified 18 candidate genes which might lead to reversion of the *ccr2* leaf-yellowing phenotype. The candidate genes serve different roles in plants. *PSY* and *ZISO* are directly involved in carotenoid biosynthesis, and *AtOR* regulates PSY protein levels (Zhou et al., 2015); the mutations in those genes likely affect the production of ACS2, the *cis*-carotenoid-derived retrograde signal. *DET1* and *RPT5B* affect chloroplast biogenesis by repressing photomorphogenesis (Yi and Deng, 2005; Guyon-Debast et al., 2010; Dong et al., 2014; Shi et al., 2015), which links the mutated genes to the antagonism of ACS2. Interestingly, *cis*-carotenoid composition in *ccr2 det1*-154 is also altered, suggesting a complex mechanism in the restoration of plastid development. *FtsH11* is another gene that may regulate chloroplast development although the molecular mechanism remains unresolved. Genes encoding receptors, such as GLRs (Chapter 3), may be involved in the perception of ACS2 and hence regulate plastid development. Mutations in membrane transporter proteins such as MFS (Table 3.5) may block the translocation of an apocarotenoid signalling molecule. Kinases and other regulatory factors may be components of signalling pathways that are modulated by ACS2.

Although all *rccr2* lines displayed restoration of greening in newly emerged leaf tissues, six *rccr2* lines showed delayed cotyledon greening similar to *ccr2* (Figure 3.6), indicating that PLB formation during skotomorphogenesis might not be restored in those lines while chloroplast

biogenesis is restored in light-grown plants.

In summary, different mechanisms are involved in the regulation of ACS2 and restoration chloroplast development when *rccr2* are grown in light (short photoperiods), while skotomorphogenesis may not be affected in all revertant lines of *ccr2*.

6.2 A threshold level of *cis*-carotenoids in specific tissues may be required to produce an ACS

Among all *rccr2* lines, only *ccr2 ziso*-155 showed complete loss of two *cis*-carotenoids, tri-*cis*-neurosporene and tetra-*cis*-lycopene, which were proposed to be substrates of ACS2 (Chapter 4). The other 25 *rccr2* lines accumulated the same group of *cis*-carotenoids detected in *ccr2*, yet the levels of *cis*-carotenoids varied in some lines, especially in *ccr2 psy* double mutants (Chapter 5). This suggests that a threshold level of *cis*-carotenoids is required to produce an apocarotenoid signal, and that reducation in flux through the carotenoid pathway can perturb the biosynthesis of ACS2 (Chapter 5). In nature, perhaps *cis*-carotenoids accumulate to levels above a threshold upon the loss of CRTISO activity or protein displacement from a metabolon. *cis*-carotenoids may only accumulate to levels above a threshold in specific tissues, such as cotyledons during skotomorphogenesis or young leaves following photomorphogenesis, and thereby regulate plastid development in those tissues. However, it still remains to be determined if there are physiologically-relevant growth conditions that activate *cis*-carotenoid signalling in wild-type plants.

6.3 ACS2 regulates both skotomorphogenesis and photomorphogenesis

In this thesis, I studied the regulation of both skotomorphogenesis and photomorphogenesis by ACS2. During skotomorphogenesis, ACS2 leads to absence of PLB formation in etioplasts, which delays cotyledon greening upon illumination. In chapter 4, I demonstrated that ACS2 acts downstream of DET1 to posttranscriptionally regulate POR A/B which are required for the formation of PLB. ACS2 upregulates PIF3 protein levels and downregulates HY5, supressing photomorphogenic development. I also show that ACS2 regulates the expression *PhANG*s which may affect chloroplast biogenesis. Therefore, it appears that ACS2 regulate plastid

development during skotomorphogenesis and photomorphogenesis. Consistently, the suppression of ACS2 by mutations in *PSY* restored PLB formation in etiolated seedlings and chloroplast biogenesis in leaf (Chapter 5). In addition to the model presented in chapter 4 (Figure 8) to describe how ACS2 affects PLB formation during skotomorphogenesis and chloroplast biogenesis during photomorphogenesis, I am proposing a model as following that describes how ACS2 regulates the expression of *PhANG*s through PIF3 and HY5 (Figure 6.1).

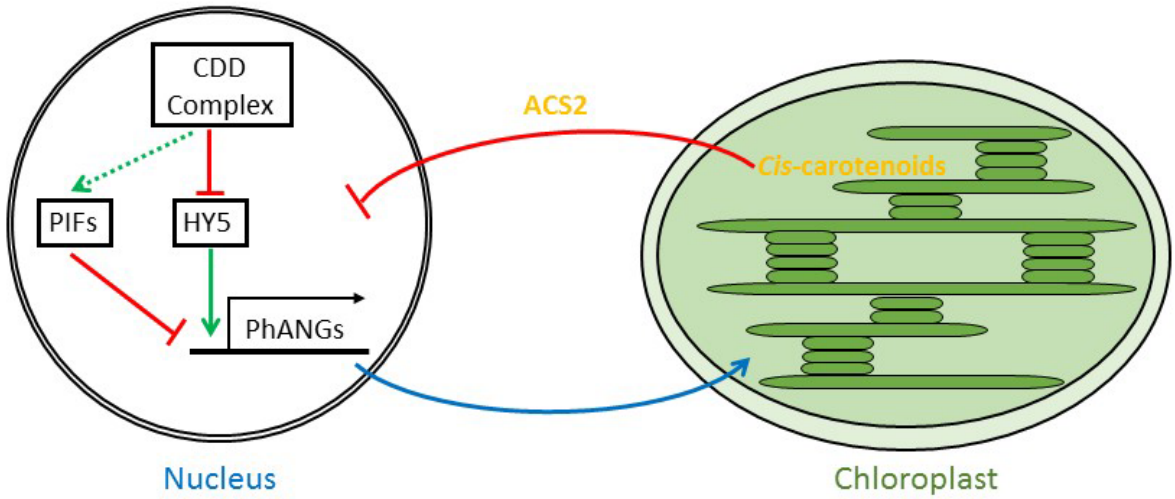

Figure 6.1 A schematic model describing how ASC2 represses the expression of *PhANG*s by modulating DET1 in the CDD complex, PIF3 and HY5. *PhANG*s: Photosynthesis Associated Nuclear Genes, DET1: Deetiolated-1, CDD complex: COP10/DET1/DDB1, PIF3: Phytochrome-Interacting Factor 3, HY5: Elongated Hypocotyl 5.

6.4 Cross-talk exists between light signalling and ACSs

The present study shows that ACS2 regulates plastid development by affecting the expression of *DET1* and protein levels of PIF3 and HY5. Interestingly, light signals also modulate carotenoid biosynthesis and plastid development, partially by regulating PIFs (Leivar and Monte, 2014). There seems to be cross-talk between light signalling and ACSs, potentially establishing a mutual regulation between carotenoid biosynthesis and plastid development. Mutations in *PSY* supress ACS2 which affects PIF3 levels in etiolated seedlings (Chapter 5), and PIFs were reported to regulate PSY expression which affects the flux of carotenoid biosynthesis (Toledo-Ortiz et al., 2010). The mutual regulation between PIFs and PSY may serve as a factor that determines the production of ACSs and controls the initiation of photomorphogenic development.

6.5 Future perspectives

For the future study of ACSs, it's essential to identify the apocarotenoids that trigger the retrograde signals. A detailed study on candidate genes identified from *rccr2* lines will aid in the elucidation of the perception and transduction of ACSs. How ACSs regulate photomorphogenesis related genes/proteins has been largely unclear and requires intensive study, and the crosstalk between ACSs and light signalling is of particular research interest. The RNA-sequencing data suggested that ACS2 modulates the expression of *GUN5*, which attracts study on the interaction between ACSs and GUN retrograde signals.

Glossary

ACS: Apocarotenoid signal

AtOR: Arabidopsis ORANGE protein

CCD: Carotenoid Cleavage Dioxygenase

ccr: *carotenoid and chloroplast regulation*

CDD complex: COP10/DET1/DDB1 complex

COP1: Constitutive Photomorphogenic 1

CRTISO: Carotenoid Isomerase

DDB1: Damaged DNA Binding Protein 1

DET1: Deetiolated 1

FTSH11: FTSH protease 11

GLR: Glutamate Receptors

HY5: Elongated Hypocotyl 5

NFZ: Norflurazon

PDS: phytoene desaturase

PhANGs: Photosynthesis associated Nuclear Genes

PhMoANGs: Photomorphogenesis associated Nuclear Genes

Phy B: Phytochrome B

PIF: Phytochrome-interacting Factor

POR: protochlorophyllide oxidoreductase

PSY: Phytoene Synthase

r*ccr2*: revertant of *ccr2*

SDC: Seed-Derived Callus

SUS: Split Ubiquitin System

Y2H: Yeast-Two-Hybrid

ZDS: ζ-carotene desaturase

ZISO: 15-*cis*-zeta-Carotene Isomerase

Bibliography

Adam, Z., Charuvi, D., Tsabari, O., Knopf, R.R., and Reich, Z. (2011). Biogenesis of thylakoid networks in angiosperms: knowns and unknowns. Plant Mol Biol **76,** 221-234.

Ahrazem, O., Trapero, A., Gomez, M.D., Rubio-Moraga, A., and Gomez-Gomez, L. (2010). Genomic analysis and gene structure of the plant carotenoid dioxygenase 4 family: a deeper study in Crocus sativus and its allies. Genomics **96,** 239-250.

Akiyama, K. (2007). Chemical identification and functional analysis of apocarotenoids involved in the development of arbuscular mycorrhizal symbiosis. Biosci Biotechnol Biochem **71,** 1405-1414.

Al-Babili, S., Hoa, T.T., and Schaub, P. (2006). Exploring the potential of the bacterial carotene desaturase CrtI to increase the beta-carotene content in Golden Rice. J Exp Bot **57,** 1007-1014.

Al-Babili, S., von Lintig, J., Haubruck, H., and Beyer, P. (1996). A novel, soluble form of phytoene desaturase from Narcissus pseudonarcissus chromoplasts is Hsp70-complexed and competent for flavinylation, membrane association and enzymatic activation. Plant J **9,** 601-612.

Al-Babili, S., Hugueney, P., Schledz, M., Welsch, R., Frohnmeyer, H., Laule, O., and Beyer, P. (2000). Identification of a novel gene coding for neoxanthin synthase from Solanum tuberosum. Febs Lett **485,** 168-172.

Al-Sady, B., Ni, W.M., Kircher, S., Schafer, E., and Quail, P.H. (2006). Photoactivated phytochrome induces rapid PIF3 phosphorylation prior to proteasorne-mediated degradation. Mol Cell **23,** 439-446.

Alba, R., Payton, P., Fei, Z., McQuinn, R., Debbie, P., Martin, G.B., Tanksley, S.D., and Giovannoni, J.J. (2005). Transcriptome and selected metabolite analyses reveal multiple points of ethylene control during tomato fruit development. Plant Cell **17,** 2954-2965.

Alboresi, A., Dall'osto, L., Aprile, A., Carillo, P., Roncaglia, E., Cattivelli, L., and Bassi, R. (2011). Reactive oxygen species and transcript analysis upon excess light treatment in wild-type Arabidopsis thaliana vs a photosensitive mutant lacking zeaxanthin and lutein. BMC Plant Biol **11,** 62.

Albrecht, M., Klein, A., Hugueney, P., Sandmann, G., and Kuntz, M. (1995). Molecular cloning and functional expression in E. coli of a novel plant enzyme mediating zeta-carotene desaturation. Febs Lett **372,** 199-202.

Alder, A., Jamil, M., Marzorati, M., Bruno, M., Vermathen, M., Bigler, P., Ghisla, S., Bouwmeester, H., Beyer, P., and Al-Babili, S. (2012). The path from beta-carotene to carlactone, a strigolactone-like plant hormone. Science **335,** 1348-1351.

Aluru, M.R., Bae, H., Wu, D., and Rodermel, S.R. (2001). The Arabidopsis immutans mutation affects plastid differentiation and the morphogenesis of white and green sectors in variegated plants. Plant Physiol **127,** 67-77.

Alvarez, D., Voss, B., Maass, D., Wuest, F., Schaub, P., Beyer, P., and Welsch, R. (2016). Carotenogenesis Is Regulated by 5 ' UTR-Mediated Translation of Phytoene Synthase Splice Variants. Plant Physiology **172,** 2314-2326.

Ament, K., Van Schie, C.C., Bouwmeester, H.J., Haring, M.A., and Schuurink, R.C. (2006). Induction of a leaf specific geranylgeranyl pyrophosphate synthase and emission of (E,E)-4,8,12-trimethyltrideca-1,3,7,11-tetraene in tomato are dependent on both

jasmonic acid and salicylic acid signaling pathways. Planta **224,** 1197-1208.

Apel, W., and Bock, R. (2009). Enhancement of carotenoid biosynthesis in transplastomic tomatoes by induced lycopene-to-provitamin A conversion. Plant Physiol **151,** 59-66.

Arango, J., Wust, F., Beyer, P., and Welsch, R. (2010). Characterization of phytoene synthases from cassava and their involvement in abiotic stress-mediated responses. Planta **232,** 1251-1262.

Armstrong, G.A., Alberti, M., Leach, F., and Hearst, J.E. (1989). Nucleotide sequence, organization, and nature of the protein products of the carotenoid biosynthesis gene cluster of Rhodobacter capsulatus. Mol Gen Genet **216,** 254-268.

Armstrong, G.A., Runge, S., Frick, G., Sperling, U., and Apel, K. (1995). Identification of NADPH:protochlorophyllide oxidoreductases A and B: a branched pathway for light-dependent chlorophyll biosynthesis in Arabidopsis thaliana. Plant Physiol **108,** 1505-1517.

Auldridge, M.E., Block, A., Vogel, J.T., Dabney-Smith, C., Mila, I., Bouzayen, M., Magallanes-Lundback, M., DellaPenna, D., McCarty, D.R., and Klee, H.J. (2006). Characterization of three members of the Arabidopsis carotenoid cleavage dioxygenase family demonstrates the divergent roles of this multifunctional enzyme family. Plant J **45,** 982-993.

Austin, J.R., Frost, E., Vidi, P.A., Kessler, F., and Staehelin, L.A. (2006). Plastoglobules are lipoprotein subcompartments of the chloroplast that are permanently coupled to thylakoid membranes and contain biosynthetic enzymes. Plant Cell **18,** 1693-1703.

Austin, R.S., Vidaurre, D., Stamatiou, G., Breit, R., Provart, N.J., Bonetta, D., Zhang, J., Fung, P., Gong, Y., Wang, P.W., McCourt, P., and Guttman, D.S. (2011). Next-generation mapping of Arabidopsis genes. Plant J **67,** 715-725.

Avendano-Vazquez, A.O., Cordoba, E., Llamas, E., San Roman, C., Nisar, N., De la Torre, S., Ramos-Vega, M., Gutierrez-Nava, M.D., Cazzonelli, C.I., Pogson, B.J., and Leon, P. (2014). An Uncharacterized Apocarotenoid-Derived Signal Generated in zeta-Carotene Desaturase Mutants Regulates Leaf Development and the Expression of Chloroplast and Nuclear Genes in Arabidopsis. Plant Cell **26,** 2524-2537.

Azari, R., Reuveni, M., Evenor, D., Nahon, S., Shlomo, H., Chen, L., and Levin, I. (2010). Overexpression of UV-DAMAGED DNA BINDING PROTEIN 1 links plant development and phytonutrient accumulation in high pigment-1 tomato. J Exp Bot **61,** 3627-3637.

Bae, G., and Choi, G. (2008). Decoding of light signals by plant phytochromes and their interacting proteins. Annu Rev Plant Biol **59,** 281-311.

Bai, L., Kim, E.H., DellaPenna, D., and Brutnell, T.P. (2009). Novel lycopene epsilon cyclase activities in maize revealed through perturbation of carotenoid biosynthesis. Plant J **59,** 588-599.

Bailey, S., Thompson, E., Nixon, P.J., Horton, P., Mullineaux, C.W., Robinson, C., and Mann, N.H. (2002). A critical role for the Var2 FtsH homologue of Arabidopsis thaliana in the photosystem II repair cycle in vivo. J Biol Chem **277,** 2006-2011.

Bak, S., Beisson, F., Bishop, G., Hamberger, B., Hofer, R., Paquette, S., and Werck-Reichhart, D. (2011). Cytochromes p450. Arabidopsis Book **9,** e0144.

Baldermann, S., Kato, M., Kurosawa, M., Kurobayashi, Y., Fujita, A., Fleischmann, P., and Watanabe, N. (2010). Functional characterization of a carotenoid cleavage dioxygenase 1 and its relation to the carotenoid accumulation and volatile emission during the floral development of Osmanthus fragrans Lour. J Exp Bot **61,** 2967-2977.

Ballesteros, M.L., Bolle, C., Lois, L.M., Moore, J.M., Vielle-Calzada, J.P., Grossniklaus, U., and

Chua, N.H. (2001). LAF1, a MYB transcription activator for phytochrome A signaling. Genes Dev **15,** 2613-2625.

Balmer, Y., Koller, A., del Val, G., Manieri, W., Schurmann, P., and Buchanan, B.B. (2003). Proteomics gives insight into the regulatory function of chloroplast thioredoxins. P Natl Acad Sci USA **100,** 370-375.

Baranski, R., and Cazzonelli, C. (2016). Carotenoid biosynthesis and regulation in plants. In Carotenoids: Nutrition, Analysis and Technology, A. Kaczor and M. Baranska, eds (Wiley-Blackwel), pp. 161-189.

Baroli, I., and Niyogi, K.K. (2000). Molecular genetics of xanthophyll-dependent photoprotection in green algae and plants. Philos T Roy Soc B **355,** 1385-1393.

Baron, M., Davies, S., Alexander, L., Snellgrove, D., and Sloman, K.A. (2008). The effect of dietary pigments on the coloration and behaviour of flame-red dwarf gourami, Colisa lalia. Anim Behav **75,** 1041-1051.

Bartley, G.E., and Scolnik, P.A. (1989). Carotenoid biosynthesis in photosynthetic bacteria. Genetic characterization of the Rhodobacter capsulatus CrtI protein. J Biol Chem **264,** 13109-13113.

Bartley, G.E., and Scolnik, P.A. (1995). Plant carotenoids: pigments for photoprotection, visual attraction, and human health. Plant Cell **7,** 1027-1038.

Bartley, G.E., Scolnik, P.A., and Beyer, P. (1999). Two Arabidopsis thaliana carotene desaturases, phytoene desaturase and zeta-carotene desaturase, expressed in Escherichia coli, catalyze a poly-cis pathway to yield pro-lycopene. Eur J Biochem **259,** 396-403.

Bassard, J.E., Richert, L., Geerinck, J., Renault, H., Duval, F., Ullmann, P., Schmitt, M., Meyer, E., Mutterer, J., Boerjan, W., De Jaeger, G., Mely, Y., Goossens, A., and Werck-Reichhart, D. (2012). Protein-protein and protein-membrane associations in the lignin pathway. Plant Cell **24,** 4465-4482.

Bassi, R., Pineau, B., Dainese, P., and Marquardt, J. (1993). Carotenoid-binding proteins of photosystem II. Eur J Biochem **212,** 297-303.

Beisel, K.G., Jahnke, S., Hofmann, D., Koppchen, S., Schurr, U., and Matsubara, S. (2010). Continuous turnover of carotenes and chlorophyll a in mature leaves of Arabidopsis revealed by 14CO2 pulse-chase labeling. Plant Physiol **152,** 2188-2199.

Benvenuto, G., Formiggini, F., Laflamme, P., Malakhov, M., and Bowler, C. (2002). The photomorphogenesis regulator DET1 binds the amino-terminal tail of histone H2B in a nucleosome context. Curr Biol **12,** 1529-1534.

Beyer, P., and Kleinig, H. (1991). Carotenoid Biosynthesis in Higher-Plants - Membrane-Bound Desaturation and Cyclization Reactions in Chromoplast Membranes from Narcissus Peudonarcissus. Biol Chem H-S **372,** 527-527.

Beyer, P., Mayer, M., and Kleinig, H. (1989). Molecular oxygen and the state of geometric isomerism of intermediates are essential in the carotene desaturation and cyclization reactions in daffodil chromoplasts. Eur J Biochem **184,** 141-150.

Beyer, P., Al-Babili, S., Ye, X., Lucca, P., Schaub, P., Welsch, R., and Potrykus, I. (2002). Golden Rice: introducing the beta-carotene biosynthesis pathway into rice endosperm by genetic engineering to defeat vitamin A deficiency. J Nutr **132,** 506S-510S.

Bonk, M., Tadros, M., Vandekerckhove, J., Al-Babili, S., and Beyer, P. (1996). Purification and characterization of chaperonin 60 and heat-shock protein 70 from chromoplasts of Narcissus pseudonarcissus. Plant Physiol **111,** 931-939.

Bonk, M., Hoffmann, B., Von Lintig, J., Schledz, M., Al-Babili, S., Hobeika, E., Kleinig, H., and

Beyer, P. (1997). Chloroplast import of four carotenoid biosynthetic enzymes in vitro reveals differential fates prior to membrane binding and oligomeric assembly. Eur J Biochem **247,** 942-950.

Booker, J., Auldridge, M., Wills, S., McCarty, D., Klee, H., and Leyser, O. (2004). MAX3/CCD7 is a carotenoid cleavage dioxygenase required for the synthesis of a novel plant signaling molecule. Curr Biol **14,** 1232-1238.

Botella-Pavia, P., Besumbes, O., Phillips, M.A., Carretero-Paulet, L., Boronat, A., and Rodriguez-Concepcion, M. (2004). Regulation of carotenoid biosynthesis in plants: evidence for a key role of hydroxymethylbutenyl diphosphate reductase in controlling the supply of plastidial isoprenoid precursors. Plant J **40,** 188-199.

Bouvier, F., Keller, Y., d'Harlingue, A., and Camara, B. (1998a). Xanthophyll biosynthesis: molecular and functional characterization of carotenoid hydroxylases from pepper fruits (Capsicum annuum L.). Biochim Biophys Acta **1391,** 320-328.

Bouvier, F., Hugueney, P., d'Harlingue, A., Kuntz, M., and Camara, B. (1994). Xanthophyll biosynthesis in chromoplasts: isolation and molecular cloning of an enzyme catalyzing the conversion of 5,6-epoxycarotenoid into ketocarotenoid. Plant J **6,** 45-54.

Bouvier, F., d'Harlingue, A., Suire, C., Backhaus, R.A., and Camara, B. (1998b). Dedicated roles of plastid transketolases during the early onset of isoprenoid biogenesis in pepper fruits. Plant Physiology **117,** 1423-1431.

Bouvier, F., Suire, C., d'Harlingue, A., Backhaus, R.A., and Camara, B. (2000). Molecular cloning of geranyl diphosphate synthase and compartmentation of monoterpene synthesis in plant cells. Plant Journal **24,** 241-252.

Bouvier, F., d'Harlingue, A., Hugueney, P., Marin, E., Marion-Poll, A., and Camara, B. (1996). Xanthophyll biosynthesis. Cloning, expression, functional reconstitution, and regulation of beta-cyclohexenyl carotenoid epoxidase from pepper (Capsicum annuum). J Biol Chem **271,** 28861-28867.

Bradbury, L.M., Shumskaya, M., Tzfadia, O., Wu, S.B., Kennelly, E.J., and Wurtzel, E.T. (2012). Lycopene cyclase paralog CruP protects against reactive oxygen species in oxygenic photosynthetic organisms. Proc Natl Acad Sci U S A **109,** E1888-1897.

Bramley, P.M. (1997). The regulation and genetic manipulation of carotenoid biosynthesis in tomato fruit. Pure Appl Chem **69,** 2159-2162.

Brandi, F., Bar, E., Mourgues, F., Horvath, G., Turcsi, E., Giuliano, G., Liverani, A., Tartarini, S., Lewinsohn, E., and Rosati, C. (2011). Study of 'Redhaven' peach and its white-fleshed mutant suggests a key role of CCD4 carotenoid dioxygenase in carotenoid and norisoprenoid volatile metabolism. BMC Plant Biol **11,** 24.

Breitenbach, J., and Sandmann, G. (2005). zeta-Carotene cis isomers as products and substrates in the plant poly-cis carotenoid biosynthetic pathway to lycopene. Planta **220,** 785-793.

Breitenbach, J., Fernandez-Gonzalez, B., Vioque, A., and Sandmann, G. (1998). A higher-plant type zeta-carotene desaturase in the cyanobacterium Synechocystis PCC6803. Plant Mol Biol **36,** 725-732.

Brenner, E.D., Martinez-Barboza, N., Clark, A.P., Liang, Q.S., Stevenson, D.W., and Coruzzi, G.M. (2000). Arabidopsis mutants resistant to S(+)-beta-methyl-alpha, beta-diaminopropionic acid, a cycad-derived glutamate receptor agonist. Plant Physiol **124,** 1615-1624.

Briggs, W.R., and Olney, M.A. (2001). Photoreceptors in plant photomorphogenesis to date. Five phytochromes, two cryptochromes, one phototropin, and one superchrome.

Plant Physiology **125,** 85-88.

Briggs, W.R., Tseng, T.S., Cho, H.Y., Swartz, T.E., Sullivan, S., Bogomolni, R.A., Kaiserli, E., and Christie, J.M. (2007). Phototropins and their LOV domains: Versatile plant blue-light receptors. Journal of Integrative Plant Biology **49,** 4-10.

Britton, G. (1993). Carotenoids in chloroplasts pigment-protein complexes. In Pigment-protein complexes in plastids: synthesis and assembly, C. Sundqvist and M. Ryberg, eds (San Diego: Academic Press), pp. 447-483.

Bruno, M., Beyer, P., and Al-Babili, S. (2015). The potato carotenoid cleavage dioxygenase 4 catalyzes a single cleavage of beta-ionone ring-containing carotenes and non-epoxidated xanthophylls. Arch Biochem Biophys **572,** 126-133.

Bruno, M., Koschmieder, J., Wuest, F., Schaub, P., Fehling-Kaschek, M., Timmer, J., Beyer, P., and Al-Babili, S. (2016). Enzymatic study on AtCCD4 and AtCCD7 and their potential to form acyclic regulatory metabolites. J Exp Bot **67,** 5993-6005.

Buchanan, B.B., Schurmann, P., Wolosiuk, R.A., and Jacquot, J.P. (2002). The ferredoxin/thioredoxin system: from discovery to molecular structures and beyond. Photosynthesis Research **73,** 215-222.

Budziszewski, G.J., Lewis, S.P., Glover, L.W., Reineke, J., Jones, G., Ziemnik, L.S., Lonowski, J., Nyfeler, B., Aux, G., Zhou, Q., McElver, J., Patton, D.A., Martienssen, R., Grossniklaus, U., Ma, H., Law, M., and Levin, J.Z. (2001). Arabidopsis genes essential for seedling viability: Isolation of Insertional mutants and molecular cloning. Genetics **159,** 1765-1778.

Burrows, P.A., Sazanov, L.A., Svab, Z., Maliga, P., and Nixon, P.J. (1998). Identification of a functional respiratory complex in chloroplasts through analysis of tobacco mutants containing disrupted plastid ndh genes. Embo J **17,** 868-876.

Busch, M., Seuter, A., and Hain, R. (2002). Functional analysis of the early steps of carotenoid biosynthesis in tobacco. Plant Physiol **128,** 439-453.

Camara, B. (1993). Plant Phytoene Synthase Complex - Component Enzymes, Immunology, and Biogenesis. Method Enzymol **214,** 352-365.

Campbell, J.A., Davies, G.J., Bulone, V., and Henrissat, B. (1997). A classification of nucleotide-diphospho-sugar glycosyltransferases based on amino acid sequence similarities. Biochemical Journal **326,** 929-939.

Campbell, R., Ducreux, L.J., Morris, W.L., Morris, J.A., Suttle, J.C., Ramsay, G., Bryan, G.J., Hedley, P.E., and Taylor, M.A. (2010). The metabolic and developmental roles of carotenoid cleavage dioxygenase4 from potato. Plant Physiol **154,** 656-664.

Cao, H., Zhang, J., Xu, J., Ye, J., Yun, Z., Xu, Q., and Deng, X. (2012). Comprehending crystalline beta-carotene accumulation by comparing engineered cell models and the natural carotenoid-rich system of citrus. J Exp Bot **63,** 4403-4417.

Carol, P., and Kuntz, M. (2001). A plastid terminal oxidase comes to light: implications for carotenoid biosynthesis and chlororespiration. Trends Plant Sci **6,** 31-36.

Carretero-Paulet, L., Cairo, A., Botella-Pavia, P., Besumbes, O., Campos, N., Boronat, A., and Rodriguez-Concepcion, M. (2006). Enhanced flux through the methylerythritol 4-phosphate pathway in Arabidopsis plants overexpressing deoxyxylulose 5-phosphate reductoisomerase. Plant Mol Biol **62,** 683-695.

Cashmore, A.R. (2003). Cryptochromes: enabling plants and animals to determine circadian time. Cell **114,** 537-543.

Castillon, A., Shen, H., and Huq, E. (2007). Phytochrome Interacting Factors: central players in phytochrome-mediated light signaling networks. Trends Plant Sci **12,** 514-521.

Cazzonelli, C.I. (2011). Carotenoids in nature: insights from plants and beyond. Funct Plant Biol **38,** 833-847.

Cazzonelli, C.I., and Pogson, B.J. (2010). Source to sink: regulation of carotenoid biosynthesis in plants. Trends Plant Sci **15,** 266-274.

Cazzonelli, C.I., Yin, K., and Pogson, B.J. (2009a). Potential implications for epigenetic regulation of carotenoid biosynthesis during root and shoot development. Plant Signal Behav **4,** 339-341.

Cazzonelli, C.I., Roberts, A.C., Carmody, M.E., and Pogson, B.J. (2010). Transcriptional control of SET DOMAIN GROUP 8 and CAROTENOID ISOMERASE during Arabidopsis development. Mol Plant **3,** 174-191.

Cazzonelli, C.I., Cuttriss, A.J., Cossetto, S.B., Pye, W., Crisp, P., Whelan, J., Finnegan, E.J., Turnbull, C., and Pogson, B.J. (2009b). Regulation of carotenoid composition and shoot branching in Arabidopsis by a chromatin modifying histone methyltransferase, SDG8. Plant Cell **21,** 39-53.

Chai, C., Fang, J., Liu, Y., Tong, H., Gong, Y., Wang, Y., Liu, M., Qian, Q., Cheng, Z., and Chu, C. (2011). ZEBRA2, encoding a carotenoid isomerase, is involved in photoprotection in rice. Plant Mol Biol **75,** 211-221.

Chamovitz, D., Pecker, I., and Hirschberg, J. (1991). The molecular basis of resistance to the herbicide norflurazon. Plant Mol Biol **16,** 967-974.

Chamovitz, D., Pecker, I., Sandmann, G., Boger, P., and Hirschberg, J. (1990). Cloning a gene coding for norflurazon resistance in cyanobacteria. Z Naturforsch C **45,** 482-486.

Chan, K.X., Mabbitt, P.D., Phua, S.Y., Mueller, J.W., Nisar, N., Gigolashvili, T., Stroeher, E., Grassl, J., Arlt, W., Estavillo, G.M., Jackson, C.J., and Pogson, B.J. (2016). Sensing and signaling of oxidative stress in chloroplasts by inactivation of the SAL1 phosphoadenosine phosphatase. Proc Natl Acad Sci U S A **113,** E4567-4576.

Chappell, J. (1995). The Biochemistry and Molecular Biology of Isoprenoid Metabolism. Plant Physiol **107,** 1-6.

Chapple, C. (1998). Molecular-genetic analysis of plant cytochrome P450-dependent monooxygenases. Annu Rev Plant Phys **49,** 311-343.

Chattopadhyay, S., Ang, L.H., Puente, P., Deng, X.W., and Wei, N. (1998). Arabidopsis bZIP protein HY5 directly interacts with light-responsive promoters in mediating light control of gene expression. Plant Cell **10,** 673-683.

Chaudhary, N., Nijhawan, A., Khurana, J.P., and Khurana, P. (2010). Carotenoid biosynthesis genes in rice: structural analysis, genome-wide expression profiling and phylogenetic analysis. Mol Genet Genomics **283,** 13-33.

Cheminant, S., Wild, M., Bouvier, F., Pelletier, S., Renou, J.P., Erhardt, M., Hayes, S., Terry, M.J., Genschik, P., and Achard, P. (2011). DELLAs regulate chlorophyll and carotenoid biosynthesis to prevent photooxidative damage during seedling deetiolation in Arabidopsis. Plant Cell **23,** 1849-1860.

Chen, J., Burke, J.J., Velten, J., and Xin, Z. (2006). FtsH11 protease plays a critical role in Arabidopsis thermotolerance. Plant J **48,** 73-84.

Chen, M., Choi, Y., Voytas, D.F., and Rodermel, S. (2000). Mutations in the Arabidopsis VAR2 locus cause leaf variegation due to the loss of a chloroplast FtsH protease. Plant J **22,** 303-313.

Chen, Y., Li, F., and Wurtzel, E.T. (2010). Isolation and characterization of the Z-ISO gene encoding a missing component of carotenoid biosynthesis in plants. Plant Physiol **153,** 66-79.

Cheng, W.H., Endo, A., Zhou, L., Penney, J., Chen, H.C., Arroyo, A., Leon, P., Nambara, E., Asami, T., Seo, M., Koshiba, T., and Sheen, J. (2002). A unique short-chain dehydrogenase/reductase in Arabidopsis glucose signaling and abscisic acid biosynthesis and functions. Plant Cell **14,** 2723-2743.

Chi, W., Sun, X., and Zhang, L. (2013). Intracellular signaling from plastid to nucleus. Annu Rev Plant Biol **64,** 559-582.

Chinnusamy, V., Gong, Z., and Zhu, J.K. (2008). Abscisic acid-mediated epigenetic processes in plant development and stress responses. J Integr Plant Biol **50,** 1187-1195.

Chiu, J., DeSalle, R., Lam, H.M., Meisel, L., and Coruzzi, G. (1999). Molecular evolution of glutamate receptors: a primitive signaling mechanism that existed before plants and animals diverged. Mol Biol Evol **16,** 826-838.

Chory, J., Peto, C., Feinbaum, R., Pratt, L., and Ausubel, F. (1989). Arabidopsis Thaliana Mutant That Develops as a Light-Grown Plant in the Absence of Light. Cell **58,** 991-999.

Clough, J.M., and Pattenden, G. (1979). Naturally Occurring Poly-Cis Carotenoids - Stereochemistry of Poly-Cis Lycopene and Its Congeners in Tangerine Tomato Fruits. J Chem Soc Chem Comm**,** 616-619.

Cordoba, E., Porta, H., Arroyo, A., Roman, C.S., Medina, L., Rodriguez-Concepcion, M., and Leon, P. (2011). Functional characterization of the three genes encoding 1-deoxy-D-xylulose 5-phosphate synthase in maize. J Exp Bot **62,** 2023-2038.

Corona, V., Aracri, B., Kosturkova, G., Bartley, G.E., Pitto, L., Giorgetti, L., Scolnik, P.A., and Giuliano, G. (1996). Regulation of a carotenoid biosynthesis gene promoter during plant development. Plant J **9,** 505-512.

Cui, L., Veeraraghavan, N., Richter, A., Wall, K., Jansen, R.K., Leebens-Mack, J., Makalowska, I., and dePamphilis, C.W. (2006). ChloroplastDB: the Chloroplast Genome Database. Nucleic Acids Res **34,** D692-696.

Cunningham, F.X., and Gantt, E. (1998). Genes and Enzymes of Carotenoid Biosynthesis in Plants. Annu Rev Plant Physiol Plant Mol Biol **49,** 557-583.

Cunningham, F.X., Jr., and Gantt, E. (2001). One ring or two? Determination of ring number in carotenoids by lycopene epsilon-cyclases. Proc Natl Acad Sci U S A **98,** 2905-2910.

Cunningham, F.X., Jr., and Gantt, E. (2007). A portfolio of plasmids for identification and analysis of carotenoid pathway enzymes: Adonis aestivalis as a case study. Photosynth Res **92,** 245-259.

Cunningham, F.X., Jr., Chamovitz, D., Misawa, N., Gantt, E., and Hirschberg, J. (1993). Cloning and functional expression in Escherichia coli of a cyanobacterial gene for lycopene cyclase, the enzyme that catalyzes the biosynthesis of beta-carotene. Febs Lett **328,** 130-138.

Cunningham, F.X., Jr., Pogson, B., Sun, Z., McDonald, K.A., DellaPenna, D., and Gantt, E. (1996). Functional analysis of the beta and epsilon lycopene cyclase enzymes of Arabidopsis reveals a mechanism for control of cyclic carotenoid formation. Plant Cell **8,** 1613-1626.

Cutler, S.R., Rodriguez, P.L., Finkelstein, R.R., and Abrams, S.R. (2010). Abscisic Acid: Emergence of a Core Signaling Network. Annual Review of Plant Biology, Vol 61 **61,** 651-679.

Cuttriss, A.J., Cazzonelli, C.I., Wurtzel, E.T., and Pogson, B.J. (2011). Carotenoids. In Biosynthesis of Vitamins in Plants, R.D. F. Rébeillé, ed (Amsterdam: Elsevier), pp. 1-36.

Cuttriss, A.J., Chubb, A.C., Alawady, A., Grimm, B., and Pogson, B.J. (2007). Regulation of lutein biosynthesis and prolamellar body formation in Arabidopsis. Funct Plant Biol **34,**

663-672.

Czechowski, T., Stitt, M., Altmann, T., Udvardi, M.K., and Scheible, W.R. (2005). Genome-wide identification and testing of superior reference genes for transcript normalization in Arabidopsis. Plant Physiol **139,** 5-17.

Dalal, M., Chinnusamy, V., and Bansal, K.C. (2010). Isolation and functional characterization of Lycopene beta-cyclase (CYC-B) promoter from Solanum habrochaites. Bmc Plant Biology **10**.

Dall'Osto, L., Cazzaniga, S., North, H., Marion-Poll, A., and Bassi, R. (2007). The Arabidopsis aba4-1 mutant reveals a specific function for neoxanthin in protection against photooxidative stress. Plant Cell **19,** 1048-1064.

Davuluri, G.R., van Tuinen, A., Fraser, P.D., Manfredonia, A., Newman, R., Burgess, D., Brummell, D.A., King, S.R., Palys, J., Uhlig, J., Bramley, P.M., Pennings, H.M., and Bowler, C. (2005). Fruit-specific RNAi-mediated suppression of DET1 enhances carotenoid and flavonoid content in tomatoes. Nat Biotechnol **23,** 890-895.

DellaPenna, D., and Pogson, B.J. (2006). Vitamin synthesis in plants: Tocopherols and carotenoids. Annu Rev Plant Biol **57,** 711-738.

Demmig-Adams, B., Gilmore, A.M., and Adams, W.W., 3rd. (1996). Carotenoids 3: in vivo function of carotenoids in higher plants. FASEB J **10,** 403-412.

Deng, X.W., Matsui, M., Wei, N., Wagner, D., Chu, A.M., Feldmann, K.A., and Quail, P.H. (1992). COP1, an Arabidopsis regulatory gene, encodes a protein with both a zinc-binding motif and a G beta homologous domain. Cell **71,** 791-801.

Deruere, J., Romer, S., d'Harlingue, A., Backhaus, R.A., Kuntz, M., and Camara, B. (1994). Fibril assembly and carotenoid overaccumulation in chromoplasts: a model for supramolecular lipoprotein structures. Plant Cell **6,** 119-133.

Diretto, G., Tavazza, R., Welsch, R., Pizzichini, D., Mourgues, F., Papacchioli, V., Beyer, P., and Giuliano, G. (2006). Metabolic engineering of potato tuber carotenoids through tuber-specific silencing of lycopene epsilon cyclase. BMC Plant Biol **6,** 13.

Dogbo, O., Laferriere, A., D'Harlingue, A., and Camara, B. (1988). Carotenoid biosynthesis: Isolation and characterization of a bifunctional enzyme catalyzing the synthesis of phytoene. Proc Natl Acad Sci U S A **85,** 7054-7058.

Dong, H., Deng, Y., Mu, J., Lu, Q., Wang, Y., Xu, Y., Chu, C., Chong, K., Lu, C., and Zuo, J. (2007). The Arabidopsis Spontaneous Cell Death1 gene, encoding a zeta-carotene desaturase essential for carotenoid biosynthesis, is involved in chloroplast development, photoprotection and retrograde signalling. Cell Res **17,** 458-470.

Dong, J., Tang, D., Gao, Z., Yu, R., Li, K., He, H., Terzaghi, W., Deng, X.W., and Chen, H. (2014). Arabidopsis DE-ETIOLATED1 represses photomorphogenesis by positively regulating phytochrome-interacting factors in the dark. Plant Cell **26,** 3630-3645.

Ducreux, L.J., Morris, W.L., Hedley, P.E., Shepherd, T., Davies, H.V., Millam, S., and Taylor, M.A. (2005). Metabolic engineering of high carotenoid potato tubers containing enhanced levels of beta-carotene and lutein. J Exp Bot **56,** 81-89.

Earley, K.W., Haag, J.R., Pontes, O., Opper, K., Juehne, T., Song, K., and Pikaard, C.S. (2006). Gateway-compatible vectors for plant functional genomics and proteomics. Plant J **45,** 616-629.

Eckardt, N.A. (2002). Tangerine dreams: cloning of carotenoid isomerase from Arabidopsis and tomato. Plant Cell **14,** 289-292.

Egea, I., Bian, W., Barsan, C., Jauneau, A., Pech, J.C., Latche, A., Li, Z., and Chervin, C. (2011). Chloroplast to chromoplast transition in tomato fruit: spectral confocal microscopy

analyses of carotenoids and chlorophylls in isolated plastids and time-lapse recording on intact live tissue. Ann Bot **108,** 291-297.

Eisenreich, W., Rohdich, F., and Bacher, A. (2001). Deoxyxylulose phosphate pathway to terpenoids. Trends Plant Sci **6,** 78-84.

Endo, T., Ishida, S., Ishikawa, N., and Sato, F. (2008). Chloroplastic NAD(P)H dehydrogenase complex and cyclic electron transport around photosystem I. Mol Cells **25,** 158-162.

Enfissi, E.M., Barneche, F., Ahmed, I., Lichtle, C., Gerrish, C., McQuinn, R.P., Giovannoni, J.J., Lopez-Juez, E., Bowler, C., Bramley, P.M., and Fraser, P.D. (2010). Integrative transcript and metabolite analysis of nutritionally enhanced DE-ETIOLATED1 downregulated tomato fruit. Plant Cell **22,** 1190-1215.

Eroglu, A., Hruszkewycz, D.P., dela Sena, C., Narayanasamy, S., Riedl, K.M., Kopec, R.E., Schwartz, S.J., Curley, R.W., Jr., and Harrison, E.H. (2012). Naturally occurring eccentric cleavage products of provitamin A beta-carotene function as antagonists of retinoic acid receptors. J Biol Chem **287,** 15886-15895.

Estavillo, G.M., Chan, K.X., Phua, S.Y., and Pogson, B.J. (2012). Reconsidering the nature and mode of action of metabolite retrograde signals from the chloroplast. Front Plant Sci **3,** 300.

Estevez, J.M., Cantero, A., Reindl, A., Reichler, S., and Leon, P. (2001). 1-deoxy-D-xylulose-5-phosphate synthase, a limiting enzyme for plastidic isoprenoid biosynthesis in plants. Journal of Biological Chemistry **276,** 22901-22909.

Estevez, J.M., Cantero, A., Romero, C., Kawaide, H., Jimenez, L.F., Kuzuyama, T., Seto, H., Kamiya, Y., and Leon, P. (2000). Analysis of the expression of CLA1, a gene that encodes the 1-deoxyxylulose 5-phosphate synthase of the 2-C-methyl-D-erythritol-4-phosphate pathway in Arabidopsis. Plant Physiology **124,** 95-103.

Fan, J., Hill, L., Crooks, C., Doerner, P., and Lamb, C. (2009). Abscisic acid has a key role in modulating diverse plant-pathogen interactions. Plant Physiol **150,** 1750-1761.

Fantini, E., Falcone, G., Frusciante, S., Giliberto, L., and Giuliano, G. (2013). Dissection of tomato lycopene biosynthesis through virus-induced gene silencing. Plant Physiol **163,** 986-998.

Farmer, E.E., and Mueller, M.J. (2013). ROS-mediated lipid peroxidation and RES-activated signaling. Annu Rev Plant Biol **64,** 429-450.

Farre, G., Sanahuja, G., Naqvi, S., Bai, C., Capell, T., Zhu, C.F., and Christou, P. (2010). Travel advice on the road to carotenoids in plants. Plant Science **179,** 28-48.

Ferro, M., Brugiere, S., Salvi, D., Seigneurin-Berny, D., Court, M., Moyet, L., Ramus, C., Miras, S., Mellal, M., Le Gall, S., Kieffer-Jaquinod, S., Bruley, C., Garin, J., Joyard, J., Masselon, C., and Rolland, N. (2010). AT_CHLORO, a Comprehensive Chloroplast Proteome Database with Subplastidial Localization and Curated Information on Envelope Proteins. Mol Cell Proteomics **9,** 1063-1084.

Fester, T., Hause, B., Schmidt, D., Halfmann, K., Schmidt, J., Wray, V., Hause, G., and Strack, D. (2002a). Occurrence and localization of apocarotenoids in arbuscular mycorrhizal plant roots. Plant & cell physiology **43,** 256-265.

Fester, T., Schmidt, D., Lohse, S., Walter, M.H., Giuliano, G., Bramley, P.M., Fraser, P.D., Hause, B., and Strack, D. (2002b). Stimulation of carotenoid metabolism in arbuscular mycorrhizal roots. Planta **216,** 148-154.

Fiedor, J., and Burda, K. (2014). Potential role of carotenoids as antioxidants in human health and disease. Nutrients **6,** 466-488.

Fitter, D.W., Martin, D.J., Copley, M.J., Scotland, R.W., and Langdale, J.A. (2002). GLK gene

pairs regulate chloroplast development in diverse plant species. Plant J **31,** 713-727.

Floss, D.S., Schliemann, W., Schmidt, J., Strack, D., and Walter, M.H. (2008). RNA interference-mediated repression of MtCCD1 in mycorrhizal roots of Medicago truncatula causes accumulation of C27 apocarotenoids, shedding light on the functional role of CCD1. Plant Physiol **148,** 1267-1282.

Forreiter, C., and Apel, K. (1993). Light-independent and light-dependent protochlorophyllide-reducing activities and two distinct NADPH-protochlorophyllide oxidoreductase polypeptides in mountain pine (Pinus mugo). Planta **190,** 536-545.

Franklin, K.A., Larner, V.S., and Whitelam, G.C. (2005). The signal transducing photoreceptors of plants. Int J Dev Biol **49,** 653-664.

Fraser, P.D., and Bramley, P.M. (2004). The biosynthesis and nutritional uses of carotenoids. Prog Lipid Res **43,** 228-265.

Fraser, P.D., Schuch, W., and Bramley, P.M. (2000). Phytoene synthase from tomato (Lycopersicon esculentum) chloroplasts - partial purification and biochemical properties. Planta **211,** 361-369.

Fraser, P.D., Truesdale, M.R., Bird, C.R., Schuch, W., and Bramley, P.M. (1994). Carotenoid Biosynthesis during Tomato Fruit Development (Evidence for Tissue-Specific Gene Expression). Plant Physiol **105,** 405-413.

Fraser, P.D., Kiano, J.W., Truesdale, M.R., Schuch, W., and Bramley, P.M. (1999). Phytoene synthase-2 enzyme activity in tomato does not contribute to carotenoid synthesis in ripening fruit. Plant Mol Biol **40,** 687-698.

Fraser, P.D., Enfissi, E.M., Halket, J.M., Truesdale, M.R., Yu, D., Gerrish, C., and Bramley, P.M. (2007). Manipulation of phytoene levels in tomato fruit: effects on isoprenoids, plastids, and intermediary metabolism. Plant Cell **19,** 3194-3211.

Fray, R.G., Wallace, A., Fraser, P.D., Valero, D., Hedden, P., Bramley, P.M., and Grierson, D. (1995). Constitutive Expression of a Fruit Phytoene Synthase Gene in Transgenic Tomatoes Causes Dwarfism by Redirecting Metabolites from the Gibberellin Pathway. Plant Journal **8,** 693-701.

Frusciante, S., Diretto, G., Bruno, M., Ferrante, P., Pietrella, M., Prado-Cabrero, A., Rubio-Moraga, A., Beyer, P., Gomez-Gomez, L., Al-Babili, S., and Giuliano, G. (2014). Novel carotenoid cleavage dioxygenase catalyzes the first dedicated step in saffron crocin biosynthesis. Proc Natl Acad Sci U S A **111,** 12246-12251.

Galpaz, N., Ronen, G., Khalfa, Z., Zamir, D., and Hirschberg, J. (2006). A chromoplast-specific carotenoid biosynthesis pathway is revealed by cloning of the tomato white-flower locus. Plant Cell **18,** 1947-1960.

Galpaz, N., Wang, Q., Menda, N., Zamir, D., and Hirschberg, J. (2008). Abscisic acid deficiency in the tomato mutant high-pigment 3 leading to increased plastid number and higher fruit lycopene content. Plant J **53,** 717-730.

Galpaz, N., Burger, Y., Lavee, T., Tzuri, G., Sherman, A., Melamed, T., Eshed, R., Meir, A., Portnoy, V., Bar, E., Shimoni-Shor, E., Feder, A., Saar, Y., Saar, U., Baumkoler, F., Lewinsohn, E., Schaffer, A.A., Katzir, N., and Tadmor, Y. (2013). Genetic and chemical characterization of an EMS induced mutation in Cucumis melo CRTISO gene. Archives of Biochemistry and Biophysics **539,** 117-125.

Garcia-Limones, C., Schnabele, K., Blanco-Portales, R., Luz Bellido, M., Caballero, J.L., Schwab, W., and Munoz-Blanco, J. (2008). Functional characterization of FaCCD1: a carotenoid cleavage dioxygenase from strawberry involved in lutein degradation during fruit ripening. J Agric Food Chem **56,** 9277-9285.

Ghassemian, M., Lutes, J., Tepperman, J.M., Chang, H.S., Zhu, T., Wang, X., Quail, P.H., and Lange, B.M. (2006). Integrative analysis of transcript and metabolite profiling data sets to evaluate the regulation of biochemical pathways during photomorphogenesis. Arch Biochem Biophys **448,** 45-59.

Gilmore, A.M. (1997). Mechanistic aspects of xanthophyll cycle-dependent photoprotection in higher plant chloroplasts and leaves. Physiol Plantarum **99,** 197-209.

Giorio, G., Stigliani, A.L., and D'Ambrosio, C. (2008). Phytoene synthase genes in tomato (Solanumlycopersicum L.) - new data on the structures, the deduced amino acid sequences and the expression patterns. FEBS J **275,** 527-535.

Giovannoni, J. (2001). Molecular Biology of Fruit Maturation and Ripening. Annu Rev Plant Physiol Plant Mol Biol **52,** 725-749.

Giuliano, G., and Diretto, G. (2007). Of chromoplasts and chaperones. Trends Plant Sci **12,** 529-531.

Giuliano, G., Bartley, G.E., and Scolnik, P.A. (1993). Regulation of carotenoid biosynthesis during tomato development. Plant Cell **5,** 379-387.

Giuliano, G., Giliberto, L., and Rosati, C. (2002). Carotenoid isomerase: a tale of light and isomers. Trends Plant Sci **7,** 427-429.

Giuliano, G., Tavazza, R., Diretto, G., Beyer, P., and Taylor, M.A. (2008). Metabolic engineering of carotenoid biosynthesis in plants. Trends Biotechnol **26,** 139-145.

Gonzalez-Jorge, S., Ha, S.H., Magallanes-Lundback, M., Gilliland, L.U., Zhou, A.L., Lipka, A.E., Nguyen, Y.N., Angelovici, R., Lin, H.N., Cepela, J., Little, H., Buell, C.R., Gore, M.A., and DellaPenna, D. (2013). CAROTENOID CLEAVAGE DIOXYGENASE4 Is a Negative Regulator of beta-Carotene Content in Arabidopsis Seeds. Plant Cell **25,** 4812-4826.

Gonzalez-Perez, S., Gutierrez, J., Garcia-Garcia, F., Osuna, D., Dopazo, J., Lorenzo, O., Revuelta, J.L., and Arellano, J.B. (2011). Early transcriptional defense responses in Arabidopsis cell suspension culture under high-light conditions. Plant Physiol **156,** 1439-1456.

Goodwin, T.W. (1983). Developments in carotenoid biochemistry over 40 years. The third Morton lecture. Biochem Soc Trans **11,** 473-483.

Green, B.R., and Durnford, D.G. (1996). The Chlorophyll-Carotenoid Proteins of Oxygenic Photosynthesis. Annu Rev Plant Physiol Plant Mol Biol **47,** 685-714.

Guevara-Garcia, A., San Roman, C., Arroyo, A., Cortes, M.E., de la Luz Gutierrez-Nava, M., and Leon, P. (2005). Characterization of the Arabidopsis clb6 mutant illustrates the importance of posttranscriptional regulation of the methyl-D-erythritol 4-phosphate pathway. Plant Cell **17,** 628-643.

Guyon-Debast, A., Lecureuil, A., Bonhomme, S., Guerche, P., and Gallois, J.L. (2010). A SNP associated with alternative splicing of RPT5b causes unequal redundancy between RPT5a and RPT5b among Arabidopsis thaliana natural variation. Bmc Plant Biology **10**.

Hager, A., and Holocher, K. (1994). Localization of the Xanthophyll-Cycle Enzyme Violaxanthin De-Epoxidase within the Thylakoid Lumen and Abolition of Its Mobility by a (Light-Dependent) Ph Decrease. Planta **192,** 581-589.

Han, S.H., Sakuraba, Y., Koh, H.J., and Paek, N.C. (2012). Leaf variegation in the rice zebra2 mutant is caused by photoperiodic accumulation of tetra-*cis*-lycopene and singlet oxygen. Mol Cells **33,** 87-97.

Harjes, C.E., Rocheford, T.R., Bai, L., Brutnell, T.P., Kandianis, C.B., Sowinski, S.G., Stapleton, A.E., Vallabhaneni, R., Williams, M., Wurtzel, E.T., Yan, J., and Buckler, E.S. (2008). Natural genetic variation in lycopene epsilon cyclase tapped for maize biofortification.

Science **319,** 330-333.

Harrison, P.J., and Bugg, T.D. (2014). Enzymology of the carotenoid cleavage dioxygenases: reaction mechanisms, inhibition and biochemical roles. Arch Biochem Biophys **544,** 105-111.

Hartwig, B., James, G.V., Konrad, K., Schneeberger, K., and Turck, F. (2012). Fast isogenic mapping-by-sequencing of ethyl methanesulfonate-induced mutant bulks. Plant Physiol **160,** 591-600.

Hausmann, A., and Sandmann, G. (2000). A single five-step desaturase is involved in the carotenoid biosynthesis pathway to beta-carotene and torulene in Neurospora crassa. Fungal Genet Biol **30,** 147-153.

Havaux, M. (1998). Carotenoids as membrane stabilizers in chloroplasts. Trends in Plant Science **3,** 147-151.

Havaux, M. (2014). Carotenoid oxidation products as stress signals in plants. Plant J **79,** 597-606.

Henikoff, S., and Henikoff, J.G. (1992). Amino acid substitution matrices from protein blocks. Proc Natl Acad Sci U S A **89,** 10915-10919.

Hieber, A.D., King, T.J., Morioka, S., Fukushima, L.H., Franke, A.A., and Bertram, J.S. (2000). Comparative effects of all-trans beta-carotene vs. 9-cis beta-carotene on carcinogen-induced neoplastic transformation and connexin 43 expression in murine 10T1/2 cells and on the differentiation of human keratinocytes. Nutr Cancer **37,** 234-244.

Hirschberg, J. (2001). Carotenoid biosynthesis in flowering plants. Curr Opin Plant Biol **4,** 210-218.

Holm, M., Ma, L.G., Qu, L.J., and Deng, X.W. (2002). Two interacting bZIP proteins are direct targets of COP1-mediated control of light-dependent gene expression in Arabidopsis. Genes Dev **16,** 1247-1259.

Hou, X., Rivers, J., Leon, P., McQuinn, R.P., and Pogson, B.J. (2016). Synthesis and Function of Apocarotenoid Signals in Plants. Trends Plant Sci **21,** 792-803.

Howitt, C.A., and Pogson, B.J. (2006). Carotenoid accumulation and function in seeds and non-green tissues. Plant Cell Environ **29,** 435-445.

Hsieh, M.H., Chang, C.Y., Hsu, S.J., and Chen, J.J. (2008). Chloroplast localization of methylerythritol 4-phosphate pathway enzymes and regulation of mitochondrial genes in ispD and ispE albino mutants in Arabidopsis. Plant Mol Biol **66,** 663-673.

Huang, F.C., Molnar, P., and Schwab, W. (2009). Cloning and functional characterization of carotenoid cleavage dioxygenase 4 genes. J Exp Bot **60,** 3011-3022.

Ibdah, M., Azulay, Y., Portnoy, V., Wasserman, B., Bar, E., Meir, A., Burger, Y., Hirschberg, J., Schaffer, A.A., Katzir, N., Tadmor, Y., and Lewinsohn, E. (2006). Functional characterization of CmCCD1, a carotenoid cleavage dioxygenase from melon. Phytochemistry **67,** 1579-1589.

Ikoma, Y., Komatsu, A., Kita, M., Ogawa, K., Omura, M., Yano, M., and Moriguchi, T. (2001). Expression of a phytoene synthase gene and characteristic carotenoid accumulation during citrus fruit development. Physiol Plantarum **111,** 232-238.

Ilg, A., Bruno, M., Beyer, P., and Al-Babili, S. (2014). Tomato carotenoid cleavage dioxygenases 1A and 1B: Relaxed double bond specificity leads to a plenitude of dialdehydes, mono-apocarotenoids and isoprenoid volatiles. FEBS Open Bio **4,** 584-593.

Ilg, A., Yu, Q., Schaub, P., Beyer, P., and Al-Babili, S. (2010). Overexpression of the rice carotenoid cleavage dioxygenase 1 gene in Golden Rice endosperm suggests apocarotenoids as substrates in planta. Planta **232,** 691-699.

Isaacson, T., Ronen, G., Zamir, D., and Hirschberg, J. (2002). Cloning of tangerine from tomato reveals a carotenoid isomerase essential for the production of beta-carotene and xanthophylls in plants. Plant Cell **14,** 333-342.

Isaacson, T., Ohad, I., Beyer, P., and Hirschberg, J. (2004). Analysis in vitro of the enzyme CRTISO establishes a poly-cis-carotenoid biosynthesis pathway in plants. Plant Physiol **136,** 4246-4255.

Ishikawa, M., Fujiwara, M., Sonoike, K., and Sato, N. (2009). Orthogenomics of photosynthetic organisms: bioinformatic and experimental analysis of chloroplast proteins of endosymbiont origin in Arabidopsis and their counterparts in Synechocystis. Plant & cell physiology **50,** 773-788.

Islam, M., Lyrene, S.A., Miller, E.M., Jr., and Porter, J.W. (1977). Dissociation of prelycopersene pyrophosphate synthetase from phytoene synthetase complex of tomato fruit plastids. J Biol Chem **252,** 1523-1525.

Jahns, P., Latowski, D., and Strzalka, K. (2009). Mechanism and regulation of the violaxanthin cycle: The role of antenna proteins and membrane lipids. Bba-Bioenergetics **1787,** 3-14.

Jefferies, R.A., and Mackerron, D.K.L. (1987). Effect of second growth on the quality of tubers as seed in the cultivar Record. Potato Res. **30,** 337-340.

Josse, E.M., and Halliday, K.J. (2008). Skotomorphogenesis: the dark side of light signalling. Curr Biol **18,** R1144-1146.

Josse, E.M., Simkin, A.J., Gaffe, J., Laboure, A.M., Kuntz, M., and Carol, P. (2000). A plastid terminal oxidase associated with carotenoid desaturation during chromoplast differentiation. Plant Physiol **123,** 1427-1436.

Joyard, J., Ferro, M., Masselon, C., Seigneurin-Berny, D., Salvi, D., Garin, J., and Rolland, N. (2009). Chloroplast Proteomics and the Compartmentation of Plastidial Isoprenoid Biosynthetic Pathways. Molecular Plant **2,** 1154-1180.

Kachanovsky, D.E., Filler, S., Isaacson, T., and Hirschberg, J. (2012). Epistasis in tomato color mutations involves regulation of phytoene synthase 1 expression by cis-carotenoids. P Natl Acad Sci USA **109,** 19021-19026.

Kato-Noguchi, H. (1996). An endogenous growth inhibitor, 3-hydroxy-β-ionone. III. Its longitudinal gradients in the first internode of Phaseolus vulgaris. Physiol Plantarum **98,** 241-244.

Kato, M., Matsumoto, H., Ikoma, Y., Okuda, H., and Yano, M. (2006). The role of carotenoid cleavage dioxygenases in the regulation of carotenoid profiles during maturation in citrus fruit. J Exp Bot **57,** 2153-2164.

Khan, A.A., Kamena, F., Timmer, M.S., and Stocker, B.L. (2013). Development of a benzophenone and alkyne functionalised trehalose probe to study trehalose dimycolate binding proteins. Org Biomol Chem **11,** 881-885.

Kilambi, H.V., Kumar, R., Sharma, R., and Sreelakshmi, Y. (2013). Chromoplast-specific carotenoid-associated protein appears to be important for enhanced accumulation of carotenoids in hp1 tomato fruits. Plant Physiol **161,** 2085-2101.

Kim, C., Meskauskiene, R., Zhang, S., Lee, K.P., Lakshmanan Ashok, M., Blajecka, K., Herrfurth, C., Feussner, I., and Apel, K. (2012). Chloroplasts of Arabidopsis are the source and a primary target of a plant-specific programmed cell death signaling pathway. Plant Cell **24,** 3026-3039.

Kim, J., and DellaPenna, D. (2006). Defining the primary route for lutein synthesis in plants: the role of Arabidopsis carotenoid beta-ring hydroxylase CYP97A3. Proc Natl Acad Sci

U S A **103,** 3474-3479.

Kim, J., Smith, J.J., Tian, L., and Dellapenna, D. (2009). The evolution and function of carotenoid hydroxylases in Arabidopsis. Plant & cell physiology **50,** 463-479.

Kim, J.E., Cheng, K.M., Craft, N.E., Hamberger, B., and Douglas, C.J. (2010). Over-expression of Arabidopsis thaliana carotenoid hydroxylases individually and in combination with a beta-carotene ketolase provides insight into in vivo functions. Phytochemistry **71,** 168-178.

Kim, Y., Schumaker, K.S., and Zhu, J.K. (2006). EMS mutagenesis of Arabidopsis. Methods Mol Biol **323,** 101-103.

Klassen, J.L. (2010). Phylogenetic and evolutionary patterns in microbial carotenoid biosynthesis are revealed by comparative genomics. PLoS One **5,** e11257.

Kleffmann, T., von Zychlinski, A., Russenberger, D., Hirsch-Hoffmann, M., Gehrig, P., Gruissem, W., and Baginsky, S. (2007). Proteome dynamics during plastid differentiation in rice. Plant Physiol **143,** 912-923.

Klingner, A., Hundeshagen, B., Kernebeck, H., and Bothe, H. (1995). Localization of the Yellow Pigment Formed in Roots of Gramineous Plants Colonized by Arbuscular Fungi. Protoplasma **185,** 50-57.

Kobayashi, K., and Masuda, T. (2016). Transcriptional Regulation of Tetrapyrrole Biosynthesis in Arabidopsis thaliana. Front Plant Sci **7,** 1811.

Kolossov, V.L., and Rebeiz, C.A. (2003). Chloroplast biogenesis 88. Protochlorophyllide b occurs in green but not in etiolated plants. J Biol Chem **278,** 49675-49678.

Kolotilin, I., Koltai, H., Tadmor, Y., Bar-Or, C., Reuveni, M., Meir, A., Nahon, S., Shlomo, H., Chen, L., and Levin, I. (2007). Transcriptional profiling of high pigment-2dg tomato mutant links early fruit plastid biogenesis with its overproduction of phytonutrients. Plant Physiol **145,** 389-401.

Krushkal, J., Pistilli, M., Ferrell, K.M., Souret, F.F., and Weathers, P.J. (2003). Computational analysis of the evolution of the structure and function of 1-deoxy-D-xylulose-5-phosphate synthase, a key regulator of the mevalonate-independent pathway in plants. Gene **313,** 127-138.

Kuhlbrandt, W. (1994). Structure and Function of the Plant Light-Harvesting Complex, Lhc-Ii. Curr Opin Struc Biol **4,** 519-528.

Kuntz, M., Romer, S., Suire, C., Hugueney, P., Weil, J.H., Schantz, R., and Camara, B. (1992). Identification of a Cdna for the Plastid-Located Geranylgeranyl Pyrophosphate Synthase from Capsicum-Annuum - Correlative Increase in Enzyme-Activity and Transcript Level during Fruit Ripening. Plant Journal **2,** 25-34.

Kwok, E.Y., and Hanson, M.R. (2004). Stromules and the dynamic nature of plastid morphology. J Microsc-Oxford **214,** 124-137.

Lam, H.M., Chiu, J., Hsieh, M.H., Meisel, L., Oliveira, I.C., Shin, M., and Coruzzi, G. (1998). Glutamate-receptor genes in plants. Nature **396,** 125-126.

Lange, B.M., and Ghassemian, M. (2003). Genome organization in Arabidopsis thaliana: a survey for genes involved in isoprenoid and chlorophyll metabolism. Plant Mol Biol **51,** 925-948.

Lange, B.M., and Ghassemian, M. (2005). Comprehensive post-genomic data analysis approaches integrating biochemical pathway maps. Phytochemistry **66,** 413-451.

Lao, Y.M., Xiao, L., Luo, L.X., and Jiang, J.G. (2014). Hypoosmotic expression of Dunaliella bardawil zeta-carotene desaturase is attributed to a hypoosmolarity-responsive element different from other key carotenogenic genes. Plant Physiol **165,** 359-372.

Lashbrooke, J.G., Young, P.R., Dockrall, S.J., Vasanth, K., and Vivier, M.A. (2013). Functional characterisation of three members of the Vitis vinifera L. carotenoid cleavage dioxygenase gene family. BMC Plant Biol **13,** 156.

Latari, K., Wust, F., Hubner, M., Schaub, P., Beisel, K.G., Matsubara, S., Beyer, P., and Welsch, R. (2015). Tissue-Specific Apocarotenoid Glycosylation Contributes to Carotenoid Homeostasis in Arabidopsis Leaves. Plant Physiol **168,** 1550-1562.

Lau, O.S., and Deng, X.W. (2012). The photomorphogenic repressors COP1 and DET1: 20 years later. Trends in Plant Science **17,** 584-593.

Lau, O.S., Huang, X., Charron, J.B., Lee, J.H., Li, G., and Deng, X.W. (2011). Interaction of Arabidopsis DET1 with CCA1 and LHY in Mediating Transcriptional Repression in the Plant Circadian Clock. Mol Cell **43,** 703-712.

Law, C.W., Chen, Y., Shi, W., and Smyth, G.K. (2014). voom: Precision weights unlock linear model analysis tools for RNA-seq read counts. Genome Biol **15,** R29.

Lee, J., He, K., Stolc, V., Lee, H., Figueroa, P., Gao, Y., Tongprasit, W., Zhao, H., Lee, I., and Deng, X.W. (2007). Analysis of transcription factor HY5 genomic binding sites revealed its hierarchical role in light regulation of development. Plant Cell **19,** 731-749.

Leenhardt, F., Lyan, B., Rock, E., Boussard, A., Potus, J., Chanliaud, E., and Remesy, C. (2006a). Wheat lipoxygenase activity induces greater loss of carotenoids than vitamin E during breadmaking. J Agr Food Chem **54,** 1710-1715.

Leenhardt, F., Lyan, B., Rock, E., Boussard, A., Potus, J., Chanliaud, E., and Remesy, C. (2006b). Genetic variability of carotenoid concentration, and lipoxygenase and peroxidase activities among cultivated wheat species and bread wheat varieties. Eur J Agron **25,** 170-176.

Leitner-Dagan, Y., Ovadis, M., Shklarman, E., Elad, Y., Rav David, D., and Vainstein, A. (2006a). Expression and functional analyses of the plastid lipid-associated protein CHRC suggest its role in chromoplastogenesis and stress. Plant Physiol **142,** 233-244.

Leitner-Dagan, Y., Ovadis, M., Zuker, A., Shklarman, E., Ohad, I., Tzfira, T., and Vainstein, A. (2006b). CHRD, a plant member of the evolutionarily conserved YjgF family, influences photosynthesis and chromoplastogenesis. Planta **225,** 89-102.

Leivar, P., and Quail, P.H. (2011). PIFs: pivotal components in a cellular signaling hub. Trends Plant Sci **16,** 19-28.

Leivar, P., and Monte, E. (2014). PIFs: systems integrators in plant development. Plant Cell **26,** 56-78.

Leivar, P., Tepperman, J.M., Monte, E., Calderon, R.H., Liu, T.L., and Quail, P.H. (2009). Definition of early transcriptional circuitry involved in light-induced reversal of PIF-imposed repression of photomorphogenesis in young Arabidopsis seedlings. Plant Cell **21,** 3535-3553.

Leivar, P., Monte, E., Oka, Y., Liu, T., Carle, C., Castillon, A., Huq, E., and Quail, P.H. (2008). Multiple Phytochrome-Interacting bHLH Transcription Factors Repress Premature Seedling Photomorphogenesis in Darkness. Curr Biol **18,** 1815-1823.

Lemaire, S.D., Guillon, B., Le Marechal, P., Keryer, E., Miginiac-Maslow, M., and Decottignies, P. (2004). New thioredoxin targets in the unicellular photosynthetic eukaryote Chlamydomonas reinhardtii. P Natl Acad Sci USA **101,** 7475-7480.

Leon, P., Arroyo, A., and Mackenzie, S. (1998). Nuclear Control of Plastid and Mitochondrial Development in Higher Plants. Annu Rev Plant Physiol Plant Mol Biol **49,** 453-480.

Levonen, A.L., Landar, A., Ramachandran, A., Ceaser, E.K., Dickinson, D.A., Zanoni, G., Morrow, J.D., and Darley-Usmar, V.M. (2004). Cellular mechanisms of redox cell

signalling: role of cysteine modification in controlling antioxidant defences in response to electrophilic lipid oxidation products. Biochem J **378,** 373-382.

Li, F., Murillo, C., and Wurtzel, E.T. (2007). Maize Y9 encodes a product essential for 15-cis-zeta-carotene isomerization. Plant Physiol **144,** 1181-1189.

Li, F., Vallabhaneni, R., and Wurtzel, E.T. (2008a). PSY3, a new member of the phytoene synthase gene family conserved in the Poaceae and regulator of abiotic stress-induced root carotenogenesis. Plant Physiol **146,** 1333-1345.

Li, F., Vallabhaneni, R., Yu, J., Rocheford, T., and Wurtzel, E.T. (2008b). The maize phytoene synthase gene family: overlapping roles for carotenogenesis in endosperm, photomorphogenesis, and thermal stress tolerance. Plant Physiol **147,** 1334-1346.

Li, H., and Durbin, R. (2009). Fast and accurate short read alignment with Burrows-Wheeler transform. Bioinformatics **25,** 1754-1760.

Li, H., Handsaker, B., Wysoker, A., Fennell, T., Ruan, J., Homer, N., Marth, G., Abecasis, G., and Durbin, R. (2009a). The Sequence Alignment/Map format and SAMtools. Bioinformatics **25,** 2078-2079.

Li, K., Gao, Z., He, H., Terzaghi, W., Fan, L.M., Deng, X.W., and Chen, H. (2015). Arabidopsis DET1 represses photomorphogenesis in part by negatively regulating DELLA protein abundance in darkness. Mol Plant **8,** 622-630.

Li, L., Paolillo, D.J., Parthasarathy, M.V., Dimuzio, E.M., and Garvin, D.F. (2001). A novel gene mutation that confers abnormal patterns of beta-carotene accumulation in cauliflower (Brassica oleracea var. botrytis). Plant J **26,** 59-67.

Li, L., Yang, Y., Xu, Q., Owsiany, K., Welsch, R., Chitchumroonchokchai, C., Lu, S., Van Eck, J., Deng, X.X., Failla, M., and Thannhauser, T.W. (2012). The Or gene enhances carotenoid accumulation and stability during post-harvest storage of potato tubers. Mol Plant **5,** 339-352.

Li, Z.R., Wakao, S., Fischer, B.B., and Niyogi, K.K. (2009b). Sensing and Responding to Excess Light. Annu Rev Plant Biol **60,** 239-260.

Liao, Y., Smyth, G.K., and Shi, W. (2014). featureCounts: an efficient general purpose program for assigning sequence reads to genomic features. Bioinformatics **30,** 923-930.

LibalWeksler, Y., Vishnevetsky, M., Ovadis, M., and Vainstein, A. (1997). Isolation and regulation of accumulation of a minor chromoplast-specific protein from cucumber corollas. Plant Physiology **113,** 59-63.

Lichtenthaler, H.K. (1968). Distribution and relative concentrations of lipophilic plastid quinones in green plants. Planta **81,** 140-152.

Lichtenthaler, H.K. (1999). The 1-Deoxy-D-Xylulose-5-Phosphate Pathway of Isoprenoid Biosynthesis in Plants. Annu Rev Plant Physiol Plant Mol Biol **50,** 47-65.

Lin, H., Wang, R., Qian, Q., Yan, M., Meng, X., Fu, Z., Yan, C., Jiang, B., Su, Z., Li, J., and Wang, Y. (2009). DWARF27, an iron-containing protein required for the biosynthesis of strigolactones, regulates rice tiller bud outgrowth. Plant Cell **21,** 1512-1525.

Lindgreen, S. (2012). AdapterRemoval: easy cleaning of next-generation sequencing reads. BMC Res Notes **5,** 337.

Linnewiel, K., Ernst, H., Caris-Veyrat, C., Ben-Dor, A., Kampf, A., Salman, H., Danilenko, M., Levy, J., and Sharoni, Y. (2009). Structure activity relationship of carotenoid derivatives in activation of the electrophile/antioxidant response element transcription system. Free Radic Biol Med **47,** 659-667.

Liu, J.R., Sun, X.R., Dong, H.W., Sun, C.H., Sun, W.G., Chen, B.Q., Song, Y.Q., and Yang, B.F. (2008). beta-Ionone suppresses mammary carcinogenesis, proliferative activity and

induces apoptosis in the mammary gland of the Sprague-Dawley rat. Int J Cancer **122,** 2689-2698.

Liu, Y., Roof, S., Ye, Z., Barry, C., van Tuinen, A., Vrebalov, J., Bowler, C., and Giovannoni, J. (2004). Manipulation of light signal transduction as a means of modifying fruit nutritional quality in tomato. Proc Natl Acad Sci U S A **101,** 9897-9902.

Lois, L.M., Rodriguez-Concepcion, M., Gallego, F., Campos, N., and Boronat, A. (2000). Carotenoid biosynthesis during tomato fruit development: regulatory role of 1-deoxy-D-xylulose 5-phosphate synthase. Plant J **22,** 503-513.

Lopez, A.B., Yang, Y., Thannhauser, T.W., and Li, L. (2008a). Phytoene desaturase is present in a large protein complex in the plastid membrane. Physiol Plantarum **133,** 190-198.

Lopez, A.B., Van Eck, J., Conlin, B.J., Paolillo, D.J., O'Neill, J., and Li, L. (2008b). Effect of the cauliflower Or transgene on carotenoid accumulation and chromoplast formation in transgenic potato tubers. J Exp Bot **59,** 213-223.

Lu, S., Van Eck, J., Zhou, X., Lopez, A.B., O'Halloran, D.M., Cosman, K.M., Conlin, B.J., Paolillo, D.J., Garvin, D.F., Vrebalov, J., Kochian, L.V., Kupper, H., Earle, E.D., Cao, J., and Li, L. (2006). The cauliflower Or gene encodes a DnaJ cysteine-rich domain-containing protein that mediates high levels of beta-carotene accumulation. Plant Cell **18,** 3594-3605.

Lundquist, P.K., Poliakov, A., Bhuiyan, N.H., Zybailov, B., Sun, Q., and van Wijk, K.J. (2012). The functional network of the Arabidopsis plastoglobule proteome based on quantitative proteomics and genome-wide coexpression analysis. Plant Physiol **158,** 1172-1192.

Lundquist, P.K., Poliakov, A., Giacomelli, L., Friso, G., Appel, M., McQuinn, R.P., Krasnoff, S.B., Rowland, E., Ponnala, L., Sun, Q., and van Wijk, K.J. (2013). Loss of Plastoglobule Kinases ABC1K1 and ABC1K3 Causes Conditional Degreening, Modified Prenyl-Lipids, and Recruitment of the Jasmonic Acid Pathway. Plant Cell **25,** 1818-1839.

Lv, F., Zhou, J., Zeng, L., and Xing, D. (2015). beta-cyclocitral upregulates salicylic acid signalling to enhance excess light acclimation in Arabidopsis. J Exp Bot **66,** 4719-4732.

Ma, G., Zhang, L., Matsuta, A., Matsutani, K., Yamawaki, K., Yahata, M., Wahyudi, A., Motohashi, R., and Kato, M. (2013). Enzymatic formation of beta-citraurin from beta-cryptoxanthin and Zeaxanthin by carotenoid cleavage dioxygenase4 in the flavedo of citrus fruit. Plant Physiol **163,** 682-695.

Maass, D., Arango, J., Wust, F., Beyer, P., and Welsch, R. (2009). Carotenoid crystal formation in Arabidopsis and carrot roots caused by increased phytoene synthase protein levels. PLoS One **4,** e6373.

Maier, W., Peipp, H., Schmidt, J., Wray, V., and Strack, D. (1995). Levels of a terpenoid glycoside (blumenin) and cell wall-bound phenolics in some cereal mycorrhizas. Plant Physiol **109,** 465-470.

Mandel, M.A., Feldmann, K.A., HerreraEstrella, L., RochaSosa, M., and Leon, P. (1996). CLA1, a novel gene required for chloroplast development, is highly conserved in evolution. Plant Journal **9,** 649-658.

Mann, V., Harker, M., Pecker, I., and Hirschberg, J. (2000). Metabolic engineering of astaxanthin production in tobacco flowers. Nature Biotechnology **18,** 888-892.

Maresca, J.A., Graham, J.E., and Bryant, D.A. (2008). The biochemical basis for structural diversity in the carotenoids of chlorophototrophic bacteria. Photosynth Res **97,** 121-140.

Marin, E., Nussaume, L., Quesada, A., Gonneau, M., Sotta, B., Hugueney, P., Frey, A., and

MarionPoll, A. (1996). Molecular identification of zeaxanthin epoxidase of Nicotiana plumbaginifolia, a gene involved in abscisic acid biosynthesis and corresponding to the ABA locus of Arabidopsis thaliana. Embo J **15,** 2331-2342.

Masamoto, K., Wada, H., Kaneko, T., and Takaichi, S. (2001). Identification of a gene required for cis-to-trans carotene isomerization in carotenogenesis of the cyanobacterium Synechocystis sp. PCC 6803. Plant & cell physiology **42,** 1398-1402.

Masuda, T., and Takamiya, K. (2004). Novel insights into the enzymology, regulation and physiological functions of light-dependent protochlorophyllide oxidoreductase in angiosperms. Photosynthesis Research **81,** 1-29.

Mathieu, S., Terrier, N., Procureur, J., Bigey, F., and Gunata, Z. (2005). A carotenoid cleavage dioxygenase from Vitis vinifera L.: functional characterization and expression during grape berry development in relation to C13-norisoprenoid accumulation. J Exp Bot **56,** 2721-2731.

Mathur, J., and Koncz, C. (1998). Callus culture and regeneration. In Arabidopsis protocols: Methods in molecular biology, J. Martinez-Zapater and J. Salinas, eds (Totowa: Humana Press, Inc), pp. 31-34.

Matthews, P.D., Luo, R., and Wurtzel, E.T. (2003). Maize phytoene desaturase and zeta-carotene desaturase catalyse a poly-Z desaturation pathway: implications for genetic engineering of carotenoid content among cereal crops. J Exp Bot **54,** 2215-2230.

Maudinas, B., Bucholtz, M.L., Papastephanou, C., Katiyar, S.S., Briedis, A.V., and Porter, J.W. (1977). The partial purification and properties of a phytoene synthesizing enzyme system. Arch Biochem Biophys **180,** 354-362.

McCarthy, D.J., Chen, Y., and Smyth, G.K. (2012). Differential expression analysis of multifactor RNA-Seq experiments with respect to biological variation. Nucleic Acids Research **40,** 4288-4297.

McCourt, P., and Desveaux, D. (2010). Plant chemical genetics. New Phytol **185,** 15-26.

McGraw, K.J., Crino, O.L., Medina-Jerez, W., and Nolan, P.M. (2006). Effect of dietary carotenoid supplementation on food intake and immune function in a songbird with no carotenoid coloration. Ethology **112,** 1209-1216.

McQuinn, R.P., Giovannoni, J.J., and Pogson, B.J. (2015). More than meets the eye: from carotenoid biosynthesis, to new insights into apocarotenoid signaling. Curr Opin Plant Biol **27,** 172-179.

Mehrshahi, P., Johnny, C., and DellaPenna, D. (2014). Redefining the metabolic continuity of chloroplasts and ER. Trends in Plant Science **19,** 501-507.

Meier, S., Tzfadia, O., Vallabhaneni, R., Gehring, C., and Wurtzel, E.T. (2011). A transcriptional analysis of carotenoid, chlorophyll and plastidial isoprenoid biosynthesis genes during development and osmotic stress responses in Arabidopsis thaliana. BMC Syst Biol **5,** 77.

Merzlyak, M.N., and Solovchenko, A.E. (2002). Photostability of pigments in ripening apple fruit: a possible photoprotective role of carotenoids during plant senescence. Plant Science **163,** 881-888.

Misawa, N., Truesdale, M.R., Sandmann, G., Fraser, P.D., Bird, C., Schuch, W., and Bramley, P.M. (1994). Expression of a tomato cDNA coding for phytoene synthase in Escherichia coli, phytoene formation in vivo and in vitro, and functional analysis of the various truncated gene products. J Biochem **116,** 980-985.

Moehs, C.P., Tian, L., Osteryoung, K.W., and Dellapenna, D. (2001). Analysis of carotenoid biosynthetic gene expression during marigold petal development. Plant Mol Biol **45,**

281-293.

Moran, N.A., and Jarvik, T. (2010). Lateral transfer of genes from fungi underlies carotenoid production in aphids. Science **328,** 624-627.

Nambara, E., and Marion-Poll, A. (2005). Abscisic acid biosynthesis and catabolism. Annu Rev Plant Biol **56,** 165-185.

Neta-Sharir, I., Isaacson, T., Lurie, S., and Weiss, D. (2005). Dual role for tomato heat shock protein 21: protecting photosystem II from oxidative stress and promoting color changes during fruit maturation. Plant Cell **17,** 1829-1838.

Nievelstein, V., Vandekerchove, J., Tadros, M.H., Lintig, J.V., Nitschke, W., and Beyer, P. (1995). Carotene desaturation is linked to a respiratory redox pathway in Narcissus pseudonarcissus chromoplast membranes. Involvement of a 23-kDa oxygen-evolving-complex-like protein. Eur J Biochem **233,** 864-872.

Nisar, N., Li, L., Lu, S., Khin, N.C., and Pogson, B.J. (2015). Carotenoid metabolism in plants. Mol Plant **8,** 68-82.

Nishimura, K., Kato, Y., and Sakamoto, W. (2016). Chloroplast Proteases: Updates on Proteolysis within and across Suborganellar Compartments. Plant Physiol **171,** 2280-2293.

Nishino, H., Tokuda, H., Murakoshi, M., Satomi, Y., Masuda, M., Onozuka, M., Yamaguchi, S., Takayasu, J., Tsuruta, J., Okuda, M., Khachik, F., Narisawa, T., Takasuka, N., and Yano, M. (2000). Cancer prevention by natural carotenoids. Biofactors **13,** 89-94.

Niyogi, K.K. (1999). Photoprotection revisited: Genetic and molecular approaches. Annu Rev Plant Phys **50,** 333-359.

Niyogi, K.K. (2000). Safety valves for photosynthesis. Current Opinion in Plant Biology **3,** 455-460.

Niyogi, K.K., Grossman, A.R., and Bjorkman, O. (1998). Arabidopsis mutants define a central role for the xanthophyll cycle in the regulation of photosynthetic energy conversion. Plant Cell **10,** 1121-1134.

Norris, S.R., Barrette, T.R., and DellaPenna, D. (1995). Genetic dissection of carotenoid synthesis in arabidopsis defines plastoquinone as an essential component of phytoene desaturation. Plant Cell **7,** 2139-2149.

North, H.M., De Almeida, A., Boutin, J.P., Frey, A., To, A., Botran, L., Sotta, B., and Marion-Poll, A. (2007). The Arabidopsis ABA-deficient mutant aba4 demonstrates that the major route for stress-induced ABA accumulation is via neoxanthin isomers. Plant Journal **50,** 810-824.

Ohmiya, A., Kishimoto, S., Aida, R., Yoshioka, S., and Sumitomo, K. (2006). Carotenoid cleavage dioxygenase (CmCCD4a) contributes to white color formation in chrysanthemum petals. Plant Physiol **142,** 1193-1201.

Okada, K., Saito, T., Nakagawa, T., Kawamukai, M., and Kamiya, Y. (2000). Five geranylgeranyl diphosphate synthases expressed in different organs are localized into three subcellular compartments in Arabidopsis. Plant Physiology **122,** 1045-1056.

Ossowski, S., Schneeberger, K., Clark, R.M., Lanz, C., Warthmann, N., and Weigel, D. (2008). Sequencing of natural strains of Arabidopsis thaliana with short reads. Genome Research **18,** 2024-2033.

Osterlund, M.T., Wei, N., and Deng, X.W. (2000a). The roles of photoreceptor systems and the COP1-targeted destabilization of HY5 in light control of arabidopsis seedling development. Plant Physiology **124,** 1520-1524.

Osterlund, M.T., Hardtke, C.S., Wei, N., and Deng, X.W. (2000b). Targeted destabilization of

HY5 during light-regulated development of Arabidopsis. Nature **405,** 462-466.

Ostersetzer, O., and Adam, Z. (1997). Light-stimulated degradation of an unassembled Rieske FeS protein by a thylakoid-bound protease: the possible role of the FtsH protease. Plant Cell **9,** 957-965.

Paddock, T., Lima, D., Mason, M.E., Apel, K., and Armstrong, G.A. (2012). Arabidopsis light-dependent protochlorophyllide oxidoreductase A (PORA) is essential for normal plant growth and development. Plant Mol Biol **78,** 447-460.

Paddock, T.N., Mason, M.E., Lima, D.F., and Armstrong, G.A. (2010). Arabidopsis protochlorophyllide oxidoreductase A (PORA) restores bulk chlorophyll synthesis and normal development to a porB porC double mutant. Plant Mol Biol **72,** 445-457.

Paik, I., Yang, S., and Choi, G. (2012). Phytochrome regulates translation of mRNA in the cytosol. P Natl Acad Sci USA **109,** 1335-1340.

Pandit, J., Danley, D.E., Schulte, G.K., Mazzalupo, S., Pauly, T.A., Hayward, C.M., Hamanaka, E.S., Thompson, J.F., and Harwood, H.J., Jr. (2000). Crystal structure of human squalene synthase. A key enzyme in cholesterol biosynthesis. J Biol Chem **275,** 30610-30617.

Paolillo, D.J., Garvin, D.F., and Parthasarathy, M.V. (2004). The chromoplasts of Or mutants of cauliflower (Brassica oleracea L. var. botrytis). Protoplasma **224,** 245-253.

Park, H., Kreunen, S.S., Cuttriss, A.J., DellaPenna, D., and Pogson, B.J. (2002). Identification of the carotenoid isomerase provides insight into carotenoid biosynthesis, prolamellar body formation, and photomorphogenesis. Plant Cell **14,** 321-332.

Passardi, F., Dobias, J., Valerio, L., Guimil, S., Penel, C., and Dunand, C. (2007). Morphological and physiological traits of three major Arabidopsis thaliana accessions. J Plant Physiol **164,** 980-992.

Pecker, I., Gabbay, R., Cunningham, F.X., Jr., and Hirschberg, J. (1996). Cloning and characterization of the cDNA for lycopene beta-cyclase from tomato reveals decrease in its expression during fruit ripening. Plant Mol Biol **30,** 807-819.

Pecker, I., Chamovitz, D., Linden, H., Sandmann, G., and Hirschberg, J. (1992). A single polypeptide catalyzing the conversion of phytoene to zeta-carotene is transcriptionally regulated during tomato fruit ripening. Proc Natl Acad Sci U S A **89,** 4962-4966.

Pepper, A., Delaney, T., Washburn, T., Poole, D., and Chory, J. (1994). DET1, a negative regulator of light-mediated development and gene expression in arabidopsis, encodes a novel nuclear-localized protein. Cell **78,** 109-116.

Pfaffl, M.W. (2001). A new mathematical model for relative quantification in real-time RT-PCR. Nucleic Acids Res **29,** e45.

Phillip, D., and Young, A.J. (1995). Occurrence of the carotenoid lactucaxanthin in higher plant LHC II. Photosynth Res **43,** 273-282.

Phillips, M.A., Leon, P., Boronat, A., and Rodriguez-Concepcion, M. (2008). The plastidial MEP pathway: unified nomenclature and resources. Trends in Plant Science **13,** 619-623.

Pizarro, L., and Stange, C. (2009). Light-dependent regulation of carotenoid biosynthesis in plants. Cienc Investig Agrar **36,** 143-161.

Pogson, B., McDonald, K.A., Truong, M., Britton, G., and DellaPenna, D. (1996). Arabidopsis carotenoid mutants demonstrate that lutein is not essential for photosynthesis in higher plants. Plant Cell **8,** 1627-1639.

Pogson, B.J., and Rissler, H.M. (2000). Genetic manipulation of carotenoid biosynthesis and photoprotection. Philos Trans R Soc Lond B Biol Sci **355,** 1395-1403.

Pogson, B.J., and Albrecht, V. (2011). Genetic dissection of chloroplast biogenesis and

development: an overview. Plant Physiol **155,** 1545-1551.

Pogson, B.J., Niyogi, K.K., Bjorkman, O., and DellaPenna, D. (1998). Altered xanthophyll compositions adversely affect chlorophyll accumulation and nonphotochemical quenching in Arabidopsis mutants. P Natl Acad Sci USA **95,** 13324-13329.

Pogson, B.J., Woo, N.S., Forster, B., and Small, I.D. (2008). Plastid signalling to the nucleus and beyond. Trends in Plant Science **13,** 602-609.

Porra, R.J. (2002). The chequered history of the development and use of simultaneous equations for the accurate determination of chlorophylls a and b. Photosynth Res **73,** 149-156.

Porra, R.J., Thompson, W.A., and Kriedemann, P.E. (1989). Determination of accurate extinction coefficients and simultaneous equations for assaying chlorophylls a and b extracted with four different solvents: verification of the concentration of chlorophyll standards by atomic absorption spectroscopy. Biochim. Biophys. Acta **975,** 384-394.

Prandi, C., Rosso, H., Lace, B., Occhiato, E.G., Oppedisano, A., Tabasso, S., Alberto, G., and Blangetti, M. (2013). Strigolactone analogs as molecular probes in chasing the (SLs) receptor/s: design and synthesis of fluorescent labeled molecules. Mol Plant **6,** 113-127.

Price, M.B., Jelesko, J., and Okumoto, S. (2012). Glutamate receptor homologs in plants: functions and evolutionary origins. Front Plant Sci **3,** 235.

Qin, G., Gu, H., Ma, L., Peng, Y., Deng, X.W., Chen, Z., and Qu, L.J. (2007). Disruption of phytoene desaturase gene results in albino and dwarf phenotypes in Arabidopsis by impairing chlorophyll, carotenoid, and gibberellin biosynthesis. Cell Res **17,** 471-482.

Querol, J., Campos, N., Imperial, S., Boronat, A., and Rodriguez-Concepcion, M. (2002). Functional analysis of the Arabidopsis thaliana GCPE protein involved in plastid isoprenoid biosynthesis. Febs Lett **514,** 343-346.

Quinlan, R.F., Shumskaya, M., Bradbury, L.M., Beltran, J., Ma, C., Kennelly, E.J., and Wurtzel, E.T. (2012). Synergistic interactions between carotene ring hydroxylases drive lutein formation in plant carotenoid biosynthesis. Plant Physiol **160,** 204-214.

Raisig, A., and Sandmann, G. (1999). 4,4'-diapophytoene desaturase: catalytic properties of an enzyme from the C(30) carotenoid pathway of Staphylococcus aureus. J Bacteriol **181,** 6184-6187.

Ramel, F., Mialoundama, A.S., and Havaux, M. (2013a). Nonenzymic carotenoid oxidation and photooxidative stress signalling in plants. J Exp Bot **64,** 799-805.

Ramel, F., Birtic, S., Ginies, C., Soubigou-Taconnat, L., Triantaphylides, C., and Havaux, M. (2012). Carotenoid oxidation products are stress signals that mediate gene responses to singlet oxygen in plants. Proc Natl Acad Sci U S A **109,** 5535-5540.

Ramel, F., Ksas, B., Akkari, E., Mialoundama, A.S., Monnet, F., Krieger-Liszkay, A., Ravanat, J.L., Mueller, M.J., Bouvier, F., and Havaux, M. (2013b). Light-induced acclimation of the Arabidopsis chlorina1 mutant to singlet oxygen. Plant Cell **25,** 1445-1462.

Rebeiz, C.A. (2002). Analysis of Intermediates and End Products of the Chlorophyll Biosynthetic Pathway. In Heme Chlorophyll and Bilins, Methods and Protocols, A. Smith and M. Witty, eds (Totowa NJ: Human Press), pp. 111-155.

Reinbothe, S., Reinbothe, C., Lebedev, N., and Apel, K. (1996). PORA and PORB, two light-dependent protochlorophyllide-reducing enzymes of angiosperm chlorophyll biosynthesis. Plant Cell **8,** 763-769.

Richly, E., and Leister, D. (2004). An improved prediction of chloroplast proteins reveals diversities and commonalities in the chloroplast proteomes of Arabidopsis and rice.

Gene **329,** 11-16.

Robinson, M.D., and Smyth, G.K. (2007). Moderated statistical tests for assessing differences in tag abundance. Bioinformatics **23,** 2881-2887.

Robinson, M.D., and Smyth, G.K. (2008). Small-sample estimation of negative binomial dispersion, with applications to SAGE data. Biostatistics **9,** 321-332.

Robinson, M.D., and Oshlack, A. (2010). A scaling normalization method for differential expression analysis of RNA-seq data. Genome Biol **11,** R25.

Robinson, M.D., McCarthy, D.J., and Smyth, G.K. (2010). edgeR: a Bioconductor package for differential expression analysis of digital gene expression data. Bioinformatics **26,** 139-140.

Rodriguez-Concepcion, M. (2010). Supply of precursors for carotenoid biosynthesis in plants. Arch Biochem Biophys **504,** 118-122.

Rodriguez-Concepcion, M., and Boronat, A. (2002). Elucidation of the methylerythritol phosphate pathway for isoprenoid biosynthesis in bacteria and plastids. A metabolic milestone achieved through genomics. Plant Physiol **130,** 1079-1089.

Rodriguez-Concepcion, M., Ahumada, I., Diez-Juez, E., Sauret-Gueto, S., Lois, L.M., Gallego, F., Carretero-Paulet, L., Campos, N., and Boronat, A. (2001). 1-Deoxy-D-xylulose 5-phosphate reductoisomerase and plastid isoprenoid biosynthesis during tomato fruit ripening. Plant Journal **27,** 213-222.

Rodriguez-Villalon, A., Gas, E., and Rodriguez-Concepcion, M. (2009a). Phytoene synthase activity controls the biosynthesis of carotenoids and the supply of their metabolic precursors in dark-grown Arabidopsis seedlings. Plant J **60,** 424-435.

Rodriguez-Villalon, A., Gas, E., and Rodriguez-Concepcion, M. (2009b). Colors in the dark: a model for the regulation of carotenoid biosynthesis in etioplasts. Plant Signal Behav **4,** 965-967.

Romer, S., and Fraser, P.D. (2005). Recent advances in carotenoid biosynthesis, regulation and manipulation. Planta **221,** 305-308.

Romer, S., Hugueney, P., Bouvier, F., Camara, B., and Kuntz, M. (1993). Expression of the genes encoding the early carotenoid biosynthetic enzymes in Capsicum annuum. Biochem Biophys Res Commun **196,** 1414-1421.

Ronen, G., Cohen, M., Zamir, D., and Hirschberg, J. (1999). Regulation of carotenoid biosynthesis during tomato fruit development: expression of the gene for lycopene epsilon-cyclase is down-regulated during ripening and is elevated in the mutant Delta. Plant J **17,** 341-351.

Ronen, G., Carmel-Goren, L., Zamir, D., and Hirschberg, J. (2000). An alternative pathway to beta -carotene formation in plant chromoplasts discovered by map-based cloning of beta and old-gold color mutations in tomato. Proc Natl Acad Sci U S A **97,** 11102-11107.

Rubio-Moraga, A., Rambla, J.L., Fernandez-de-Carmen, A., Trapero-Mozos, A., Ahrazem, O., Orzaez, D., Granell, A., and Gomez-Gomez, L. (2014). New target carotenoids for CCD4 enzymes are revealed with the characterization of a novel stress-induced carotenoid cleavage dioxygenase gene from Crocus sativus. Plant Mol Biol **86,** 555-569.

Rubio, A., Rambla, J.L., Santaella, M., Gomez, M.D., Orzaez, D., Granell, A., and Gomez-Gomez, L. (2008). Cytosolic and plastoglobule-targeted carotenoid dioxygenases from Crocus sativus are both involved in beta-ionone release. J Biol Chem **283,** 24816-24825.

Ruckle, M.E., DeMarco, S.M., and Larkin, R.M. (2007). Plastid signals remodel light signaling networks and are essential for efficient chloroplast biogenesis in Arabidopsis. Plant Cell **19,** 3944-3960.

Rudowska, L., Gieczewska, K., Mazur, R., Garstka, M., and Mostowska, A. (2012). Chloroplast biogenesis - correlation between structure and function. Biochim Biophys Acta **1817,** 1380-1387.

Ruiz-Sola, M.A., and Rodriguez-Concepcion, M. (2012). Carotenoid biosynthesis in Arabidopsis: a colorful pathway. Arabidopsis Book **10,** e0158.

Ruiz-Sola, M.A., Coman, D., Beck, G., Barja, M.V., Colinas, M., Graf, A., Welsch, R., Rutimann, P., Buhlmann, P., Bigler, L., Gruissem, W., Rodriguez-Concepcion, M., and Vranova, E. (2016). Arabidopsis GERANYLGERANYL DIPHOSPHATE SYNTHASE 11 is a hub isozyme required for the production of most photosynthesis-related isoprenoids. New Phytol **209,** 252-264.

Saijo, Y., Sullivan, J.A., Wang, H., Yang, J., Shen, Y., Rubio, V., Ma, L., Hoecker, U., and Deng, X.W. (2003). The COP1-SPA1 interaction defines a critical step in phytochrome A-mediated regulation of HY5 activity. Genes Dev **17,** 2642-2647.

Sakamoto, W., Miyagishima, S.Y., and Jarvis, P. (2008). Chloroplast biogenesis: control of plastid development, protein import, division and inheritance. Arabidopsis Book **6,** e0110.

Sakamoto, W., Zaltsman, A., Adam, Z., and Takahashi, Y. (2003). Coordinated regulation and complex formation of yellow variegated1 and yellow variegated2, chloroplastic FtsH metalloproteases involved in the repair cycle of photosystem II in Arabidopsis thylakoid membranes. Plant Cell **15,** 2843-2855.

Sandmann, G. (2009). Evolution of carotene desaturation: the complication of a simple pathway. Arch Biochem Biophys **483,** 169-174.

Sandmann, G., Romer, S., and Fraser, P.D. (2006). Understanding carotenoid metabolism as a necessity for genetic engineering of crop plants. Metab Eng **8,** 291-302.

Schaub, P., Al-Babili, S., Drake, R., and Beyer, P. (2005). Why is golden rice golden (yellow) instead of red? Plant Physiol **138,** 441-450.

Schaub, P., Yu, Q.J., Gemmecker, S., Poussin-Courmontagne, P., Mailliot, J., McEwen, A.G., Ghisla, S., Al-Babili, S., Cavarelli, J., and Beyer, P. (2012). On the Structure and Function of the Phytoene Desaturase CRTI from Pantoea ananatis, a Membrane-Peripheral and FAD-Dependent Oxidase/Isomerase. PLoS One **7**.

Schermelleh, L., Heintzmann, R., and Leonhardt, H. (2010). A guide to super-resolution fluorescence microscopy. Journal of Cell Biology **190,** 165-175.

Schledz, M., al-Babili, S., von Lintig, J., Haubruck, H., Rabbani, S., Kleinig, H., and Beyer, P. (1996). Phytoene synthase from Narcissus pseudonarcissus: functional expression, galactolipid requirement, topological distribution in chromoplasts and induction during flowering. Plant J **10,** 781-792.

Schliemann, W., Schmidt, J., Nimtz, M., Wray, V., Fester, T., and Strack, D. (2006). Accumulation of apocarotenoids in mycorrhizal roots of Ornithogalum umbellatum. Phytochemistry **67,** 1196-1205.

Schmidt-Dannert, C., Umeno, D., and Arnold, F.H. (2000). Molecular breeding of carotenoid biosynthetic pathways. Nat Biotechnol **18,** 750-753.

Schneeberger, K., Ossowski, S., Lanz, C., Juul, T., Petersen, A.H., Nielsen, K.L., Jorgensen, J.E., Weigel, D., and Andersen, S.U. (2009). SHOREmap: simultaneous mapping and mutation identification by deep sequencing. Nat Methods **6,** 550-551.

Schneider, C.A., Rasband, W.S., and Eliceiri, K.W. (2012). NIH Image to ImageJ: 25 years of image analysis. Nat Methods **9,** 671-675.

Schroeder, D.F., Gahrtz, M., Maxwell, B.B., Cook, R.K., Kan, J.M., Alonso, J.M., Ecker, J.R.,

and Chory, J. (2002). De-etiolated 1 and damaged DNA binding protein 1 interact to regulate Arabidopsis photomorphogenesis. Curr Biol **12,** 1462-1472.

Schwartz, S.H., Qin, X., and Loewen, M.C. (2004). The biochemical characterization of two carotenoid cleavage enzymes from Arabidopsis indicates that a carotenoid-derived compound inhibits lateral branching. J Biol Chem **279,** 46940-46945.

Schwartz, S.H., Tan, B.C., McCarty, D.R., Welch, W., and Zeevaart, J.A. (2003). Substrate specificity and kinetics for VP14, a carotenoid cleavage dioxygenase in the ABA biosynthetic pathway. Biochim Biophys Acta **1619,** 9-14.

Seo, H.S., Yang, J.Y., Ishikawa, M., Bolle, C., Ballesteros, M.L., and Chua, N.H. (2003). LAF1 ubiquitination by COP1 controls photomorphogenesis and is stimulated by SPA1. Nature **423,** 995-999.

Seo, M., and Koshiba, T. (2002). Complex regulation of ABA biosynthesis in plants. Trends in Plant Science **7,** 41-48.

Sergeant, M.J., Li, J.J., Fox, C., Brookbank, N., Rea, D., Bugg, T.D., and Thompson, A.J. (2009). Selective inhibition of carotenoid cleavage dioxygenases: phenotypic effects on shoot branching. J Biol Chem **284,** 5257-5264.

Seto, Y., and Yamaguchi, S. (2014). Strigolactone biosynthesis and perception. Curr Opin Plant Biol **21C,** 1-6.

Shahbazi, M., Gilbert, M., Laboure, A.M., and Kuntz, M. (2007). Dual role of the plastid terminal oxidase in tomato. Plant Physiology **145,** 691-702.

Sharoni, Y., Linnewiel-Hermoni, K., Khanin, M., Salman, H., Veprik, A., Danilenko, M., and Levy, J. (2012). Carotenoids and apocarotenoids in cellular signaling related to cancer: a review. Mol Nutr Food Res **56,** 259-269.

Shen, H., Zhu, L., Castillon, A., Majee, M., Downie, B., and Huq, E. (2008). Light-induced phosphorylation and degradation of the negative regulator PHYTOCHROME-INTERACTING FACTOR1 from Arabidopsis depend upon its direct physical interactions with photoactivated phytochromes. Plant Cell **20,** 1586-1602.

Shi, H., Wang, X., Mo, X., Tang, C., Zhong, S., and Deng, X.W. (2015). Arabidopsis DET1 degrades HFR1 but stabilizes PIF1 to precisely regulate seed germination. Proc Natl Acad Sci U S A **112,** 3817-3822.

Shin, J., Kim, K., Kang, H., Zulfugarov, I.S., Bae, G., Lee, C.H., Lee, D., and Choi, G. (2009). Phytochromes promote seedling light responses by inhibiting four negatively-acting phytochrome-interacting factors. Proc Natl Acad Sci U S A **106,** 7660-7665.

Shumbe, L., Bott, R., and Havaux, M. (2014). Dihydroactinidiolide, a high light-induced beta-carotene derivative that can regulate gene expression and photoacclimation in Arabidopsis. Mol Plant **7,** 1248-1251.

Shumskaya, M., and Wurtzel, E.T. (2013). The carotenoid biosynthetic pathway: thinking in all dimensions. Plant Sci **208,** 58-63.

Shumskaya, M., Bradbury, L.M., Monaco, R.R., and Wurtzel, E.T. (2012). Plastid localization of the key carotenoid enzyme phytoene synthase is altered by isozyme, allelic variation, and activity. Plant Cell **24,** 3725-3741.

Simkin, A.J., Breitenbach, J., Kuntz, M., and Sandmann, G. (2000). In vitro and in situ inhibition of carotenoid biosynthesis in Capsicum annuum by bleaching herbicides. J Agric Food Chem **48,** 4676-4680.

Simkin, A.J., Zhu, C., Kuntz, M., and Sandmann, G. (2003). Light-dark regulation of carotenoid biosynthesis in pepper (Capsicum annuum) leaves. J Plant Physiol **160,** 439-443.

Simkin, A.J., Schwartz, S.H., Auldridge, M., Taylor, M.G., and Klee, H.J. (2004a). The tomato

carotenoid cleavage dioxygenase 1 genes contribute to the formation of the flavor volatiles beta-ionone, pseudoionone, and geranylacetone. Plant J **40,** 882-892.

Simkin, A.J., Moreau, H., Kuntz, M., Pagny, G., Lin, C., Tanksley, S., and McCarthy, J. (2008). An investigation of carotenoid biosynthesis in Coffea canephora and Coffea arabica. J Plant Physiol **165,** 1087-1106.

Simkin, A.J., Underwood, B.A., Auldridge, M., Loucas, H.M., Shibuya, K., Schmelz, E., Clark, D.G., and Klee, H.J. (2004b). Circadian regulation of the PhCCD1 carotenoid cleavage dioxygenase controls emission of beta-ionone, a fragrance volatile of petunia flowers. Plant Physiol **136,** 3504-3514.

Smirra, I., Halevy, A.H., and Vainstein, A. (1993). Isolation and Characterization of a Chromoplast-Specific Carotenoid-Associated Protein from Cucumis sativus Corollas. Plant Physiol **102,** 491-496.

Smyth, G.K. (2004). Linear models and empirical bayes methods for assessing differential expression in microarray experiments. Stat Appl Genet Mol Biol **3,** Article3.

Smyth, G.K. (2005). limma: Linear Models for Microarray Data. In Bioinformatics and Computational Biology Solutions Using R and Bioconductor, R. Gentleman, V.J. Carey, W. Huber, R.A. Irizarry, and S. Dudoit, eds (New York: Springer), pp. 397-420.

Snodderly, D.M. (1995). Evidence for protection against age-related macular degeneration by carotenoids and antioxidant vitamins. Am J Clin Nutr **62,** 1448S-1461S.

Solymosi, K., and Schoefs, B. (2010). Etioplast and etio-chloroplast formation under natural conditions: the dark side of chlorophyll biosynthesis in angiosperms. Photosynth Res **105,** 143-166.

Sperling, U., Franck, F., van Cleve, B., Frick, G., Apel, K., and Armstrong, G.A. (1998). Etioplast differentiation in arabidopsis: both PORA and PORB restore the prolamellar body and photoactive protochlorophyllide-F655 to the cop1 photomorphogenic mutant. Plant Cell **10,** 283-296.

Stephenson, P.G., Fankhauser, C., and Terry, M.J. (2009). PIF3 is a repressor of chloroplast development. P Natl Acad Sci USA **106,** 7654-7659.

Sullivan, J.A., and Deng, X.W. (2003). From seed to seed: the role of photoreceptors in Arabidopsis development. Dev Biol **260,** 289-297.

Sun, Z., Gantt, E., and Cunningham, F.X., Jr. (1996). Cloning and functional analysis of the beta-carotene hydroxylase of Arabidopsis thaliana. J Biol Chem **271,** 24349-24352.

Sundqvist, C., and Dahlin, C. (1997). With chlorophyll pigments from prolamellar bodies to light-harvesting complexes. Physiol Plantarum **100,** 748-759.

Takaichi, S., and Mochimaru, M. (2007). Carotenoids and carotenogenesis in cyanobacteria: unique ketocarotenoids and carotenoid glycosides. Cell Mol Life Sci **64,** 2607-2619.

Tan, B.C., Joseph, L.M., Deng, W.T., Liu, L., Li, Q.B., Cline, K., and McCarty, D.R. (2003). Molecular characterization of the Arabidopsis 9-cis epoxycarotenoid dioxygenase gene family. Plant J **35,** 44-56.

Tao, L., Schenzle, A., Odom, J.M., and Cheng, Q. (2005). Novel carotenoid oxidase involved in biosynthesis of 4,4'-diapolycopene dialdehyde. Appl Environ Microbiol **71,** 3294-3301.

Teardo, E., Formentin, E., Segalla, A., Giacometti, G.M., Marin, O., Zanetti, M., Lo Schiavo, F., Zoratti, M., and Szabo, I. (2011). Dual localization of plant glutamate receptor AtGLR3.4 to plastids and plasmamembrane. Biochim Biophys Acta **1807,** 359-367.

Tepperman, J.M., Zhu, T., Chang, H.S., Wang, X., and Quail, P.H. (2001). Multiple transcription-factor genes are early targets of phytochrome A signaling. Proc Natl Acad Sci U S A **98,** 9437-9442.

Tian, L., and DellaPenna, D. (2001). Characterization of a second carotenoid beta-hydroxylase gene from Arabidopsis and its relationship to the LUT1 locus. Plant Mol Biol **47,** 379-388.

Tian, L., and DellaPenna, D. (2004). Progress in understanding the origin and functions of carotenoid hydroxylases in plants. Arch Biochem Biophys **430,** 22-29.

Tian, L., Magallanes-Lundback, M., Musetti, V., and DellaPenna, D. (2003). Functional analysis of beta- and epsilon-ring carotenoid hydroxylases in Arabidopsis. Plant Cell **15,** 1320-1332.

Tian, L., Musetti, V., Kim, J., Magallanes-Lundback, M., and DellaPenna, D. (2004). The Arabidopsis LUT1 locus encodes a member of the cytochrome p450 family that is required for carotenoid epsilon-ring hydroxylation activity. Proc Natl Acad Sci U S A **101,** 402-407.

Toledo-Ortiz, G., Huq, E., and Rodriguez-Concepcion, M. (2010). Direct regulation of phytoene synthase gene expression and carotenoid biosynthesis by phytochrome-interacting factors. Proc Natl Acad Sci U S A **107,** 11626-11631.

Tuan, P.A., Kim, J.K., Lee, S., Chae, S.C., and Park, S.U. (2013a). Molecular characterization of carotenoid cleavage dioxygenases and the effect of gibberellin, abscisic acid, and sodium chloride on the expression of genes involved in the carotenoid biosynthetic pathway and carotenoid accumulation in the callus of Scutellaria baicalensis Georgi. J Agric Food Chem **61,** 5565-5572.

Tuan, P.A., Thwe, A.A., Kim, J.K., Kim, Y.B., Lee, S., and Park, S.U. (2013b). Molecular characterisation and the light-dark regulation of carotenoid biosynthesis in sprouts of tartary buckwheat (Fagopyrum tataricum Gaertn.). Food Chem **141,** 3803-3812.

Urantowka, A., Knorpp, C., Olczak, T., Kolodziejczak, M., and Janska, H. (2005). Plant mitochondria contain at least two i-AAA-like complexes. Plant Mol Biol **59,** 239-252.

Utama, I.M., Wills, R.B., Ben-Yehoshua, S., and Kuek, C. (2002). In vitro efficacy of plant volatiles for inhibiting the growth of fruit and vegetable decay microorganisms. J Agric Food Chem **50,** 6371-6377.

Vainstein, A., Halevy, A.H., Smirra, I., and Vishnevetsky, M. (1994). Chromoplast Biogenesis in Cucumis sativus Corollas (Rapid Effect of Gibberellin A3 on the Accumulation of a Chromoplast-Specific Carotenoid-Associated Protein). Plant Physiol **104,** 321-326.

Vallabhaneni, R., and Wurtzel, E.T. (2009). Timing and biosynthetic potential for carotenoid accumulation in genetically diverse germplasm of maize. Plant Physiol **150,** 562-572.

Vallabhaneni, R., Bradbury, L.M., and Wurtzel, E.T. (2010). The carotenoid dioxygenase gene family in maize, sorghum, and rice. Arch Biochem Biophys **504,** 104-111.

Van Norman, J.M., Zhang, J., Cazzonelli, C.I., Pogson, B.J., Harrison, P.J., Bugg, T.D., Chan, K.X., Thompson, A.J., and Benfey, P.N. (2014). Periodic root branching in Arabidopsis requires synthesis of an uncharacterized carotenoid derivative. Proc Natl Acad Sci U S A **111,** E1300-1309.

Verhounig, A., Karcher, D., and Bock, R. (2010). Inducible gene expression from the plastid genome by a synthetic riboswitch. Proc Natl Acad Sci U S A **107,** 6204-6209.

Vierheilig, H., Maier, W., Wyss, U., Samson, J., Strack, D., and Piche, Y. (2000). Cyclohexenone derivative- and phosphate-levels in split-root systems and their role in the systemic suppression of mycorrhization in precolonized barley plants. J. Plant Physiol. **157,** 593-599.

Vincill, E.D., Bieck, A.M., and Spalding, E.P. (2012). Ca(2+) conduction by an amino acid-gated ion channel related to glutamate receptors. Plant Physiol **159,** 40-46.

Vishnevetsky, M., Ovadis, M., and Vainstein, A. (1999a). Carotenoid sequestration in plants: the role of carotenoid-associated proteins. Trends Plant Sci **4,** 232-235.

Vishnevetsky, M., Ovadis, M., Itzhaki, H., and Vainstein, A. (1997). CHRC, encoding a chromoplast-specific carotenoid-associated protein, is an early gibberellic acid-responsive gene. J Biol Chem **272,** 24747-24750.

Vishnevetsky, M., Ovadis, M., Zuker, A., and Vainstein, A. (1999b). Molecular mechanisms underlying carotenogenesis in the chromoplast: multilevel regulation of carotenoid-associated genes. Plant J **20,** 423-431.

Vogel, J.T., Tan, B.C., McCarty, D.R., and Klee, H.J. (2008). The carotenoid cleavage dioxygenase 1 enzyme has broad substrate specificity, cleaving multiple carotenoids at two different bond positions. J Biol Chem **283,** 11364-11373.

Vogel, J.T., Walter, M.H., Giavalisco, P., Lytovchenko, A., Kohlen, W., Charnikhova, T., Simkin, A.J., Goulet, C., Strack, D., Bouwmeester, H.J., Fernie, A.R., and Klee, H.J. (2010). SlCCD7 controls strigolactone biosynthesis, shoot branching and mycorrhiza-induced apocarotenoid formation in tomato. Plant Journal **61,** 300-311.

von Lintig, J., Welsch, R., Bonk, M., Giuliano, G., Batschauer, A., and Kleinig, H. (1997). Light-dependent regulation of carotenoid biosynthesis occurs at the level of phytoene synthase expression and is mediated by phytochrome in Sinapis alba and Arabidopsis thaliana seedlings. Plant J **12,** 625-634.

von Zychlinski, A., Kleffmann, T., Krishnamurthy, N., Sjolander, K., Baginsky, S., and Gruissem, W. (2005). Proteome analysis of the rice etioplast: metabolic and regulatory networks and novel protein functions. Mol Cell Proteomics **4,** 1072-1084.

Vranova, E., Hirsch-Hoffmann, M., and Gruissem, W. (2011). AtIPD: A Curated Database of Arabidopsis Isoprenoid Pathway Models and Genes for Isoprenoid Network Analysis. Plant Physiology **156,** 1655-1660.

Wagner, D., Przybyla, D., Op den Camp, R., Kim, C., Landgraf, F., Lee, K.P., Wursch, M., Laloi, C., Nater, M., Hideg, E., and Apel, K. (2004). The genetic basis of singlet oxygen-induced stress responses of Arabidopsis thaliana. Science **306,** 1183-1185.

Wagner, R., Aigner, H., and Funk, C. (2012). FtsH proteases located in the plant chloroplast. Physiol Plant **145,** 203-214.

Wagner, R., von Sydow, L., Aigner, H., Netotea, S., Brugiere, S., Sjogren, L., Ferro, M., Clarke, A., and Funk, C. (2016). Deletion of FtsH11 protease has impact on chloroplast structure and function in Arabidopsis thaliana when grown under continuous light. Plant Cell Environ **39,** 2530-2544.

Walter, M.H., and Strack, D. (2011). Carotenoids and their cleavage products: Biosynthesis and functions. Nat Prod Rep **28,** 663-692.

Walter, M.H., Hans, J., and Strack, D. (2002). Two distantly related genes encoding 1-deoxy-D-xylulose 5-phosphate synthases: differential regulation in shoots and apocarotenoid-accumulating mycorrhizal roots. Plant Journal **31,** 243-254.

Walter, M.H., Stauder, R., and Tissier, A. (2015). Evolution of root-specific carotenoid precursor pathways for apocarotenoid signal biogenesis. Plant Sci **233,** 1-10.

Wang, H., Ma, L.G., Li, J.M., Zhao, H.Y., and Deng, X.W. (2001). Direct interaction of Arabidopsis cryptochromes with COP1 in light control development. Science **294,** 154-158.

Wei, S., Li, X., Gruber, M.Y., Li, R., Zhou, R., Zebarjadi, A., and Hannoufa, A. (2009). RNAi-mediated suppression of DET1 alters the levels of carotenoids and sinapate esters in seeds of Brassica napus. J Agric Food Chem **57,** 5326-5333.

Wei, S., Hannoufa, A., Soroka, J., Xu, N., Li, X., Zebarjadi, A., and Gruber, M. (2011). Enhanced beta-ionone emission in Arabidopsis over-expressing AtCCD1 reduces feeding damage in vivo by the crucifer flea beetle. Environ. Entomol. **40,** 1622-1630.

Weigel, D., and Glazebrook, J. (2006). EMS Mutagenesis of Arabidopsis Seed. CSH Protoc **2006**.

Welsch, R., Beyer, P., Hugueney, P., Kleinig, H., and von Lintig, J. (2000). Regulation and activation of phytoene synthase, a key enzyme in carotenoid biosynthesis, during photomorphogenesis. Planta **211,** 846-854.

Welsch, R., Medina, J., Giuliano, G., Beyer, P., and von Lintig, J. (2003). Structural and functional characterization of the phytoene synthase promoter from Arabidopsis thaliana. Planta **216,** 523-534.

Welsch, R., Wust, F., Bar, C., Al-Babili, S., and Beyer, P. (2008). A third phytoene synthase is devoted to abiotic stress-induced abscisic acid formation in rice and defines functional diversification of phytoene synthase genes. Plant Physiology **147,** 367-380.

Welsch, R., Arango, J., Bar, C., Salazar, B., Al-Babili, S., Beltran, J., Chavarriaga, P., Ceballos, H., Tohme, J., and Beyer, P. (2010). Provitamin A accumulation in cassava (Manihot esculenta) roots driven by a single nucleotide polymorphism in a phytoene synthase gene. Plant Cell **22,** 3348-3356.

Wille, A., Zimmermann, P., Vranova, E., Furholz, A., Laule, O., Bleuler, S., Hennig, L., Prelic, A., von Rohr, P., Thiele, L., Zitzler, E., Gruissem, W., and Buhlmann, P. (2004). Sparse graphical Gaussian modeling of the isoprenoid gene network in Arabidopsis thaliana. Genome Biol **5,** R92.

Woitsch, S., and Romer, S. (2003). Expression of xanthophyll biosynthetic genes during light-dependent chloroplast differentiation. Plant Physiology **132,** 1508-1517.

Wong, J.H., Balmer, Y., Cai, N., Tanaka, C.K., Vensel, W.H., Hurkman, W.J., and Buchanan, B.B. (2003). Unraveling thioredoxin-linked metabolic processes of cereal starchy endosperm using proteomics. Febs Lett **547,** 151-156.

Woodson, J.D., and Chory, J. (2008). Coordination of gene expression between organellar and nuclear genomes. Nat Rev Genet **9,** 383-395.

Woodson, J.D., Perez-Ruiz, J.M., and Chory, J. (2011). Heme Synthesis by Plastid Ferrochelatase I Regulates Nuclear Gene Expression in Plants. Curr Biol **21,** 897-903.

Wu, D.Y., Wright, D.A., Wetzel, C., Voytas, D.F., and Rodermel, S. (1999). The immutans variegation locus of Arabidopsis defines a mitochondrial alternative oxidase homolog that functions during early chloroplast biogenesis. Plant Cell **11,** 43-55.

Wurtzel, E.T. (2004). Genomics, genetics, and biochemistry of maize carotenoid biosynthesis. Recent Adv Phytochem **38,** 85-110.

Xie, X.N., Yoneyama, K., and Yoneyama, K. (2010). The Strigolactone Story. Annu Rev Phytopathol **48,** 93-117.

Xing, S.F., Miao, J., Li, S.A., Qin, G.J., Tang, S., Li, H.N., Gu, H.Y., and Qu, L.J. (2010). Disruption of the 1-deoxy-D-xylulose-5-phosphate reductoisomerase (DXR) gene results in albino, dwarf and defects in trichome initiation and stomata closure in Arabidopsis. Cell Res **20,** 688-700.

Yadav, V., Kundu, S., Chattopadhyay, D., Negi, P., Wei, N., Deng, X.W., and Chattopadhyay, S. (2002). Light regulated modulation of Z-box containing promoters by photoreceptors and downstream regulatory components, COP1 and HY5, in Arabidopsis. Plant Journal **31,** 741-753.

Yahyaa, M., Berim, A., Isaacson, T., Marzouk, S., Bar, E., Davidovich-Rikanati, R., Lewinsohn, E., and Ibdah, M. (2015). Isolation and Functional Characterization of Carotenoid

Cleavage Dioxygenase-1 from Laurus nobilis L. (Bay Laurel) Fruits. J Agric Food Chem **63,** 8275-8282.

Yamamoto, H.Y. (2006). Functional roles of the major chloroplast lipids in the violaxanthin cycle. Planta **224,** 719-724.

Yamauchi, R., Tsuchihashi, K., and Kato, K. (1998). Oxidation Products of beta-Carotene during the Peroxidation of Methyl Linoleate in the Bulk Phase. Biosci Biotechnol Biochem **62,** 1301-1306.

Yanagawa, Y., Sullivan, J.A., Komatsu, S., Gusmaroli, G., Suzuki, G., Yin, J., Ishibashi, T., Saijo, Y., Rubio, V., Kimura, S., Wang, J., and Deng, X.W. (2004). Arabidopsis COP10 forms a complex with DDB1 and DET1 in vivo and enhances the activity of ubiquitin conjugating enzymes. Genes Dev **18,** 2172-2181.

Yi, C., and Deng, X.W. (2005). COP1 - from plant photomorphogenesis to mammalian tumorigenesis. Trends Cell Biol **15,** 618-625.

Ytterberg, A.J., Peltier, J.B., and van Wijk, K.J. (2006). Protein profiling of plastoglobules in chloroplasts and chromoplasts. A surprising site for differential accumulation of metabolic enzymes. Plant Physiol **140,** 984-997.

Yu, Q., Ghisla, S., Hirschberg, J., Mann, V., and Beyer, P. (2011). Plant carotene cis-trans isomerase CRTISO: a new member of the FAD(RED)-dependent flavoproteins catalyzing non-redox reactions. J Biol Chem **286,** 8666-8676.

Yu, Q., Schaub, P., Ghisla, S., Al-Babili, S., Krieger-Liszkay, A., and Beyer, P. (2010). The lycopene cyclase CrtY from Pantoea ananatis (formerly Erwinia uredovora) catalyzes an FADred-dependent non-redox reaction. J Biol Chem **285,** 12109-12120.

Zhang, L., and Ren, G. (2012). IPET and FETR: experimental approach for studying molecular structure dynamics by cryo-electron tomography of a single-molecule structure. PLoS One **7,** e30249.

Zhou, X., Welsch, R., Yang, Y., Alvarez, D., Riediger, M., Yuan, H., Fish, T., Liu, J., Thannhauser, T.W., and Li, L. (2015). Arabidopsis OR proteins are the major posttranscriptional regulators of phytoene synthase in controlling carotenoid biosynthesis. Proc Natl Acad Sci U S A **112,** 3558-3563.

Zhu, C., Bai, C., Sanahuja, G., Yuan, D., Farre, G., Naqvi, S., Shi, L., Capell, T., and Christou, P. (2010). The regulation of carotenoid pigmentation in flowers. Arch Biochem Biophys **504,** 132-141.

Zybailov, B., Rutschow, H., Friso, G., Rudella, A., Emanuelsson, O., Sun, Q., and van Wijk, K.J. (2008). Sorting signals, N-terminal modifications and abundance of the chloroplast proteome. PLoS One **3,** e1994.